GEOLOGICAL SURVEY OF WESTERN AUSTRALIA

BULLETIN 138

THE GEOLOGY OF THE SYLVANIA INLIER AND THE SOUTHEAST HAMERSLEY BASIN

By
I.M. TYLER

DEPARTMENT OF MINES
WESTERN AUSTRALIA

THE GEOLOGY OF THE SYLVANIA INLIER AND THE SOUTHEAST HAMERSLEY BASIN

02208-1

GSWA 25881

FRONTISPIECE

Large-scale overturned D_{2c} fold in the upper Dales Gorge Member of the Brockman Iron Formation near Mount Newman. The structure forms part of a northerly directed foreland fold and thrust belt, which developed in the southeastern Hamersley Basin during the Early Proterozoic Capricorn Orogeny. The cliff is 30 m high.

GEOLOGICAL SURVEY OF WESTERN AUSTRALIA

BULLETIN 138

THE GEOLOGY OF THE SYLVANIA INLIER AND THE SOUTHEAST HAMERSLEY BASIN

by
I. M. Tyler

Perth 1991

MINISTER FOR MINES
The Hon. Gordon Hill, J.P., M.L.A.

DIRECTOR GENERAL OF MINES
D. R. Kelly

DIRECTOR, GEOLOGICAL SURVEY OF WESTERN AUSTRALIA
Phillip E. Playford

National Library of Australia
Cataloguing-in-publication entry

Tyler, I. M.
The geology of the Sylvania Inlier and the southeast Hamersley Basin

Bibliography.
ISBN 0 7309 1187 X.

1. Geology, Structural—Western Australia—Hamersley Basin.
2. Hamersley Basin (W.A.).
I. *Geological Survey of Western Australia.*
II. Title. (Series: Bulletin (Geological Survey of Western Australia); 138).

551.8099413

ISSN 0085 8137

Copies available from:
The Director
Geological Survey of Western Australia
100 Plain Street
EAST PERTH Western Australia 6004
Ph. (09) 222 3168

CONTENTS

CHAPTER 3 HAMERSLEY BASIN

CHAPTER 4 CAPRICORN OROGENY

CHAPTER 5 POST-CAPRICORN OROGENY EVOLUTION

CHAPTER 6 ECONOMIC GEOLOGY

APPENDIX

PLATES

(in separate wallet)

1. Jimblebar greenstone belt, scale 1:50 000
2. Geological map and representative diagrammatic cross-sections of the Sylvania Inlier and southeast Hamersley Basin, scale 1:250 000
3. Structural interpretation map, scale 1:500 000

FIGURES

TABLES

Summary

This bulletin describes the geology of the Sylvania Inlier and related rocks along the southeast margin of the Hamersley Basin. Archaean (older than 2750 Ma) granite–greenstone is exposed in the Sylvania Inlier; it is unconformably overlain by mafic volcanics, felsic volcanics and intrusive rocks, carbonates, clastic metasedimentary rocks, and banded iron-formation, all of which were deposited in the late Archaean to early Proterozoic (2750–2300 Ma) Hamersley Basin. In the eastern part of the area studied, the Hamersley Basin rocks are overlain by clastic metasedimentary rocks, carbonate rocks, and mafic volcanic rocks, of the Wyloo Group (1.84 Ga) which were deposited in the Ashburton Basin.

Most of the Sylvania Inlier is granitoid, but there are also discontinuous greenstone belts which have been intruded by the granitoid. The rocks of the greenstone belts were deposited near exposed granitoid basement, and form layered sequences of low-to medium-grade metavolcanics, mafic intrusions, and metasedimentary rocks. Deposition of these rocks was followed by intrusion of an early granitoid. The ultramafic intrusion at Coobina intrudes the Jimblebar greenstone belt and the early granitoid. It comprises two parts: a serpentinite sill emplaced along the granitoid–greenstone contact; and a feeder dyke. Chromitite pods and lenses occur at the junction between the feeder dyke and the sill.

The earliest deformation (D_{1g}) formed a layer-parallel foliation (S_{1g}) and may be related to thrusting. Deformation was accompanied by greenschist-facies metamorphism (M_g). A second deformation (D_{2g}) produced tight, northwest-facing folds which are locally overturned. A third deformation (D_{3g}) produced open, upright folds that plunge steeply to the southwest and to the southeast, and refold D_{2g} structures.

The D_{3g} event was followed by the intrusion of the gabbro at Western Creek and a layered mafic body between Sylvania and Woggaginna Hill. The greenstone belts, the early granitoid, the ultramafic intrusion at Coobina, and the later, layered mafic bodies, were all intruded by granitoid that was post-tectonic with respect to the D_{3g} deformation. This later granitoid forms most of the outcrop within the inlier. The later granitoid and the rocks that it intrudes are cut by several suites of mafic dykes. The oldest mafic dykes (Suite 1) are numerous in the western and central parts of the inlier and are correlated with the Black Range dyke suite in the northern Pilbara.

Field relationships in the granite–greenstone of the Sylvania Inlier resembles those of the northern Pilbara. There are differences in isotope and rare-earth-element patterns, however, suggesting separate evolution of the Sylvania Inlier prior to 3.0 Ga. The role of the Sylvania Inlier as cratonic basement to the Hamersley Basin implies that it is older than the granite–greenstone of the Yilgarn Craton.

The Hamersley Basin sequence, which overlies the granite–greenstone, comprises three groups of rocks: the mafic volcanic-dominated Fortescue Group; the banded iron-formation-dominated Hamersley Group, and the more areally restricted, clastic metasediment-dominated Turee Creek Group. Two successions are recognized in the Fortescue Group around the Sylvania Inlier. To the southwest of the inlier, the Fortescue Group succession is similar to that in the southwestern part of the Hamersley Basin; it consists of a basal metasedimentary unit, a lower mafic volcanic unit, a felsic pyroclastic unit, and an upper mafic volcanic unit. The upper mafic volcanic unit contains several pyroxene spinifex-textured metabasalt flows. Along the northern margin of the Sylvania Inlier the Fortescue Group succession comprises a basal metasedimentary unit overlain by a mafic volcanic unit. Both successions are overlain by the Jeerinah Formation. A regional palaeohigh north of the Sylvania Inlier was progressively on-lapped, and ultimately buried by the Fortescue Group.

In the western part of the Sylvania Inlier, a static metamorphic event has recrystallized—to albite–epidote–amphibolite facies—the gabbro at Western Creek, the later granitoid, and Suite 1 mafic dykes. This metamorphism post-dates the M_g event and is thought to be equivalent to a burial metamorphism (M_b) recognized in the overlying Hamersley Basin rocks. In the eastern part of the inlier, rocks were extensively deformed during the Capricorn Orogeny; however, evidence of the M_b event is preserved in zones of low strain. Temperatures and pressures are estimated to have been at least 550°C and 300 MPa. This can be combined with previously published data to construct a geothermal gradient for the Hamersley Basin.

The geological history of the Hamersley Basin records evolution from a rift phase (Fortescue Group) to a passive-margin phase (Hamersley Group) when banded iron-formation was deposited on an outer continental shelf in a period of tectonic quiescence. A return to a more active tectonic environment is marked by the Turee Creek Group.

The Pilbara and Yilgarn Cratons and their margins have quite different geological histories, and the available evidence suggests that they were juxtaposed for the first time during the Early Proterozoic (2200–1600 Ma) Capricorn Orogeny. This orogeny appears to reflect modern B-subduction-style plate tectonics and is interpreted as the result of an oblique continent–continent collision between the Pilbara Craton and the Yilgarn Craton.

Tectonic activity during the early stages of convergence between the two cratons occurred at the end of Turee Creek Group time and resulted in uplift along the southern margin of the Pilbara Craton. The Ophthalmia Fold Belt developed in rocks forming the southern part of the Hamersley Basin. Large open dome-and-basin-style folding forms the western part of the Ophthalmia Fold Belt.

In the southeast Hamersley Basin, deformation occurred later, during the deposition of the Wyloo Group. Two phases of deformation have affected the southeast part of the Ophthalmia Fold Belt. The earliest (D_{1c}) produced small-scale, layer-parallel folds and associated mylonites of restricted occurrence. D_{1c} structures were refolded by a regional-scale fold and thrust event (D_{2c}). D_{1c} structures are thought to have resulted from gravity spreading on bedding planes as a response to uplift during the development of incipient D_{2c} thrusts. D_{2c} deformation is most intense north of the Sylvania Inlier, where thrusts and overturned folds are abundant.

Numerous ductile shear zones that post-date the intrusion of suite 1 and 2 mafic dykes occur in the eastern part of the Sylvania Inlier. The shear zones can be linked to the D_{1c} and D_{2c} events in the overlying Hamersley Basin rocks. Together they form part of a foreland fold and thrust belt developed at the northern margin of the Capricorn Orogen. Deformation was accompanied by metamorphism (M_c). Hamersley Basin rocks were metamorphosed to the pumpellyite–actinolite and lower greenschist facies; similar grades were established in these rocks during the earlier burial metamorphism. The deepest structural levels and highest metamorphic grades (up to the amphibolite facies) are exposed at the southern margin of the Sylvania Inlier.

The orientation of folds, thrusts, and shear zones, suggests that the Yilgarn Craton moved north-northwest relative to the Pilbara Craton. Collision initially occurred at the southeast corner of the Pilbara Craton. Uplift associated with thrusting supplied sediment which was deposited in a foreland basin on the southern edge of the Pilbara Craton to form the middle and upper Wyloo Group.

As collision progressed, deformation migrated westward. The Ashburton Fold Belt includes rocks of the Capricorn Formation, Wyloo Group, and adjacent Hamersley Basin. The earliest deformation produced recumbent folding (D_{1a}) in the southern part of the Ashburton Basin. Large-scale, west-northwest-orientated dextral wrench faulting and associated folding (D_{2a}) developed along the margin between the Ashburton and Hamersley Basins. Extensive faulting occurs in the Paraburdoo area. Rotation of the Turee Creek Syncline produced reorientation of local D_{2c} folds as well as minor thrusting. The dextral movement is explained in terms of westward extrusion of material trapped between the converging craton margins. Corresponding northeast-orientated sinistral faults have been reported from the northern edge of the Yilgarn Craton.

After the Capricorn Orogeny, the region acted as basement to later Proterozoic sedimentary basins. Deformation was dominated by faulting and associated folding. The Mount Whaleback Fault system comprises northeast-orientated normal faults connected by west-northwest-orientated sinistral transfer faults consistent with a southeast-directed extension. Faulting controlled deposition of alluvial fans in the Bresnahan Basin. Later faults (Prairie Downs and Poonda Faults) were active during deposition in the Bangemall Basin.

The Shovelanna Bore and Murramunda Faults have a sinistral movement, and this age of faulting can be related to the occurrence of minor fold structures throughout the southeast Hamersley Basin. Locally D_{2c} folds are refolded. The youngest faults include the sinistral Fortescue River Fault, which may have been active during the Tertiary.

Four sets of mafic dykes which post-date the Capricorn Orogeny have been recognized.

The economic potential of the area is dominated by large hematite orebodies. They were produced by a combination of supergene enrichment processes and burial metamorphism operating from about 2000 Ma to the present. The largest orebodies are controlled by zones of complex faulting. The development of orebodies in the southeast Hamersley Basin can be related to the development of the Bresnahan Basin.

Gold has been mined at Jimblebar, and Australia's largest known deposit of chromite occurs at Coobina. Copper mineralization is present in rocks of the Jimblebar greenstone belt and in the Fortescue Group.

Acknowledgements

As part of this study, three weeks of the 1985 field season were spent looking in detail at the structural geology of the Mount Whaleback Mine. Mr Malcolm Kneeshaw of Mount Newman Mining is thanked for his co-operation, and for arranging unrestricted access to all areas of the mine.

Chapter One

Introduction

This report forms part of a major reassessment of the southern margin of the Pilbara Craton by the Geological Survey of Western Australia. It had its roots in the revision of the stratigraphy of the Mount Bruce Supergroup by Trendall (1979). Remapping of WYLOO* (Seymour et al., 1988) followed, and was extended to a regional study of the Ashburton Basin (Thorne and Seymour, 1991). In 1983, the author began fieldwork aimed at a better understanding of the age and tectonic position of the Sylvania Inlier. As work progressed it was recognized that deformation in the inlier could be related to deformation in the cover rocks of the southeast Hamersley Basin. In 1985 the project was extended to include the strongly folded Mount Bruce Supergroup rocks on ROBERTSON, NEWMAN, and TUREE CREEK, as well as parts of ROY HILL and MOUNT BRUCE (Fig. 1). Second editions of ROBERTSON, NEWMAN and TUREE CREEK have been prepared (Williams and Tyler, 1991; Tyler et al., 1990; Thorne and Tyler, in press) as well as a first edition NEWMAN 1:100 000 sheet (Tyler, 1990).

The major concern of this report is the structural development of the area, and its role as the northern foreland of the Capricorn Orogen. It compliments work on the sedimentology of the Wyloo Group, which was deposited in the Ashburton Basin and has been reported on by Thorne and Seymour (1991). The resulting model for the tectonic evolution of the Capricorn Orogen draws heavily on the relationship between deformation in the Sylvania Inlier and southeast Hamersley Basin, and sedimentation in the Ashburton Basin.

The area contains a number of large hematite orebodies. Given the structural and metamorphic controls on ore formation, the understanding of the structure of the area and its relationship to the tectonic history is important for exploration models. The complex folding and faulting is also important when designing large open-cut mining operations.

Location, communications, and access

The area covered by this report (Fig 1) lies across the boundary between the Pilbara and Gascoyne regions of Western Australia. Two major towns are present, Newman (population 5466 in 1981) and Paraburdoo (population 2357 in 1981). They were both established in the early 1970s to provide accommodation for workers in the Pilbara iron-ore mining industry.

Newman is reached from the south via the sealed Great Northern Highway. A highway northwards to Port Hedland– via Wonmunna, Mount Robinson, and Packsaddle was completed in 1990. A standard-gauge, single-track railway connects the Mount Whaleback Mine near Newman with the deep-water port at Port Hedland. The Ophthalmia Dam, built across the Fortescue River and Warrawanda Creek, ensures the town's water supply by catching seasonal rainfall to recharge underground aquifers.

Paraburdoo is connected to the iron-ore mining town of Tom Price, 80 km to the north, by a sealed two-lane road; it may also be reached from Nanutarra on the Coastal Highway via a sealed two-lane road and well-maintained graded roads. A standard-gauge, single-track railway connects the Paraburdoo Mine with Tom Price, from where ore is despatched by rail to the deep-water port of Dampier. Both Newman and Paraburdoo have airports which are served by regular daily flights to Perth.

The country comprises vacant crown land, National Park, and pastoral lease. Pastoral leases are mainly found in the south and east. Homesteads at Sylvania, Prairie Downs, and Juna Downs, together with a small holding at Mundiwindi, are occupied,. Other leases which extend into the area are Marillana, Roy Hill, Ethel Creek, Walagunya, Weelarrana, Bulloo Downs, Turee Creek, Mininer, and Rocklea. An Aboriginal Reserve occupies the eastern end of the area. The Jigalong Community is located to the northeast. Access in these areas is via graded roads and station tracks.

Extensive exploration for iron ore in the 1960s and 1970s has provided access into many areas of vacant crown land. Exploration camps are maintained at McCamey's Monster, Rhodes Ridge, Giles, West Angelas, and Packsaddle. Only the main access roads to the camps are maintained; and extreme care should be taken when negotiating other roads and tracks, particularly steep drill tracks, as they may be badly washed out.

The southern part of the Hamersley Range National Park occurs in the northwest part of the area.

Physiography

The area straddles the divide between three major drainages: the Fortescue, flowing to the north; the Ashburton,

*1:250 000 map sheet names are printed in capitals to avoid confusion with identical place names

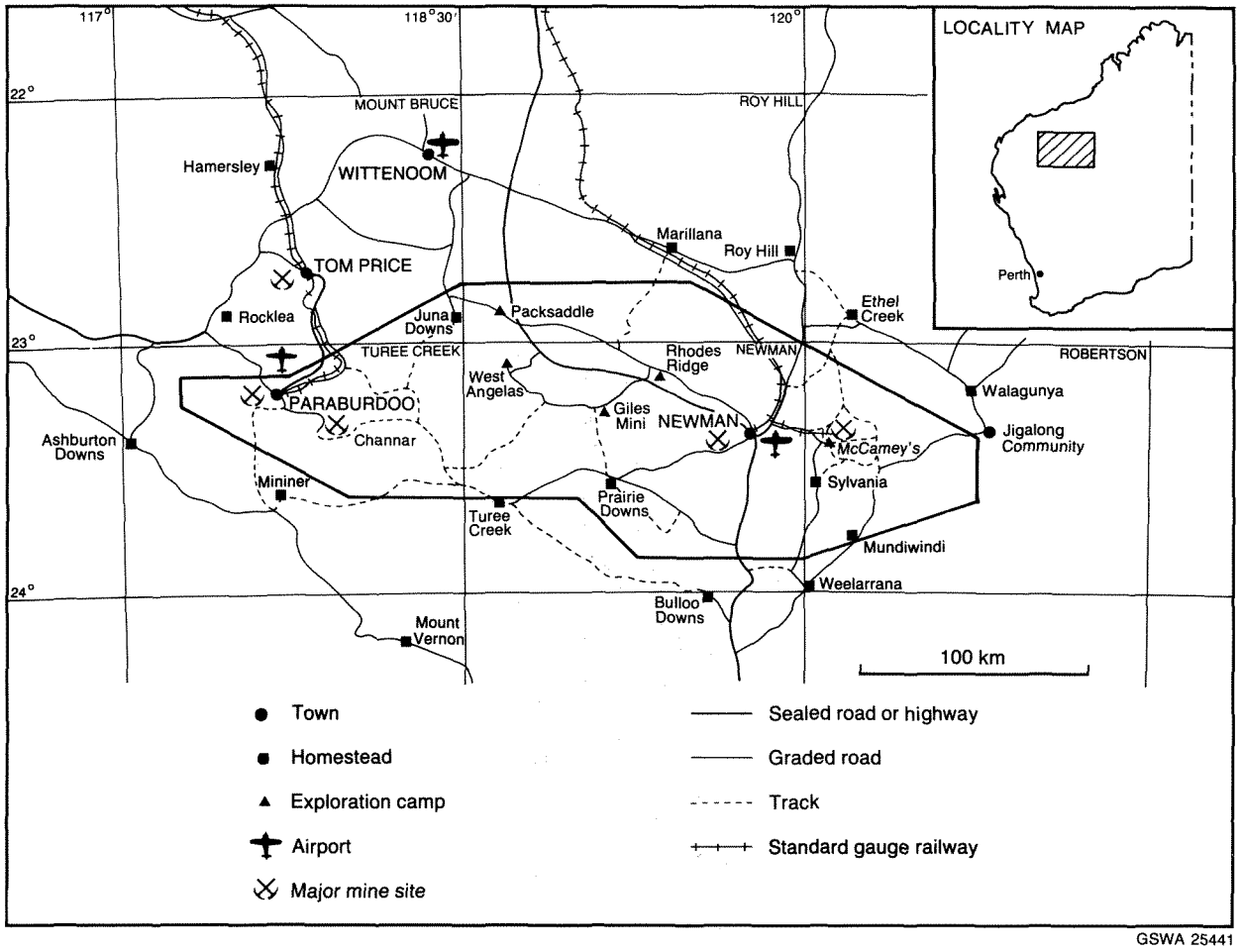

Figure 1. Location and access map for the southeast Pilbara with index to 1:250 000 map sheets. Area covered by Plate 2 is outlined.

flowing to the southwest; and the Savory, flowing to the east. Watercourses are intermittent and only flow after periods of heavy rainfall.

The main physiographic units are the Hamersley Plateau, the Fortescue Valley, the Kumerina Hills, and the Ashburton Valley (Beard, 1975, fig. 3). The Hamersley Plateau is rugged hill country. The Ophthalmia and Hamersley Ranges are characterized by long strike-ridges that rise 300 m above the intervening valley floors. Prominent are Wheelarra Hill (727 m), Shovelanna Hill (802 m), Mount Newman (1055 m), Pamelia Hill (874 m), Mount Robinson (1142 m), Snowy Mountain (860 m), and Mount Channar (720 m). The highest point is Mount Meharry–at 1245 m, the highest point in Western Australia. Valley floors may contain extensive alluvial flats. In the northeast, high plateau country is dissected by deep gorges.

The Fortescue Valley contains extensive alluvial flats and sand plain; these form the flood plain of the Fortescue River. The Ashburton Valley and Kumerina Hills are gently undulating plains broken by low rocky hills. Prominent landmarks include Deadman Hill (731 m) and the Kunderong Range. The area underlain by the granite–greenstone of the Sylvania Inlier is a stony, poorly vegetated plain scattered with low granite tors.

Climate and vegetation

The average annual rainfall, mainly the result of tropical cyclones in late summer, is between 200 and 300 mm. The area may also be affected by winter rains from the southwest. The temperature range is large: maximum temperatures can rise above 45°C in summer. In winter minimum temperatures may drop below freezing: -5°C has been recorded at Mundiwindi.

Vegetation can be divided into four types coinciding with the physiographic units identified above (Beard, 1975). In hill country of the Hamersley Plateau, vegetation is described as tree steppe, and comprises buck spinifex (*Triodea wiseana*) and snappy gum (*Eucalyptus brevifolia*); shrub steppe, comprising mulga (*Acacia aneura*) and spinifex, becomes more important to the west. Valleys are filled with low mulga woodland. The Fortescue Valley is characterized by low woodland dominated by mulga and shrub steppe (*E. gamophylla* and spinifex) on sandplain. The Kumerina Hills are covered by low mulga woodland and scrub. In the Ashburton Valley, scrub, consisting of mulga and other acacias, together with snakewood and teatree, is dominant.

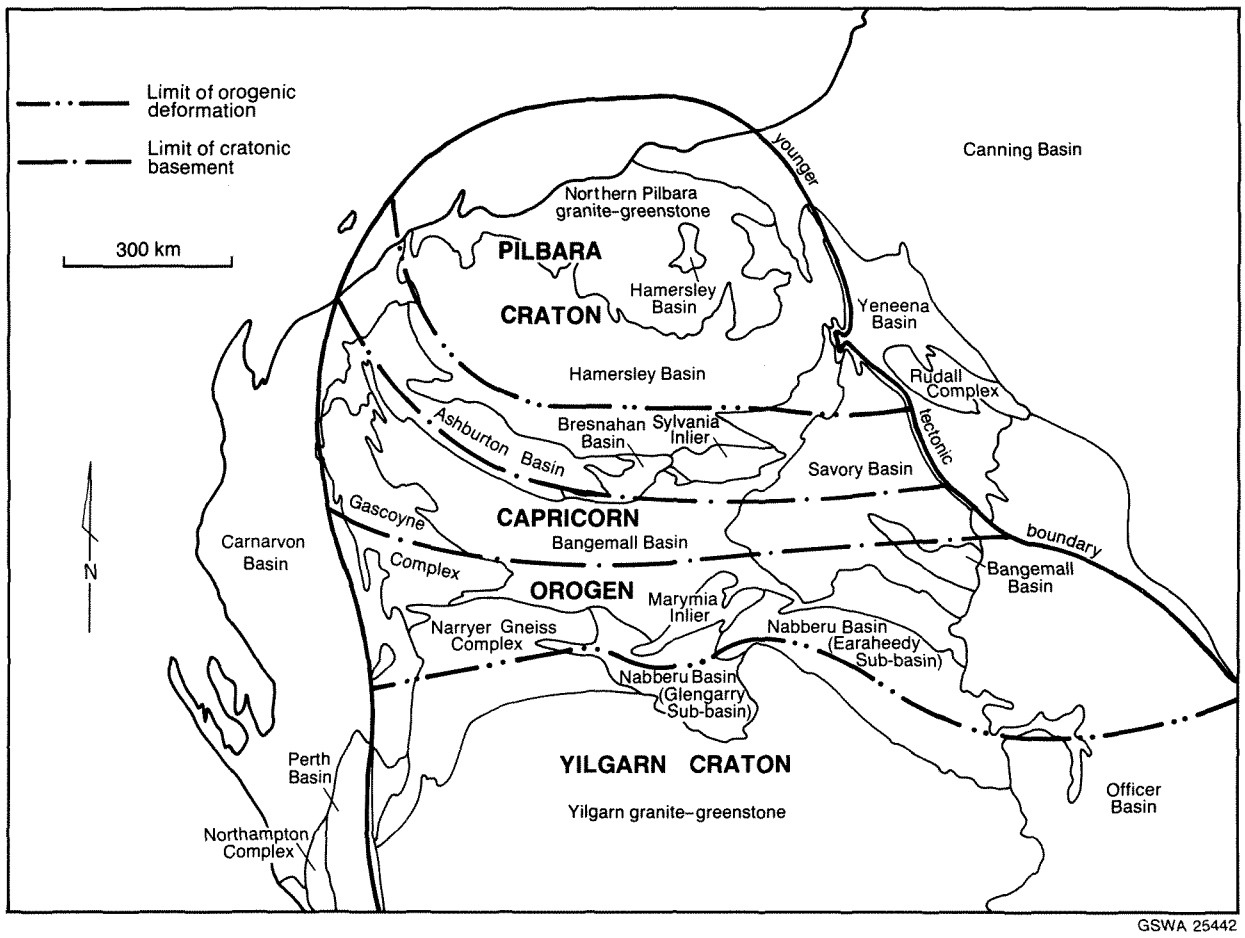

Figure 2. Map showing the main tectonic units forming the Pilbara Craton, the northern Yilgarn Craton and the Capricorn Orogen. Later sedimentary basins are also shown.

Previous investigations

Summaries of exploration and early geological work in the southeast Pilbara are given in the various first edition volumes of the 1:250 000 Geological Series—Explanatory Notes (Daniels and MacLeod, 1965; de la Hunty, 1965; MacLeod and de la Hunty, 1966; Daniels, 1968; de la Hunty, 1969), and by MacLeod (1966). More recent work will be referred to in the text as appropriate.

Regional geological setting

The area under investigation lies at the southeast corner of the Pilbara Craton (Fig. 2). Archaean granite–greenstone (older than 2750 Ma) is exposed in the Sylvania Inlier, and represents cratonic basement similar to that seen in the northern Pilbara. It is unconformably overlain by rocks of the late Archaean to Early Proterozoic (2765 Ma to 2300 Ma) Hamersley Basin. This basin, evolving from an initial rift in already cratonized crust to a stable shelf, has developed as a passive continental margin .

Rocks between the Pilbara and Yilgarn Cratons were involved in the Capricorn Orogeny (2200 Ma to 1600 Ma). These rocks include low-grade metasedimentary and metavolcanic rocks of the Ashburton and Nabberu Basins, and the higher grade metamorphic and igneous rocks of the Gascoyne Complex. The southern Pilbara Craton and northern Yilgarn Craton acted as stable forelands that were deformed during the orogenic event. In the southern Pilbara Craton, deformation produced the Ophthalmia Fold Belt. The Ashburton Basin developed as a foreland basin during the orogeny. The basin was itself deformed at a late stage to form the Ashburton Fold Belt.

Rocks which were involved in the Capricorn Orogeny are unconformably overlain by the Middle Proterozoic Bresnahan Basin (about 1600 Ma). This is a series of large alluvial fans—prograding to the southeast—that can be related to an extensive extensional fault system.

The Bresnahan Basin is unconformably overlain by the Middle to Late Proterozoic (1500 Ma to 1100 Ma) Bangemall Basin. Rocks deposited in the Bangemall Basin have been deformed to form the Edmund Fold Belt. The deformation was controlled by re-activation of previously established basement structures. To the south and east, the Bangemall Basin is unconformably overlain by rocks of the Savory Basin.

Extensive faulting post-dates rocks of the Savory Basin; and further movements may have taken place periodically throughout the Phanerozoic.

Cainozoic geology

A prominent feature of the Cainozoic geology of the southeast Pilbara is the Hamersley Surface (MacLeod et al., 1963; Campana et al., 1964), an uplifted and dissected surface of late Mesozoic to early Tertiary peneplanation (Twidale et al., 1985).

Three landscapes may be recognized (Twidale et al., 1985). Hamersley I, characterized by deep weathering of the peneplanation surface under warm humid conditions, is the earliest. Residual deposits developed on this surface are lateritic and may be ferruginous. On banded iron-formation, surficial iron enrichment has produced thin deposits of hematite–goethite ore (Morris, 1980; Kneeshaw, 1984). The surface is best preserved in the north and northeast where it is incised by deep gorges. Ridges of banded iron-formation rise above the surface as monadnocks and are cloaked by the residual deposits.

The Hamersley II landscape has been produced by stripping and dissection of the primary surface. Extensive valley-fill deposits take the form of partly consolidated and cemented colluvium. Locally, colluvium may be deposited on the Hamersley I landscape. Pisolitic limonite deposits of this age occur in the headwaters of the Angelo River and Yandicoogina Creek: they are correlated with the Robe Pisolite of MacLeod (1966). Calcrete occurs extensively along the main drainages, particularly where they cross carbonate rocks. Ridges of massive opaline silica may be associated with the calcrete.

The present erosional system may be regarded as the Hamersley III landscape. It has been produced by a lowering of the base level, which has led to dissection of colluvium, pisolite, and calcrete, as well as to further dissection of the primary surface. Relief inversion occurs: colluvium and pisolite, which once formed valley floors, stand up as mesas. Extensive areas of recent alluvium and sheetwash plain are associated with this landscape. Sandplain, forming dunes and sheets, occurs within the Fortescue Valley.

Chapter Two

Granite–greenstone—The Sylvania Inlier

Introduction

Archaean granite–greenstone (>2750 Ma) crops out over an area of 5600 km^2 between Prairie Downs on NEWMAN and the Jigalong Community on ROBERTSON (Fig. 3). Daniels and MacLeod (1965) originally referred to this as the Sylvania "Dome", believing it to be analogous to outcrops of granite–greenstone, which occupy the cores of relatively simple domical structures within the Hamersley Basin succession in the southwestern Hamersley Basin (Halligan and Daniels, 1964). As will be shown in a later section, the structural controls on the Sylvania outcrop are much more complex. In addition, it is unconformably overlain by the Middle Proterozoic Bresnahan Group to the west, and by the Middle to Late Proterozoic Bangemall Group to the south and east. The outcrop cannot be described as domical and the term inlier is preferred.

The granite–greenstone that forms the inlier comprises layered sequences of low- to medium-grade metavolcanics, mafic intrusions, and metasedimentary rocks (greenstone belts), which have been intruded extensively by granitoid rocks. Also present are numerous mafic dykes of a variety of ages and orientations.

Areas of greenstone occur at Jimblebar, Woggaginna Hill, Warrawanda Creek, Spearhole Creek, Western Creek and Spearhole Yard, and Deadman Flat. Several smaller inclusions are scattered throughout the inlier. At Coobina a large chromite-bearing ultramafic body intrudes the Jimblebar greenstone belt, but is itself intruded by granitoid. Granitoid forms the majority of outcrop within the inlier. A summary of events which took place during the evolution of the granite–greenstone forming the inlier is given in Table 1. The largest area of greenstone belt, and by far the most complete stratigraphy, occurs within the Jimblebar greenstone belt.

Jimblebar greenstone belt

Introduction

The Jimblebar greenstone belt (Plate 1) is in the northeast portion of the inlier, 50 km east-southeast of Newman. It is an arcuate outcrop of felsic, mafic, and ultramafic volcanics, together with clastic metasedimentary rocks, cherts, and banded iron-formation. It has been intruded by a number of mafic to ultramafic sills that have been deformed and metamorphosed along with the greenstone belt. The intensity of deformation is such that primary sedimentary and volcanic structures have not been preserved.

The belt can be divided into two parts which are separated by the Battery Fault. In the western part, the rocks strike from east to northeast and dip to the south and southeast. Northward younging is interpreted from layering in the mafic to ultramafic sills. Much of this sequence is inverted. Strikes in the eastern half are east to north. Younging directions from layered sills near Coobina are north and west.

The successions of the two halves are outlined in Figure 4. The lithologies at the top of the eastern succession are similar to those at the base of the western succession. Together, the two successions (including sills) are nearly 12 km thick. An early fold and thrust event may have caused unrecognized tectonic thickening of the sequence.

TABLE 1. SEQUENCE OF ARCHAEAN EVENTS IN GRANITE–GREENSTONE

1.	Greenstone sequence deposited on granitoid basement (inferred from granitic detritus forming metasedimentary rocks). Contemporaneous intrusion of mafic sills.
2.	Intrusion of pre-granitoid mafic dykes.
3.	Intrusion of the precursor to the foliated and/or banded granitoid.
4.	Emplacement of the Coobina ultramafic intrusion.
5.	D_{1g} deformation forming layer-parallel S_{1g} foliation, ?thrusting, and greenschist facies metamorphism (M_g).
6.	D_{2g} deformation produced tight, northwest-facing folds which may have become overturned.
7.	D_{3g} deformation produced open, upright, steeply southwest- and southeast-plunging folds. Refolds D_{2g} structures.
8.	Emplacement of Western Creek gabbro and a layered intrusion between Sylvania and Woggaginna Hill.
9.	Intrusion of main granitoid.
10.	Intrusion of hornblende-bearing granitoid.
11.	Intrusion of Suite 1 and Suite 2 mafic dykes.

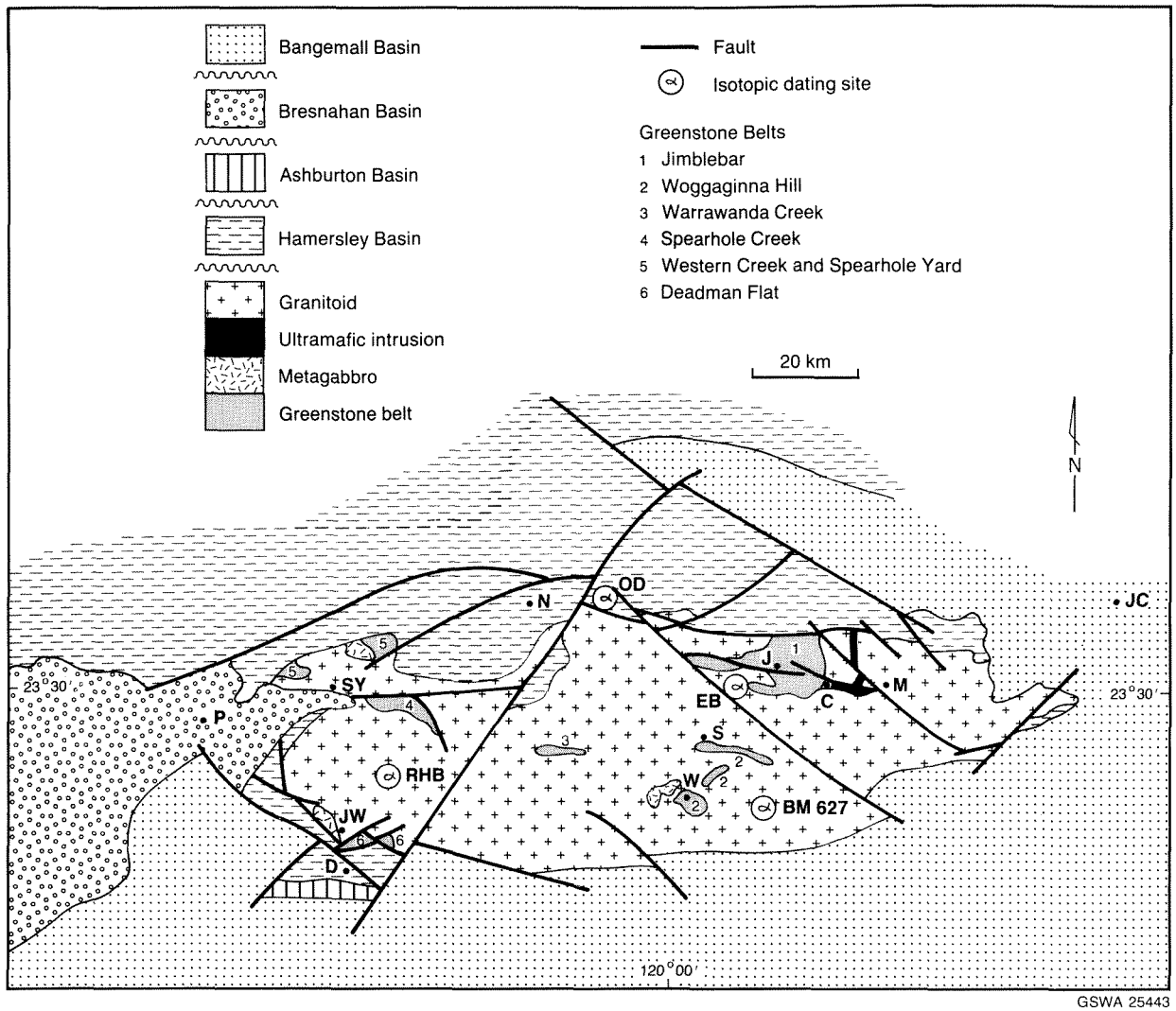

Figure 3. Simplified geological map of the Sylvania Inlier. Locations of sampling sites for isotopic dating are shown: BM627—Benchmark 627; C—Coobina; D—Deadman Hill; EB—Emerald Bore; J—Jimblebar; JC—Jigalong Community; JW—Jillary Well; M—Murramunda; N—Newman; OD—Ophthalmia Dam; P—Prairie Downs; RHB—Round Hill Bore; S—Sylvania; SY—Spearhole Yard; W—Woggaginna Hill.

Mafic to ultramafic volcanic rocks

A 500 m thick sequence of ultramafic rocks consisting of interlayered amphibole–talc–chlorite schists and tremolite– talc schists occurs 2 km northwest of Coobina. Individual layers range from 1 to 50 m thick; and a rapid alternation of the two rock types is seen. The amphibole–talc–chlorite schist may represent the altered olivine-rich, peridotitic basal parts of ultramafic lava flows, and the coarse-grained tremolite–talc schist may represent the more pyroxenitic upper parts. Spinifex textures have not been preserved.

One kilometre northwest of the old battery, a fine-grained, weakly foliated, amygdaloidal metabasalt comprises ragged laths of actinolite, interstitial microgranular plagioclase, clinozoisite, and accessory sphene. Amygdales are flattened quartz, or quartz–epidote aggregates, up to 5 mm long.

Amphibolitic schist, apparently derived from metabasalt, is observed in a similar stratigraphic position south of the Mindoona Bore Thrust. Similar rocks, containing aligned laths and needles of actinolite, and subordinate microgranoblastic plagioclase, orientated chlorite, and small amounts of epidote, occur north of the battery.

North of Coobina, amphibolitic schist in several horizons preserves textures in thin section which indicate that the rocks may originally have been komatiitic basalts. They consist of tremolite (pseudomorphing pyroxene) which shows a relic skeletal–platy texture, plagioclase (partially replaced by granular epidote), and lesser chlorite.

Mafic to ultramafic intrusive rocks

A zone of mafic to ultramafic sills, which has a strike length of 20 km and a thickness of up to 1.5 km, occurs south and east of Copper Knob. The sills intrude the

greenstone belt. The dominant rock is metagabbro. Discontinuous layers of coarse-grained metaleucogabbro, which has good cumulate texture, are present. Pods and lenses of serpentinite (originally dunite), serpentine–talc or serpentine–tremolite rocks (after peridotite), and chlorite–tremolite rocks (after pyroxenite) are also present. Extensive areas of silicified ultramafic rocks occur 4 km northeast of Copper Knob

Metagabbro and metaleucogabbro consist of actinolite (pseudomorphing pyroxene) in a matrix of microcrystalline epidote, actinolite, feldspar, and chlorite (pseudomorphing plagioclase laths). In some specimens, actinolite pseudomorphs ?orthopyroxene, suggesting the original occurrence of gabbronorite.

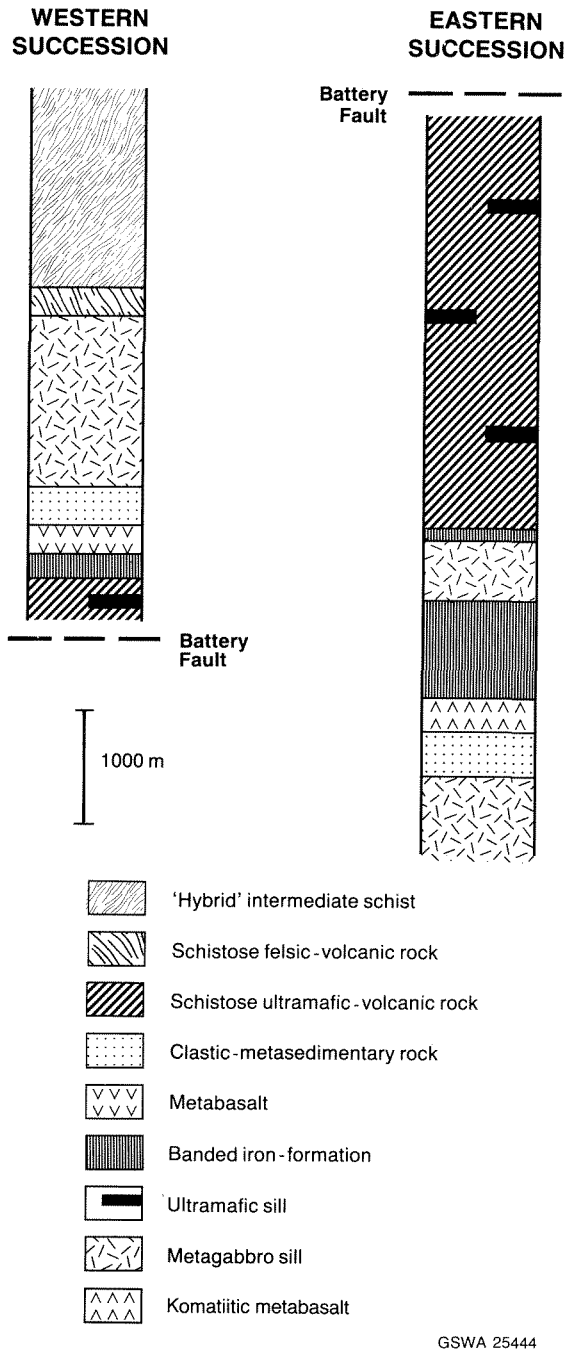

Figure 4. Stratigraphy of the Jimblebar greenstone belt.

Layered mafic to ultramafic sills crop out elsewhere in the Jimblebar greenstone belt, most notably to the north and east of Coobina. One sill shows a succession from serpentinite, through a distinctive feldspathic metapyroxenite containing large, centimetre-sized tremolite pseudomorphs of pyroxene phenocrysts, into a metagabbro which becomes leucocratic towards the top. Other metagabbro sills occur 4.5 km northeast of Copper Knob and at the eastern margin of the belt, north of Coobina. The latter may be quite leucocratic, and, locally, becomes anorthositic.

A series of layered, dominantly ultramafic sills have intruded ultramafic schist between Coobina and Jimblebar. They are mainly of metapyroxenite with medium-grained tremolite–actinolite pseudomorphs of laths and plates of pyroxene. Relic pyroxene may be present in the cores of amphibole pseudomorphs. The sills may be differentiated, becoming more gabbroic (up to 5% epidote–clinozoisite replacing feldspar) towards the top. Serpentinite or metaperidotite, preserving the texture of former olivine cumulates with intercumulus pyroxene, may occur at the base. Olivine may be preserved.

Felsic volcanic rocks

A prominent ridge of distinctive reddish-purple-weathering schist occurs towards the northwest margin of the belt. The rock is a fine-grained felsic schist. At Copper Knob it is porphyroclastic rock and comprises 40–50% quartz–feldspar (K-feldspar and plagioclase) porphyroclasts and composite quartz–feldspar fragments set in an anastomosing fabric of quartz, feldspar and dark-green chlorite, which wraps around the porphyroclasts. The internal textures of the porphyroclasts vary: some show beta-quartz forms; others, microcrystalline intergrowths of quartz and feldspar—a texture normally associated with devitrified felsic volcanic rocks. Also present is a quartz–albite–chlorite–hornblende–biotite–garnet schist (Fig. 5). The garnet has a spessartine–almandine composition (Barley, 1974)

A fine-grained quartz–chlorite schist occurs north of Coobina. Relic textures include cryptocrystalline felsic fragments, which may represent devitrified volcanic glass, suggesting that the rock was a felsic tuff.

Clastic metasedimentary rocks and chert

Two main horizons of clastic metasedimentary rocks interlayered with chert occur within the belt. A mixed metasedimentary sequence of interlayered chert, metaquartzite, quartzofeldspathic schist, metapelitic schist and calcareous metapsammite, up to 400 m thick, crops out from just northwest of Jimblebar to south of Mindoona Bore.

Chert is best developed near Jimblebar; it is grey and white with a well-developed alternation of milky and dark layers up to 1 cm thick. Locally the chert may be ferruginous. It is associated with quartzofeldspathic schist which may have a felsic volcanic origin.

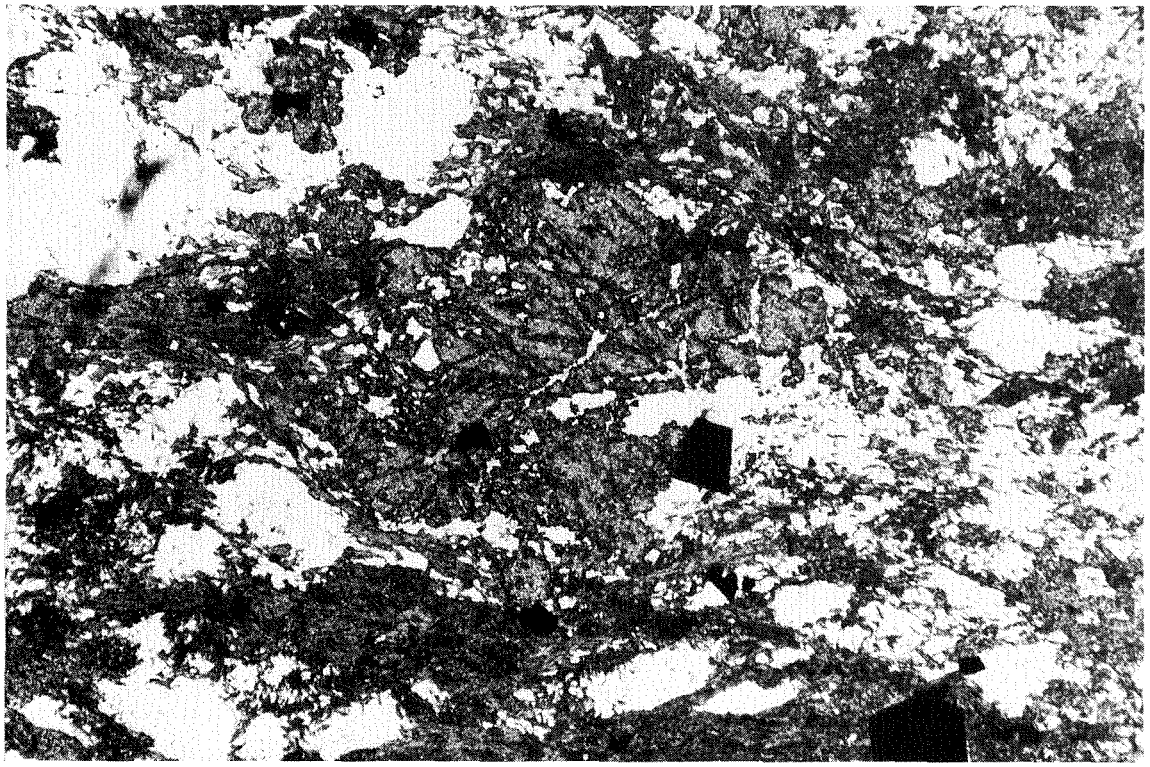

GSWA 25445

Figure 5. Quartz–albite–chlorite–hornblende–biotite–garnet schist, Copper Knob (x35). GSWA sample 49156.

Fine-grained, well-foliated, granoblastic to lepidoblastic, fuchsitic metaquartzite that has a distinctly flaggy appearance crops out as prominent ridges 1.5 km south of Copper Knob and 2 km southeast of Mindoona Bore.

Associated with the metaquartzite, a layered, calcareous metapsammite crops out 1 km southwest of Jimblebar. The layering, which is up to 30 cm thick, is probably a primary sedimentary feature. The rock is fine grained, foliated, and leucocratic; it comprises 50–60% quartz, 20% feldspar (K-feldspar dominant), 15% hornblende, and 5% clinozoisite. The texture is slightly mylonitic: quartz or feldspar porphyroclasts are wrapped by domains of fine-grained quartz, hornblende, feldspar, and clinozoisite. The rock is probably a metamorphosed sandstone or arkose which, judging from the abundant amphibole and clinozoisite, had a significant calcic plagioclase content. Two kilometres southeast of Mindoona Bore, a similar, but even more calcareous, metapsammite is present.

Metapelites are scarce and are typically fine-grained granoblastic to lepidoblastic rocks that containing of sub-equal amounts of quartz and muscovite, and either biotite or chlorite.

A conglomerate containing well-rounded, undeformed boulders of granitoid up to 0.5 m in diameter that are supported in a strongly cleaved quartzofeldspathic matrix occurs 2.7 km southeast of Mindoona Bore (Fig. 6). The unit is intraformational.

North of Coobina, a prominent ridge, 200 m wide, consists of two well-laminated metaquartzite horizons separated by a thin chlorite schist. South and east of this is a well-foliated, fine-grained, semi-pelitic schist consisting predominantly of quartz with lesser muscovite and chlorite.

Banded iron-formation

Banded iron-formation occurs at Jimblebar and to the west and north of Coobina. It is of the magnetite–hematite type and is well layered and typically flaggy. Locally it may grade into ferruginous chert. To the west of Coobina is a thinly banded iron-formation which has a distinctive "shaly" appearance in outcrop. It contains two amphiboles: deep blue-green hornblende; and colourless grunerite. Both form porphyroblastic laths which make up 50% of the rock and are orientated parallel to the layering. Granoblastic quartz and magnetite form the rest of the rock.

Other greenstone belts

Woggaginna Hill

The Woggaginna Hill greenstone belt crops out in the southern part of the inlier (Fig. 3); it comprises ultramafic rock and banded iron-formation. The belt has been intruded by mafic–ultramafic layered sills and by granitoid prior to intense deformation that has disrupted and dismembered it.

Ultramafic rock, comprising tremolite–chlorite schist with or without talc, is interlayered with the banded iron-formation. East of Sylvania, a silicified cap rock has developed on ultramafic schist.

GSWA 25446

Figure 6. Deformed, matrix-supported boulder conglomerate. Large, rounded boulders in schistose granitic matrix, southeast of Mindoona Bore.

Banded iron-formation occurs at Woggaginna Hill and near Sylvania as a fine- to medium-grained rock consisting of quartz and magnetite and accessory apatite. Textures indicate extensive recrystallization, and magnetite grains may reach 3 mm in diameter. Clay pseudomorphs suggest that amphibole was formerly a constituent.

Warrawanda Creek

The Warrawanda Creek greenstone belt (Fig. 3) crops out 16 km south of the Capricorn Roadhouse; it consists of east-trending banded iron-formation, schistose amphibolite, and serpentinite, all of which have been intruded by granitoid.

The banded iron-formation is moderately recrystallized, fine- to medium-grained quartz and magnetite. Magnetite may have been oxidized to goethite and hematite. Minor quantities of chert are associated with the BIF.

Schistose amphibolite occurs at the southern margin of the BIF; it is fine- to medium-grained; it consists of pale-green actinolite, plagioclase (oligoclase–andesine), quartz, and small amounts of sphene, chlorite, and epidote. A strong anastomosing fabric is defined by fine-grained, granoblastic plagioclase, orientated amphibole, and quartz, all of which wrap laths and plates of amphibole up to 3 mm long.

A serpentinite body, 300 m thick and 4 km long, occurs at the southern margin of the belt; it is massive, unfoliated, and capped with opaline silica.

Spearhole Creek

The Spearhole Creek greenstone belt crops out along the southern side of Spearhole Creek, 7 km southwest of Outcamp Well. It is dominated by banded iron-formation. Lithologies related to a layered sill are exposed south of the BIF. These are amphibolitic rocks—now consisting of actinolite, epidote, albite, and sphene—after pyroxenite and gabbro. Primary igneous textures are not preserved; however, local layering, defined by iron oxides and variations in the proportions of silicate minerals, probably represents small-scale igneous layering. Further west, weakly foliated amygdaloidal metabasalt, together with serpentinite and ultramafic schist, is exposed.

Western Creek and Spearhole Yard

Two areas of greenstone occur in the northwest part of the inlier, one on Western Creek and the other north of Spearhole Yard. Both are dominated by clastic metasedimentary rocks and BIF, but subordinate mafic volcanic rocks are also exposed.

The clastic metasedimentary rocks at Western Creek are interlayered fuchsitic quartzite and metasandstone. They are thoroughly recrystallized, and the well-developed foliation tends to wrap original quartz clasts that reach 0.5 mm across. They are overlain by amphibolite (comprising actinolite, albite, epidote, and sphene) which is interlayered with thin layers of a calcareous semi-pelitic rock. Quartz–biotite–muscovite pelitic schist overlies this unit and occupies the core of a synform.

North of Spearhole Yard, matrix-supported fuchsitic metaconglomerate (Fig. 7), containing recrystallized quartz pebbles 2–3 cm long, overlies metasandstone in the core of a major synform. Banded iron-formation consisting of quartz and hydrated iron-oxide underlies the metasandstone. Limonite pseudomorphs of ?amphibole occur.

Deadman Flat

The Deadman Flat greenstone belt is exposed as a series of discontinuous xenoliths in granitoid at the southeastern margin of the inlier north of Deadman Hill. It consists of deformed remnants of a layered intrusion together with an interlayered sequence of amygdaloidal metabasalt, ultramafic schist, chert, and quartz–muscovite schist.

Rocks which formed the layered intrusion outcrop around Jillary Well, but are now thoroughly recrystallized. Metagabbro is typically a foliated and lineated medium- to coarse-grained assemblage of amphibole (actinolite and grunerite), patches of epidote–sericite–albite after calcic plagioclase, and sphene. Locally, small- and medium-scale primary layering can be recognized, and metapyroxenite, serpentinite, tremolite–chlorite–talc schist, and anorthosite layers are developed. The local occurrence of grunerite suggests the occurrence of aluminium-poor layers in the intrusion.

At Deadman Flat, fine- to medium-grained amphibolite is moderately foliated; it consists of amphibole (transitional from actinolite to hornblende), epidote, albite, sphene, and quartz. In some amphibolites, large knots of epidote–quartz represent either original plagioclase phenocrysts or recrystallized amygdales. Ultramafic schist is poorly exposed and typically silicified.

Well-layered chert, which may be ferruginous, forms strike ridges up to 50 m wide. Quartz–muscovite schist is fine to medium grained, and contains quartz augen, wrapped by a strong mylonitic foliation, up to 1 mm across. The augen look like the embayed quartz bipyramids found in felsic volcanics, and taken together with mica-rich patches possibly derived from lithic fragments, suggest that the rock was a crystal–lithic tuff.

A medium-grained, well-foliated and lineated amphibolite is exposed in granitoid 1.5 km northwest of Curley Bore. It is composed of hornblende, plagioclase and quartz. Ptygmatically folded quartz–feldspar veins are present.

Environment of greenstone belt deposition

The discontinuous nature of the greenstone belts, together with the general lack of primary sedimentary and igneous features, makes the interpretation of an environment of deposition difficult. Perhaps the most useful information comes from the nature of the metasedimentary rocks present.

In the Jimblebar belt, the upper metasedimentary unit in the western part of the belt contains a variety of rock types including a coarse, matrix-supported conglomerate. Matrix-supported conglomerate is also seen north of Spearhole Yard. This suggests a high-energy environment. The occurrence of granitic boulders in the conglomerates, together with metasandstones and calcareous metapsammites of granitic provenance, indicates proximity to exposed granitic basement. In the absence of sedimentary structures, the environment of deposition is uncertain, but it may have been the proximal part of a submarine fan (cf. Walker, 1984), or part of an alluvial fan (cf. Rust and Koster, 1984). From the degree of volcanic activity, the area must have been one of tectonic instability: the available evidence is compatible with the intracratonic rift model described by Ayers and Thurston (1985).

Minor intrusions

Low, typically thin, sinuous ridges of schistose mafic to ultramafic rocks cut across felsic schist and mafic to ultramafic sills in the Copper Knob area of the Jimblebar

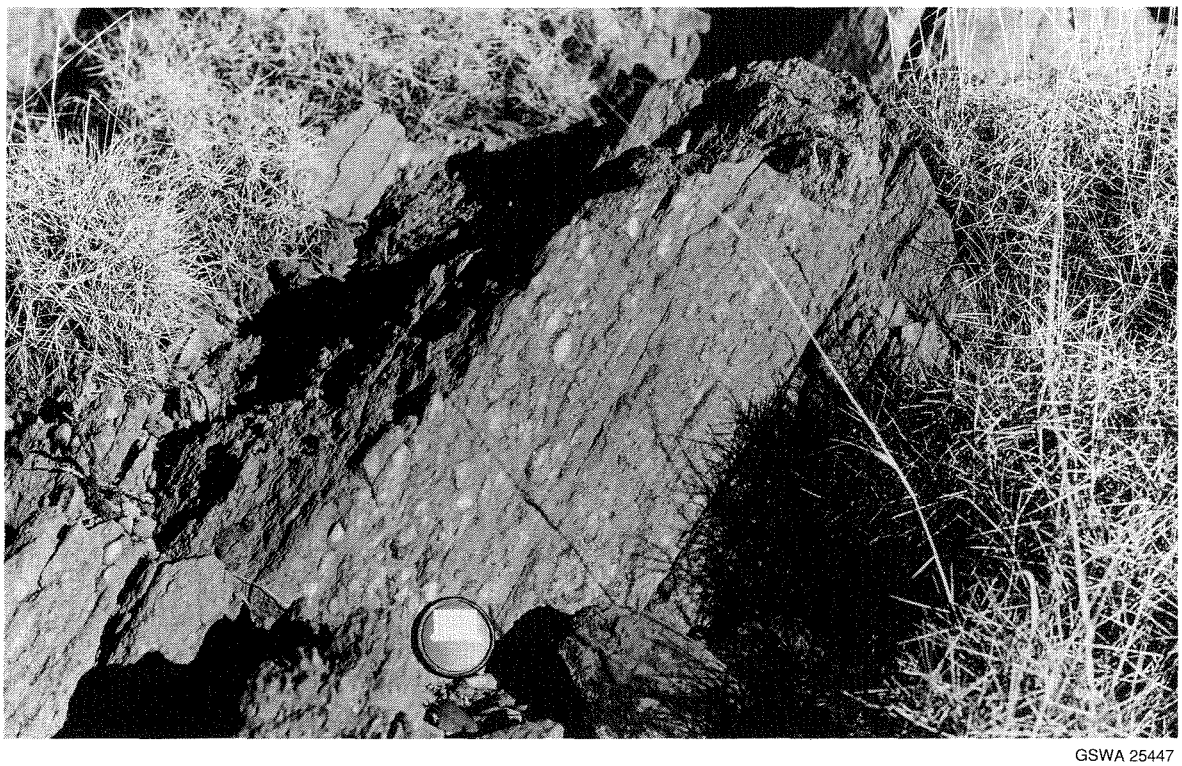

GSWA 25447

Figure 7. Foliated, matrix-supported fuchsitic metaconglomerate, north of Spearhole Yard.

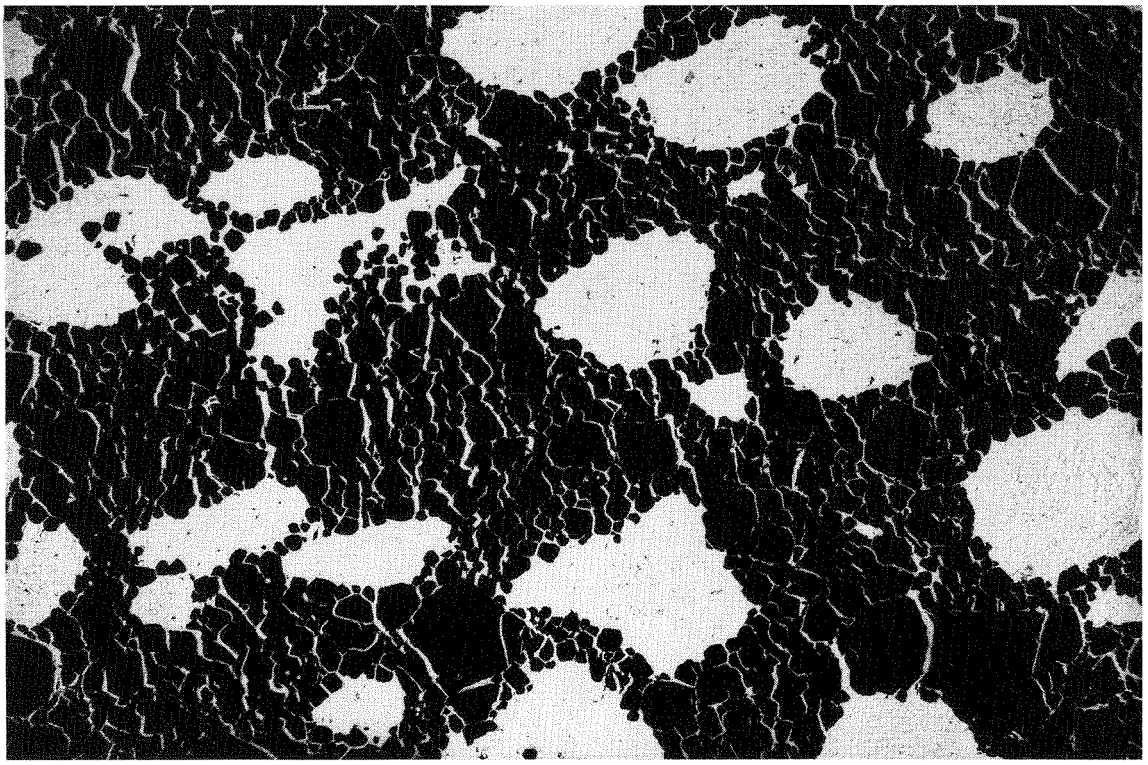

GSWA 25448

Figure 8. Olivine–chromite cumulate, Coobina ultramafic intrusion (x13). Olivine is pseudomorphed by serpentine. GSWA sample 81842.

greenstone belt. They contain medium-sized tremolite pseudomorphs—after pyroxene—in a finer matrix of chlorite and tremolite. The foliation, which is parallel to the main foliation in the belt, tends to wrap tremolite crystals, and in outcrop is seen to cut across contacts. More mafic examples contain up to 25% plagioclase. The rocks are thought to be dykes that were intruded into the greenstone succession prior to deformation.

Ultramafic intrusion at Coobina

The Coobina ultramafic intrusion, which crops out at the eastern end of the Jimblebar greenstone belt, is a 10 km long dyke-like body that ranges from 0.2–1.5 km wide. At its eastern end, a 300 m wide body of ultramafic rocks extends to the northern boundary of the Sylvania Inlier. Two shorter subsidiary bodies extend up to 4 km southwest from Murramunda. Chromitite pods and lenses occur extensively in serpentinite at the west end of the intrusion.

At Coobina, the ultramafic intrusion is conformable with the greenstone succession, and crops out against metaquartzite. A sill containing chromitite lenses is exposed at the same stratigraphic level 5.5 km further west. To the north of Coobina, metagabbro separates the serpentinite from the metaquartzite. Baxter (1978) reported the contact between the metagabbro and the serpentinite as "diffuse", and regarded the metagabbro as part of the main intrusion—indicating younging to the west. In this study, the contact is interpreted as a shear zone along which amphibole–talc–chlorite schist has developed. Anorthositic metagabbro was sheared against the serpentinite during later deformation and is not thought to be related to the ultramafic intrusion.

The western end of the ultramafic intrusion is largely massive, generally silicified serpentinite. It comprises fine-grained serpentine minerals and subordinate opaques (chromite and magnetite) and chlorite. The rock was originally a dunite; pseudomorphed olivine crystals up to 2 mm across show an adcumulate texture.

Interlayered with the serpentinite are numerous pods and lenses of chromitite. More than 200 have been identified; some reach 250 m in length and 6 m in width (Bye, 1975; Baxter, 1978). Layering may be preserved; and fine- to medium-grained chromitite, comprising 85% chromite and 15% chlorite may grade into a serpentine–chromite rock derived from sub-equal amounts of olivine and chromite. This rock shows well-preserved cumulate textures (Fig. 8).

In the eastern part of the ultramafic intrusion, rocks were more pyroxene-rich. Coarse-grained (about 1 cm) tremolite crystals—in a groundmass of serpentine and chlorite after fine-grained pyroxene pseudomorphing olivine—were noted.

Metagabbro is locally preserved adjacent to the ultramafic ridges, most notably 4.5 km northwest of Murramunda. It is not certain whether this is part of the intrusion or a remnant of the Jimblebar greenstone belt.

The ultramafic intrusion is extensively veined by late granitoid and pegmatite. However, in most cases, contacts against granitoid are either faulted or sheared, and marked by quartz veining and local development of cleavage. The general trend of layering, picked out by chromitite pods and lenses, is truncated by the granitoid contacts.

The ultramafic intrusion shows field relations that indicate both sill-like and dyke-like intrusion. Chromitite pods and lenses are preserved at the junction between the sill-like and the dyke-like parts; they are thought to represent relic primary layering that developed in a magma chamber feeding a major sill that intruded the greenstone belt. Much of the ultramafic intrusion has been obscured by later granitoid intrusion. The dyke-like part, then, represents a feeder system to the sill.

Patches of well-foliated, mafic-rich granitoid, which may represent the country rock into which the feeder dyke system was intruded, occur within a much more voluminous late granitoid. The ultramafic body was intruded as a dyke; when it reached the granitoid–greenstone boundary, the greenstone acted as a barrier to further upward intrusion, and the dyke spread to form a sill (Fig. 9). The intrusion is now a large, wall-like xenolith within the later granitoid, and its sheared contacts resulted from later deformation.

This interpretation is in agreement with that of Bye (1975); however, the layers have been dismembered by later deformation. The restriction of layering to one specific area, and the absence of mafic rocks at the top of the sill, seem to preclude the presence of a major stratiform body. The evidence suggests that the body has been derived from an ultramafic magma, rather than by differentiation *in situ* of a mafic magma.

On the basis of petrology, Bye (1975) concluded that there was no evidence for the intrusion having ophiolitic affinities as suggested by McCall (1971). Two, and probably three, events affected the body after it was intruded (*see* Structure section, this chapter). The intrusion crops out on the eastern limb of a major syncline that faces northwest. The sill-like part was folded with the greenstone belt, and its present orientation is the result of that folding. As the sill-like part, now steeply dipping, must have been initially horizontal, the current outcrop is a vertical section through the intrusion.

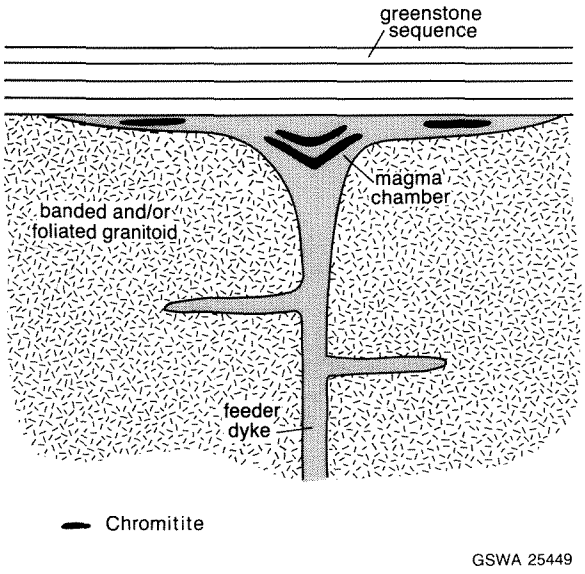

Figure 9. Diagrammatic cross-section showing interpreted original form of the Coobina ultramafic intrusion.

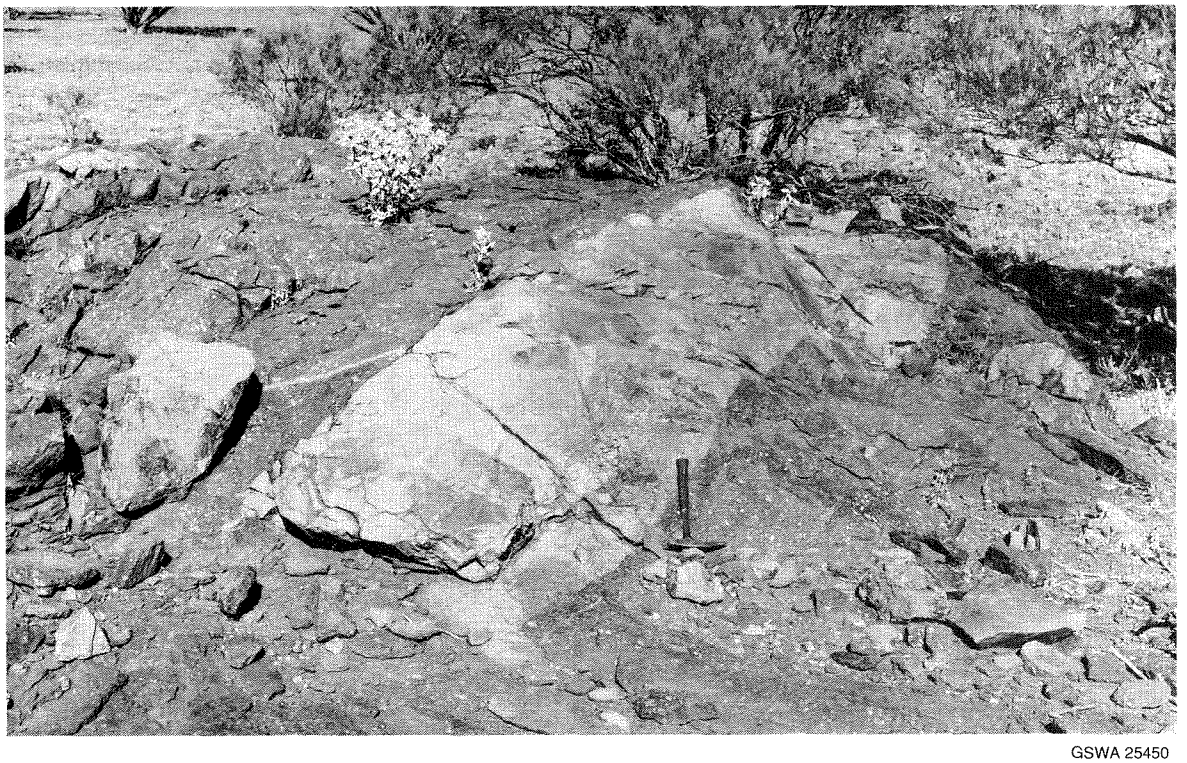

Figure 10. Undeformed dyke of granitoid rock intruded into medium- to coarse-grained melanocratic rock.

GSWA 25451

Figure 11. Leucocratic rock comprising feldspar megacrysts in medium-grained matrix.

Other mafic to ultramafic intrusive bodies

Gabbro at Western Creek

Fine- to coarse-grained metagabbro has intruded the Western Creek greenstone belt in the northwest part of the inlier. Many of the exposed contacts with granitoid are faulted; but there is also extensive veining of the gabbro by granitoid; and the veins are undeformed. The rock is typically massive, homogeneous, and has no obvious layering. It comprises actinolite, epidote, quartz, albite, and minor amounts of biotite and sphene. Some specimens contain grunerite. The present mineral assemblages formed during metamorphism; however, primary igneous texture can still be recognized. This was ophitic: poikilitic pyroxenes enclosed finer plagioclase laths. In some samples, elongate feldspar laths up to 5 mm long are present.

An unusual suite of mafic to felsic coarse-grained rocks crops out near the Western Creek crossing on the Newman to Prairie Downs road. The field relations of this suite are similar to the gabbro at Western Creek: they are undeformed and veined by granitoid (Fig. 10). On the western side of the creek crossing, a leucocratic rock (Fig. 11) containing numerous subhedral megacrysts of albite up to 3 cm long in a matrix of medium-grained albite, biotite and quartz (Fig. 12) is exposed. Accessory sphene, apatite, and allanite, together with carbonate and chlorite, are also present. On the eastern side of the crossing,the leucocratic rock can be seen to intrude a medium- to coarse-grained melanocratic unit that lacks the albite megacrysts but contains K-feldspar and magnetite. Intrusive contacts where leucocratic material penetrates melanocratic material and includes it as xenoliths are well exposed (Fig. 13). A distinctive, lobate intrusive contact suggests that the earlier melanocratic rock may have been only partly solidified when the leucocratic rock was intruded. Poorly developed primary igneous layering is locally present.

Many of the textures seen in hand specimen suggest a cumulate origin for the leucocratic rock. The contacts between megacrystic and non-megacrystic rocks are clearly intrusive rather than having been controlled by secondary metasomatic alteration. Feldspar:quartz ratios define quartz dioritic to monzodioritic, rather than gabbroic compositions. The occurrence of a distinctive green biotite rather than amphibole in these rocks suggests a high K:Al ratio, which is not typical of an igneous chemistry. This is borne out by the widespread occurrence of carbonate. The evidence suggests hydrothermal alteration of an originally gabbroic rock. However, the rocks show little evidence of low-grade hydrothermal alteration; and fresh feldspar and biotite are probably the result of later metamorphism that has homogenized and recrystallized the mineral assemblage. This effect has tended to mask the earlier alteration. The later granitoid may have provided the source of alteration.

Sylvania–Woggaginna Hill

Between Sylvania and Woggaginna Hill, medium- to coarse-grained, foliated or banded amphibolite is present. It has been intruded by granitoid and extensively disrupted by later shearing. Associated with the amphibolite are ultramafic rocks that are typically tremolite–chlorite(–talc) schist. Serpentinite may occur as remnant pods within these

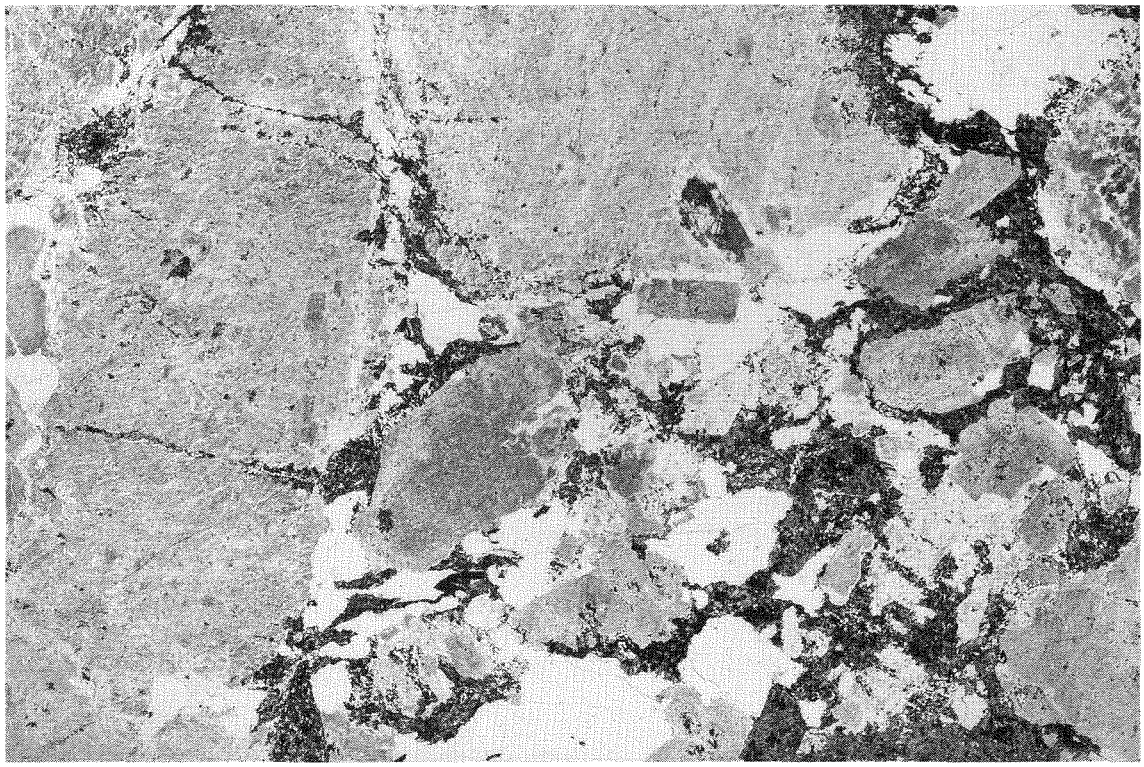

GSWA 25452

Figure 12. Leucocratic rock seen in Figure 11. Albite megacrysts in a medium-grained matrix of albite, biotite and quartz (x6). GSWA sample 84557.

GSWA 25453

Figure 13. Leucocratic rock veining medium-grained melanocratic rock.

schistose units. Metapyroxenite is also present. The amphibolite consists of bluish-green to green hornblende, plagioclase (oligoclase–andesine), epidote, clinozoisite, quartz, and biotite. Opaques are ilmenite and/or magnetite; sphene and apatite occur as accessory minerals. Some sericitization of plagioclase has occurred.

The rocks typically show extensive recrystallization and limited preservation of primary textures. However, cumulus textures have been recognized and are consistent with an intrusive gabbro. Primary igneous layering may also be recognized on a small scale. This can be distinguished from quartzofeldspathic segregation veins, 2–3 cm thick, which run parallel to the foliation. Leucocratic units representing primary layering tend to grade into adjacent melanocratic rock, whereas segregation veins have sharp, well-defined margins. Larger scale layering, whose ultramafic units grade into amphibolite, can be recognized in several exposures.

Anorthosite crops out 6 km south-southeast of Sylvania; it contains labradoritic plagioclase, bluish-green hornblende, clinozoisite, quartz, chlorite, and sphene. Recrystallization during deformation produced a protomylonitic texture: porphyroclasts of plagioclase are wrapped by anastomosing layers of plagioclase, hornblende and clinozoisite.

A fine- to medium-grained, weakly-foliated calc-silicate rock comprising quartz, plagioclase (may be very calcic, ranging up to bytownite composition), hornblende, epidote, garnet, and small amounts of opaques, apatite, and allanite, is exposed 2 km north-northwest of Woggaginna Hill (Fig. 14). Garnet and hornblende are porphyroblastic. This is interpreted as a metamorphosed granophyric top to a layered unit.

The proximity of amphibolite (after gabbro) to ultramafic schist, serpentinite, and anorthosite and calc-silicate rocks, is consistent with derivation from one or more, now deformed and metamorphosed, layered intrusions. The intrusions may be equivalent to the gabbro at Western Creek in the western part of the inlier.

Minor outcrops

Metapyroxenite, chlorite–tremolite schist, and amphibolite, occur in granitoid 9 km north-northeast of Mundiwindi. The amphibolite and chlorite–tremolite schist tend to be well foliated, but metapyroxenite is generally massive. All are veined by granitoid.

The metapyroxenite is composed of tremolite–actinolite and minor amounts of clinopyroxene. Large sub-rectangular grains of tremolite up to 1 cm long (pseudomorphs of pyroxene) are set in a matrix of finer, moderately well-foliated tremolite. This aligned fabric wraps the megacrysts to give an augen texture.

Metagabbro, veined by granitoid and pegmatite, crops out south of Shovelanna Hill, 3.5 km east of Noddy Bore. It is a medium- to coarse-grained rock with a well-preserved primary cumulate texture and shows little evidence of deformation. Pyroxene laths have been pseudomorphed by actinolite, and highly mottled plagioclase is now principally albite.

Granitoid rocks

Introduction

Granitoid rocks make up most of the inlier. Three main types are recognized. The oldest is scarce, well-foliated, and/or banded. The second type, referred to as the "main granitoid", is the most widespread; it varies considerably in composition (syenogranite to granodiorite), grain size, and in the content of K-feldspar or plagioclase megacrysts. The main granitoid intrudes both the foliated and/or banded granitoid (Fig. 15) and the greenstone belts. The greenstone belts form "mega-xenoliths" within the main granitoid. The third granitoid, which intrudes the greenstones, has alkaline affinities, indicated by the occurrence of alkali amphibole and pyroxene. When naming a granitoid rock where the metamorphic assemblage albite–epidote is present, albite is included as plagioclase, rather than alkali feldspar.

Foliated and/or banded granitoid

Foliated and/or banded granitoid is most extensively developed in the western part of the inlier south and east of a line running from just west of Round Hill Bore to just west

GSWA 25454

Figure 14. Calc-silicate rock comprising quartz, plagioclase, hornblende, epidote, and garnet (x37). GSWA sample 81840.

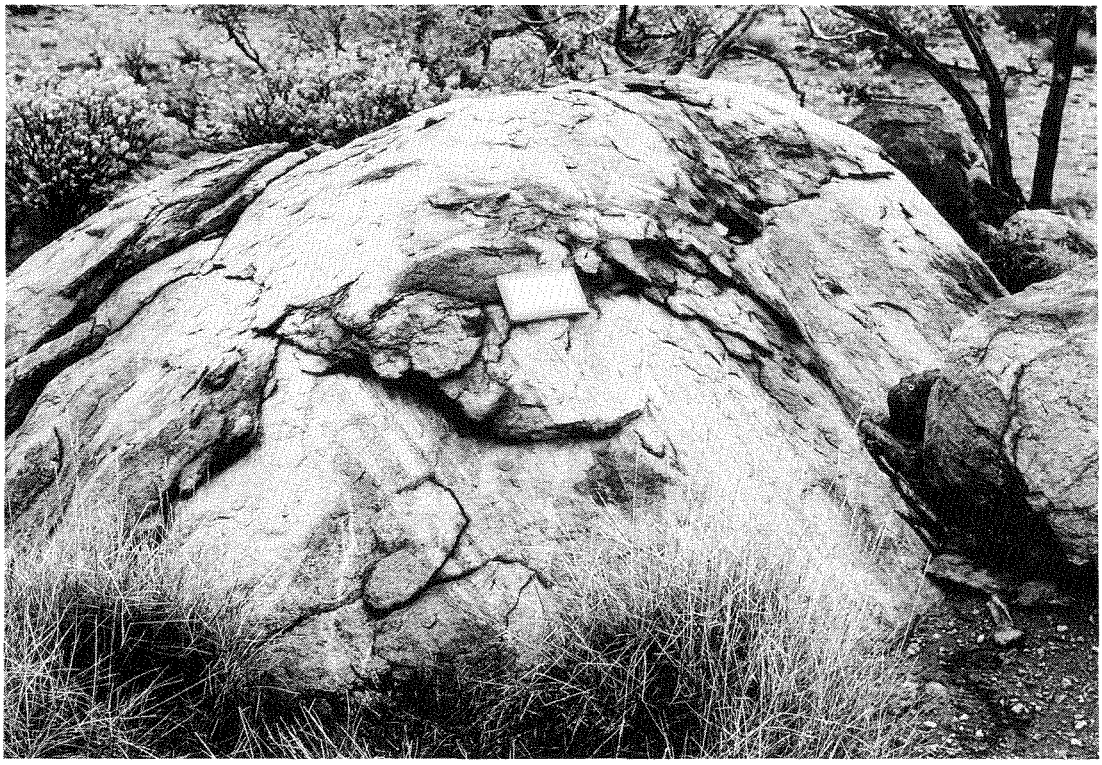

GSWA 25455

Figure 15. Foliated and/or banded granitoid intruded by the undeformed main granitoid.

of Jillary Well (Plate 2). Other small patches occur throughout the main granitoid outcrop, most notably 4 km southwest of Bubbacurry Well (Plate 2). Xenoliths have also been recognized between Coobina and Murramunda near the southern margin of the Coobina ultramafic intrusion. These are probably best seen on the eastern side of a granitoid tor 5 km southwest of Murramunda. The relationship between the foliated and/or banded granitoid and the greenstone belts has not been seen.

The foliated and/or banded granitoid is typically monzogranitic. The rock varies considerably in grain size from a coarse-grained, well-foliated to banded rock to a fine- to medium-grained rock which may be schistose. The coarser varieties are more leucocratic. Associated pegmatites are generally orientated sub-parallel to the foliation (Fig. 16). Pegmatites may show "pinch and swell" structures and both the pegmatites and the foliation may be folded. In areas of lower strain the pegmatites can be seen to cross-cut banding.

The rocks have been thoroughly recrystallized during deformation and metamorphism. In the Round Hill Bore - Jillary Well area, the general assemblage is greenish-brown biotite, epidote, albite, microcline (usually perthitic), muscovite, quartz, and minor amounts of sphene, apatite, fluorite and opaques. There has been some alteration of biotite to chlorite and of feldspar to sericite. The foliation is defined by strings of randomly orientated biotite flakes and rounded epidote grains, usually 0.2 to 0.3 mm across. The foliation tends to wrap around the larger feldspar crystals.

The feldspars show a range of sizes, reaching 5 mm in length, and occur both as megacrysts and as groundmass crystals. They are typically unzoned; and albite is characteristically sieved by fine, disorientated grains of epidote and muscovite. Sphene is widespread and ilmenite is associated with it. Mafic clots (2–3 mm diameter) of randomly orientated, fine-grained biotite, epidote, and subordinate sphene, are abundant. They apparently replace an earlier, coarser grained mafic mineral, probably biotite. Fine quartz grains, 0.2 to 0.3 mm across, occur in patches 1 to 2 mm across, pseudomorphing earlier, coarser grained quartz crystals that were wrapped by the foliation.

In the eastern part of the inlier, compositions are similar, but assemblages differ in that the plagioclase is oligoclase. As a result, plagioclase does not show the fine sieving of epidote and muscovite that is so characteristic of albite grains in the western part of the inlier. It may, however, be riddled with fine, rounded blebs of quartz. Epidote is restricted to rounded grains associated with biotite.

As will be discussed in Chapter 4, the eastern part of the inlier was extensively reworked during the Capricorn Orogeny. A foliation (S_c) associated with deformation and metamorphism is well developed. The distribution of mafic and quartzofeldspathic minerals in the foliated and/or banded granitoid probably reflects earlier, Archaean deformation and metamorphism. S_c is defined by biotite flakes, strings of fine-grained quartz and feldspar, and by orientated quartz crystals. It envelopes sub-rounded megacrysts of feldspar that can reach 6 mm in length.

Main granitoid

Two distinct phases of the main granitoid are seen: medium-grained syenogranite to monzogranite occurs as widespread dykes, veins, and patches, in a medium- to coarse-grained, locally sparsely porphyritic, monzogranite to granodiorite. A widespread pegmatite phase is also present as veins and dykes. As with the early foliated and/or banded granitoid, the main granitoid is recrystallized. Megacrysts, where present, are either microcline or plagioclase and reach 2 cm in length. Megacrysts rarely exceed 15% of the rock. Contacts between even-grained and sparsely porphyritic granitoids are gradational.

In the western part of the inlier, the assemblage of the syenogranite to monzogranite phase is quartz, microcline (perthite), albite, muscovite (locally phengitic), and minor amounts of biotite, epidote, sphene, garnet (rare), apatite, zircon, and opaques (ilmenite or magnetite). Biotite may have been altered to chlorite and feldspar to sericite.

The monzogranite to granodiorite phase in the western part of the inlier has a similar assemblage to that of the foliated and/or banded granodiorite. It comprises greenish-brown biotite, epidote, albite, microcline (usually perthitic), muscovite, quartz, and minor sphene, apatite, allanite, fluorite, carbonate, and opaques. Some biotite and feldspar have been altered to chlorite and sericite; prehnite and pumpellyite may occur. Again, albite contains fine-grained inclusions of epidote and muscovite. Sphene typically rims opaque minerals that are up to 5 mm in length. The rock is not foliated, but some fracturing of twin lamellae in plagioclase and internl subgraining of quartz may be present. Groundmass crystals of biotite and epidote are generally of the order of 0.3 mm across. Rounded aggregates of fine quartz up to 3 mm across pseudomorph earlier, coarse-grained, magmatic crystals. Feldspar crystals are generally around 2–5 mm, but megacrysts can range up to 2 cm.

In the eastern part of the inlier, assemblages are generally similar to those in the west except for the widespread occurrence of more calcic plagioclase. These rocks were reworked during the Capricorn Orogeny, and extensive recrystallization has taken place. The S_c foliation is defined by orientated sheet silicates, elongate quartz crystals, and strings of fine quartz and feldspar. The foliation envelopes feldspar megacrysts that may have been recrystallized to aggregates of fine-grained crystals. K-feldspar may be replaced by myrmekite. Limited zoning may be present in plagioclase: oligoclase cores grade into albite rims. Some crystals show relic, possibly magmatic, euhedral cores. Concentric structures in these grains may represent primary oscillatory zoning, but are now picked out by sericitic alteration. In many samples, typically unsieved oligoclase—with discrete albitic patches and rims containing inclusions of epidote and muscovite—has developed and appears to represent a later retrograde metamorphism. In some of the more strongly foliated specimens, chlorite forms part of the mineral assemblage.

Hornblende-bearing granitoid

Hornblende-bearing granitoid is restricted to three outcrops in the eastern part of the inlier. Two, which are no more than 3 km across, occur 6 km and 15 km southeast of Sylvania; the third a smaller one, occurs 8 km southeast of

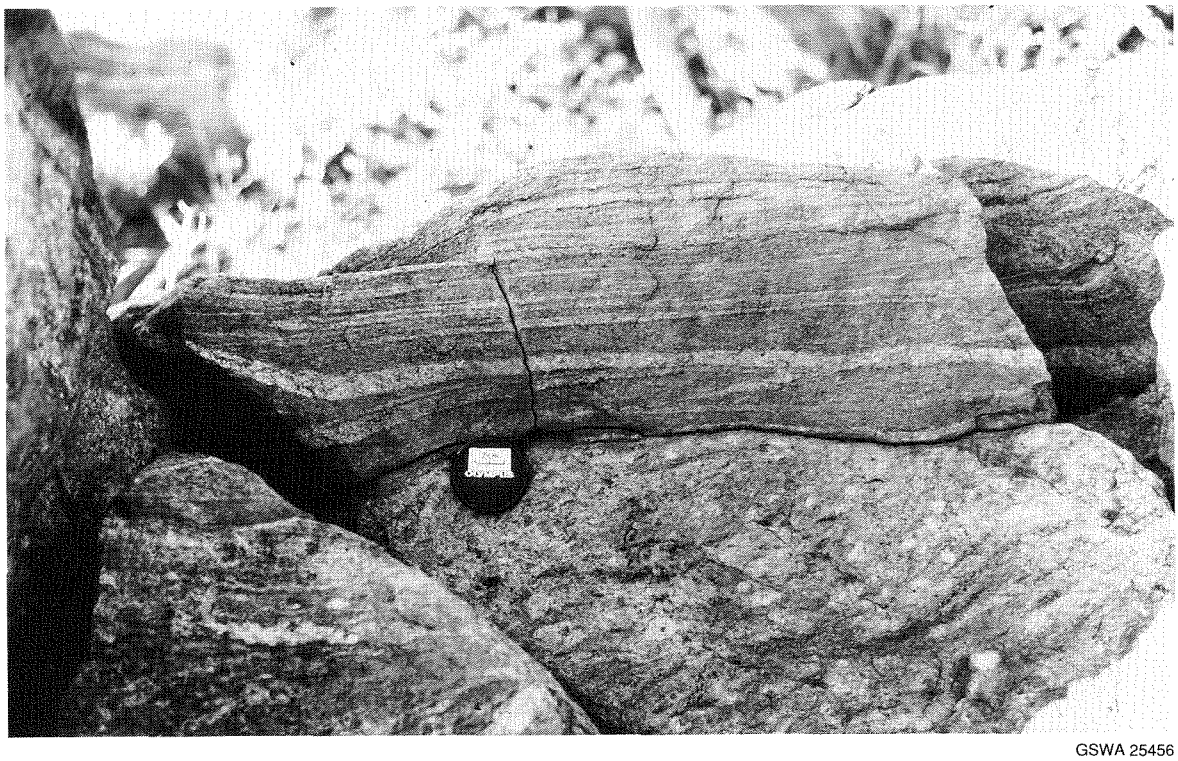

GSWA 25456

Figure 16. Foliated and/or banded granitoid containing a foliated pegmatite phase.

Garden Well. Other small patches occur locally. The rock is seen to intrude both the main granitoid and the Woggaginna Hill greenstone belt. The contact with the greenstone belt is well exposed 6 km south-southeast of Sylvania.

The unit is a medium- to coarse-grained syenogranite to monzogranite which contains numerous mafic clots up to 3 cm in diameter (Fig. 17). The typical mineral assemblage is quartz, microcline (perthite), oligoclase, hornblende, epidote, myrmekite, sphene, apatite, allanite, zircon, carbonate, and biotite. Weakly zoned plagioclase may show later sericitic alteration. Feldspar crystals range up to 1 cm across. There is evidence of partial recrystallization of the coarse-grained texture: trails of fine crystals occurring along grain boundaries, and extensive alteration of K–feldspar to myrmekite. Hornblende, 7–8 mm long and pleochroic from yellow-green through green to blue-green, indicates a relatively high sodium content. Some crystals show optical zoning: green rims surround lighter cores. Rounded aggregates of quartz crystals 3–5 mm across pseudomorph earlier, possibly magmatic, quartz crystals.

South of Sylvania, the rock is thoroughly recrystallized and the S_c foliation is developed. The quartzofeldspathic portion forms a fine- to medium-grained matrix of interlocking lobate to amoeboid grains around distinct clots and patches of mafic material 7–8 mm in diameter. The general assemblage is similar to that described above but with the addition of clinopyroxene. The clinopyroxene is up to 5 mm long; it is pleochroic from pale green to yellow-green, suggesting sodic augite. In some samples it may be rimmed by hornblende (intergrown with epidote and sphene) in a well-developed replacement texture (Fig. 18).

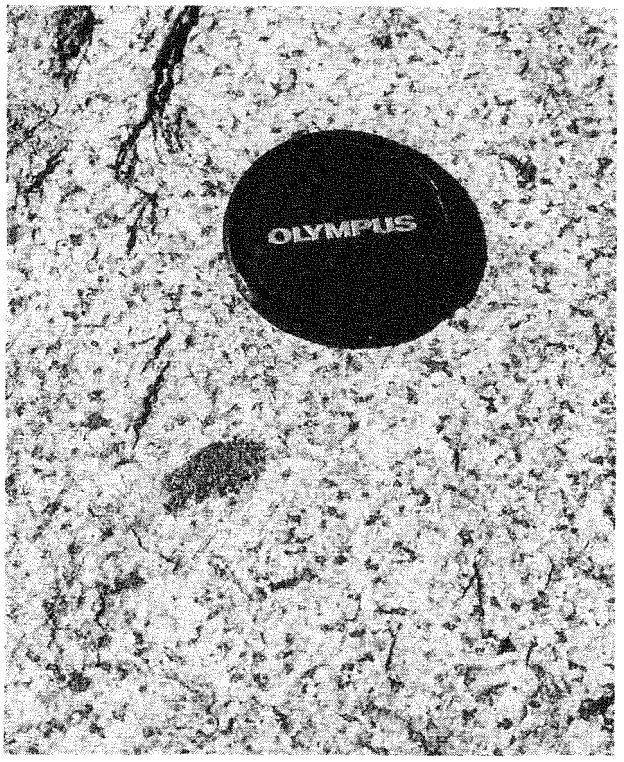

GSWA 25457

Figure 17. Mafic clot in hornblende-bearing granitoid.

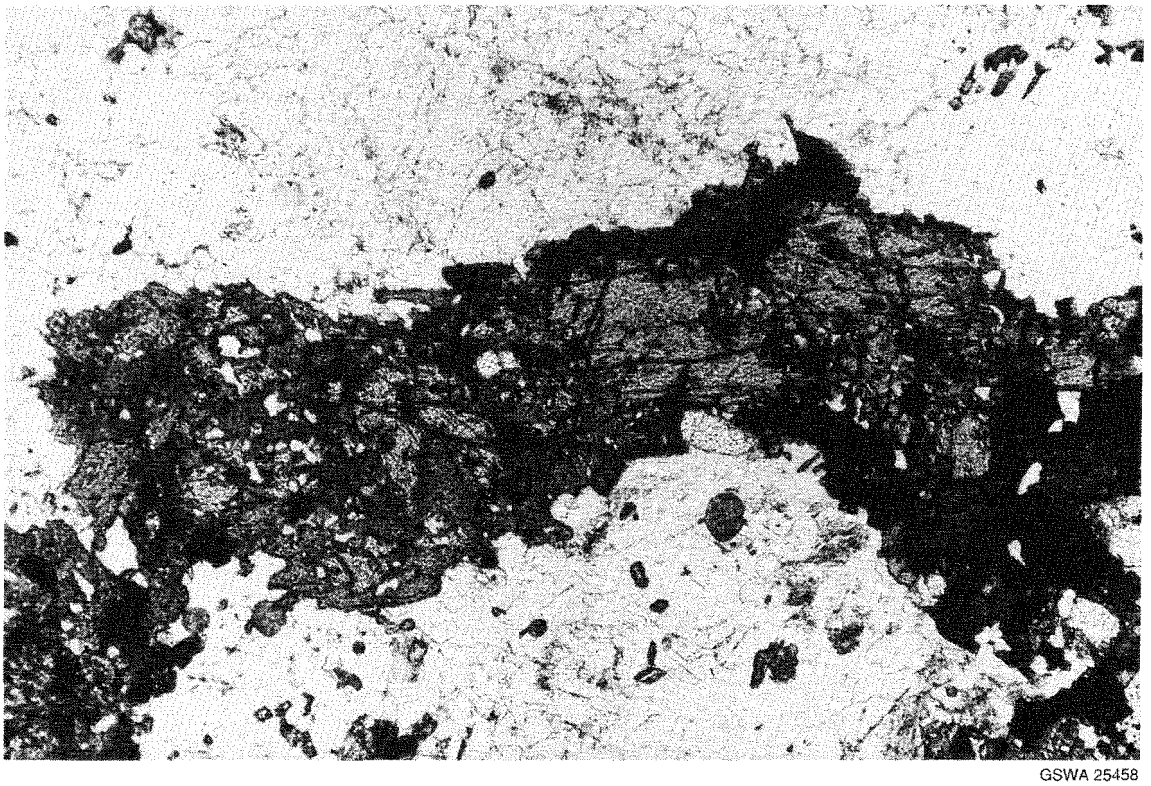

GSWA 25458

Figure 18. Sodic augite rimmed by hornblende, in a matrix of quartz–microcline–oligoclase–epidote–sphene. Hornblende–bearing granitoid (x35), GSWA sample 81835.

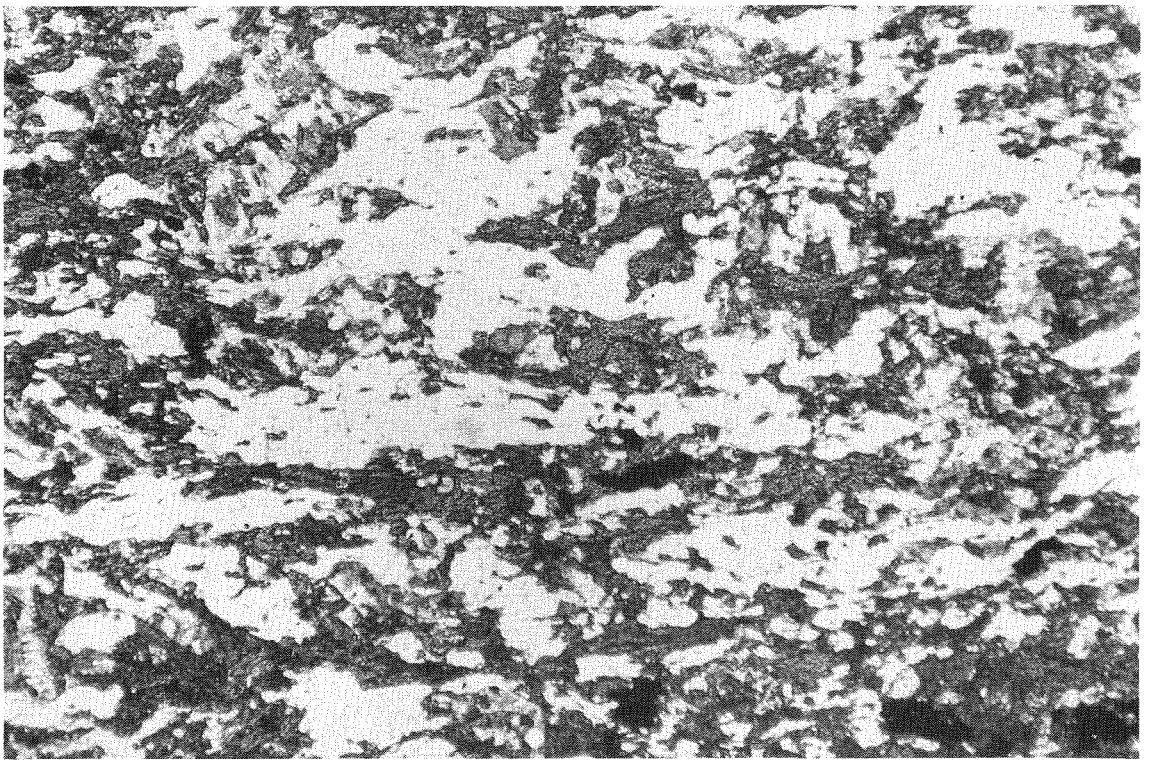

GSWA 25459

Figure 19. Hybrid rock comprising quartz–blue-green amphibole–albite (x30). GSWA sample 73360.

GSWA 25460

Figure 20. Isoclinal D_{1g} fold in banded chert.

Hybrid rock

An unusual rock of intermediate composition crops out along the northern and western margin of the Jimblebar greenstone belt. It is usually weakly foliated, and varies from fine- to medium-grained. The rock consists of 60% quartz (ovoid to elongate in shape and highly strained), 30% blue-green amphibole, 5% albite laths, and minor amounts of apatite (typically very coarse crystals up to 3.5 mm long), opaque minerals, and zircon (Fig. 19). Amphibole, as fine-grained, felted, moderately well-orientated laths, forms large, irregular aggregates, possibly pseudomorphing a former mafic mineral, scattered through the rock. Also present are a number of patches of fine-grained granoblastic quartz-rich material.

The origin of this rock is uncertain. It is associated with veins and patches of an altered granitoid. Intermediate material grades into the granitoid, possible igneous contacts occur, and mafic xenoliths and textures indicate the assimilation of mafic material by granitoid. The granitoid itself is very fine to medium grained, strongly recrystallized, and partly mylonitized. Mafic minerals, biotite (partly chloritized), garnet, and epidote, make up some 2–4% of the rock.

At the northern end of the greenstone belt, a metagabbro crops out at this horizon (Plate 1); and it seems as if the medium-grained intermediate rock developed from the assimilation of this unit by a granitic magma, probably the main granitoid.

GSWA 25461

Figure 21. M-type D_{2g} fold in banded iron-formation.

Structure

Introduction

The structural development of the granite–greenstone rocks in the inlier is complex; two quite distinct periods of tectonism, each resulting in more than one phase of deformation, can be recognized. The first is Archaean and has affected only greenstone belts and the foliated and/or banded granitoid. The second post-dates the main granitoid and the intrusion of Suite 1 and Suite 2 mafic dykes; it represents deformation during the early Proterozoic Capricorn Orogeny. This will be dealt with in Chapter 4.

Three periods of deformation (D_{1g}, D_{2g}, and D_{3g}) have been recognized as having occurred during the first, Archaean tectonic period. These are seen to have affected most greenstone outcrops, and are best developed in the Jimblebar greenstone belt.

First deformation phase

The earliest phase of deformation (D_{1g}) is inferred from the presence of a widespread, generally pervasive, layer–parallel foliation (S_{1g}) in greenstone belts. This may reflect isoclinal folding and/or thrusting as suggested by Myers and Watkins (1986) for rocks in the Murchison Province of the Yilgarn Craton. Alternatively, it may be the result of large-scale extensional detachment faulting and shearing; Wernicke (1981) and Lister et al. (1986) have discussed crustal extension models. Rare small-scale isoclinal folds are present (Fig. 20); however, major fold structures have not been identified.

Second deformation phase

The second phase of deformation (D_{2g}) is well developed; large-scale close-to-tight fold structures are recognized. Extensive small-scale folding is present in banded iron-formation and banded chert (Fig. 21). Axial-plane cleavage is not well developed, and is typically restricted to small-scale fold hinges.

An anticline forms the western part of the Jimblebar greenstone belt; a syncline, the eastern part (Plate 1). The anticline is seen to close 3 km north of the Jimblebar battery. The two structures are separated by a north-trending fault zone which passes through the site of the old battery and which will be referred to as the Battery Fault. The fold

GSWA 25462

Figure 22. D_{3g} crenulations in ultramafic schist.

structures are inclined and generally overturned. They face to the northwest and their axial surfaces dip south and east. Plunges vary because of refolding, but are essentially north and east. Much of the western part of the belt, which forms the northwestern limb of the anticline, is inverted.

The closure of the eastern syncline, which previously lay to the west of the present greenstone outcrop, has been obliterated by intrusion of the main granitoid. M-type folds (Fig. 21) in a large xenolith of banded iron-formation in granitoid to the west of Garden Well are probably related to the hinge zone.

The Battery Fault is marked by a zone of high strain, where strong local foliation has developed. The fault is subparallel to the axial planes of the D_{2g} folds and probably represents a limb failure or thrust developed during D_{2g}.

A large-scale, west-plunging, tight to isoclinal synformal fold closure is present 5 km northwest of Spearhole Yard (Plate 3). A southeast-plunging synclinal fold closure occurs in metasedimentary rocks to the east of Western Creek.

Third deformation phase

The third deformation is evidenced by a set of upright, open to close, steeply plunging folds. These may be conjugate in form and have box-type profiles. The present outcrop pattern of the Jimblebar greenstone belt is formed by the interference of southeast-plunging D_{3g} structures with large-scale D_{2g} folds. As small-scale D_{3g} fold hinges in the western end of the greenstone belt have a dominantly southwest plunge, this pattern may be the remnant eastern half of a conjugate structure. The D_{2g} fold northwest of Spearhole Yard has been refolded by an open, steeply southwesterly plunging D_{3g} fold.

In schistose rocks, small-scale structures take the form of crenulation and kink banding of the D_{1g} foliation (Fig. 22). An associated crenulation cleavage (S_{3g}) may develop. In more massive rocks, particularly banded iron-formation and chert, a spaced, disjunctive cleavage is present (Fig. 23).

Structures in the ultramafic intrusion at Coobina

A foliation is only weakly developed in the ultramafic intrusion at Coobina. Zones of high strain are present: chromitite pods typically have strongly sheared margins against serpentinite, and may show slickensiding. Bye (1975) thought that the pods and lenses defined elongate zones up to 35 m wide and that they were folded about northeasterly trending axes. This probably corresponds to D_{2g} folding in the greenstone belt. The high strain associated with the chromitite pods and lenses is consistent with initially continuous layers within the body having been pulled apart during deformation. Boudinage took place parallel to layering. Pull-apart textures have developed in the smaller lenses (Bye, 1975). Boudinage apparently predates D_{2g} folding. The layering also defines later, open, southeast-plunging folds, which correspond to D_{3g}.

GSWA 25463

Figure 23. Spaced S_{3g} cleavage axial planar to an open D_{3g} fold in banded iron-formation.

Structures in the foliated and/or banded granitoid

Foliated and/or banded granitoid was not seen in contact with greenstone belts; and, as a result, the correlation of fold structures is uncertain. Folding of banding is generally tight and is also seen to affect pegmatite veins. It is probable that establishment of the banding corresponds to D_{1g} while the later folds of banding correspond to D_{2g}.

Discussion

The structural development of granite–greenstone in the Western Australian Shield has generally been interpreted in terms of solid-state diapiric emplacement of granitoid batholiths into an initially flat-lying sequence of greenstone (Gee, 1979; Gee et al., 1981; Hickman, 1984). The pattern of the greenstone belt outcrop, then, results from the preservation of downwarped synclinal keels between the granitoid batholiths.

An alternative explanation for this pattern in part of the northwest Yilgarn Craton has been presented by Myers and Watkins (1986). In their study, the dome-and-basin pattern was shown to have developed as a result of interaction between two upright fold phases intersecting at right angles. Similar interpretations, as described by Snowden (1984), and Dimroth et al. (1983), have been presented for granite –greenstone patterns elsewhere in the world.

In the northern Pilbara, the area in Western Australia to which the diapiric model has been most comprehensively applied, Hickman (1975, 1983) described a structural sequence in which the earliest structures (D_1) only occurred as folds within greenstone xenoliths in the batholiths. The greenstone that forms these xenoliths may be older than the main greenstone, which forms the Pilbara Supergroup, where these early structures have not been seen. D_1 structures also included gneissic banding in granitoid.

A "regional foliation" (S_2), parallel to granitoid–greenstone contacts, was identified, and was seen to be most strongly developed at the contacts themselves. D_2 deformation was regarded as synchronous with diapiric emplacement. It was noted, however, that although the foliation was D_2 in age, it was not axial planar to the main synclines, but was essentially parallel to bedding. Major D_2 age faults and slides were present. The third deformation (D_3) typically formed large- to small-scale brittle kinks and conjugate folds. The D_4 event is represented by locally developed recumbent folds.

Bickle et al. (1980, 1985) identified pre-D_2 structures in greenstone belt rocks marginal to the Shaw Batholith (i.e. Pilbara Supergroup), and interpreted these as having resulted from a major recumbent fold structure produced by overthrusting prior to doming. Crustal thickening because of overthrusting produced the instability necessary to trigger diapiric emplacement of the batholiths. Hickman (1984) regarded emplacement of the different domes as taking place at different times and interpreted these pre-D_2 structures as being related to an early diapir located to the west of the Shaw Batholith.

The shape of the greenstone belts in the Sylvania Inlier is the result of the refolding of tight D_{2g} folds with moderately inclined to sub-horizontal fold axes and steeply inclined axial surfaces, about moderately to steeply plunging, open D_{3g} folds with upright axial surfaces. This has produced "hooked" type 3 refold structures as described by Ramsay and Huber (1987). The structural sequence for the Sylvania Inlier (Fig. 24) appears consistent with that for the northern Pilbara granite–greenstone described by Bickle et al., (1980, 1985). The layer-parallel D_{1g} foliation is folded by D_{2g}, and provides evidence for a set of early, flat-lying fold structures. The current exposure level is such that both the early banded and/or foliated granitoid, and the greenstone belts, form xenoliths within the main granitoid. It is not, therefore, possible to establish whether D_{2g} folds were produced by the diapiric emplacement of a granitoid batholith now obscured by intrusion of the later granitoid.

Metamorphism

Metamorphism of the greenstone belts in the Sylvania Inlier, an event here designated M_g, took place under greenschist-facies conditions. Peak metamorphism was synchronous with the D_{1g} fold event and the formation of the S_{1g} foliation.

In mafic rocks, mineral assemblages are typically actinolite–chlorite–albite–epidote–biotite–quartz. In pelitic metasedimentary rocks, assemblages are quartz–chlorite–muscovite, or quartz–muscovite–biotite, and are indicative of at least biotite-zone conditions. Higher grade (albite–epidote amphibolite facies) assemblages may be seen in some greenstone belts, but can be related either to later Hamersley Basin burial metamorphism (M_h) or Capricorn Orogeny metamorphism (M_c).

The mineral assemblages seen in the foliated and/or banded granitoid are also consistent with recrystallization under middle to upper greenschist-facies conditions.

Post-granitoid mafic dykes

Introduction

The Sylvania Inlier has been extensively intruded by several suites of mafic dykes that post-date the main granitoid. These display a variety of orientations and fall into two distinct petrographic groups: one shows metamorphism under conditions equivalent to the upper greenschist–lower amphibolite transition; the other, only very low-grade alteration.

This section will deal only with the first group, those which were intruded before the Capricorn Orogeny. It is dominated by a suite of north-northeasterly trending dykes (Suite 1). These are best developed in the western part of the inlier, where they show little evidence of deformation. In the east, they are cut by numerous shear zones and have been rotated by deformation to a more east-northeasterly orientation. Less abundant east-trending dykes constitute the second suite of the group (Suite 2). A large ultramafic dyke-like body, the southern ultramafic intrusion, forms part of this suite.

Suite 1

Suite 1 dykes post-date both the greenstone belts and the granitoids, but are not seen to intrude the overlying Fortescue Group. They are presumed to pre-date the unconformity in this part of the Hamersley Basin. Based on their

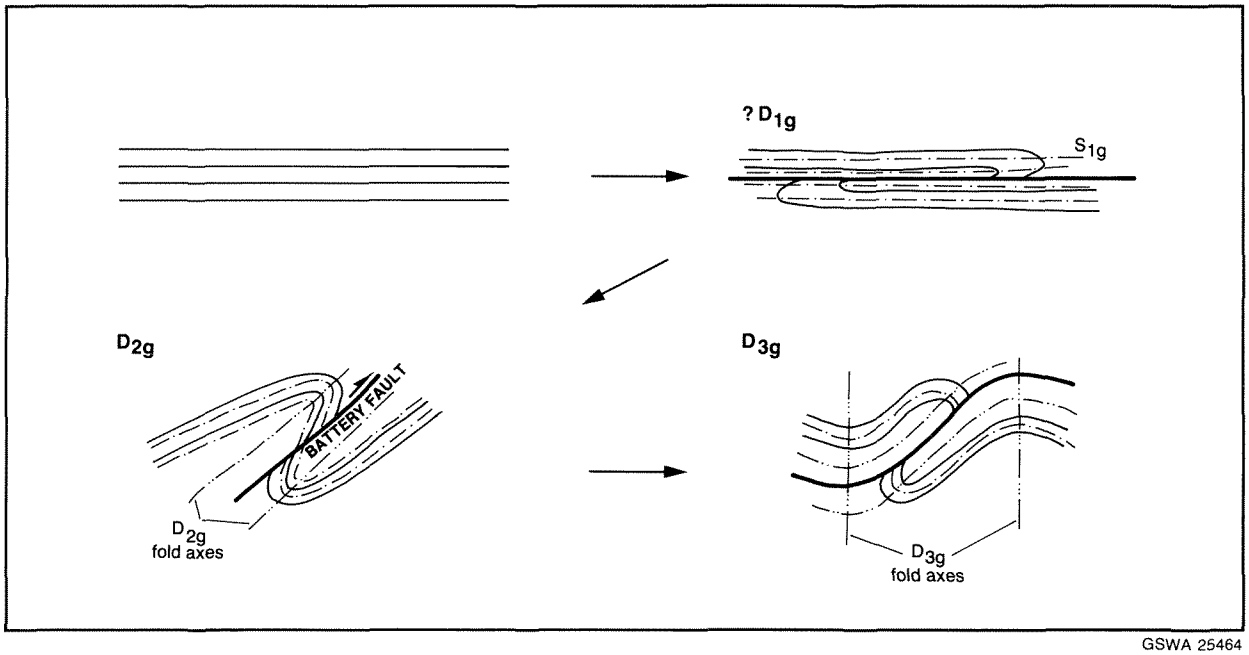

GSWA 25464

Figure 24. Sequence of deformation events in the Jimblebar greenstone belt.

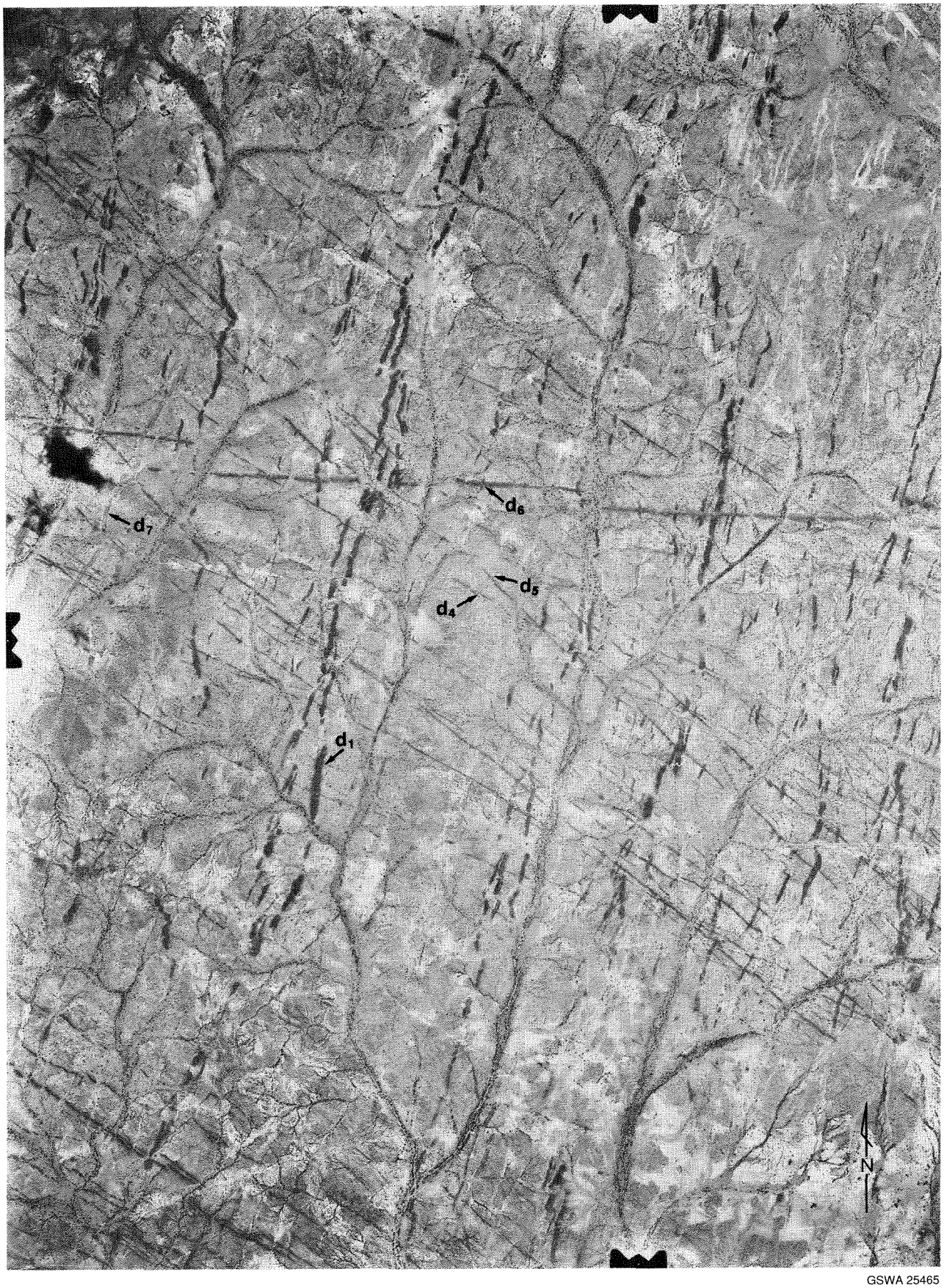

GSWA 25465

Figure 25. 1:40 000 scale aerial photograph of part of the Sylvania Inlier. Five phases of mafic dyke intrusion may be identified: d_1 — north-northeast (Suite 1); d_4 — west-northwest (Suite 4); d_5 — northwest (Suite 5); d_6 — east-west (Suite 6); d_7 — north-northeast (Suite 7, note double intrusion). (WA 1423 NEWMAN Run 12 - 5107; reproduced by courtesy of the Department of Land Administration, Perth).

field relations and their orientation, they are correlated with the Black Range dyke suite, which was identified in the northern Pilbara and which has been described by Hickman and Lipple (1975).

In the western part of inlier, individual dykes range from a few, to more than two hundred, metres wide. Typically they are complex in form, tending to branch and rejoin, and enclose sheets of country rock. Several dykes may coalesce to produce continuous outcrop over several hundred metres, and later dykes in the suite cut across earlier formed ones.

Some of the larger dykes show a distinctive pattern of intrusion: individual sections are arranged *en echelon* and offset by as much as 100 m. A distinctive form to the dyke terminations can be seen in aerial photographs (Fig. 25). The intrusion is presumed to be continuous at depth. Similar features have been recorded from dyke swarms elsewhere in the world (Harker, 1904; Watterson, 1968).

The area of most intense intrusion occurs north of the main Prairie Downs road, in the vicinity of Round Hill Bore. Here dykes occur at the rate of approximately 2 per kilometre. A section measured normal to the trend of the dykes in this area indicates a local extension of 14% has occurred during emplacement of the dykes.

In the eastern part of the inlier, the dykes are deformed. As well as having been rotated, they may locally have been folded. Foliations are best developed at the margins: the cores of larger intrusions may show little or no deformation.

The dykes are typically medium to coarse grained, and primary igneous features and textures have been preserved. Their mineral assemblages were mostly produced during metamorphism and deformation, and they now vary from metadolerite to amphibolite according to grade variations within the inlier. The dominant mineralogy is amphibole–plagioclase–quartz–sphene–apatite–iron oxides (–epidote–biotite). Variations in grade are reflected in the compositions of amphibole and plagioclase, and in the presence or absence of epidote. Amphibole is typically well recrystallized; and in undeformed examples, forms pseudomorphs after pyroxene. It ranges from grassy-green actinolite through blue-green transitional types to olive-green hornblende. The transitional actinolite–hornblende varieties are by far the most abundant. Variations in plagioclase composition are more complex and range from albite through oligoclase–andesine to labradorite. Labradorite occurs as relic laths that show extensive alteration at their margins to albite and/or oligoclase–andesine. In more thoroughly recrystallized examples, the laths are pseudomorphed by intergrowths of albite or oligoclase–andesine, quartz, and epidote. Where hornblende is present, plagioclase (which is invariably oligoclase–andesine) and quartz have been recrystallized; and little evidence of a former igneous texture is preserved.

Quartz is usually present; however, the rocks were probably not primary quartz dolerites. Typically, quartz is intergrown with the more sodic metamorphic feldspar and is metamorphic in origin. Chlorite is present in some samples intergrown with amphibole. Minor quantities of biotite also occur in some samples and may have been present in the primary igneous assemblage. Sphene is abundant, and is often seen to replace an opaque mineral, most probably ilmenite. Another iron oxide is magnetite, which may show alteration to hematite.

Suite 2

Suite 2 dykes have a general east–west orientation, and are restricted to the centre of the eastern part of the inlier. They have a similar mineralogy to Suite 1 dykes, and they vary from transitional amphibole-bearing examples to hornblende-bearing ones. Both foliated and unfoliated examples occur.

Southern ultramafic intrusion

Towards the southern margin of the inlier, a 30 km long, 200–800 m wide, easterly trending, dyke-like intrusion of ultramafic rock is exposed (Plate 2). At its western end, the body swings first to the west-southwest and then back to the northwest.

The intrusion is typically capped by massive opaline silica. The opaline silica may locally develop an apple-green colour (chrysoprase). Fresh rock is exposed at the western end of the outcrop. Here it is a serpentinite (consisting dominantly of serpentine with a small amount of talc and secondary magnetite) derived from greenschist-facies metamorphism of a coarse-grained dunite or peridotite. Minor quantities of metapyroxenite are present, but the rock is not obviously layered.

Contacts between the serpentinite and main granitoid, where exposed, are usually faulted or sheared. Suite 1 dykes are truncated by the intrusion, and late-stage aplites and pegmatite veins (common in the adjacent granitoid) do not intrude the ultramafic. However, the intrusion is not continuous, and a gap occupied by the main granitoid occurs 8 km east of the Great Northern Highway. The morphology of the intrusion terminations is similar to that seen on Suite 1 dykes. The ultramafic intrusion post-dates the main granitoid and is probably continuous at depth.

Geochronology

Prior to this study, few geochronological data for the Sylvania Inlier were available. A Rb–Sr age of 2235±54 Ma was obtained by Blockley et al. (1980) from a small inlier of granitoid near the Ophthalmia Dam; this granitoid is unconformably overlain by the Jeerinah Formation of the Fortescue Group. As this age is much younger than ages obtained for the base of the Fortescue Group (c. 2.76 Ga; Pidgeon, 1984; Richards and Blockley, 1984; Arndt et al., 1991) and the Hamersley Group (c. 2.5 Ga; Compston et al., 1981) it was thought to represent the time at which uplift of the inlier led to the dewatering of the Hamersley Basin.

As part of the present study, samples for isotopic analysis were collected from the foliated and/or banded granitoid and the undeformed main granitoid near Round Hill Bore in the western part of the inlier (Fig. 3). In the eastern inlier, foliated main granitoid was sampled near Emerald Bore,

TABLE 2. GEOCHRONOLOGY DATA FROM THE SYLVANIA INLIER

Locality	*Rock type*	*Rb–Sr*			*Sm–Nd*
		Age (Ma)	R_i	*MSWD*	T_{DM}
Ophthalmia Dam	Main granitoid	(a) 2235±54	0.7015	0.45	...
Round Hill Bore	Foliated and/or banded granitoid	(b) 2755±200	0.7032	20	(b) 3155
Round Hill Bore	Main granitoid	(b) 2800±240	0.7007	68	(b) 3315
Emerald Bore	Foliated main granitoid	(b) 2520±130	0.7160	100	(b) 3154
Benchmark 627	Hornblende-bearing granitoid	(b) 2720±350	0.7027	37	(b) 3312

NOTES: (a) Blockley et al. (1980). (b) Tyler et al. (in press)

and the hornblende-bearing granitoid was sampled 14.5 km southeast of Sylvania, near Benchmark 627. Results are shown in Table 2.

The dates for the main granitoid are typical of the post-tectonic "tin granites" (Blockley, 1980) which have intruded the granite–greenstone of the northern Pilbara—see compilations by Trendall (1983) and by Blake and McNaughton (1984). The Rb–Sr dates are younger than the age for the lower Fortescue Group. In the Sylvania Inlier, the main granitoid is unconformably overlain by the Fortescue Group and is intruded by dykes regarded as equivalent to the Black Range dyke suite.

This would appear to limit the age of intrusion of the main granitoid to pre-2.76 Ga, because lower Fortescue Group rocks unconformably overlie dykes of the Black Range suite in the northern Pilbara. Blake and McNaughton (1984) suggested that the "young" Rb–Sr ages of these granitoids may be due to slow cooling rates. An alternative explanation, (Blake and McNaughton, 1984; Nelson et al., in press; Tyler et al., in press), is that the isotopic system has been at least partially disturbed by metamorphism and metasomatism during burial under the Hamersley Basin.

Sm–Nd model ages have been obtained from single samples selected from each of the sample suites used to obtain the Rb–Sr dates (Table 2). These results differ from published data for equivalent rocks of the northern Pilbara granite–greenstone (McCulloch, 1987; Bickle et al., 1989).

Comparison with other areas of granite–greenstone—Pilbara or Yilgarn?

The Sylvania Inlier lies within the current limits of the Pilbara Craton as defined on geophysical evidence (Fraser, 1976; Drummond, 1981). However, its relationship to the main outcrops of granite–greenstone in the Yilgarn Craton and in the northern Pilbara Craton is a matter of debate. Does it form part of the older granite–greenstone of the northern Pilbara—within the "Pilbara egg" of Trendall (1983); or is it younger, equivalent to the Yilgarn, but isolated from it by formation of the Capricorn Orogen (see Rutland, 1981, fig. 1.3); or is it a fragment of crust which has a history different to both the major cratons.

The stratigraphy of the Jimblebar greenstone belt shows some similarities with the upper part of the Pilbara Super-

TABLE 3. STRATIGRAPHY OF THE GORGE CREEK GROUP

Formation	*Thickness* (km)	*Lithology*
Mosquito Creek Formation	>5.0	Psammitic to pelitic schistose rocks Greywacke and turbidites subordinate sandstone and conglomerate
Lalla Rookh Sandstone	0–0.5	Sandstone, grit and conglomerate.
Honeyeater Basalt	0–1.0	Pillow basalt containing sills of dolerite and gabbro. Minor subordinate high-magnesium basalt.
Cleaverville Formation	0.5–1.0	BIF, and ferruginous chert and shale.
Charteris Basalt	0–1.0	Pillow basalt, subordinate high-magnesium basalt, and dolerite. Local thin units of chert and felsic lava.
Corboy Formation	1.0–2.0	Quartzite, sandstone, psammopelite and ferruginous sediments.

NOTE: After Hickman (1983)

group as described by Hickman (1983). The main BIF horizon at Jimblebar could be correlated with the Cleaverville Formation of the Gorge Creek Group—the only major development of BIF in the Pilbara Supergroup. The stratigraphy of the Gorge Creek Group is shown in Table 3. On this basis, the lower metasedimentary unit (Fig. 4) would correlate with the Corboy Formation, and the upper metasedimentary unit with the Lalla Rookh Sandstone. There do not seem to be any such similarities with stratigraphies, such as those described by Watkins and Hickman (1990), and Griffin (1990), from greenstone belts in the Yilgarn Craton. However, as with any lithostratigraphic correlation made over long distances where outcrop is not continuous, there must remain considerable doubt as to its validity.

Tyler et al., (in press) have recognized differences in rare-earth-element patterns, $^{87}Rb/^{86}Sr$, $^{146}Sm/^{144}Nd$, and Sm–Nd model ages between the northern Pilbara and southeastern Pilbara granite–greenstone, despite the apparently similar field relations. These differences are fundamental, and Tyler et al. (in press) have suggested that the Sylvania Inlier, together with granite–greenstone basement underlying the southeastern Hamersley Basin, formed a separate terrane that amalgamated with the northern Pilbara to form the Pilbara Craton between 3.0 and 2.76 Ga.

The two terranes are "stitched" together by the Black Range dyke swarm, and are both unconformably overlain by the basal Fortescue Group. The Pilbara Craton was sufficiently cratonized to allow rifting and dyke-emplacement at that time. The rifting of the Fortescue Group marks the initiation of the Hamersley Basin: it took place at about the same time as the Norseman–Wiluna greenstone belt was developing within the Yilgarn Craton (Blake and Groves, 1987); and as voluminous granitoids were being intruded into the Murchison Province (Watkins and Hickman, 1990; Wiedebeck and Watkins, in prep.). The available evidence indicates that the Sylvania Inlier formed an integral part of the Pilbara Craton after 3.0 Ga, and that its evolution was not related to events that produced the Yilgarn Craton.

Chapter Three

Hamersley Basin

Introduction

The Hamersley Basin, a late Archaean to early Proterozoic depositional basin, occupies the southern part of the Pilbara Craton. It was the subject of an extensive review by Trendall (1983) to which the reader is directed for an historical overview of research prior to 1983 and a comprehensive bibliography. Three groups of rocks, which together make up the Mount Bruce Supergroup, have been recognized within the basin (Table 4). These unconformably overlie Archaean granite–greenstone basement and comprise: the mafic volcanic-dominated Fortescue Group, the base of which has been dated at 2765 Ma (Arndt et al., in press); the banded iron-formation-dominated Hamersley Group, dated at about 2500 Ma (Compston et al., 1981); and the more restricted, clastic-dominated Turee Creek Group (Trendall, 1979).

Fortescue Group

Stratigraphy

The Fortescue Group is the oldest group within the Hamersley Basin and lies unconformably on Archaean granite–greenstone cratonic basement. Two stratigraphic successions are recognized (Table 5), one occurring in the northern part of the basin, the other in the southern part (Fig. 26). Correlation between the two is a matter of some debate.

The northern succession was summarized by Hickman (1983) and Trendall (1983) and is set out in Table 5. The southern succession was first described by de la Hunty

TABLE 4. HAMERSLEY BASIN STRATIGRAPHY

Ashburton Basin	
—unconformity—	
Turee Creek Group Hamersley Group Fortescue Group	Mount Bruce Supergroup
—unconformity—	
granite–greenstone	

TABLE 5. FORTESCUE GROUP STRATIGRAPHY

Northern Pilbara Craton(a)	*Southern Hamersley Basin(b)*
Jeerinah Formation Siltstone; shale and chert; sandstone; local felsic lava, tuff and agglomerate; basalt; mafic sills locally abundant	**Jeerinah Formation** Mudstone and siltstone; chert; sandstone; basalt, pillow basalt and agglomerate; dolerite
Maddina Basalt Vesicular and amygdaloidal basalt and andesite	**Bunjinah Formation** Pillow basalt, vesicular basalt and volcanic breccia
Kuruna Siltstone Sandstone and siltstone; shale; ooidal sediments; pisolitic tuff and banded siliceous limestone	**Pyradie Formation** Ultramafic flows and pillow lavas, tuff, chert
Nymerina Basalt Basalt	**Boongal Formation** Basalt; pillow basalt; volcanic breccia; mafic tuff
Tumbiana Formation (Pillingini Tuff) Siliceous limestone (stromatolitic) and pisolitic tuff; subordinate tuff, basalt and sediments	
Kylena Basalt Massive amygdaloidal and vesicular basalt and andesite; subordinate but widespread interbedded sediments	
Hardey Sandstone Sandstone and conglomerate; local tuff, shale, mudstone and basalt	**Hardey Sandstone** Sandstone, siltstone, mudstone, tuff, basalt, and chert; ultramafic and mafic sills
Mount Roe Basalt Basalt and andesite with thin basal metasedimentary rocks	**Mount Roe Basalt** Basalt, tuff, and volcanic breccia **Bellary Formation** Mudstone, siltstone, and sandstone; conglomerate, basalt, volcanic breccia, and tuff

NOTES: (a) From Trendall (1983), Table 3-11. (b) After Thorne and Tyler (in press)

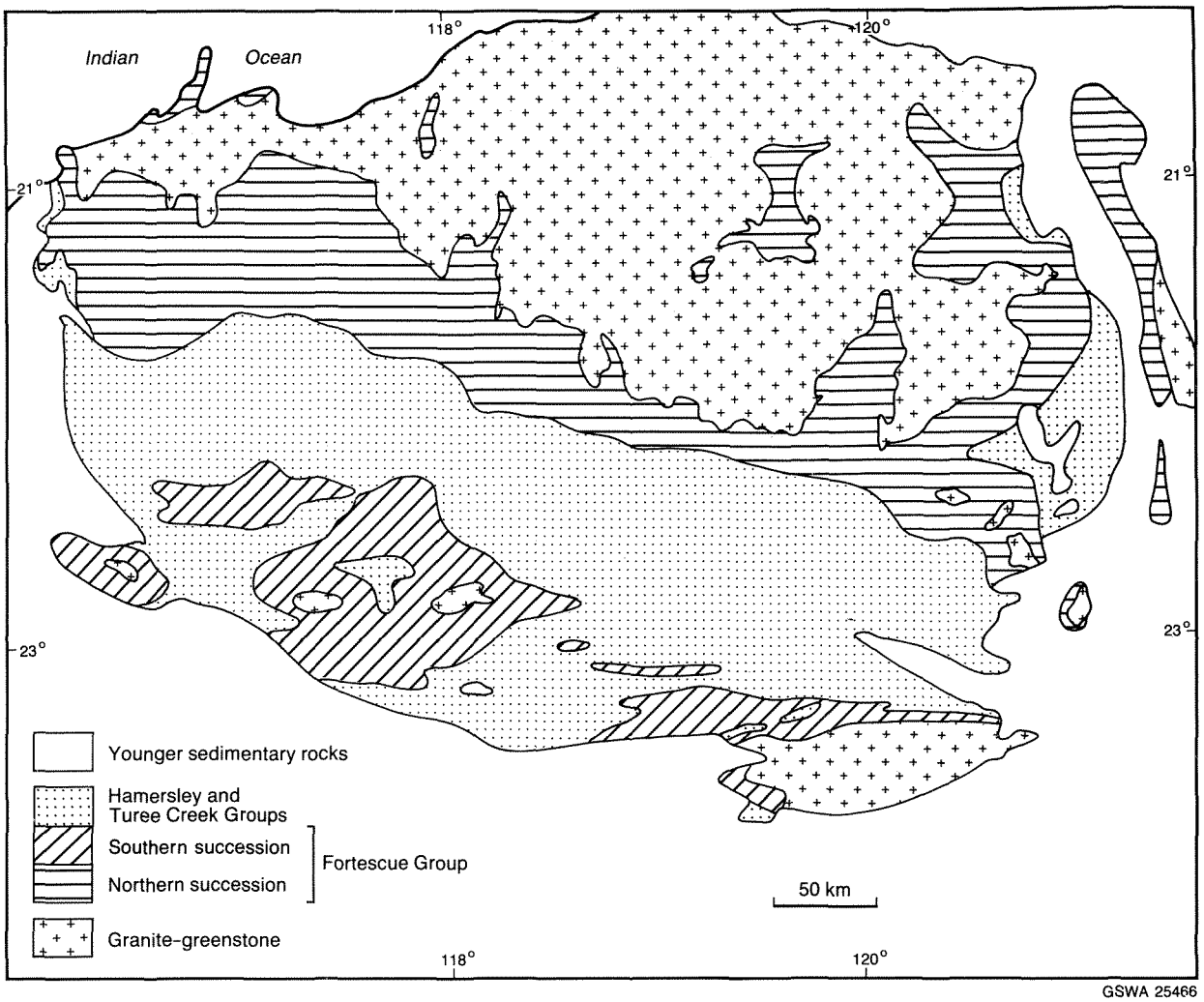

Figure 26. Outcrop of Hamersley Basin rocks. Fortescue Group rocks are separated into northern and southern successions.

(1965) for MOUNT BRUCE and extended onto WYLOO and TUREE CREEK by Daniels (1968, 1970). Seymour et al. (1988) retained the nomenclature for the second edition of WYLOO, but also recognized the Mount Roe Basalt. Thorne and Tyler (in press) have recognized, on TUREE CREEK, the Bellary Formation beneath the Mount Roe Basalt. The southern succession is set out in Table 5 for comparison with the northern succession.

In the eastern part of the southern Hamersley Basin, Fortescue Group rocks crop out adjacent to the Sylvania Inlier (Plates 2 and 3). They occur along the inlier's northern contact and also to the southwest, between Deadman Hill and Prairie Downs. Where exposed, the contact is typically faulted or sheared. However, unconformities are seen locally around small inliers of granite–greenstone that crop out as anticlinal fold cores. Examples are present 4 km south of Shovelanna Hill and 1 km southwest of Noddy Bore. Blockley et al. (1980), described an unconformity at the eastern end of the Ophthalmia Dam. An unconformity, where Fortescue Group rocks lie directly on the Sylvania Inlier, is also exposed near the Murramunda–Jigalong road.

Away from the Sylvania Inlier, upper Fortescue Group rocks are exposed extensively south and southwest of the Ophthalmia Range, and in the cores of the Wonmunna and Alligator Anticlines.

During first edition mapping, Daniels and MacLeod (1965) did not recognize any mafic volcanic rocks within the Fortescue Group on NEWMAN. They mapped Jeerinah Formation as overlying a basal clastic sedimentary unit correlated with the Hardey Sandstone. De la Hunty (1969), however, did recognize mafic volcanics below the Jeerinah Formation on ROBERTSON, and these were placed within the Mount Jope Volcanics.

Two successions, both containing mafic volcanic rocks, have subsequently been recognized adjacent to the Sylvania Inlier (Fig. 27): a northern (Outcamp Well) succession, which was described by Horwitz (1976), who correlated units with the Tumbiana Formation/Pillingini Tuff and the Maddina Basalt of the northern Pilbara; and a southwestern (Prairie Downs–Deadman Hill) succession, which was described by Tyler (1986), who correlated units with the succession exposed in the western part of the southern Hamersley Basin. Recent remapping in the western part of the southern Hamersley Basin (Thorne and Tyler, in press) has established the ultramafic and komatiitic nature of the Pyardie Formation. Thorne (1990) has revised the

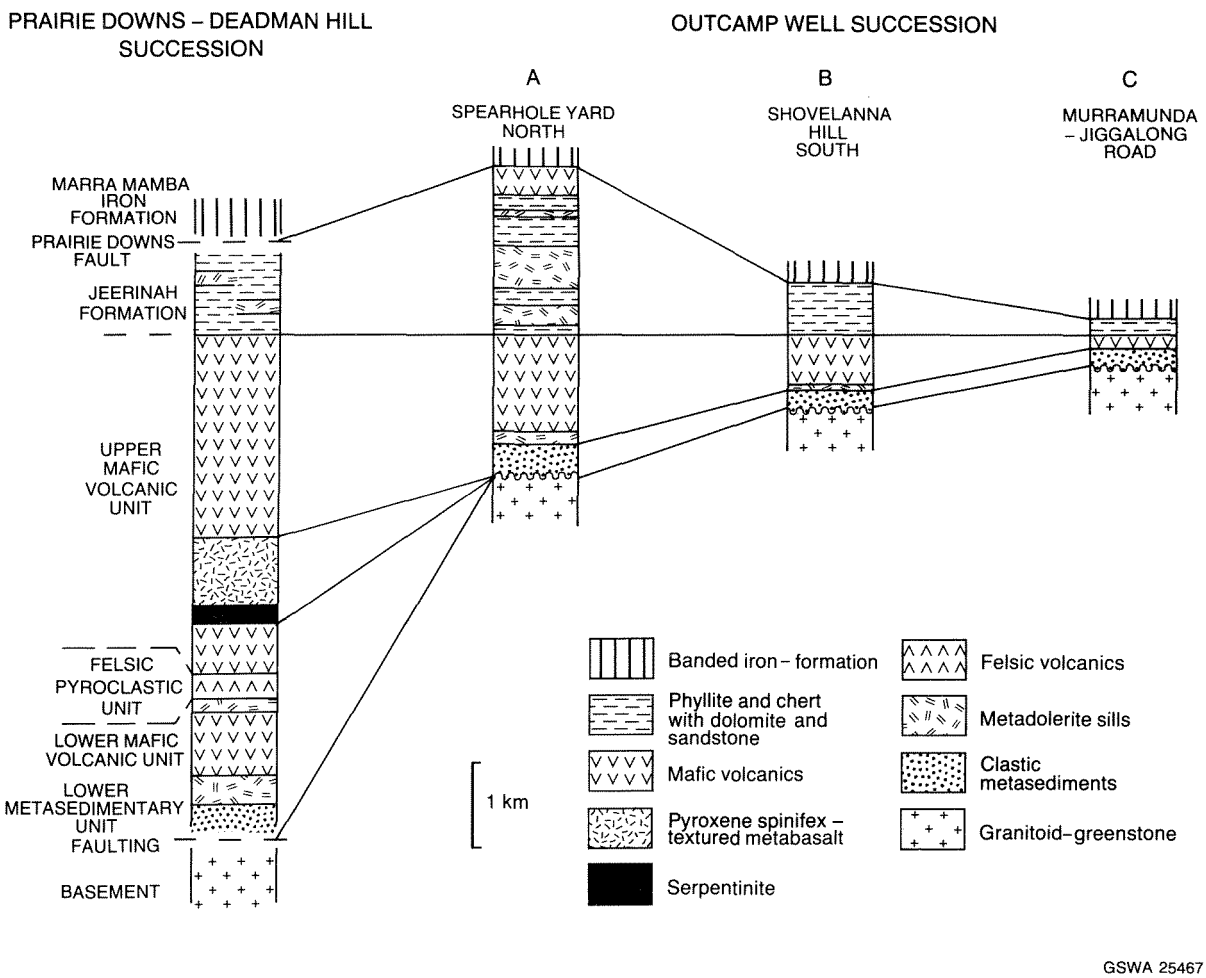

Figure 27. Stratigraphy of Fortescue Group rocks adjacent to the Sylvania Inlier.

Figure 28. Thin peloidal carbonate unit in quartz–muscovite schist, basal metasedimentary unit.

correlation of Tyler (1986) so that the unit of pyroxene spinifex-textured metabasalt and serpentinite correlates with the Pyradie Formation. The felsic pyroclastic unit, the lower mafic volcanic unit, and the lower metasedimentary unit are all thought to correlate with the Hardey Formation.

Basal metasedimentary unit

In the Prairie Downs–Deadman Hill succession, the basal metasedimentary unit is 200 m thick and consists of interbedded phyllite, quartz–muscovite schist, metasandstone, and peloidal carbonate. Conglomeratic units, containing vein quartz and lithic fragments in a shaly matrix, are also locally present.

The metasandstone is 5 m thick, medium- to coarse-grained, and may show poorly developed cross-lamination. It consists of strained and elongate clasts of quartz and, typically, ragged muscovite. Iron oxides are locally abundant. The metasandstone is underlain by purple-brown phyllite. This is now altered and comprises degraded biotite, leucoxene, and lesser amounts of quartz. It represents an original mudstone lithology. Above the metasandstone, quartz–muscovite schist is interlayered with 10–15 cm thick bands of carbonate. The schist is generally fine-grained, but may contain large quartz clasts together with some carbonate, and accessory tourmaline and iron oxides. The carbonate bands are characterized by numerous lenticles and ovoids (peloids) of carbonate reaching 3–5 mm in diameter (Fig. 28). Conglomerate occurs locally between the Prairie Downs road and Spearhole Creek.

In the Outcamp Well succession, the basal metasedimentary unit is 400–500 m thick and consists of interbedded, parallel-laminated, polymict conglomerate, coarse sandstone, and shale. The conglomerate is poorly sorted with sub-angular to sub-rounded clasts. Both clast-supported cobble conglomerate with a coarse, sandy matrix, and matrix-supported pebble conglomerate with a fine, shaly matrix occur. Beds vary in thickness from a few centimetres for pebble-rich bands in coarse sandstone to several metres for the coarsest material.

Clasts are varied: they include locally derived metasedimentary rocks, banded iron-formation, mafic volcanics, and vein quartz. The type and nature of the clasts is apparently controlled by local sources within the underlying granite–greenstone. Matrix material, and interlayered sandstone and shale units, comprise varying amounts of quartz, sericite, and chlorite. The chlorite has typically replaced degraded biotite.

The nature and thickness of the basal metasedimentary unit varies along the northern contact of the inlier, particularly east of the Fortescue River. South of Shovelanna Hill, a 10–20 m thick, very immature, poorly sorted conglomeratic sandstone comprising sand- to pebble-sized clasts of quartz and microcline, and lesser amounts of matrix clay, lies unconformably on granitoid. The pre-Fortescue Group land surface was irregular here. The conglomeratic sandstone passes directly into mafic volcanics. Three kilometres to the east, the unit comprises at least 100 m of distinctive iron-stained shale.

At the east end of the Sylvania Inlier, the Fortescue Group is seen to directly overlie the inlier proper. Two lithologies, both having a distinctive purple-brown colour, are recognized: a shaly unit, and a more massive unit. In thin section they show almost complete replacement by clay and silica, and their origin is uncertain.

Lower mafic volcanic unit

This unit is exposed in the Prairie Downs–Deadman Hill succession, where it overlies the basal metasedimentary unit. It is 750 m thick and comprises interlayered, 2–3 m thick, units of fine- to medium-grained mafic tuff (Fig. 29), and metabasalt.

The tuffaceous units contain numerous clasts of devitrified volcanic glass. Less frequent are subrounded to euhedral plagioclase grains. Some lithic fragments, dominantly chloritic, are also present. Metabasaltic units contain quartz phenocrysts 1–2 mm in diameter. Typically, both the tuffs and the lavas consist of amphibole, chlorite (both in lithic fragments and in the matrix), muscovite, albite, epidote, and minor amounts of sphene and opaques. Thin metasedimentary horizons are calcium rich and now form quartz–actinolite–epidote schists.

Felsic pyroclastic unit

The felsic pyroclastic unit overlies the lower mafic volcanic unit in the Prairie Downs–Deadman Hill succession. It is 300 m thick and comprises felsic tuff overlain by a 5–10 m thick banded chert. Much of the tuff is massive and has been extensively recrystallized to produce a structureless to weakly foliated assemblage of quartz, biotite, muscovite, and lesser amounts of feldspar. Opaques are generally iron oxides after sulphides. A well-laminated rock occurs locally and suggests that at least part of the unit was deposited in a subaqueous environment. Original igneous textures may be preserved: elongate curved grains (now recrystallized), recognizable shards, and subhedral feldspar crystal, indicate a devitrified crystal-vitric tuff (Fig. 30).

Upper mafic volcanic unit

The upper mafic volcanic unit, a monotonous, 4 km thick sequence of metabasalt, occurs above the felsic pyroclastic unit in the Prairie Downs–Deadman Hill succession. The metabasalt is typically fine- to medium-grained, locally feldspar-phyric, and comprises epidote, chlorite, amphibole, and some remnant feldspar. Original igneous textures are generally preserved, but intergrowths of epidote, sericite, and feldspar pseudomorph feldspar laths. Feldspar phenocrysts reach 1 cm in length. Some flows show quench textures.

Within the succession, a thick (1 km) unit of pyroxene spinifex-textured metabasalt with serpentinite at its base is present. The serpentinite is massive, and relic texture indicates that the rock was dunite. The pyroxene spinifex-textured metabasalt is interbedded with thin interflow ultramafic tuffs. It consists of tremolite–actinolite, epidote, chlorite, and lesser amounts of sphene, quartz, and albite. The spinifex needles are 4–5 mm long and were pyroxene

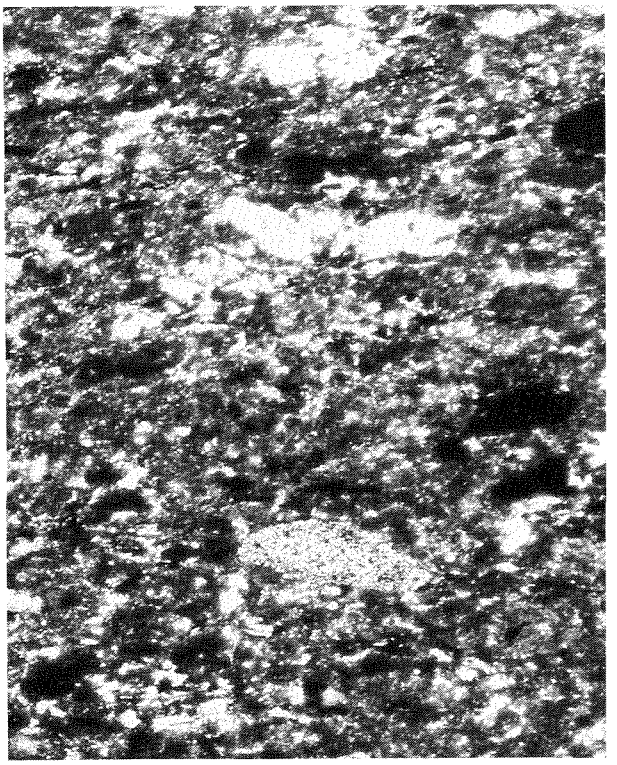

GSWA 25469

Figure 29. Mafic tuff from the lower mafic volcanic unit containing clasts of devitrified volcanic glass and lithic fragments, together with feldspar crystals (x35). GSWA sample 84523.

GSWA 25470

Figure 30. Felsic tuff from the felsic pyroclastic unit containing elongate curved shards together with feldspar crystals (x40). GSWA sample 84530.

GSWA 25471

Figure 31. Pyroxene spinifex-textured metabasalt, with amphibole replacing pyroxene needles, upper mafic volcanic unit (x10). GSWA sample 84534.

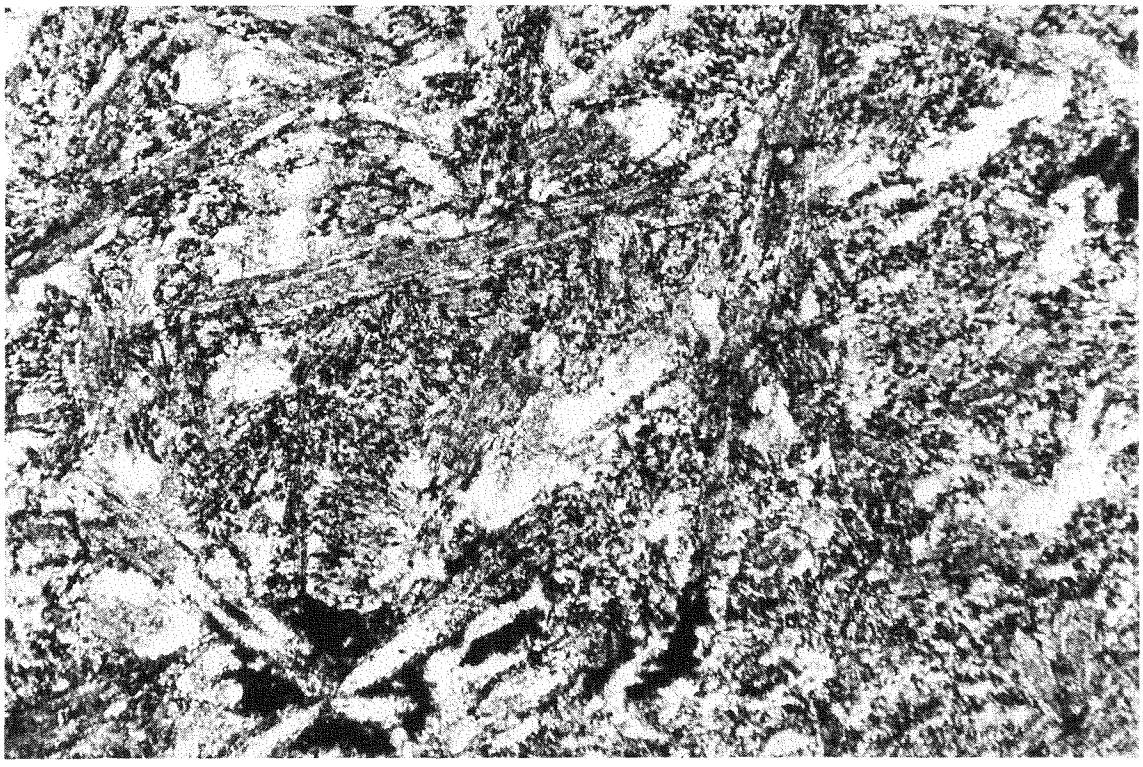

GSWA 25472

Figure 32. Spinifex-texture developed in metabasalt, upper mafic volcanic unit (x32). GSWA sample 84550.

rather than olivine (Fig. 31). Locally, the unit may have a variolitic texture. The serpentinite may represent a separate flow rather than the differentiated base of a single komatiite flow as suggested by Tyler (1986).

In the Outcamp Well succession, a single mafic volcanic unit less than 1.2 km thick, is exposed above the basal metasedimentary unit. This is probably at least a partial equivalent of the upper mafic volcanic unit in the Prairie Downs–Deadman Hill succession, but it comprises a sequence of massive and amygdaloidal metabasalts, and mafic tuffs. Towards the western end of the sequence, tuff is absent. A flow low in the succession shows spinifex texture defined by coarse, elongate to acicular, tremolite crystals in a devitrified matrix (Fig. 32). The rock is rather felsic, and there is evidence of silicification. A true komatiitic (i.e. high-Mg) origin is unlikely, although there is a metapyroxenitic base to the unit. Elsewhere in the sequence, individual flows may have also developed spinifex texture formed by randomly orientated, rather short, amphibole crystals. This texture does not seem to be metamorphic in origin, as relic igneous crystals, particularly feldspar laths, are recognizable. It is probably a primary quench texture. Several flows within the sequence contain rounded and amoeboid amygdales: these reach 2–3 mm across, are filled with quartz, and quartz–epidote, and may be as much as 40% of the rock in some cases.

Beds of mafic tuff are exposed towards the base of the unit at Outcamp Well. These contain fine to medium clasts of a very fine-grained material, probably devitrified glass, together with scattered plagioclase crystals. The rocks represent vitric and crystal-vitric tuffs. Subsequent metamorphism has produced widespread fine epidote and amphibole. Beds vary from a few centimetres to several metres thick and some are well laminated.

East of the Fortescue River, the upper mafic volcanic unit consists dominantly of metabasalt and meta-andesite interlayered with thin minor tuffaceous beds. The metabasalts and meta-andesites show relic igneous textures with abundant feldspar laths. These form both groundmass crystals and phenocrysts, and are now altered to albite. The mafic portion of the rock comprises chlorite, amphibole, epidote, and traces of sphene. Feldspar with only minor amounts of epidote may form 65% of the rock. This suggests an initially calcium-poor plagioclase (An<50) typical of an andesitic composition; this is also reflected in the high, relative to amphibole, chlorite content. Amygdales, 3–4 mm in diameter and filled with chlorite and epidote-calcite, may show an alignment, as do feldspar laths. This is probably related to deformation rather than primary flow banding.

Tuffaceous units also have an intermediate composition: they consist of amphibole and feldspar crystals in a dominantly quartzofeldspathic matrix containing small amounts of sphene and chlorite. Amphibole crystals are typically well aligned, and a foliation tends to wrap the feldspar crystals. Lithic fragments are also present.

Jeerinah Formation

In the Prairie Downs–Deadman Hill succession, the Jeerinah Formation is dominated by phyllite interbedded with 2–3 m thick silicified mudstone and chert units. Including mafic sills, it is at least 900 m thick.

Similar lithologies occur in the Outcamp Well succession, where the unit is 2 km thick. Of this 2 km, 850 m is made up of mafic sills. At the base of the formation, Horwitz (1976) records 100 m of "chertified current-bedded sediment" overlain by "125 m of sandy and gritty, ferruginized quartzitic sandstone and some shales". He later correlated these sediments with the Woodiana Sandstone Member, a unit well developed at the base of the Jeerinah Formation in the northern Pilbara (Horwitz, 1987). East of Western Creek, the lower part of the Jeerinah Formation comprises interbedded shaly mudstone and laminated siltstone, and no sandstone or cross-laminations have been recognized. Felsic tuff and thin dolomite occur in the upper part of the unit, and are well exposed in the Wonmunna Anticline. Near Mount Whaleback, a metabasalt that has well-developed pillows is exposed beneath the Marra Mamba Iron Formation (Blockley et al., 1980). This unit is developed in both the Wonmunna and the Alligator Anticlines.

East of the Fortescue River, mafic sills are absent from the Jeerinah Formation: the principal lithologies are phyllite, chert, and subordinate tuff. Two chert horizons, each up to 5 m thick, have been recognized: one towards the base, and the other very near the top. The top is marked by a transition from phyllite into cherts distinctive of the lower part of the Marra Mamba Iron Formation.

Further east, north of Junction Pool, a cross-laminated, medium-grained sandstone appears at the base of the formation. This probably correlates with the Woodiana Sandstone Member. Above the sandstone is a relatively thin succession of interlayered phyllite and chert.

Mafic sills

Mafic sills have been intruded throughout the Fortescue Group. They are best developed within the Jeerinah Formation, where they can make up over 50% of the exposed section. The sills are fine- to coarse-grained metadolerite and preserve ophitic to poikilitic igneous textures. Clinopyroxene may be preserved as plates up to 7 mm across, which show alteration to chlorite, and/or actinolite. Plagioclase

TABLE 6. HAMERSLEY GROUP STRATIGRAPHY

Formation	*Member*	*Lithology*	*Thickness*	
			Paraburdoo (m)	*Newman* (m)
Boolgeeda Iron Formation		BIF, shale	260	220
Woongarra Volcanics		Rhyodacitic to rhyolitic ?sills, BIF	800	294
Weeli Wolli Formation		BIF, chert, shale, dolerite sills	600	366
Brockman Iron Formation	Yandicoogina Shale	Shale, BIF	45	30
	Joffre Member	BIF, shale	280	340
	Whaleback Shale	Shale, chert, BIF	43+	30
	Dales Gorge Member	BIF, chert, shale	135	119
Mount McRae Shale		Shale, chert, BIF	55	30
Mount Sylvia Formation		Shale, chert, BIF, dolomite, sandstone	30	45
Wittenoom Dolomite		Dolomite, shale, chert	246	152
Marra Mamba Iron Formation	Mount Newman Member	BIF, chert, shale	60	50
	MacLeod Member	Shale, chert	30	25
	Nammuldi Member	Chert, BIF, shale	115	70

laths are invariably albitized and can be replaced by intergrowths of sericite and epidote or clinozoisite. Iron-oxides are leucoxenized. Pumpellyite is present in some samples. Large-scale primary igneous layering occurs in metapyroxenite at the base of several sills.

Hamersley Group

Introduction

In the southeast Hamersley Basin, the Hamersley Group conformably overlies the Fortescue Group and shows the same stratigraphic sequence described for the basin as a whole (MacLeod et al., 1963; MacLeod, 1966; Trendall and Blockley, 1970; Trendall, 1979). The group is dominated by banded iron-formation. Thickness variations for each of the eight formations and their constituent members between Paraburdoo and the Newman area are shown in Table 6.

Marra Mamba Iron Formation

The Marra Mamba Iron Formation can be divided into three units (Trendall and Blockley, 1970), which have been formally established as members (Kneeshaw, 1984; Blockley et al., in press).

The basal unit is the Nammuldi Member, which consists of yellow-weathering chert and cherty BIF with some shale bands. The top of this unit is marked by distinctive podding of chert with the development of a band known as the "potatoes". The middle unit is the MacLeod Member, which consists of shale and thin BIF interbeds. The upper unit is the Mount Newman Member, which consists of BIF interbedded with 18 thin shale horizons (Slepecki, 1981).

Wittenoom Dolomite

Typically, the Wittenoom Dolomite is poorly exposed; however, good exposures are present in the headwaters of Weeli Wolli Creek and near Paraburdoo. Slepecki (1981) described a 36 m thick manganese-rich shale unit, with occasional BIF and chert layers, overlying the Mount Newman Member of the Marra Mamba Iron Formation. It was included in a four-fold sub-division of that formation. Subsequently the shale has been named the West Angelas Shale (Blockley et al., in press) and has been placed at the base of the Wittenoom Dolomite. The shale is absent from the western part of the basin, e.g. Radio Hill near Paraburdoo (B. M. Simonsen, written comm., 1986) prompting the suggestion that it is the result of leaching during ore formation. However, its presence above unmineralized Marra Mamba Iron Formation in the eastern part of the basin has been proved by drilling (Slepecki, 1981).

Above the basal shale, the Wittenoom Dolomite can be divided into two. The lower is massive crystalline dolomite. At Radio Hill, B. M. Simonsen (written comm., 1986) has reported 246 m of thinly to thickly bedded dolomite in which infrequent small-scale cross-stratification is present. The massive dolomite passes up into interbedded thin shales, cherts, dolomites and occasional BIF.

Mount Sylvia Formation

The Mount Sylvia Formation consists of shale, dolomite, and three BIF units. The top and bottom of the unit are marked by BIF units. The top BIF unit is the distinctive Bruno's Band, which can be traced throughout the Hamersley Basin. Kneeshaw (1975) records the occurrence of a 21 m thick feldspathic sandstone between the central and upper BIF bands at Mount Whaleback.

Mount McRae Shale

The Mount McRae Shale comprises interlayered shales, cherts and BIF. Shales, some of which are graphitic, dominate the lower part of the unit. Banded iron-formation interbedded with shale forms the upper part. Shales in the middle of the unit carry abundant pyrite nodules up to 5 cm across.

Brockman Iron Formation

The Brockman Iron Formation is the thickest, and economically the most important, iron-formation unit within the Hamersley Group. It forms prominent strike ridges that rise 200–400 m above the surrounding country. It has been subdivided into four members.

The lowermost member is the Dales Gorge Member which has been described in detail by Trendall and Blockley (1970) and Ewers and Morris (1981). It comprises an alternating sequence of 17 BIF and 16 shale macrobands which can be traced throughout the Hamersley Basin.

The Dales Gorge Member is overlain by the Whaleback Shale, which can be divided into three zones (Kneeshaw, 1975; McConchie, 1984). The lower zone comprises pyritic black shale. It is overlain by a central chert band, which includes a prominent BIF. The upper zone is dominated by carbonate-rich shales.

The Joffre Member consists dominantly of BIF, and thin shale layers. It has not been studied in as much detail as the Dales Gorge Member; however, McConchie (1984) suggested that mesoband continuity over the Hamersley Basin is similar to that seen in the Dales Gorge Member. Ward et al. (1975) identified a median shale–tuff zone, informally known as the Ferro Gully shale.

The uppermost unit is the Yandicoogina Shale. This is generally poorly exposed and consists of shale, chert, and small amounts of BIF.

Weeli Wolli Formation

The Weeli Wolli Formation, a sequence of interbedded BIF, chert, and shale, which has been intruded by several metadolerite sills, overlies the Brockman Iron Formation. Banded iron-formation is often jaspilitic and individual units are of the order of 10 m thick.

Metadolerite may form over half of the formation. It is fine- to medium-grained and a subophitic igneous texture has been preserved. Relic pyroxene is often present and may be altered to chlorite or, less frequently, to stilpnomelane and/or actinolite. Feldspar is albitized. Chlorite, epidote, pumpellyite and prehnite are also present. Iron oxides are typically leucoxenized. A. F. Trendall (pers. comm., 1987) has reported pillows in outcrops from Coondiner Creek, 3 km north of Eagle Pool. From their morphology, they are thought to represent intrusion into wet sediment.

Woongarra Volcanics

The Woongarra Volcanics comprises quartz-phyric and K-feldspar-phyric rhyodacitic to rhyolitic rocks. Albitized plagioclase and secondary chlorite are present in a devitrified, often spherulitic, quartzofeldspathic groundmass. In some rocks, textures consistent with a fragmental, tuffaceous origin are preserved . As discussed by Kokelaar (1982), such textures may be produced by intrusion into wet sediment. A prominent, but discontinuous, band of jaspilitic banded iron-formation occurs centrally within the unit.

Boolgeeda Iron Formation

The Boolgeeda Iron Formation is the uppermost unit of the Hamersley Group. Trendall and Blockley (1970) suggested a three-fold subdivision with upper and lower iron-formations separated by a poorly exposed median shale unit. The lower BIF is typically a dense, black to brownish, well-laminated rock, having a flaggy appearance. The upper BIF is finer grained and finely laminated, and has a shaly appearance.

Turee Creek Group

The Turee Creek Group (Trendall, 1979) conformably overlies the Hamersley Group and is exposed in the cores of synclines in the southwest Hamersley Basin. Tyler et al., (1990) report the occurrence of shales conformably overlying Boolgeeda Iron Formation in a syncline 26 km northeast of Newman (Plate 2). These are presumed to belong to the Turee Creek Group.

The lowest unit, a monotonous sequence of thin-bedded greyish-green siltstone, fine-grained greywacke, and fine-grained sandstone, was named the Kungarra Formation by Trendall (1979). Thin beds of carbonate appear in the upper part of the unit. Dolerite sills occur frequently. Within the formation, a mixtite of possible glacial origin was named the Meteorite Bore Member. The Kungarra Formation is overlain by a sequence of quartzite units interbedded with an unnamed carbonate unit.

In the Turee Creek Syncline, only the upper part of the Turee Creek Group, which consists of coarse sandstone and a stromatolitic carbonate unit, is well exposed (Thorne and Tyler, in press). At Mount Maguire, the unit, consisting of siltstone and shale overlain by a coarse sandstone, is thin.

Palaeogeography and basin evolution

The palaeogeography of the Hamersley Basin is incompletely known and has been the subject of some controversy. It was initially thought that the thickest succession occurred in the central part of the basin on MOUNT BRUCE. This was used as evidence for a restricted basin, closed to the south (Trendall and Blockley, 1970; Trendall, 1975a). More recently measured sections (Horwitz and Smith, 1978; Horwitz, 1980) indicate a general thickening of rocks in the Fortescue Group from northeast to southwest across the basin.

Blake and Groves (1987) recognized a three-phase tectonic history in the Fortescue Group. The earliest was ?pre-rift volcanism (Mount Roe Basalt). This was followed by an east–west tensional event that generated linear, northerly trending sedimentary basins (Hardey Sandstone). This tensional event may have been related to the generation of a rift to either the east or west of the present craton. The intrusion of the Black Range dyke swarm was probably related to this rift. The final regional subsidence reflected a later rift close to the present southern margin of the craton. Geochemistry of basalts associated with this last phase indicates them to be continental tholeiites (Cowley, 1979).

The model presented by Blake and Groves (1987) was based mainly on work done in the northern succession. Blight (1985) investigated the lower part of the Fortescue Group succession in the western part of the southern Hamersley basin. The lowest unit, deposited in a chaotic environment within a palaeovalley, was correlated with the Mount Roe Basalt of the northern succession. It was overlain by a unit correlated with the Hardey Sandstone, which was deposited by a braided river system. Palaeocurrent data indicate a westward flow (Fig. 33), and the "Hardey braidplain" was confined to the south by an east-trending topographic high or fault-controlled escarpment.

Horwitz and Smith (1978) interpreted the presence of a "geanticline" or broad basement ridge, plunging northwestwards and extending along the line of the present Fortescue Valley. This "geanticline" controlled deposition of the Fortescue Group, and effectively separated the northern succession, dominated by subaerial volcanism, from the southern succession, dominated by subaqueous volcanism. Units progressively lapped onto, and ultimately buried the ridge. Blake (1984) identified a regional gravity low coincident with the eastern end of this ridge, and interpreted it as a source region for northeasterly directed palaeocurrents in the Hardey Sandstone to the north. This palaeohigh would also be the source area for the Hardey Sandstone in the southern part of the basin. The stratigraphy of the

Fortescue Group around the Sylvania Inlier can be interpreted in terms of progressive on-lap of units onto the southeastern margin of this basement ridge.

The Fortescue Group succession southwest of the Sylvania Inlier is one of the thickest known—compare with sections in Horwitz (1980)—and is consistent with the deepening or more rapid subsidence of the basin to the south and west. Proximity to a rift is supported by the occurrence of komatiite, a lithology not seen in the northern Pilbara succession and which has been suggested as representative of Archaean to early Proterozoic ocean crust (Nisbet, 1984). A summary of Fortescue Group palaeogeography is given in Figure 33.

Along the northern margin of the Sylvania Inlier, the lower part of the sequence seen in the Prairie Downs–Deadman Hill area is absent. The base of the Fortescue Group occurs at a relatively high stratigraphic level. The occurrence of parallel-laminated, clast-supported conglomerate and conglomeratic sandstone, together with matrix-supported conglomerates, west of the Fortescue River is consistent with proximity to a palaeohigh. These rocks may represent high-energy, alluvial deposits and debris flows (similar to those described by Rust and Kostor, 1984) at the southern margin of the basement ridge.

From local variations in thickness and stratigraphy, it seems that an irregular topography was present below the Fortescue Group unconformity. The general thinning of the Fortescue Group eastwards, together with the appearance of cross-laminated sandstone at the base of the Jeerinah Formation, can be interpreted as a change to a shallow-water, ?basin-margin, environment.

The Western Creek Fault separates the Prairie Downs–Deadman Hill succession from the Outcamp Well succession and may represent an early, syn-Fortescue Group, extensional fault at the margin of the basement ridge. The fault was reactivated as a thrust during the Early Proterozoic Capricorn Orogeny (see Chapter 4).

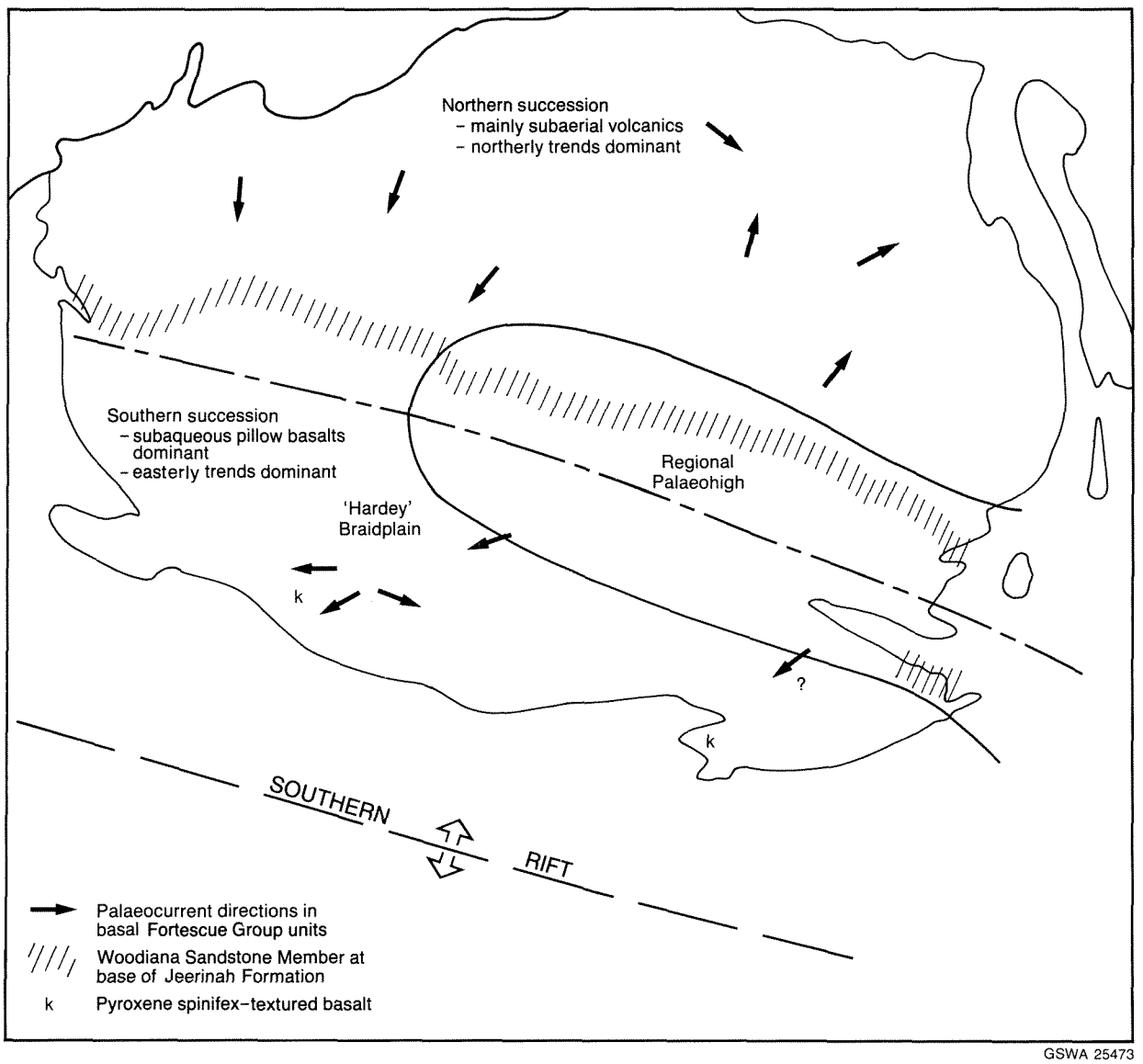

Figure 33. Palaeogeography of the Fortescue Group. Palaeocurrent data from Blake (1984) and Blight (1985). Present limits of combined granite–greenstone and Hamersley Basin rocks outlined.

The Jeerinah Formation represents a change in the evolution of the basin and the establishment of basin-wide tectonic stability; this remains typical of the basin throughout Hamersley Group times. Coarse, terrigenous sediment is absent; and shale, which is prominent within the sequence, has been linked to periodic volcanicity from a source remote from the present limits of the basin (Trendall and Blockley, 1970; Morris and Horwitz, 1983).

Trendall and Blockley (1970), using an isopach map for the Dales Gorge Member—the only unit for which reliable basin-wide thickness data are available—interpreted the environment of deposition of the BIFs in the Hamersley Group as a barred basin having a restricted oceanic connection to the northwest. Microbands in the BIFs were interpreted as varves produced by seasonal climatic variations. Fumerolic activity was postulated as a source for the iron.

In view of the increasing thickness of the Fortescue Group to the southwest, Horwitz and Smith (1978) preferred BIF deposition to have taken place on a shelf open to the ocean to the west. This view was also taken by Ewers and Morris (1981) based on the need to supply sufficient iron to the area of deposition. This they supposed to have been achieved by the periodic upwelling of deep ocean currents. Deposition of iron was not disturbed by wave action and must have been triggered by some chemical control in deep water on the outer part of the shelf.

Morris and Horwitz (1983) and McConchie (1984) took this model one step further by postulating deposition on a platform or bank that was separated from the inner part of the shelf. The necessity for a platform was based on the apparent lack of evidence of proximity to a basin margin within the Hamersley Group. Recent work by Hassler (1990) has identified turbidites within the Wittenoom Dolomite. These would appear to confirm a shelf rather than a platform as the environment of deposition. Palaeocurrent data, which indicate a source area for the turbidites to the north and east of the outcrop are consistent with this conclusion (Fig. 34).

In the eastern part of the Hamersley Basin, the normal stratigraphic sequence of the Hamersley Group has not developed (Williams, 1989; Williams and Tyler, 1991). Cherty iron-formation corresponding to the Marra Mamba

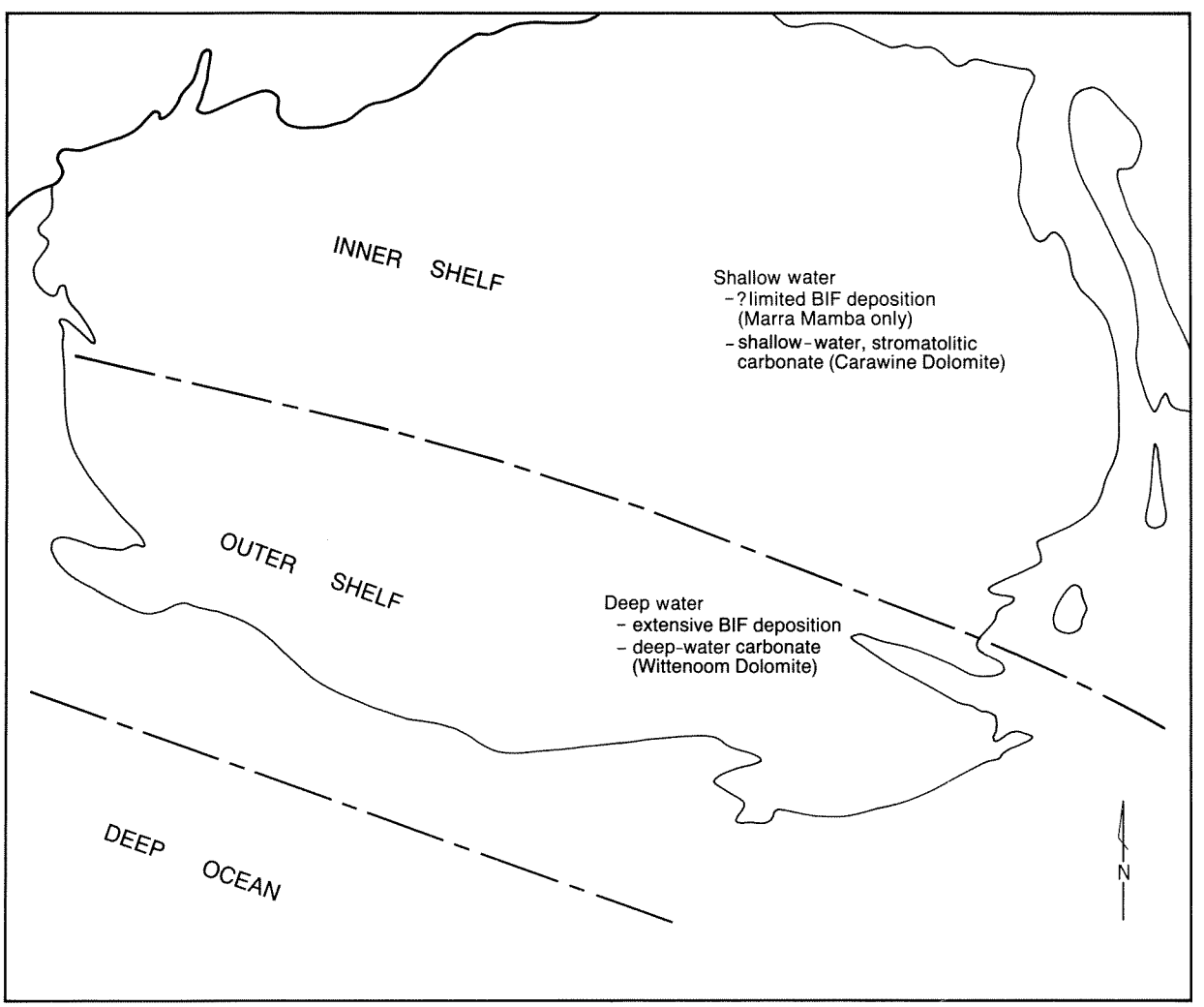

Figure 34. Palaeogeography of the Hamersley Group. Present limits of combined granite–greenstone and Hamersley Basin rocks outlined.

Iron Formation overlies the Jeerinah Formation; however, this is overlain by a stromatolitic carbonate, the Carawine Dolomite, which, from its stratigraphic position, is assumed to be a lateral equivalent of the Wittenoom Dolomite (Hickman, 1983). The top of the dolomite is not seen because the unit is unconformably overlain by the Pinjian Chert Breccia, and the upper part of the Hamersley Group has either been removed by erosion, or was not deposited in this area. As well as stromatolitic bioherms, Simonsen (written comm., 1986) also recognized structures and textures consistent with an evaporitic environment. Cross-stratification displays features characteristic of wave ripples suggesting a shallow-water, possible inner-shelf, environment.

In the southeast Pilbara, the change in Hamersley Group stratigraphy occurs at the east end of the Sylvania Inlier. The Wittenoom Dolomite is exposed near Wheelarra Hill, and upper Hamersley Group units are seen between Limestone Well and the Murramunda–Jigalong road. Some 20 km to the north, stromatolitic Carawine Dolomite is exposed (Williams and Tyler, 1991). This change in the Hamersley Group reflects a long-lived feature of the palaeogeography of the Hamersley Basin. It also corresponds to the limit of the northern Fortescue Group succession which is seen on BALFOUR DOWNS and northern ROBERTSON (Williams, 1989; Williams and Tyler, 1991), and to the appearance of the Woodiana Sandstone Member at the base of the Jeerinah Formation (Figs 33 and 34).

The Turee Creek Group represents the resumption of pronounced tectonic activity. There is an influx of dominantly clastic sediment together with an overall shallowing of the basin. Shales conformably overlie the Boolgeeda Iron Formation; and, together with the siltstone and greywacke that form the Kungarra Formation, represent a deep-water environment. Towards the top of the group, shallower water deposits, characterized by cross-stratified sandstones and stromatolitic carbonates (Trendall, 1979; Thorne and Tyler, in press) appear.

Metamorphism

It was initially thought that rocks in the Hamersley Basin were little affected by regional metamorphism (Trendall and Blockley, 1970). Later work on oxygen isotopes (Becker and Clayton, 1976) and on mineral paragenesis (Ayers, 1972) in the iron formations of the Wittenoom area suggested burial metamorphism at temperatures of about 300°C and pressures of 400 to 600 MPa (100 MPa = 1 kb). More recently, a study by Smith et al. (1982) has established a zonal pattern, based mainly on mineral assemblages in mafic volcanics of the Fortescue Group, of very low- and low-grade metamorphism. Grade increases from north to south concomitant with increasing stratigraphic thickness; and metamorphism was attributed to a static burial metamorphism. Four zones, ranging from the prehnite–pumpellyite facies through to the lowermost greenschist facies, were recognized (Fig. 35). The southeast Pilbara falls within the two highest grade zones recognized by Smith et al. (1982), the prehnite–pumpellyite–epidote–actinolite zone (Z III) and the (prehnite)–epidote–actinolite zone (Z IV). The highest grades (with conditions reaching 460°C at 250 MPa) occurred in the deepest observed part of the basin along its southern margin.

As will be discussed in the next chapter, much of the Sylvania Inlier, and the southeastern part of the Hamersley Basin, were deformed during the Early Proterozoic Capricorn Orogeny. Rocks are foliated and were recrystallized during an accompanying metamorphic event, designated M_c. Metamorphic grades are similar to those established during the Hamersley Basin burial metamorphism—here designated M_h–recognized by Smith et al. (1982)—and, to the west of the Turee Creek, the effects of the two metamorphic events merge.

In the Sylvania Inlier, evidence of a static metamorphic event is present. Static recrystallization affects the main granitoid and is, therefore, younger than the M_g event, which affected only the greenstone belts and the early banded and/or foliated granitoid. In the western part of the inlier, reworking during the Capricorn Orogeny was limited. Granitoid rocks, metagabbroic intrusions such as the gabbro at Western Creek, and Suite 1 mafic dykes, preserve extensive evidence of the static recrystallization. In contrast, the eastern part of the inlier was extensively reworked. However, evidence of the earlier static recrystallization is preserved in zones of low strain. The static metamorphic event in the inlier is presumed to be equivalent to the M_h event recognized in the Hamersley Basin rocks.

Mineral assemblages characteristic of the greenschist facies and the albite–epidote amphibolite facies in mafic rocks have been discussed by Miyashiro (1973), Laird (1980), and Maruyama et al. (1983), and involve variations within the common assemblage as defined by Laird (1980). This comprises amphibole–chlorite–epidote–plagioclase–quartz–Ti phase(–Fe^{3+} oxide–carbonate–K-mica). Unlike pelitic rocks where, in general, the mineral assemblage changes with changing grade, mafic rocks retain a fairly constant mineral assemblage, but mineral composition and modal abundances vary continuously. The typical greenschist-facies assemblage is actinolite–chlorite–epidote–albite–quartz. The assemblage hornblende–chlorite–epidote–albite–quartz characterizes the albite–epidote amphibolite facies.

The western part of the Sylvania Inlier has been metamorphosed under greenschist facies and albite–epidote amphibolite facies conditions. In the metagabbroic rocks at Western Creek and in the Suite 1 mafic dykes, greenschist facies assemblages are marked by the occurrence of actinolite and albite, accompanied by epidote, chlorite, and biotite. Actinolite–chlorite intergrowths completely pseudomorph igneous pyroxenes, while albite–epidote replaces igneous plagioclases. The albite–epidote amphibolite facies is marked by the appearance of a distinctive blue-green amphibole, which is probably edenitic (Holland and Richardson, 1979), and transitional between actinolite and true hornblende.

In granitoid rocks, assemblages of metamorphic minerals pseudomorph original igneous minerals. The assemblage albite–epidote–muscovite replaces calcium-rich igneous plagioclases. Albite is typically sieved by scattered crystals of fine-grained epidote and muscovite (Fig. 36). Intergrowths of medium-grained biotite–epidote–muscovite

pseudomorph what was once coarse-grained igneous biotite.

In the eastern two-thirds of the Sylvania Inlier, there are little-deformed rocks in which a static recrystallization, presumed to be equivalent to M_h, can be recognized. In the country between Sylvania Homestead and Woggaginna Hill, the remnants of a dismembered layered mafic sill are present. Pods of amphibolite and associated meta-anorthosite, metapyroxenite, and serpentinite, occur. Cumulus textures, together with small-scale igneous layering, are preserved. Mineral assemblages in amphibolite are hornblende–epidote–oligoclase to andesine–biotite (–chlorite). The assemblage, quartz–plagioclase (andesine to bytownite)–hornblende–epidote–garnet, which has been interpreted as the metamorphosed, granophyric top of a layered mafic sill, occurs in a calc-silicate rock near Woggaginna Hill. The static recrystallization is interpreted as having taken place under albite–epidote–amphibolite facies conditions.

The hornblende-bearing granitoid in the eastern part of the inlier contains hornblende and clinopyroxene, both of which are sodium rich. They occur with oligoclase, quartz, and epidote. The rock is thoroughly recrystallized, and neither the hornblende nor the clinopyroxene appears to be a primary igneous phase. Hornblende typically forms replacement rims around the clinopyroxene (Fig. 18). Hornblende is aligned in a foliation and has recrystallized during the M_c event. The clinopyroxene, however, may represent a remnant phase belonging to the earlier M_h event.

The occurrence of clinopyroxene is unusual in these low- to medium-grade rocks. Clinopyroxene is more normally associated with granulite facies metamorphism (Winkler, 1979). However, Droop (1982) reported a similar occurrence of clinopyroxene in metasyenite from the albite–epidote–amphibolite facies of the Austrian Alps, where its stability was controlled by the rock's bulk Al:Na+K ratio. The occurrence of clinopyroxene does not reflect a zone of anomalous high-grade metamorphism.

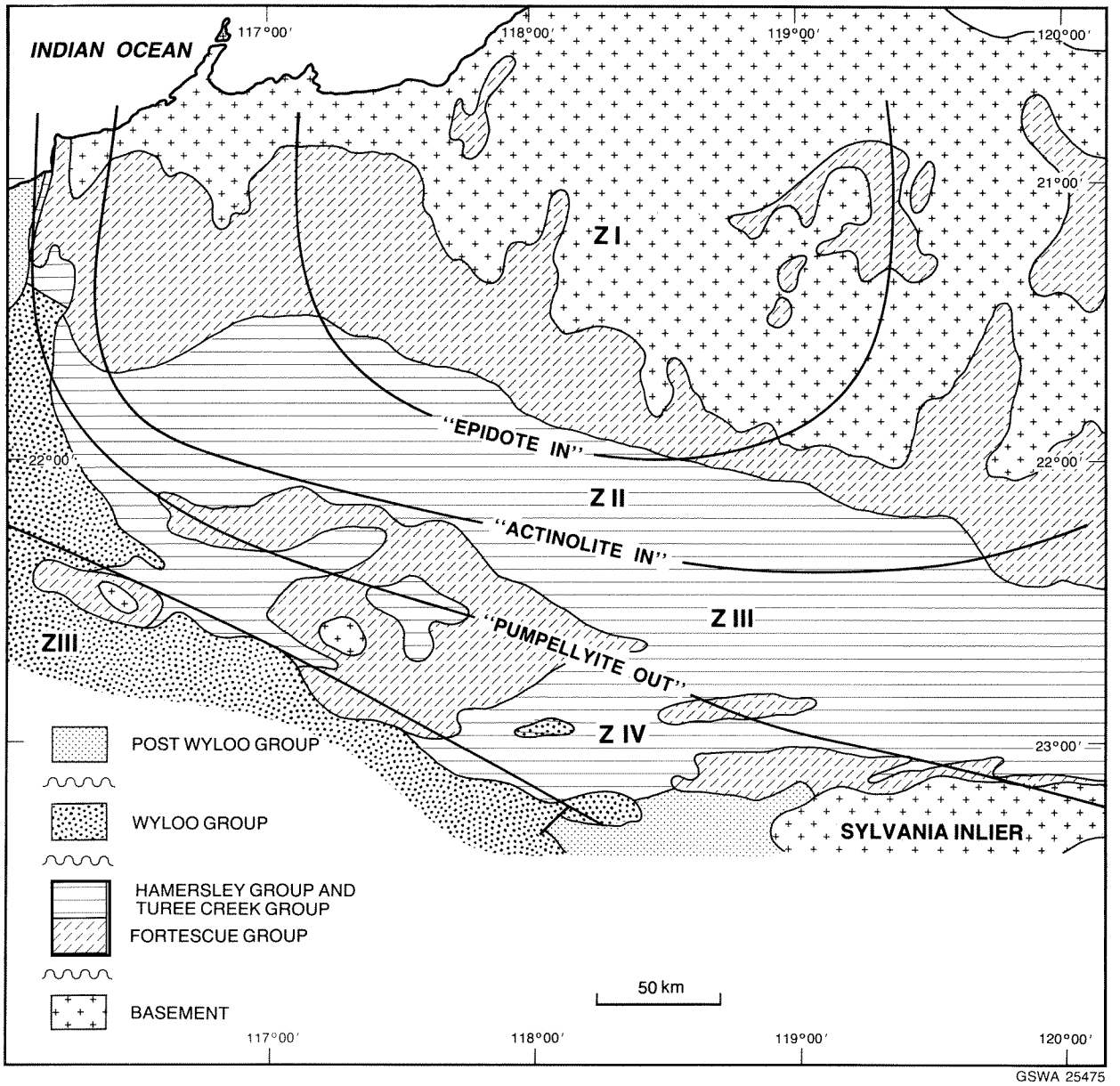

Figure 35. Metamorphic zones and intervening isograds in the Hamersley Basin as identified by Smith et al. (1982).

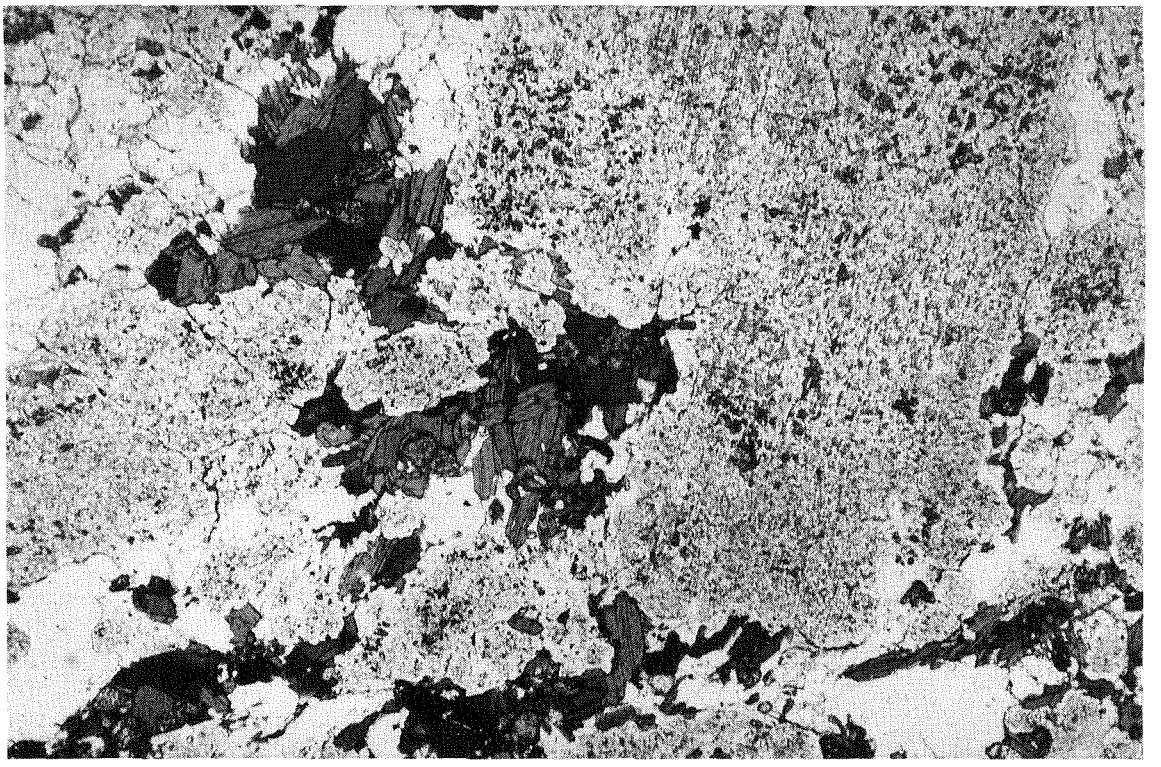

GSWA 25476

Figure 36. Metagranodiorite comprising albite laths (sieved by fine epidote and muscovite), biotite, epidote and quartz (x30). GSWA sample 81885.

Experimental studies on phase relations in mafic rocks involved in the transitions between the greenschist facies, the albite–epidote–amphibolite facies, and the amphibolite facies, have been carried out by Liou et al. (1974) and by Apted and Liou (1983). Three reactions are of interest: a chlorite-decreasing reaction; a low-pressure, epidote– chlorite-out reaction; and a higher pressure, epidote-out reaction (Fig. 37 curves 1, 2, and 3). The intersection of the epidote–chlorite-out and the epidote-out curves provides a lower pressure limit to the albite–epidote amphibolite facies. At pressures below this limit, the greenschist facies passes directly into the amphibolite facies.

The occurrence of statically recrystallized assemblages in mafic rocks, which are characteristic of the albite–epidote amphibolite facies indicates that the M_h metamorphic event in the Sylvania Inlier must have taken place at pressures above the intersection of the chlorite–epidote-out and epidote-out curves.

Fluid-phase compositions, particularly variations in fO_2, can drastically affect the temperature and pressure at which reactions take place. Liou et al. (1974), Apted and Liou (1983), and Moody et al. (1983), provide data for reactions 1, 2, and 3, where fO_2 values were controlled by the QFM, NNO, and HM buffers. Opaque minerals are generally magnetite and/or ilmenite plus sphene, and are consistent with relatively high fO_2 values, such as those represented by the NNO and QFM buffers. Intersection of curves 2 and 3 for the NNO buffer occurs at 550°C and 300 MPa. Higher fO_2 values push the intersection to higher pressures.

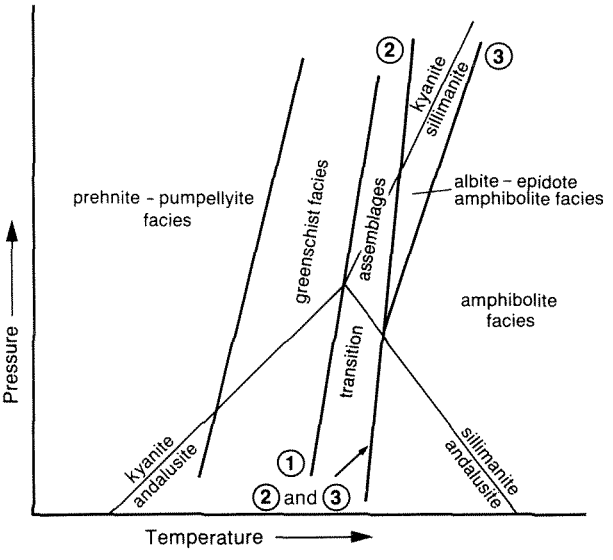

Reactions

① 'Chlorite decreasing' (Liou et al., 1974)

② 'Chlorite - epidote out' (Liou et al., 1974)

③ 'Epidote out' (Apted and Liou, 1983)

GSWA 25477

Figure 37. Temperature (T) and pressure (P) diagram illustrating the reactions which control the transitions between the greenschist facies, the albite–epidote–amphibolite facies, and the amphibolite facies in mafic rocks.

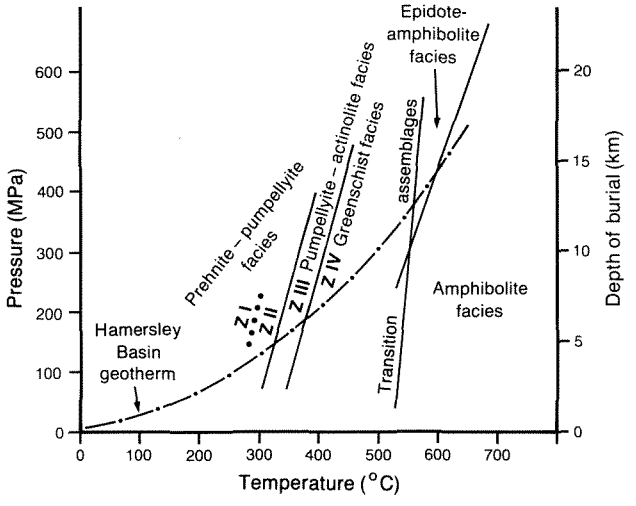

GSWA 25478

Figure 38. The Hamersley Basin geotherm, based on data from Smith et al. (1982) and from the present study.

It is not possible, with the data available, to place an upper limit on the observed assemblages other than to note that, according to Laird and Albee (1981), the absence of glaucophane seems to restrict conditions to medium pressures (less than 900 MPa).

Smith et al. (1982) constructed a temperature–depth curve for burial metamorphism in the Hamersley Basin. Their investigation involved only rocks of the Hamersley Basin succession; and the inferred depth limit was 9 km—equivalent to an overburden pressure of 250 MPa. The southwestern part of the Fortescue Group succession, adjacent to the Sylvania Inlier, has a minimum thickness of 6.6 km (Tyler, 1986). The Hamersley Group in the Newman area is 1.8 km thick (Table 6). When taken together with possible Turee Creek Group strata now removed—according to Trendall (1979) as much as 4 km—the thickness of Hamersley Basin strata in the Deadman Hill–Prairie Downs area was between 8.4 and 12.4 km. This represents overburden pressures of between 240 MPa and 350 MPa, and is consistent with metamorphism at the lower pressure end of the albite–epidote–amphibolite facies in the underlying Sylvania Inlier.

Figure 38 extends the temperature–depth diagram of Smith et al. (1982) to pass through the lower pressure end of the albite–epidote–amphibolite facies. Deposition in the basin appears to have been continuous for at least 260 Ma and probably as long as 450 M—to the end of Turee Creek Group time (Trendall, 1983). As metamorphism is regarded as being due to burial, this length of time is consistent with the curve in Figure 38 representing the true geothermal gradient of the basin, the Hamersley Basin geotherm. Tectonothermal metamorphic geotherms evolve over much shorter time periods (England and Richardson, 1977).

In the eastern inlier, the Hamersley Basin cover was much thinner (3–7 km); this requires the uplift and removal of large volumes of granitoid material (at least 4–8 km) to expose the observed albite–epidote–amphibolite facies assemblages near Woggaginna Hill.

Chapter Four

Capricorn Orogeny

Introduction

The Capricorn Orogen (Fig. 2) was defined by Gee (1979, p.352) as "a major orogenic zone involving geosynclinal sedimentation, metamorphism, basement reworking and granitoid emplacement in the region between the Yilgarn Block—now Craton (Geological Survey of Western Australia, 1990)—and the Pilbara Craton. It takes its name from the Tropic of Capricorn, at which latitude it is approximately located." Tectonic units included within the orogen were the Ashburton Basin, the Gascoyne Complex, the Nabberu Basin, and the basement rocks beneath the Bangemall Basin. In the present study the orogen is also taken to include areas on the margins of the Yilgarn and Pilbara Cratons where foreland deformation has occurred. Deformation which can be related to the Capricorn Orogeny occurs in the Sylvania Inlier, the Hamersley Basin, the Marymia Inlier, and the Narryer Gneiss Complex (Fig. 2). Available geochronological data (Libby et al., 1986) suggest that the orogen developed between 2200 Ma and 1600 Ma.

In the southern part of the Pilbara Craton (Fig. 39), Halligan and Daniels (1964) and MacLeod (1966) considered all the major folding (Fig. 40) that affected rocks within the Hamersley Basin—as it was then defined (MacLeod et al., 1963; MacLeod, 1966)—part of the Ophthalmia Fold Belt. The Wyloo Group, a sequence of terrestrial and shallow- and deep-marine sediments, was included as part of the Hamersley Basin succession. Deformation that affected the Wyloo Group was therefore included within the Ophthalmia Fold Belt. In a revision of the stratigraphy of the Hamersley Basin succession by Trendall (1979), a major unconformity between the base of the revised Wyloo Group and the Mount Bruce Supergroup (Fortescue Group, Hamersley Group, and the newly defined Turee Creek Group), was documented. This allowed Gee (1979) to recognize a separate Ashburton Basin (referred to by him as the Ashburton Trough), in which the Wyloo Group was deposited. He also recognized two separate fold belts: an older Ophthalmia Fold Belt, within which rocks of the redefined Hamersley Basin were deformed; and a later Ashburton Fold Belt, within which rocks of the Wyloo Group were deformed, and which was coincident with the geographical extent of the Ashburton Basin (Fig. 39). The Ophthalmia Fold Belt was thought to have formed as a response to block movements in the almost completely cratonized granite–greenstone basement (MacLeod, 1966; Gee, 1979). These movements took place before, or during, formation of the Ashburton Basin; and the fold belt was regarded as essentially pre-orogenic (Gee, 1979).

In the present study, numerous shear zones have been identified within the granite–greenstone rocks of the Sylvania Inlier; they post-date Suites 1 and 2 mafic dykes, and record different metamorphic conditions to those established during burial metamorphism beneath the Hamersley Basin. Structural and stratigraphic relationships in the Turee Creek Syncline (Plates 2 and 3), and the Hardey Syncline area (Trendall, 1979), indicate that folds within the Ophthalmia Fold Belt, as redefined by Gee (1979), can be divided into two groups. Folds in the western part of the fold belt form open dome-and-basin structures that trend northwest (Figs 39 and 40); these represent the central structural zone of MacLeod et al. (1963). Folding took place at the end of Turee Creek Group time and appears to be pre-orogenic. Folds in the southeast part of the fold belt, however, are orientated east–west, are close to tight, and have short wavelengths (Figs 39 and 40). These folds correspond to the southern structural zone of MacLeod et al. (1963), and formed during the evolution of the Ashburton Basin, which is regarded by Thorne and Seymour (1991) as a foreland basin that developed as part of the Capricorn Orogeny. Two periods of deformation have been recognized in the Ashburton Fold Belt (Seymour et al., 1988; Thorne and Seymour, 1991). Both are younger than deformation in the Ophthalmia Fold Belt. The southeast part of the Ophthalmia Fold Belt and the Ashburton Fold Belt are the deformed foreland at the northern margin of the Capricorn Orogen. The sequence of fold events, and their relationship to the stratigraphy of the southern margin of the Pilbara Craton, are set out in Table 7.

Ashburton Basin

The Ashburton Basin, which developed along the southern margin of the Pilbara Craton (Figs 2 and 39), is an integral part of the Capricorn Orogen. It has been the subject of an extensive study by Thorne and Seymour (1991); see also Thorne (1985) and Thorne and Seymour (1986), from which this description is derived. Rocks deposited within the basin form the Wyloo Group, which records a change from terrestrial and shallow-marine to "deep-water" sedimentation. During this evolution, the distribution of sedimentary facies was strongly influenced by local and regional tectonic activity. Pidgeon and Hor-

witz (1991) have reported a U–Pb age of 1843 ± 2 Ma from zircons obtained from an acid tuff or fragmental volcanic rock within the June Hill Volcanics near Mount Stuart, which is west of the area described in this bulletin. The June Hill Volcanics occurs locally in the upper part of the Wyloo Group.

In the Paraburdoo and Turee Creek Syncline areas, the group consists of five formations (Table 7). The lowest, comprising cream- or white-weathering, silicified quartz sandstone and locally developed BIF-derived conglomerate, mudstone, and carbonate that were deposited as part of a fan-delta system, is the Beasley River Quartzite. The Wyloo Dome–Hardey Syncline area was tectonically active during deposition; and the formation unconformably overlies folded Hamersley Basin sediments. At Paraburdoo, relationships are complicated by later strike-slip faulting (Thorne and Tyler, in press; this study). In the Turee Creek Syncline and at Mount Maguire (Plate 2), the Beasley River Quartzite and the Hamersley Basin succession are disconformable; and sedimentation took place as part of a braided-delta system, whose sediment was derived from the northeast. The delta was subsequently abandoned, and marine sedimentation extended northeast into the Turee Creek Syncline. Further east, Beasley River Quartzite unconformably overlies Woongarra Volcanics near Divide Well (Thorne and Tyler, in press) and the Weeli Wolli Formation near Deadman Hill (Tyler et al., 1990).

The overlying Cheela Springs Basalt is mainly vesicular basalt, but includes subordinate fine- to coarse-grained tuff, immature sandstone, siltstone, and mudstone, which were deposited in a coastal to shallow-marine environment. Dolerite sills are abundant.

The Mount McGrath Formation disconformably overlies the Cheela Springs Basalt and overlaps older formations (Horwitz, 1980; 1982). It unconformably overlies Hamersley Group rocks south of the Channar iron-ore deposit (Bourn and Jackson, 1979) and 12 km southeast of Snowy Mountain (Thorne and Tyler, in press). The unit comprises ferruginous conglomerate and sandstone, and quartz sandstone, siltstone, mudstone, and locally developed carbonate. The lower part of the unit was deposited on eroded lower Wyloo Group and Hamersley Basin rocks as part of a delta system associated with an uplifted source area to the north and east of Paraburdoo. In contrast, the upper part records a period of gradually deepening shelf water accompanied by a waning supply of sediment and, finally, abandonment of the delta.

The Duck Creek Dolomite rests conformably on Mount McGrath Formation and consists of thin- to thick-bedded, buff or grey-mauve dolomite. It is commonly stromatolitic. Intense silicification may have occurred locally. Carbonate, as part of a carbonate shelf fringing the landmass, accumulated in low-lying intertidal and supratidal flats and a shallow lagoon. Further off shore, deposition took place on a slope of moderate gradient. The carbonate shelf underwent a period of progradation while the middle part of the formation was being deposited. The upper part of the formation records the collapse and drowning of the prograded shelf and a return to slope and basin deposition.

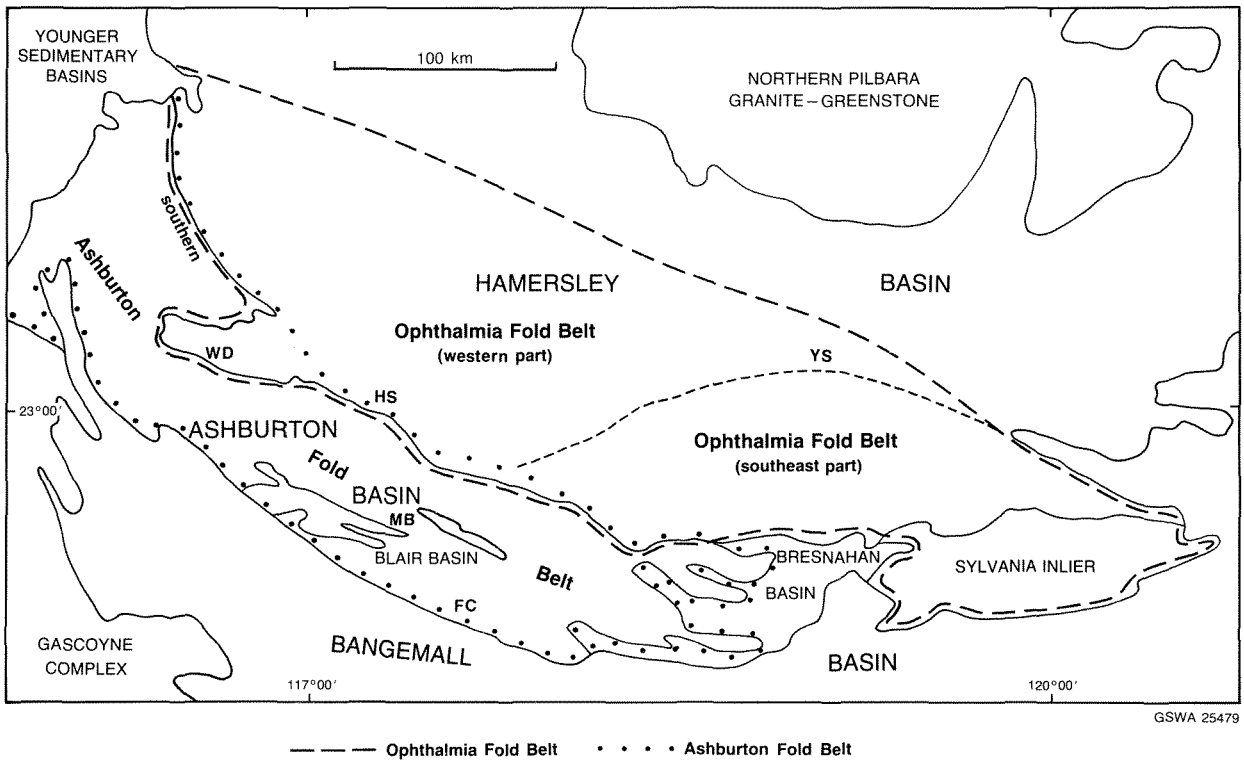

Figure 39. Map of the southern part of the Pilbara Craton showing the main tectonic units and the geographical extent of the Ophthalmia and Ashburton Fold Belts. FC - Fords Creek; HS - Hardey Syncline; MB - Mount Blair; WD - Wyloo Dome.

The Ashburton Formation, which consists of mudstone and immature sandstone interbedded with a small amount of conglomerate, BIF and chert, and felsic to mafic volcanics, conformably overlies the Duck Creek Dolomite. The sandstone was derived from a dominantly granitic source. Granitic sand and mud were shed into the eastern end of a deep marine basin, and were distributed westward by a submarine fan system extending as far as the Wyloo Dome. Later uplift southwest of the basin supplied sediment to a submarine fan system south of the Wyloo Dome. Sediment derived from the Hamersley Basin supplied a third submarine fan complex northwest of the Wyloo Dome.

The Ashburton Formation is conformably overlain by an unnamed stromatolitic dolomite unit near Saltwater Pool in the southwest corner of NEWMAN (Tyler et al., 1990).

Blair Basin

The Blair Basin is occupied by the Capricorn Formation (Fig. 39), which rests with angular unconformity on the Ashburton Formation. The Capricorn Formation was described by Thorne and Seymour (1991); it consists of sandstone, siltstone, mudstone, and small amounts of conglomerate, dolomite, and felsic volcanic rock. The lower part was deposited by braided streams that entered a shallow-marine (or lacustrine) environment. The middle part was influenced by a relative rise in sea level, which drowned much of the basin. This was followed by uplift of the source area and progradation by braided-fluvial systems. In the final stages of basin filling, alluvial-fan deposits were dominant.

TABLE 7. STRATIGRAPHY, AND SEQUENCE OF CAPRICORN OROGENY DEFORMATION EVENTS: SOUTHERN MARGIN OF THE PILBARA CRATON

Stratigraphy	*Fold belt*	*Event*	*Nature of deformation*
BLAIR BASIN			
Capricorn Formation	ASHBURTON FOLD BELT	D_{2a}	Dextral wrench faulting and associated folding.
— unconformity —		D_{1a}	Recumbent folding and thrusting.
ASHBURTON BASIN			
Wyloo Group			
Ashburton Formation			
Duck Creek Dolomite			
Mount McGrath Formation			
— unconformity or disconformity —	OPHTHALMIA FOLD BELT (southeast part)	D_{2c} & D_{1c}	Folding and thrusting of Hamersley Basin succession. Shear zones in Sylvania Inlier.
Cheela Springs Basalt			
Beasley River Quartzite			
— unconformity —	OPHTHALMIA FOLD BELT (western part)		Open dome-and-basin folding.
HAMERSLEY BASIN			
Turee Creek Group			
Hamersley Group			
Fortescue Group		rifting of cratonic basement	Normal faulting
— unconformity —			
granite - greenstone			

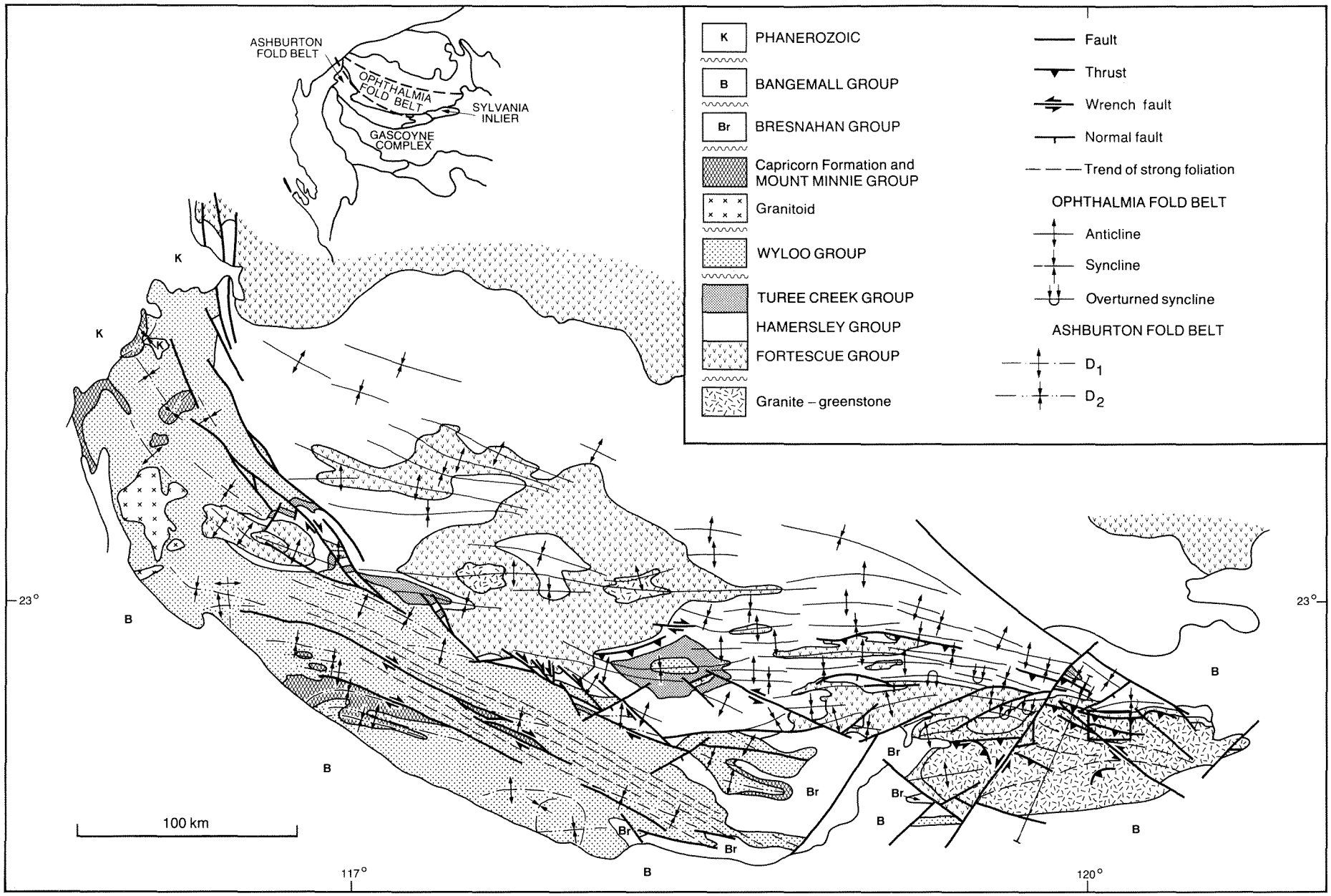

Figure 40. Simplified geological map of the southern Pilbara showing the main structural features (folds, faults, and cleavage trends).

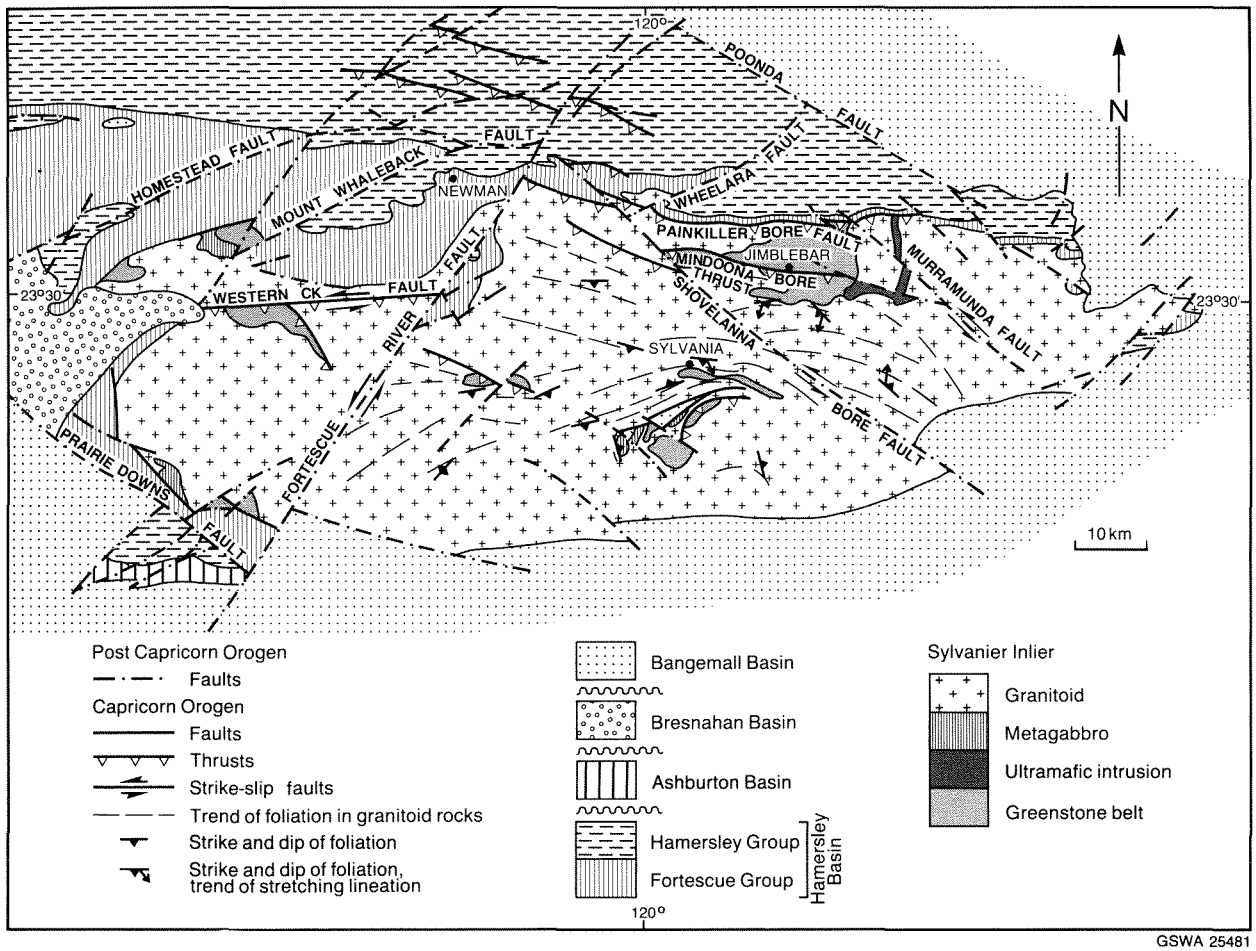

Figure 41. Simplified geological map showing the main structural features within the Sylvania Inlier.

Figure 42. Schistose granitoid in a shear zone in the Sylvania Inlier.

Capricorn Orogen structures in the Sylvania Inlier

Within the Sylvania inlier east of the Fortescue River Fault, numerous shear zones are present (Figs 41 and 42). These shear zones are seen to cut across large-scale D_{2g} and D_{3g} structures in the greenstone belts. They also post-date Suite 1 and 2 mafic dykes, which are probably related to rifting during the early stages of the formation of the Hamersley Basin. As will be discussed, the shear zones can be related to folding in the southeast part of the Ophthalmia Fold Belt and are here regarded as having formed during the Capricorn Orogeny. Blockley et al. (1980) reported a Rb - Sr isochron, giving an age of 2235±54 Ma, from an inlier of Archaean granitoid unconformably overlain by Fortescue Group rocks at the eastern end of the Ophthalmia Dam. This age is anomalous when compared with the known age, 2750–2500 Ma (Trendall, 1983), of the overlying Fortescue Group rocks, and has been interpreted as the product of equilibration, during uplift, of Sr isotopes with Proterozoic water from the Hamersley Basin. As such it may represent a maximum age for deformation.

Granitoid in the eastern part of the Sylvania Inlier developed a foliation (S_c) parallel to the shear zones. Megacrystic varieties developed augen that are wrapped by the S_c foliation. Strain was inhomogeneous, and it is possible to trace foliated granitoid into chlorite- and mica-bearing quartzofeldspathic schist. The shear zones, and the S_c foliation in less deformed granitoid, trend generally east–west, although there is a swing to the southwest as the Fortescue River is approached. A swing to the southeast occurs towards the eastern end of the inlier, and is well exposed near Red Hill. Shear zones and foliation dip moderately to steeply southwards in the northern part of the inlier. In the southern part of the inlier, the shear zones are folded, and vertical to northerly dips are present. Rocks within the shear zones often show a pronounced stretching lineation (L_c) on foliation surfaces, and this maintains a generally north-northeast orientation independent of the foliation trend.

The most intense deformation is observed towards the southern margin of the inlier, between Sylvania and Woggaginna Hill. Here, blocks of greenstone belt, which may be up to 700 m across, form boudins within shear zones. The shear zones are also seen to pass from granitoid into the blocks of greenstone, and mylonitic fabrics are common in both. In the Woggaginna Hill area, shear zones and greenstone belts have been folded into open-to-close easterly trending fold structures. Where small-scale folds of banding occur, a new axial-plane cleavage, defined by biotite, has formed (Fig. 43).

Rocks within the shear zones in the Woggaginna Hill area are typically blastomylonitic. In well-banded and foliated mylonites, elongate medium- to coarse-grained quartz, together with finer aggregates of quartz, form ribbon structures around granoblastic lenticular aggregates of feldspar, which may contain relics of primary igneous feldspar crystals (Fig. 44). In more intensely deformed rocks, complete recrystallization has occurred, and a new, typically schistose, fabric can be seen. The best example of this is a chlorite–biotite–muscovite–kyanite–quartz schist that crops out 6 km south of Sylvania (Fig. 45). It occurs on the margins of a strip of greenstone, and grades northwards into foliated granitoid.

Rocks in shear zones in the northern part of the inlier are also blastomylonitic; however, the intensity of recrystallization is less. Again, shear zones cut both granitoid and greenstone, and one such structure is demonstrably a south-dipping thrust. It is named the Mindoona Bore Thrust (Plates 1 and 3) and trends east–west to form the northern margin of the Jimblebar greenstone belt near Mindoona Bore. To the east, the thrust cuts across the trend of the greenstone belt offsetting D_{2g} structures near the old battery. Small-scale D_{2g} folds south of Mindoona Bore were refolded by this event. The thrust dies out as it nears Coobina. Within the greenstone belt, its position is marked by sheared, strongly foliated and lineated amphibolite, which is best exposed near Mindoona Bore and to the south of Copper Knob. Adjacent granitoid is also foliated and lineated, and near Shovelanna Bore, the thrust passes into mylonitic granitoid. A similar south-dipping shear zone occurs at the margin of the Warrawanda Creek greenstone belt.

Typically, the granitoid rocks in the northern part of the inlier have a strongly developed anastomosing foliation: trails and strings of fine-grained quartz and phyllosilicates wrap around medium to coarse feldspar porphyroclasts (Fig. 46). Chloritization of pre-shearing biotite is common. The amount of fine-grained material present is an approximate indication of the amount of strain suffered by the rock (White, 1979), and all stages, from weakly deformed to

GSWA 25483

Figure 43. Recrystallized mylonite with a new axial-plane cleavage defined by orientated biotite crystals (x35). GSWA sample 81845.

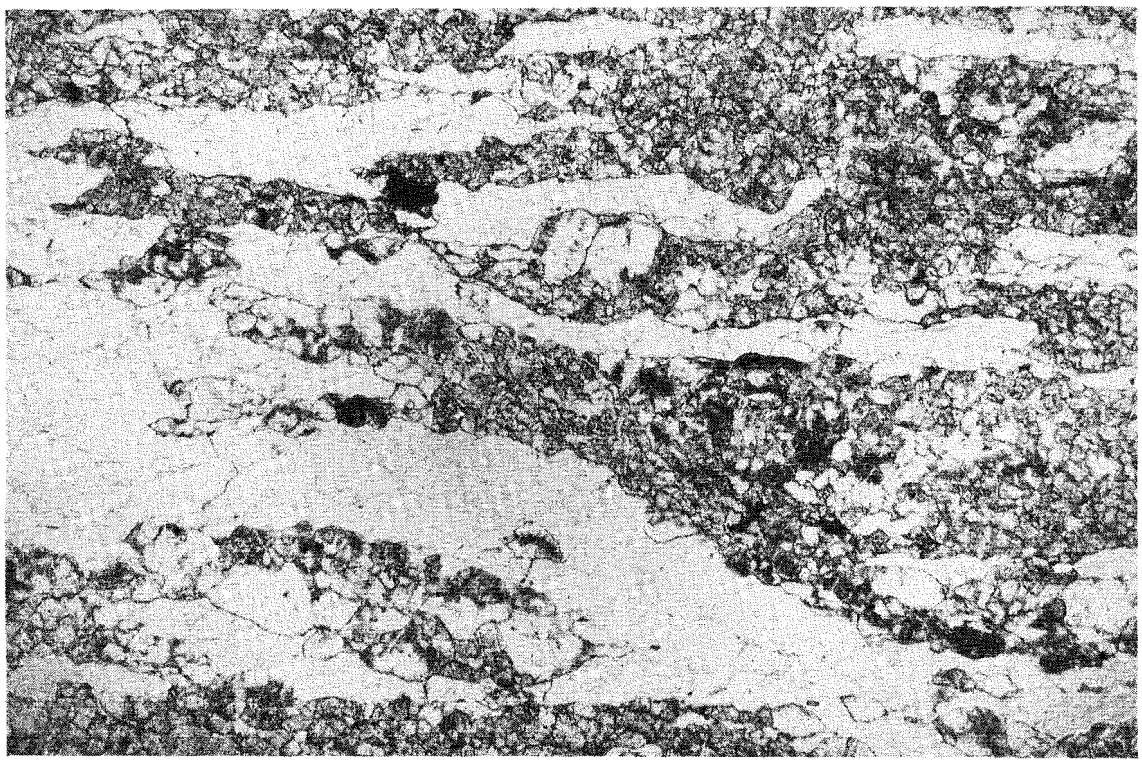

GSWA 25484

Figure 44. Blastomylonite; quartz ribbons interlayered with lenticular aggregates of granoblastic feldspar. Relics of primary igneous feldspar crystals may be seen within the aggregates (x28). GSWA sample 81818.

strongly mylonitized rock, are seen. The anastomosing form of the foliation gives the granitoid rocks their distinctive augen-gneiss appearance. Mafic rocks show similar fabrics, although the S_c foliation is defined by an alignment of amphibole with quartzofeldspathic strings (Fig. 47). Medium- to coarse-feldspar porphyroclasts may be present.

Pre-Capricorn Orogeny structures tend to have been re-orientated and intensified. This is seen in the orientation of Suite 1 dykes. Near the southern ultramafic intrusion, the dykes have a north-northeast orientation. In the centre of the eastern part of the inlier, their orientation is east-northeast (Plate 2). This re-orientation is accompanied by an increasing intensity of deformation, both of the dykes themselves and the adjacent granitoid. Open to close folds of the dykes, whose axial planes are parallel to the trend of the S_c foliation and shear zones, may occur.

Although not directly exposed, the contact between the inlier and Fortescue Group cover-rocks—from north of Jimblebar to south of the Ophthalmia Dam—is interpreted as a south-dipping thrust fault or shear zone, rather than an unconformity as previously mapped (de la Hunty, 1969). The contact is marked by a zone of lateritized quartz veining, which is offset by later, conjugate, northwest- and northeast-trending faults. This contact is parallel to the shear zones in the inlier, most notably the Mindoona Bore Thrust. A well-developed south-dipping foliation is seen in both Fortescue Group rocks and adjacent granitoid. Folds within the Fortescue Group, which are overturned to the

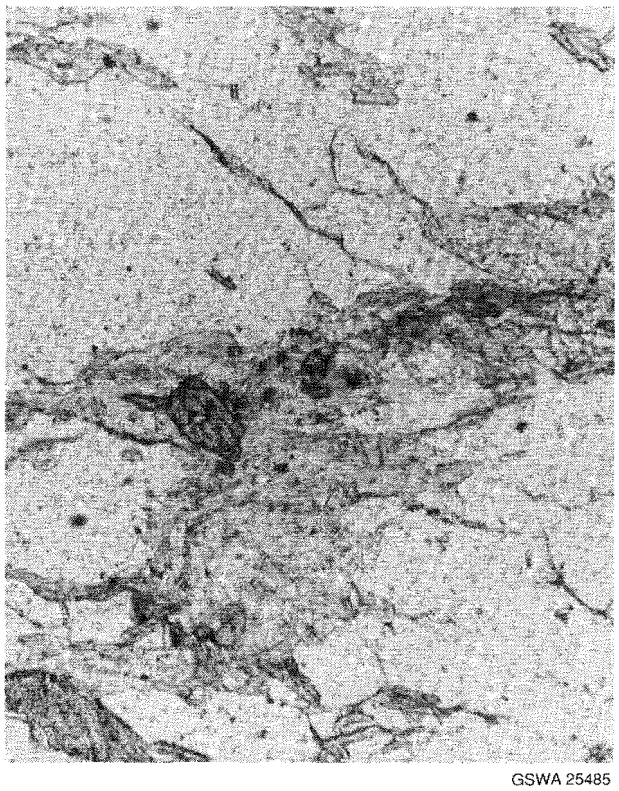

GSWA 25485

Figure 45. Quartz–chlorite–biotite–muscovite–kyanite schist from a shear zone south of Sylvania (x40). GSWA sample 81832.

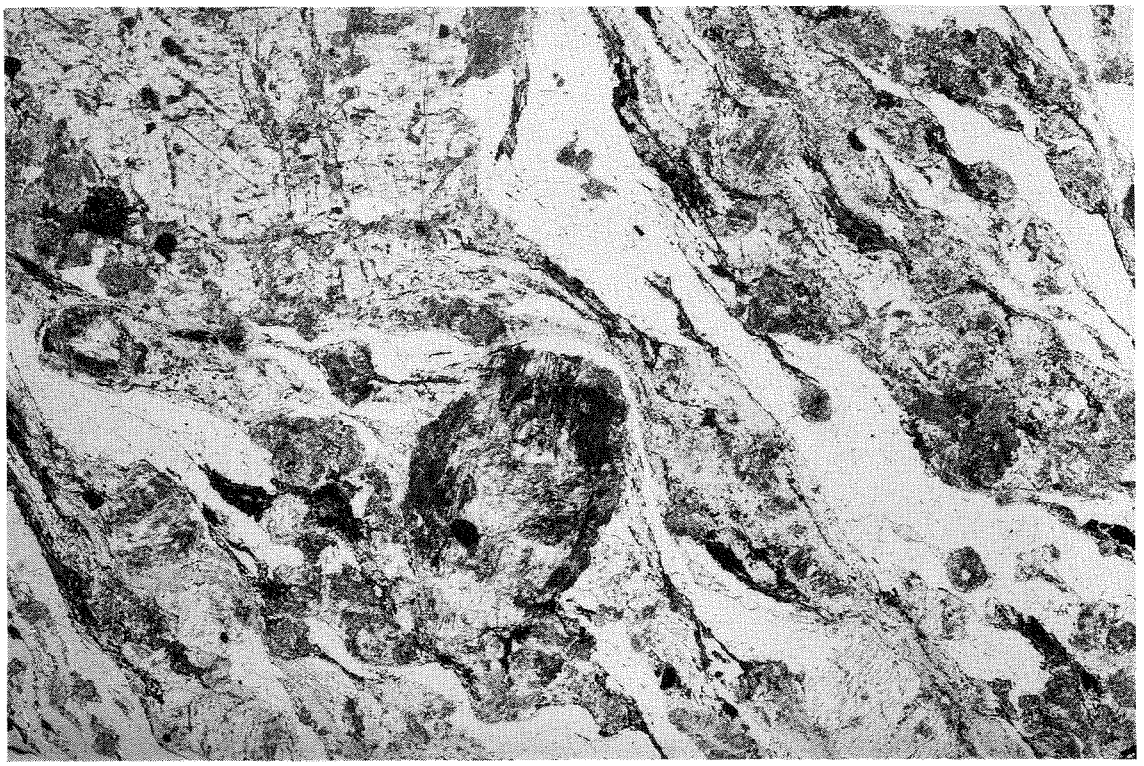

GSWA 25486

Figure 46. Mylonitic "augen" granitoid with quartz–phyllosilicate strings defining the S_c foliation and wrapping around feldspar porphyroclasts (x8). GSWA sample 85352.

GSWA 25487

Figure 47. Mylonitic amphibolite, near Mindoona Bore (x30). GSWA sample 73370.

GSWA 25488

north, become tighter and, ultimately, isoclinal as the contact is approached. The contact thrust and the folding in the cover are, therefore, interpreted as having formed contemporaneously. Like the Mindoona Bore Thrust, this structure, which will be referred to as the Painkiller Bore Fault, dies out to the east. An unconformity is present where the Murramunda–Jigalong road crosses the contact at the eastern end of the inlier.

In the western part of the inlier, relatively few shear zones are present. One occurs in granitoid 1.5 km northwest of Deadman Flat. A major east-trending fault, the Western Creek Fault, is interpreted along the line of Western Creek, east of its junction with Spearhole Creek (Plates 2 and 3). The offset of the Fortescue Group rocks where they are cut by the Western Creek Fault indicates an apparent sinistral movement of the order of 10 km (Plate 2 and 3). A southeasterly trending splay from the Western Creek Fault forms the northeast margin of the Spearhole Creek greenstone belt. The splay is characterized by a zone of high strain in banded iron-formation. Small, tight to isoclinal folds with sub-horizontal axes are common. These folds are orientated parallel to the fault zone and, in areas of particularly high strain, have become rootless structures (Fig. 48), and a southwest-dipping foliation has formed in adjacent granitoid.

Figure 48. Highly strained BIF. Isoclinal small-scale folds of banding become rootless, intrafolial folds in areas of highest strain.

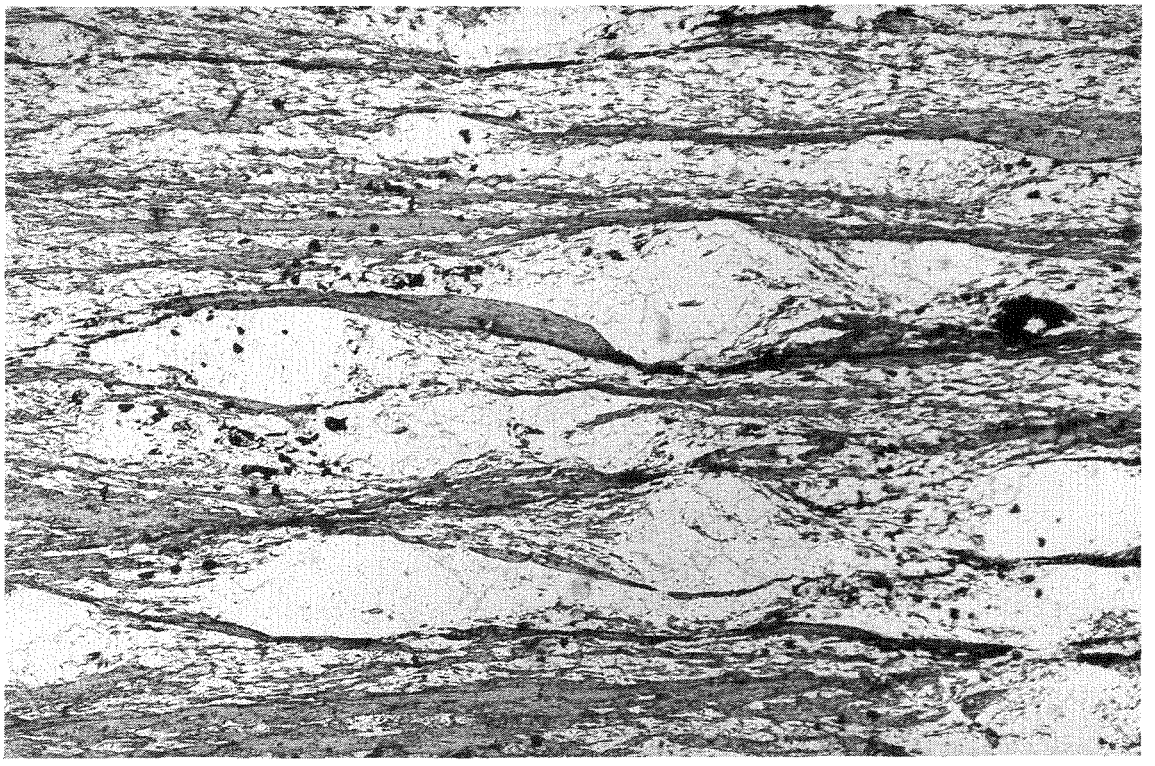

GSWA 25489

Figure 49. Mylonitic psammitic metasedimentary rock with an anastomosing foliation wrapping around porphyroclasts of quartz (x25). GSWA sample 81873.

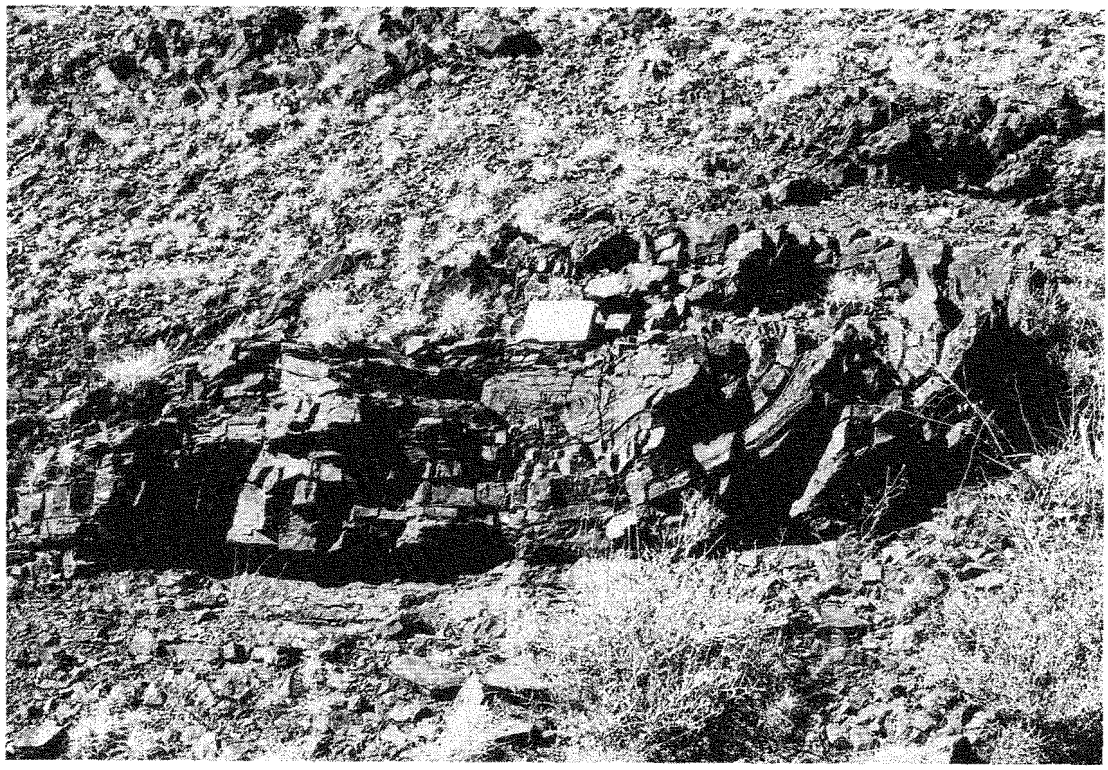

GSWA 25490

Figure 50. Flat-lying, isoclinal D_{1c} fold in lowermost Boolgeeda Iron Formation.

Southeastern Ophthalmia Fold Belt

The area which has been investigated in the present study includes all those folds which form the younger southeastern grouping within the Ophthalmia Fold Belt (Fig. 39). Within this group, two phases of deformation have been recognized which will be distinguished by the suffix "c". An early event (D_{1c}) is marked by small, layer-parallel folds and associated mylonites which are restricted in their occurrence, and a later regional fold event (D_{2c}).

First deformation phase

D_{1c} structures were seen at a few localities. They are restricted to particular stratigraphic horizons, and have, so far, been recognized in the basal metasedimentary unit of the Fortescue Group, in the upper Jeerinah Formation and basal Marra Mamba Iron Formation, in the central BIF unit of the Woongarra Volcanics, and at the base of the Boolgeeda Iron Formation. Although not abundant, they have a wide geographical distribution, and have been recognized north of Wheelara Hill, in the Newman area, in the Wonmunna Anticline, and in the Turee Creek Syncline.

Mylonitic rocks in the basal metasedimentary unit of the Fortescue Group crop out 8 km south of the Capricorn Roadhouse, where schistose psammitic and semi-pelitic metasedimentary rocks are present. The foliation is flat-lying, typically anastomosing, and wraps around porphyroclasts of quartz, which may reach 5 mm in length (Fig. 49). It is defined by well-orientated muscovite and strings of recrystallized fine-grained, granular, polygonal quartz. Mica crystals are commonly so well aligned that they go to extinction together over wide areas of a single thin section. Coarser grained, more conglomeratic beds, which show variable amounts of strain and recrystallization are also present. Textures are essentially blastomylonitic.

At the other stratigraphic horizons, folding is well developed in chert and BIF: it comprises small-scale tight to elastica (Figs 50 and 51) folds; elastica folds have a negative inter-limb angle (Ramsay and Huber, 1987, p.313). The axial surfaces of these folds are sub-parallel to bedding. The development of an axial-plane cleavage (S_{1c}) (Fig. 52) indicates that these are tectonic rather than soft-sediment folds. An intersection lineation (L_{1c}) is commonly seen on bedding surfaces. Usually, fold hinges have gentle to moderate plunges; but even where steep down-dip plunges are seen, a stretching lineation has not developed.

Folding is restricted to zones of high strain no more than 5 m thick, and often localized by bedding planes. Strain was inhomogeneous, and folds become tighter in these zones. Near the radio transmitter 32 km north-northeast of Newman, a zone of high strain occurs at the base of the Boolgeeda Iron Formation. Strain increased downwards, and the high strain zone is truncated by the contact with the underlying Woongarra Volcanics. No evidence for high strain can be seen in the underlying rocks.

D_{1c} structures have clearly been refolded by the later regional D_{2c} structures. This relationship can be seen in a west-plunging D_{2c} syncline 8 km northwest of Newman.

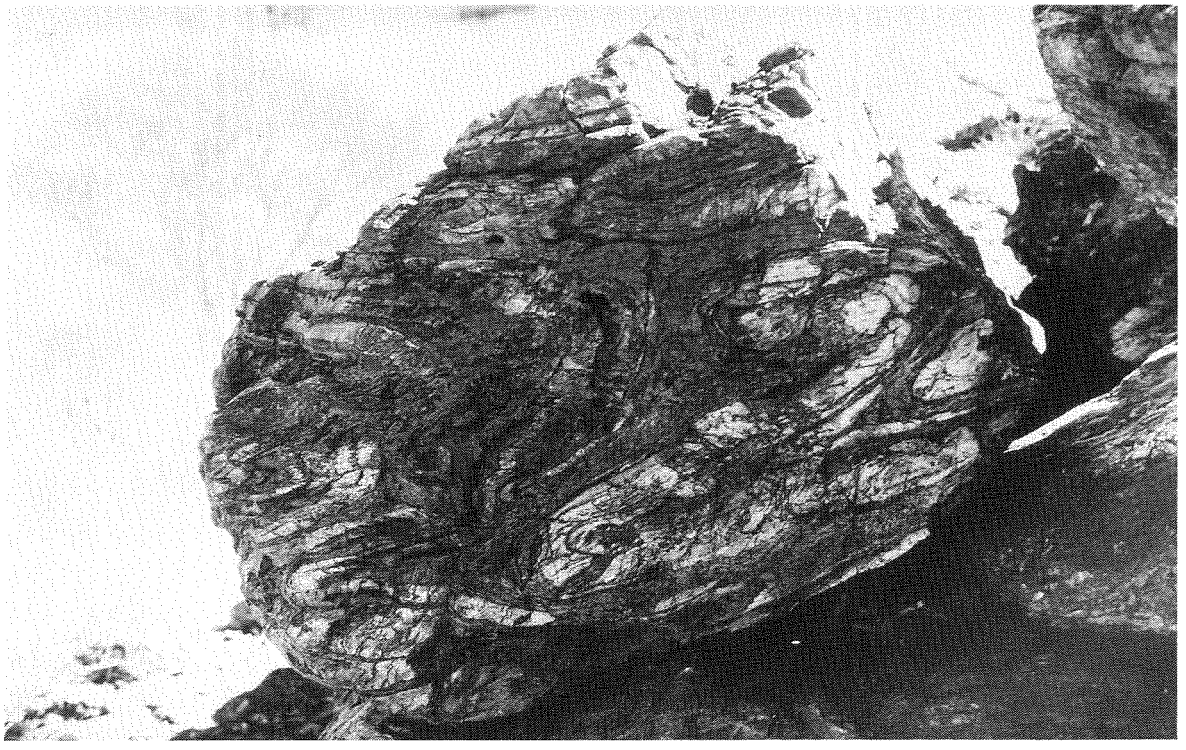

GSWA 25491

Figure 51. Tight to isoclinal D_{1c} folds in upper Jeerinah Formation chert.

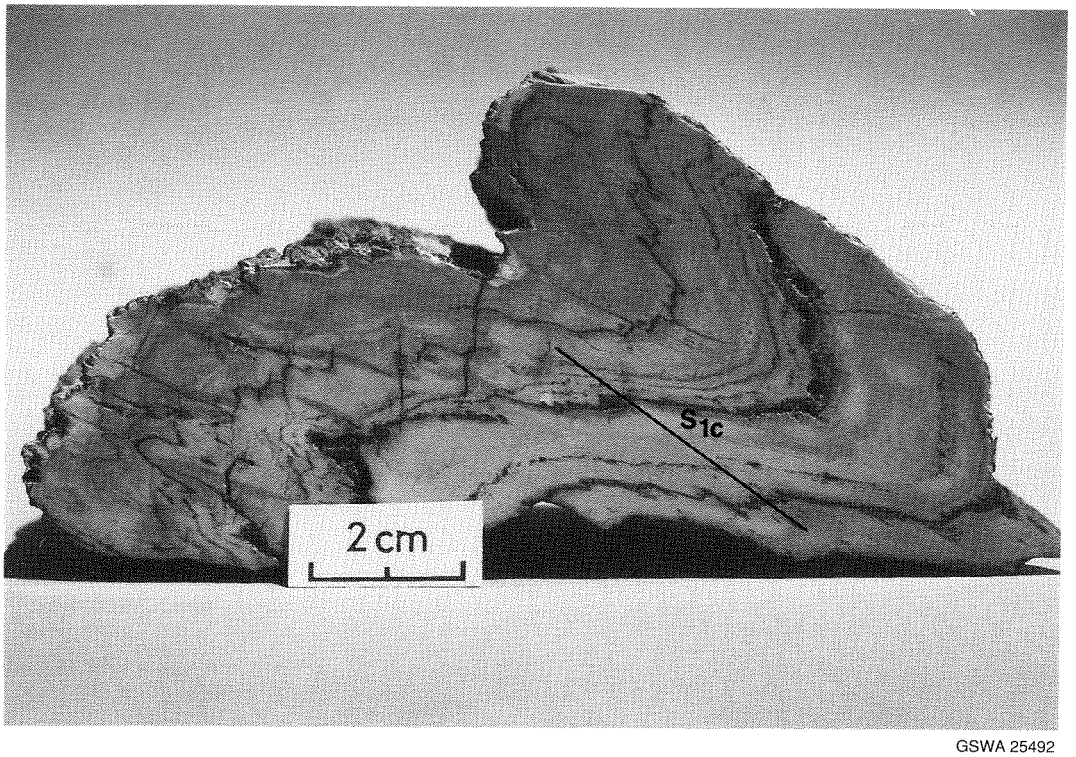

GSWA 25492

Figure 52. D_{1c} fold from upper Jeerinah Formation showing a well-developed axial-plane S_{1c} cleavage.

Here, layer-parallel D_{1c} isoclinal folds in the upper part of the Jeerinah Formation can be traced from the overturned and steeply dipping southern limb to the shallowly dipping northern limb. Small-scale hooked, refolded folds—Type 3 of Ramsay (1967)—occur in the fold nose.

Second deformation phase

The D_{2c} event is the most prominent deformation event in the southeast Hamersley Basin, and folding can be recognized from Limestone Well in the east to the Turee Creek Syncline in the west (Plates 2 and 3). The northern limit, which is south of the Yandicoogina Syncline and which is marked by a general northwest, rather than a west or west-northwest, orientation of the folds, is gradational. The southern limit is marked by contacts with the Bresnahan and Bangemall Groups.

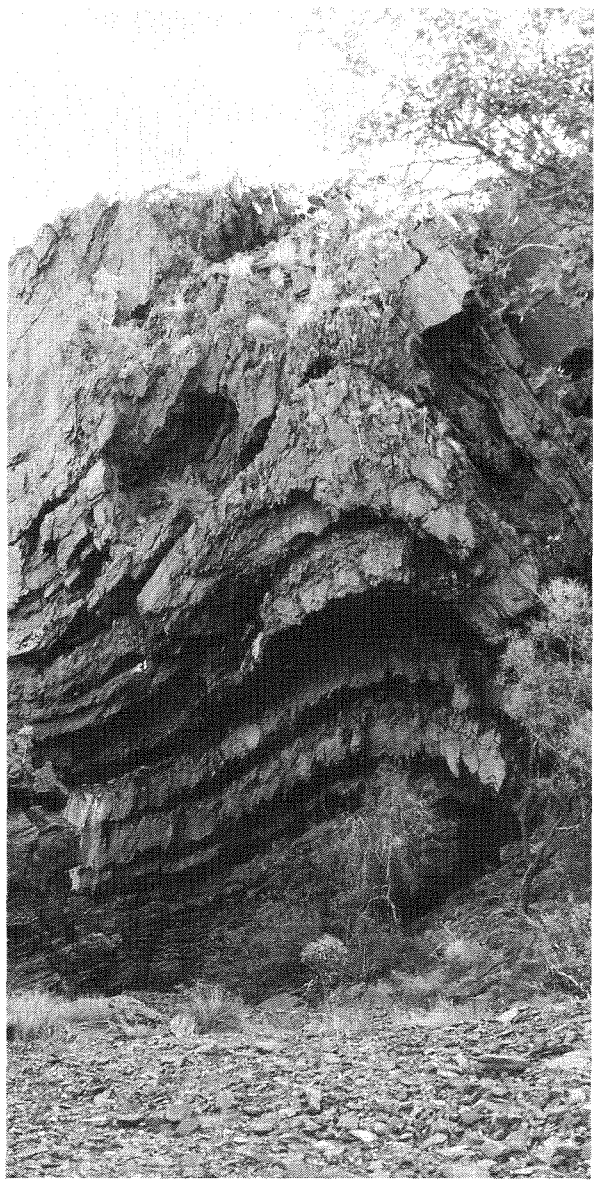

GSWA 25493

Figure 53. Upright, open to close D_{2c} fold in the Dales Gorge Member of the Brockman Iron Formation, near Weeli Wolli Spring.

Deformation is pervasive and is seen on all scales. It takes the form of generally north-facing, open to elastica folds with upright to recumbent axial surfaces (Figs 53 and 54) that often have a conjugate, box-type form (Fig. 55). Folds are typically buckle-type with rounded hinges, non-cylindrical, and impersistent, and die out both laterally and vertically along their axial surfaces (e.g. Fig. 56). Fold profiles vary considerably from parallel to flattened parallel, near similar forms (cf. Ramsay and Huber, 1987) (Figs 57 and 58). Plunges are usually gentle to moderate, to either the east or west. A cleavage is present, which becomes weak or absent in the west.

On the basis of intensity of deformation, two main areas of folding can be identified: an area of high strain north of the Sylvania Inlier that involves some 10 km of shortening (Plate 2, Section E–F); and an area of low to moderate strain northwest and west of the inlier that involves only 2 km of shortening (Plate 2, Section C–D). North of the Sylvania Inlier, two zones can be recognized: a zone of overturned north-facing folds; and, to the north of that, a zone of reverse faulting and folds with steeply inclined to upright axial surfaces (Plate 3).

Within the zone of overturned folds, which extends as far north as the northern limb of the Mount Newman Syncline (Fig. 59), fold traces are orientated west-northwest. Deformation is at its most intense adjacent to the Painkiller Bore Fault, a feature well illustrated throughout Fortescue and lower Hamersley Group rocks between the Fortescue River and Wheelara Hill. Overturned folds with moderately to gently inclined axial surfaces, are ubiquitous. Local thrusting is present: 6 km west-southwest of Shovelanna Hill, Jeerinah Formation and lower Marra Mamba Iron Formation have been thrust over Marra Mamba Iron Formation. At the eastern end of the Ophthalmia Dam, rocks of the south-dipping Jeerinah Formation are seen to structurally overlie rocks of the Marra Mamba Iron Formation that form the core of a north-facing syncline.

Along the northwest margin of the Sylvania Inlier is a series of overturned synclines and anticlines comprising the east-plunging Eastern Ridge Syncline, and the west-plunging Mount Whaleback and Western Ridge Synclines (Plate 3). A plunge reversal has produced a doubly plunging anticline–syncline pair north of Outcamp Well.

The Mount Whaleback iron-ore mine has been developed within the Brockman Iron Formation, which forms the core of the Mount Whaleback Syncline. Ore is found primarily in the Dales Gorge Member of the Brockman Iron Formation and the upper part of the Mount McRae Shale. The other members of the Brockman Iron Formation are also present in the mine area, as is the Mount Sylvia Formation. The mine provides an excellent opportunity for a detailed look at the anatomy of the folds, particularly with regard to the relationship of smaller to larger structures.

As part of the regional Mount Whaleback Syncline, the rocks have been folded into two overturned, asymmetrical synclines; the east syncline and the south syncline are separated by the central anticline (Kneeshaw, 1975). In the following discussion large-scale structures are those on a

GSWA 25494

Figure 54. Recumbent D_{2c} fold in Marra Mamba Iron Formation south of Newman.

scale equivalent to the east and south synclines and the central anticline. Medium-scale structures are folds varying from a few tens to a hundred metres in wavelength. Small-scale fold structures vary from a few centimetres to several metres in wavelength.

Folds are usually overturned, and the south-dipping axial surfaces vary from steeply inclined to near-recumbent (Figs 60 and 61). Thrusts may occur on the overturned limbs. Local downward-facing folds have gently north-dipping axial surfaces (Fig. 62). In the central part of the mine, axial surfaces become flat lying, and dips are westward, coincident with the overall moderate to gentle westward plunge (Fig. 63).

The typical, asymmetrical fold can be divided into a shallowly dipping limb and a steeply dipping, typically overturned, limb (Fig. 64). A structural fanning of smaller folds about large structures can be recognized; tightness and orientation of small structures vary according to their position on the larger structure. The tightness of small structures also varies as a response to lithological controls within stratigraphic units. On shallowly dipping limbs, small structures are tight and have moderately to steeply inclined axial surfaces (e.g. Fig. 60). On steep limbs, open folding is present in massively bedded units such as the

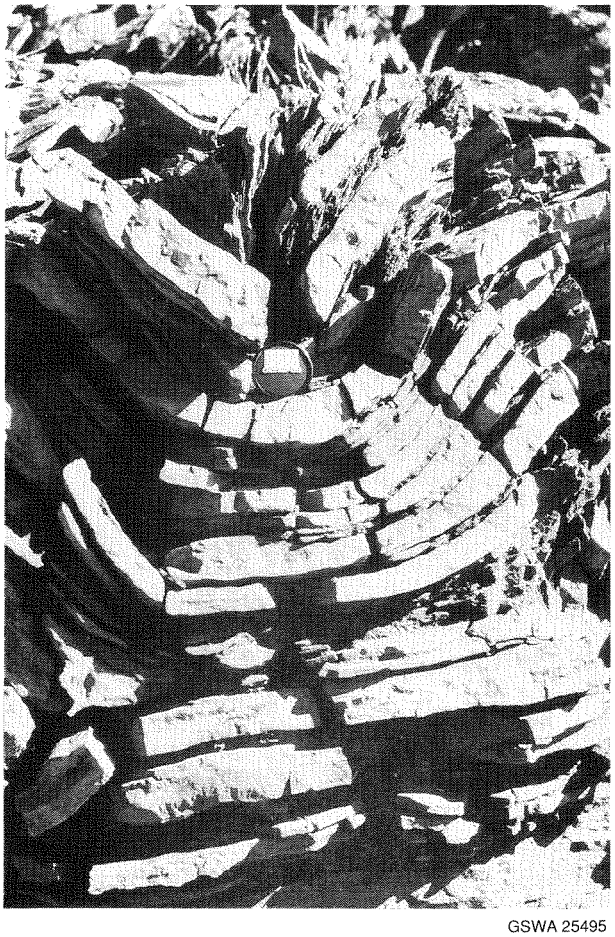

GSWA 25495

Figure 55. Upright conjugate D_{2c} fold in Weeli Wolli Formation BIF, Kalgan Creek.

GSWA 25496

Figure 56. D_{2c} buckle folds in Mount McRae Shale near Paraburdoo. Note how folds die out down their axial planes.

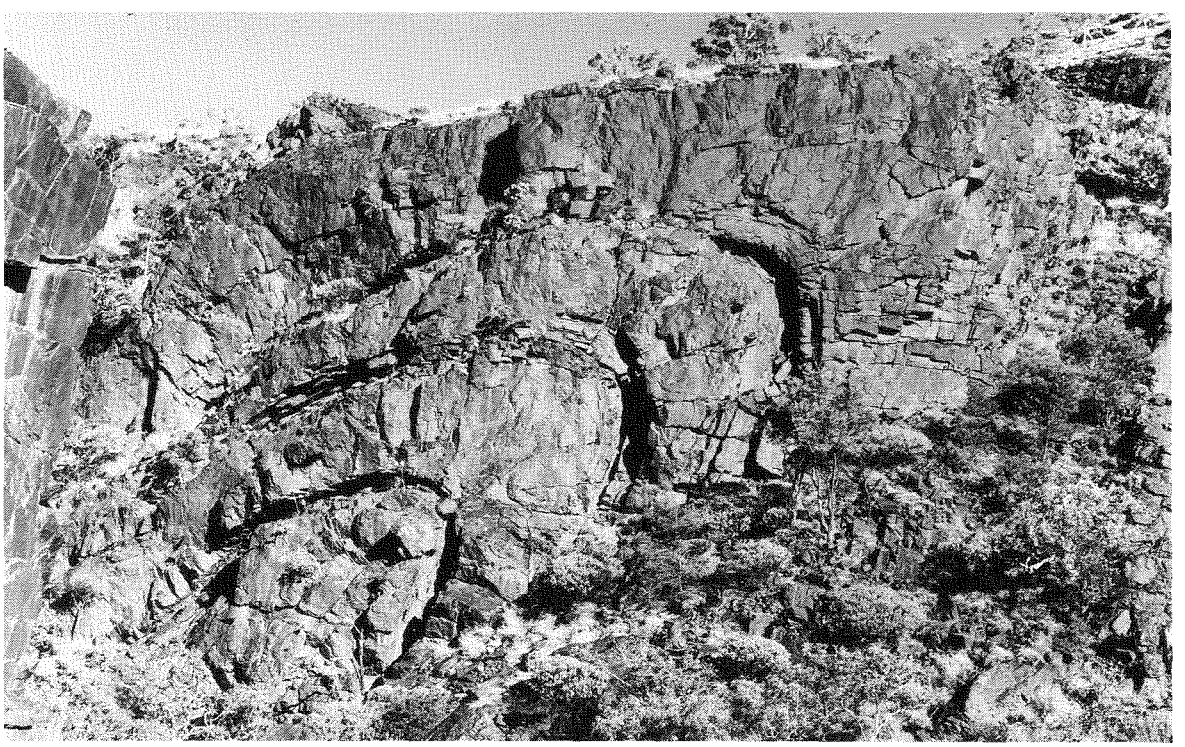

GSWA 25497

Figure 57. Large, overturned D_{2c} fold in the Dales Gorge Member of the Brockman Iron Formation, near Mount Newman. Note flattened, parallel, near similar profile.

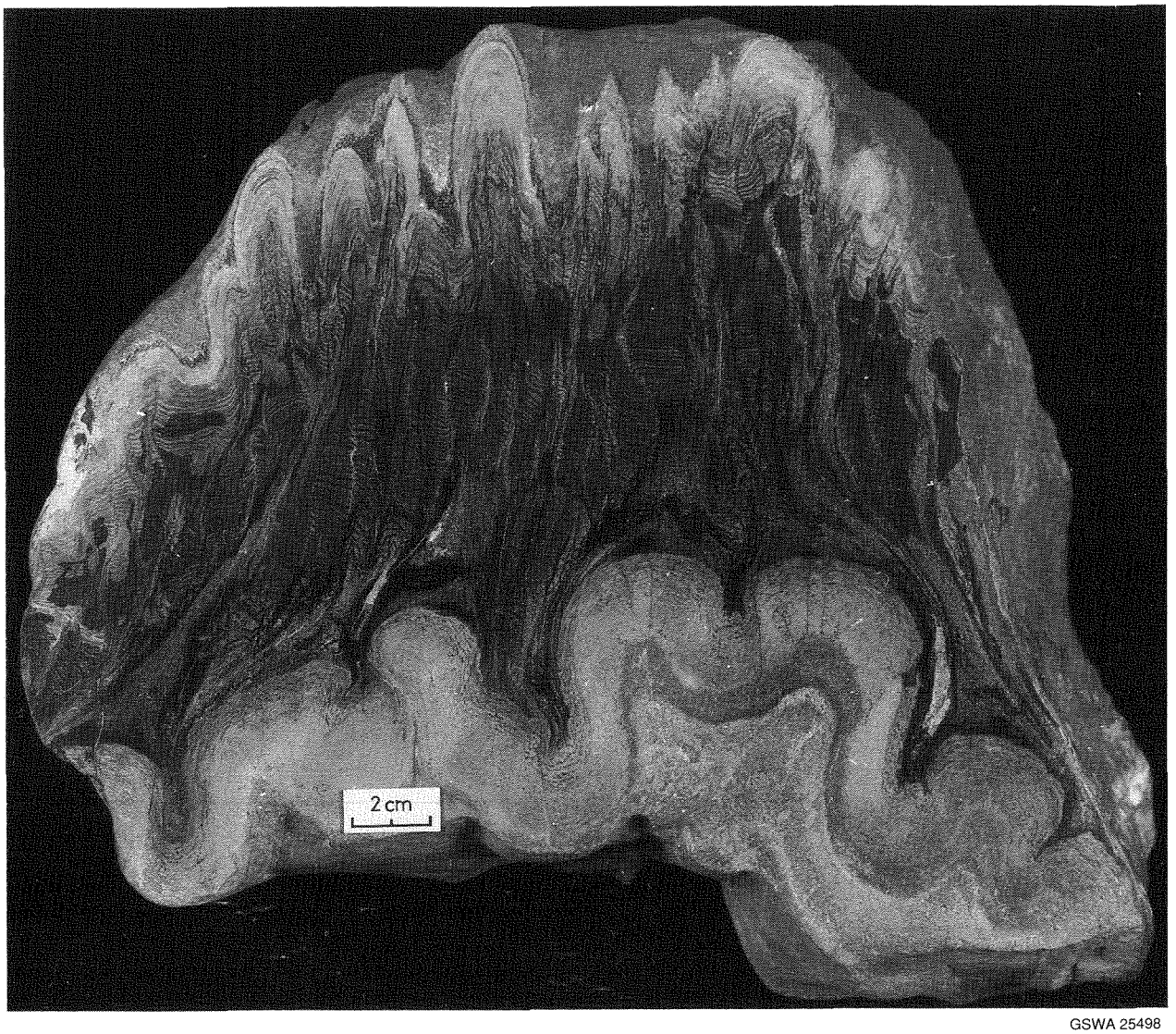

GSWA 25498

Figure 58. Polished slab from the Joffre Member, Brockman Iron Formation, Mount Whaleback Mine. Note parallel, conjugate D_{2c} folding in lower part and compare with flattened parallel D_{2c} folds in upper part. A wavy, anastomosing spaced S_{2c} cleavage, defined by seams of hematite, is well developed. GSWA sample 42229.

Joffre Member, where competency contrasts between individual beds are small (Fig. 65). The Mount Sylvia Formation and the Mount McRae Shale comprise thinly bedded, rapidly alternating shale, siltstone, chert, and BIF bands. Here competency contrasts are large, and stacks of isoclinal to elastica folds are common in the more competent chert and BIF (Fig. 61). Examples of disharmonic folding are widespread. Both the open folds and the isoclinal folds have near-recumbent axial surfaces.

Boudinage features, principally pinch and swell structures in chert on shallow limbs, have been caused by rotation of the fold limbs into the extension direction during folding (Fig. 66).

The zone of reverse faulting that can be seen in the Kalgan area (Plate 2 and 3) is characterized by moderately to steeply south-dipping, west-northwest-trending faults (Fig. 67). One of the best exposed examples is on the north side of a short railway cutting in Ethel Gorge (Fig. 68). At this locality, a BIF unit low in the Weeli Wolli Formation, which forms the northern limb of a regional-scale syncline, is faulted against the Woongarra Volcanics. Sheared felsic rock can be seen occupying the fault zone. The throw on this structure is at least 360 m (the thickness of the Weeli Wolli Formation in this area). The reverse faults may pass laterally into fold structures, but can be continuous over 25 km. Conjugate folds with steeply inclined to upright axial surfaces are the characteristic folding style in this zone (Fig. 55).

The area to the northwest and west of the Sylvania Inlier is characterized by more upright, though generally asymmetrical, folding. Typically, structures are north-facing, but south-facing structures are seen in some places. The overall lower strain environment is typified by the conjugate, box-type nature of much of the folding (Fig. 69). Structures are orientated east–west. A northwest orientation becomes dominant from east to west across the Turee

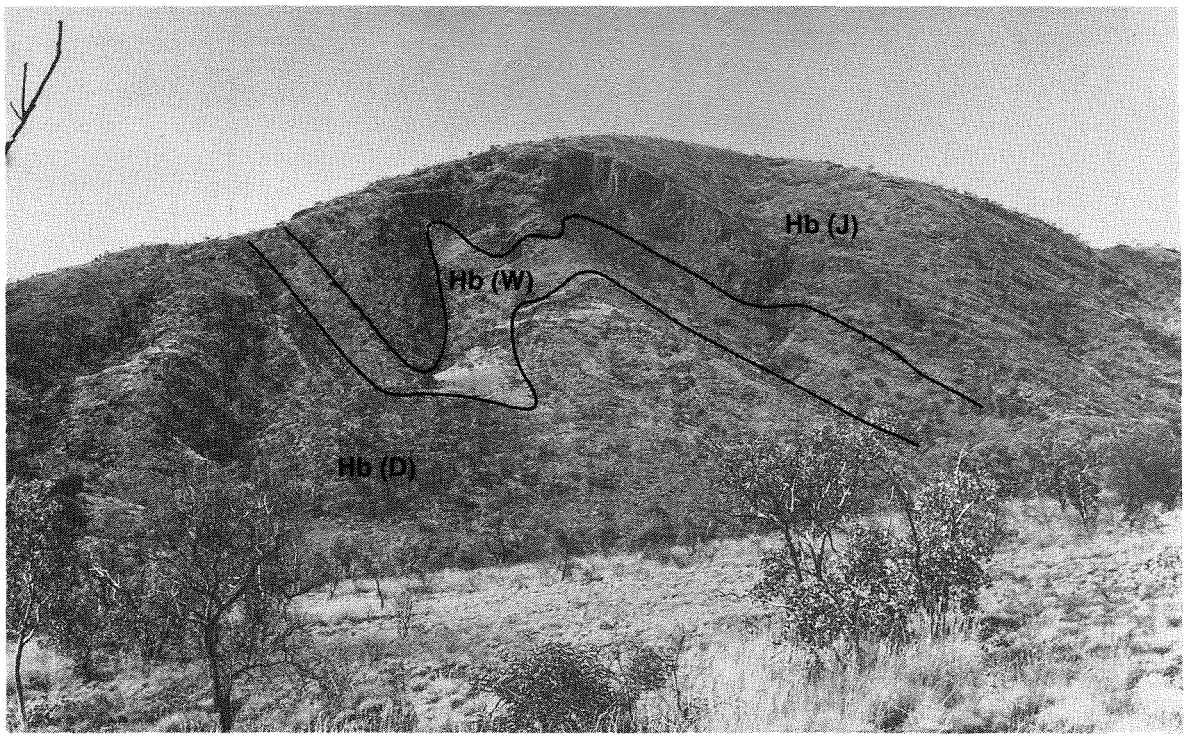

GSWA 25499

Figure 59. Large, overturned D_{2c} folding in Brockman Iron Formation forming the northern limb of the Mount Newman Syncline. Hb(D) — Dales Gorge Member; Hb(W) — Whaleback Shale Member; Hb(J) — Joffre Member.

GSWA 25500

Figure 60. Medium D_{2c} folds in the Joffre Member, Brockman Iron Formation, Mount Whaleback Mine. Axial planes are moderately to steeply inclined. Bench height in this and subsequent photographs taken at the Mount Whaleback Mine is 15 m.

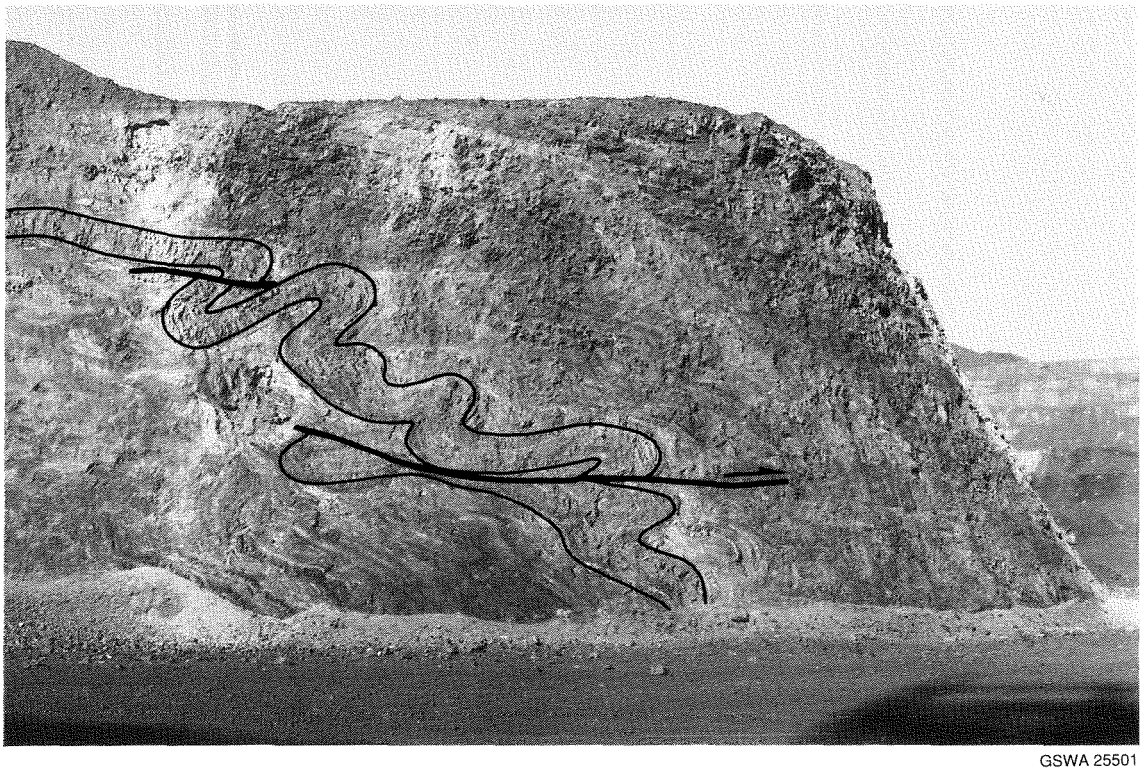

GSWA 25501

Figure 61. D_{2c} folds of a chert band in Mount Sylvia Formation, Mount Whaleback Mine, having recumbent to gently inclined axial surfaces. Folds are isoclinal. Note local flat-lying thrusts.

GSWA 25502

Figure 62. Downward-facing D_{2c} fold in Mount McRae Shale, Mount Whaleback Mine. Stratigraphic way-up is to the right-hand side (north) of the photograph.

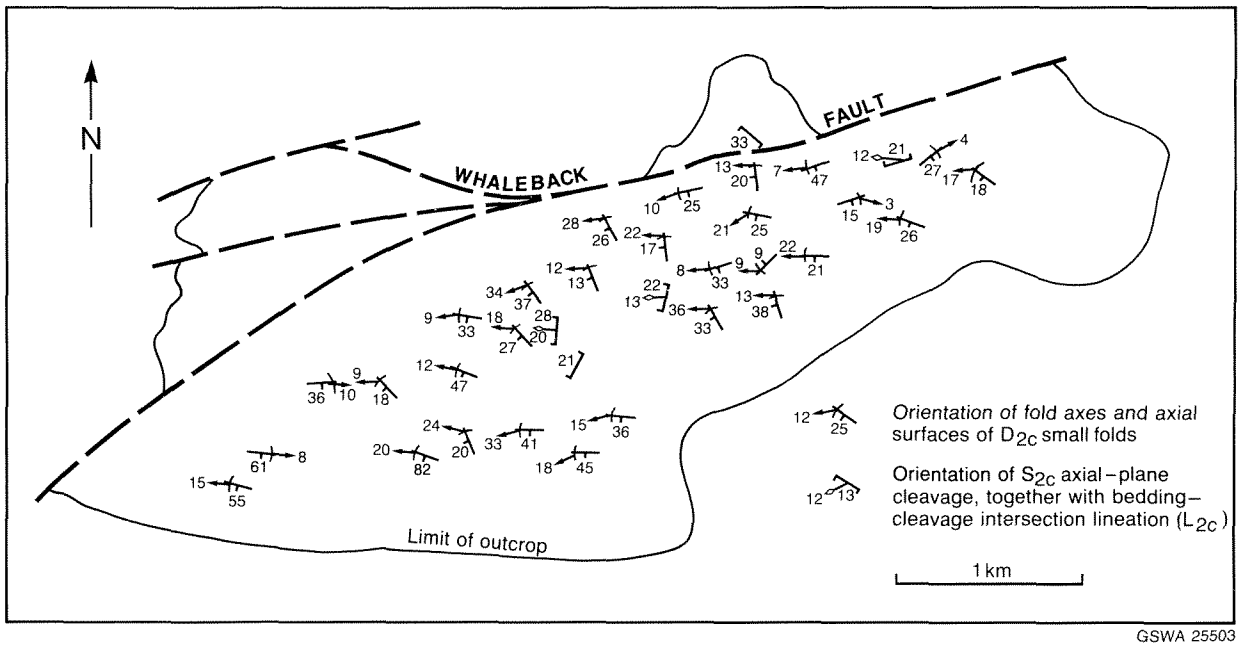

Figure 63. Map of the Mount Whaleback Mine area showing the orientation of D_{2c} folds, S_{2c} cleavage and L_{2c} lineation.

Creek Syncline (Plate 3). Major structures include the Weeli Wolli Anticline, the Alligator Anticline, the Wonmunna Anticline, the Mount Robinson Syncline, the Rhodes Ridge Syncline, and the Turee Creek Syncline (Plate 3). Some structures, such as the Pamelia Syncline and the Mount Newman Syncline have curved axial traces that can be followed out from the more deformed area north of the Sylvania Inlier (Plate 3). Locally, overturned folding, possibly associated with steep reverse faulting such as that developed along the northern limb of the Wonmunna Anticline, may be present. Upper Jeerinah Formation is thrust over upper Marra Mamba Iron Formation 5 km southwest of Rhodes Ridge camp. Further west the Marra Mamba Iron Formation is thrust onto the Wittenoom Dolomite.

The vergence and orientation of small folds in Fortescue and Hamersley Group rocks north of Prairie Downs are consistent with the northwest end of the Sylvania Inlier cropping out as the core of a west-plunging anticline (Plate 3). To the south of the Western Creek Fault, the inlier also forms the core of a regional west-plunging anticline. The intervening syncline has been removed by the Western Creek Fault, which has a reverse component of movement as well as the sinistral offset already noted. Overturned lower Fortescue Group rocks crop out to the south of the fault and form the northern limb of the anticline, which faces to the north. The hinge zone and southern shallowly dipping limb are represented by the Prairie Downs–Deadman Hill Fortescue Group succession. The fold closure is in the vicinity of Nirran Nirrie Bore. Faulting, which characterizes the contact between Fortescue Group rocks and granitoid in this area, is probably related to local thrusting during folding. The Hamersley Group rocks at Deadman Hill are the structurally higher part of the southern limb which has been downfaulted along the younger Prairie Downs Fault.

An axial-plane cleavage (S_{2c}) is well developed in much of the southwestern part of the Ophthalmia Fold Belt; and a bedding–cleavage intersection lineation (L_{2c}) is also seen (Fig. 70). The cleavage is not pervasive, and is best seen in shale units in both the Fortescue Group and the Hamersley Group (Fig. 71), where it takes the form of a continuous slaty cleavage as defined by Powell (1979). Cleavage refraction is particularly well developed between shale and silt horizons in the Jeerinah Formation (Fig. 72) and in

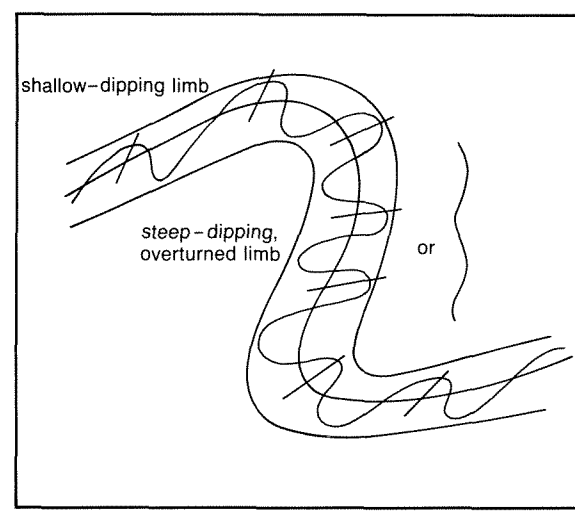

Figure 64. Sketch of typical overturned D_{2c} fold showing the relationship between small-scale folds and larger structures. On steeply dipping limbs the tightness of small folds is controlled by differing viscosity contrasts between layers in each of the stratigraphic units present.

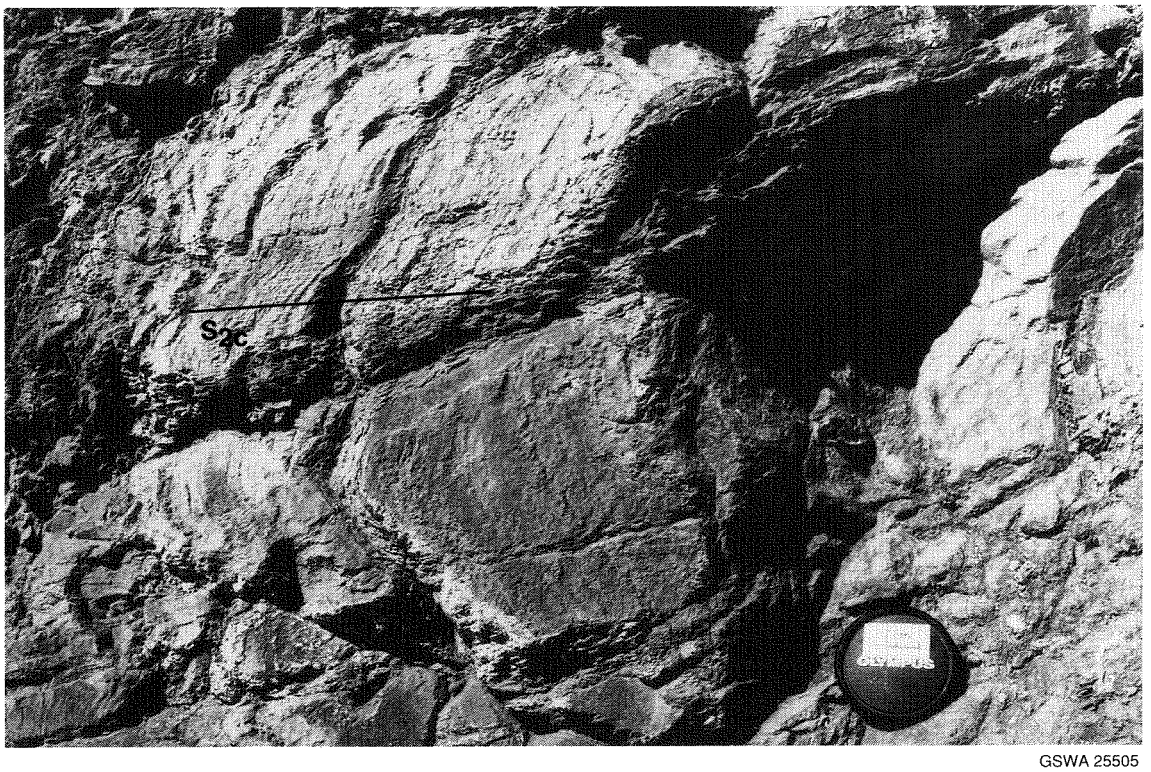

GSWA 25505

Figure 65. Open fold in the Joffre Member of the Brockman Iron Formation, Mount Whaleback Mine. Note sub-horizontal S_{2c} cleavage.

parts of the Whaleback Shale. In the more silty horizons (Fig. 71), cleavage has a planar form and is closely (<1 mm) spaced (after Engelder and Marshak, 1985).

Pyrite nodules are well developed in a particular zone in the central part of the Mount McRae Shale. In samples collected at Mount Whaleback, the slaty cleavage can be seen to wrap around the nodules, and pressure shadows have developed in the plane of the cleavage (Figs 73 and 74). Some pressure shadows have a sigmoidal form, also seen in quartz fibres within the shadows, suggesting local rotation within the stress field during deformation (Ramsay and Huber, 1983).

The slaty cleavage seen in shale passes into a spaced cleavage in more massive chert and BIF horizons. This is best seen in samples from the Joffre Member at Mount Whaleback. Here the primary sedimentary fabric, in the form of microbanding, is preserved in microlithons separated by domains or seams of dark iron oxide material which form the cleavage. Close examination of the polished slab in Figure 58, and observations made at exposures within the mine, indicate that the seams have developed on microfolds of the microbanding. The cleavage is therefore properly described as a discrete crenulation cleavage (Powell, 1979). Spacing and form varies from a strong planar type (Fig. 75) (spacing <1 cm) to a moderate, wavy to anastomosing type (Fig. 58) (spacing >1 cm). Although large apparent displacements between adjacent microlithons can be seen in Figure 58, these are not seen to offset the chert mesobands at the top and bottom of the specimen. This suggests that internal volume reduction as a response to stress rather than simple shear along the cleavage seams has taken place, and provides evidence for the operation of a mass transfer—pressure solution of Rutter (1983)—process preferentially removing silica.

A metamorphic foliation has developed in mafic units in the Fortescue Group and in metadolerite sills in the Weeli Wolli Formation. It is defined by the preferred orientation of chlorite and amphibole crystals.

Away from the more deformed area along the northern margin of the Sylvania Inlier, the axial-plane cleavage is confined principally to shale horizons and to areas of local high strain. It is often prominent in the hinge zones of folds. Further west it is apparently absent; it is not seen in the Paraburdoo area.

Age of folding in the southeast Hamersley Basin

The occurrence of lowermost Wyloo Group (Beasley River Quartzite and Cheela Springs Basalt) in the core of the Turee Creek Syncline provides a lower limit to the age of D_{2c} folding. Along the margin of the Hamersley Basin, D_{2c} folds are cut by west-northwest-trending mafic dykes. At Paraburdoo these dykes pre-date the formation of hematite ore in the Brockman Iron Formation (Morris, 1980). Pebbles of hematite occur in the Mount McGrath Formation near Paraburdoo, and limit the age of ore formation to pre-Mount McGrath Formation time (Morris, 1980). D_{2c}

folding must, therefore, have taken place after eruption of the Cheela Springs Basalt; but before dyke intrusion and ore formation, and before deposition of the Mount McGrath Formation.

Near Paraburdoo, the Beasley River Quartzite, which was involved in the D_{2c} fold event, unconformably overlies Marra Mamba Iron Formation, Brockman Iron Formation, and Weeli Wolli Formation (Plates 2 and 3; Bourn and Jackson, 1979). Further east, it lies on Woongarra Volcanics south of Divide Well, and on Weeli Wolli Formation southwest of Deadman Hill (see Plates 2 and 3). Prior to D_{2c} folding, therefore, extensive uplift must have taken place in the southeastern Hamersley Basin, probably at the same time as folding in the southwestern Hamersley Basin. D_{2c} folding is, therefore, younger than the open dome-and-basin style of folding seen in the southwest part of the Hamersley Basin.

Ashburton Fold Belt

The evolution of the Ashburton Fold Belt (Figs 39 and 40) is described by Thorne and Seymour (1991). Two periods of deformation, which, in this study, will be referred to as D_{1a} and D_{2a} to distinguish them from the D_{1c} and D_{2c} deformation events in the Ophthalmia Fold Belt, have been recognized. Both deformations of the Ashburton Fold Belt post-date deposition of the Wyloo Group, and both are younger than the two deformation events described above for the Ophthalmia Fold Belt. D_{1a} structures post-date the Wyloo Group and pre-date the Capricorn Formation. D_{2a} structures post-date the Capricorn Formation as well as the intrusion of the Boolaloo Batholith, a body of granitic rock that intrudes the Wyloo Group.

Structures associated with the D_{1a} event are best seen in the Ashburton Formation, where an S_{2a} cleavage is com-

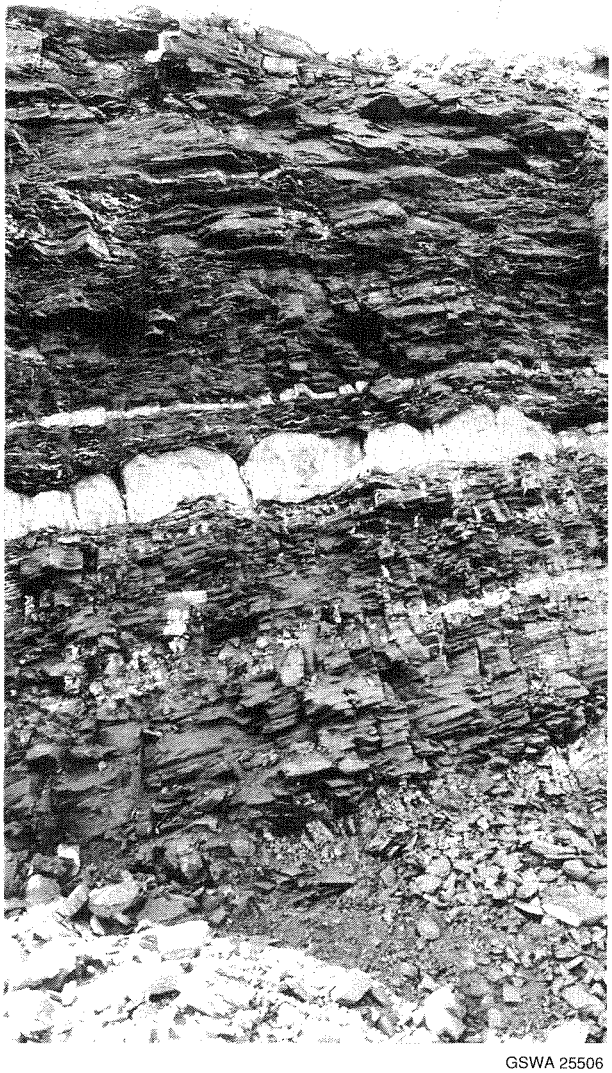

GSWA 25506

Figure 66. Pinch-and-swell structure in chert band of the Mount McRae Shale, Mount Whaleback Mine.

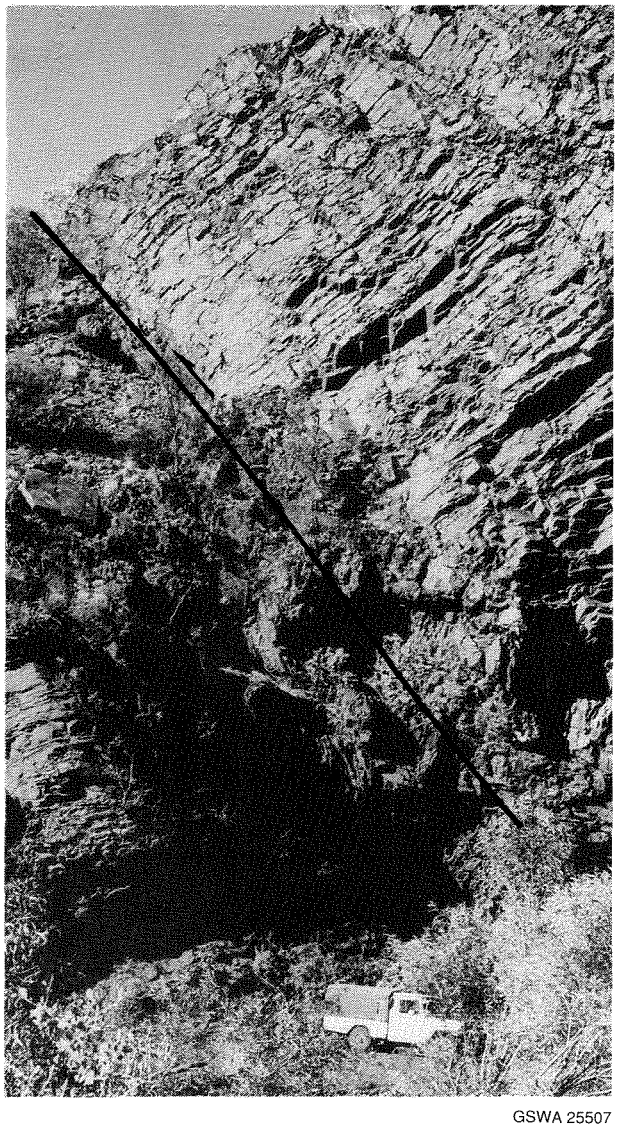

GSWA 25507

Figure 67. Steep reverse fault in Brockman Iron Formation, Kalgan Creek.

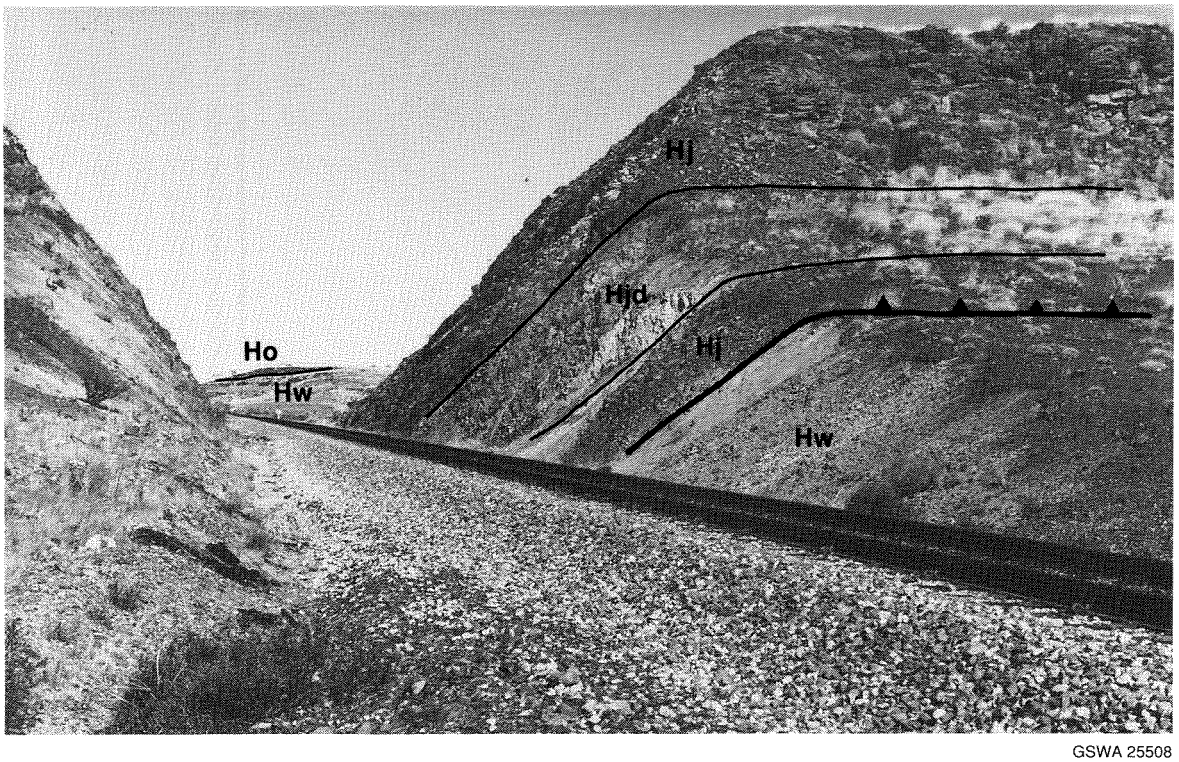

GSWA 25508

Figure 68. Reverse fault exposed in railway cutting in Ethel Gorge. Boolgeeda Iron Formation (Ho) and Woongarra Volcanics (Hw) are exposed in the core of a syncline to the south. The fault juxtaposes lower Weeli Wolli Formation BIF (Hj) and metadolerite (Hjd) against Woongarra Volcanics.

monly developed as a crenulation of an earlier S_{1a} fabric (Thorne and Seymour, 1991). Large-scale fold-interference patterns were also recognized. With increasing metamorphic grade, the cleavage passes into metamorphic schistosity, which is sub-parallel to bedding. Bedding–cleavage intersections typically produce a horizontal to gently plunging L_{1a} lineation.

Evidence concerning the pre-D_{2a} orientation of D_{1a} structures is limited (Thorne and Seymour, 1991). At Mount Blair, unfolding the Capricorn Formation unconformity indicated that S_{1a} dipped steeply to the south while the D_{1a} folds faced north. Beneath the Bangemall Group unconformity at Fords Creek, there is evidence that large-scale, tight D_{1a} folds had moderately inclined, northeast-dipping axial surfaces and faced the southwest.

D_{2a} structures are dominant in the Ashburton Fold Belt, and three structural zones were recognized (Thorne and Seymour, 1991). Zone A is adjacent to the Hamersley Basin and is dominated by large open to tight folds and dextral wrench faults. Zone B is characterized by tight to isoclinal, non-cylindrical folds with wavelengths of 5–200 m. Folds are associated with a strong axial-plane cleavage (S_{2a}) that dips southwest. High-angle reverse faults that are orientated sub-parallel to D_{2a} fold axes occur along the northern margin of the zone. Zone C is distinguished from Zone B by the presence of D_{2a} folds which have wavelengths of up to 5 km. Folds are generally open but become tighter as Zone B is approached.

Extensive dextral wrench faulting occurred throughout the fold belt. Outliers of Capricorn Formation are partially or completely fault-bounded; this has produced a distinctive rhombohedral outcrop geometry, also recognized by Tyler and Thorne (1990).

The area currently under discussion lies within Zone A, and forms the boundary with the Ophthalmia Fold Belt. D_{1a} structures are not seen, and the most prominent structures are a set of west-northwesterly to northwesterly orientated faults of D_{2a} age (Plate 3). These extend from Bukardi Creek to Cairn Hill Well. Dextral offset on individual faults may be as great as 7.5 km. In the southern limb of the Bellary Anticline, faulting has taken place parallel to strike, and has removed the Wittenoom Dolomite as well as parts of the overlying lower Wyloo Group. The contact between Beasley River Quartzite and Hamersley Group exposed 3.5 km west of the Paraburdoo mine is a fault (Fig. 76). A resilicified fault breccia occurs in quartzite at the contact (Fig. 77). Further faulting is indicated by the juxtaposition of Beasley River Quartzite and Duck Creek Dolomite 9 km west-northwest of Ratty Spring, and by the truncation of fold structures immediately south of the mine (Plates 2 and 3). Dips on fault surfaces range from vertical to moderate to the southwest.

Low-angle normal faults are preserved within the Paraburdoo orebody (Morris, 1985). These pre-date ore formation, but post-date the formation of folds belonging to the Ophthalmia Fold Belt

The north-trending, east-dipping fault which truncates the Marra Mamba and Brockman Iron Formations near Radio Hill (Plates 2 and 3), has a sinistral offset, and is here regarded as antithetic to the main dextral system (Fig. 78). This differs from the interpretation of Bourn and Jackson (1979), who regarded movement as having occurred prior to the deposition of the Wyloo Group. Other north-trending faults, which are well developed west of the mine and in the vicinity of Mount Maguire (Plate 3), have a normal sense of displacement and minimal lateral offsets. These correspond to the "antithetic–normal" faults described from model wrench systems by Wilcox et al. (1973).

Several folds in the Wyloo Group southeast of Mount Maguire trend east–west and are arranged *en echelon* to a west-northwest-trending fault, the Nanjilgardy Fault (Plate 3). This relationship is consistent with these folds having also developed as part of a dextral wrench system (Fig. 78). An axial-plane cleavage, a feature not seen associated with Ophthalmia Fold Belt D_{2c} folds in the Turee Creek Syncline, is well developed in Boolgeeda Iron Formation and Turee Creek Group shale south of Nanjilgardy Pool (Fig. 79).

GSWA 25509

Figure 69. Upright conjugate D_{2c} fold in Weeli Wolli Formation BIF near Mount Channar.

The Hamersley and Turee Creek Group rocks that crop out at Mount Maguire are separated from the main Hamersley Basin outcrop by the Nanjilgardy Fault. Locally, faulting is complex; and thrusting, which involves Mount McGrath Formation and Beasley River Quartzite, and which causes a repetition of the upper Hamersley Group–Turee Creek Group–lower Wyloo Group sequence 2.5 km and 4 km south of Nanjilgardy Pool (Plate 3), is well developed. Faulting is interpreted as having developed within an extensional fault jog similar to those described by Sibson (1987). The fault jog formed within the dextral wrench system (see Plate 3) and is the result of segmentation of the Nanjilgardy Fault.

Folding is associated with D_{2a} faulting in the Hamersley Group, and is most spectacularly developed in Doggers Gorge, where medium-scale, north-facing chevron folds occur adjacent to a fault zone (Fig. 80). Elsewhere folding takes the form of medium and small conjugate folds (Fig. 81).

On the northwest limb of the Turee Creek Syncline, anticlines, whose axial surfaces trend east-northeast (Plate 3), have developed locally in Brockman Iron Formation. Thrusts have developed at the base of these structures, and a decollement occurs in the Wittenoom Dolomite. Movement was to the northwest and placed Brockman Iron Formation directly on Marra Mamba Iron Formation.

Ophthalmia Fold Belt D_{2c} folds have a northwest trend throughout the Turee Creek syncline, rather than the general east–west trend seen further to the east. The Alligator Anticline (Plate 3) can be seen to be re-orientated from the east–west trend into this northwest trend. The reorientation is interpreted as the effect of the Ashburton Fold Belt D_{2a} deformation on pre-existing Opthalmia Fold Belt D_{2c} fold structures.

Metamorphism

As has been described above, an axial-plane cleavage is associated with D_{2c} folds in the southeast part of the Ophthalmia Fold Belt. Formation of this cleavage took place under low- and very low-grade metamorphic conditions. In pelitic and semi-pelitic rocks, the cleavage is defined by the preferred orientation of chlorite, sericitic muscovite, and iron oxides. In mafic volcanic rocks and mafic sills, a foliation defined by the orientation of chlorite and amphibole is present. Smith et al. (1982) have interpreted low- and very low-grade metamorphic mineral assemblages throughout the Hamersley Basin as the product of burial metamorphism (M_h), which reached a peak at the end of Turee Creek Group time. The formation of the S_{2c} cleavage, however, implies that a later, Capricorn age metamorphic event (M_c) was superimposed onto the burial metamorphic event. Grades reached in the M_c event were similar to those reached during M_h.

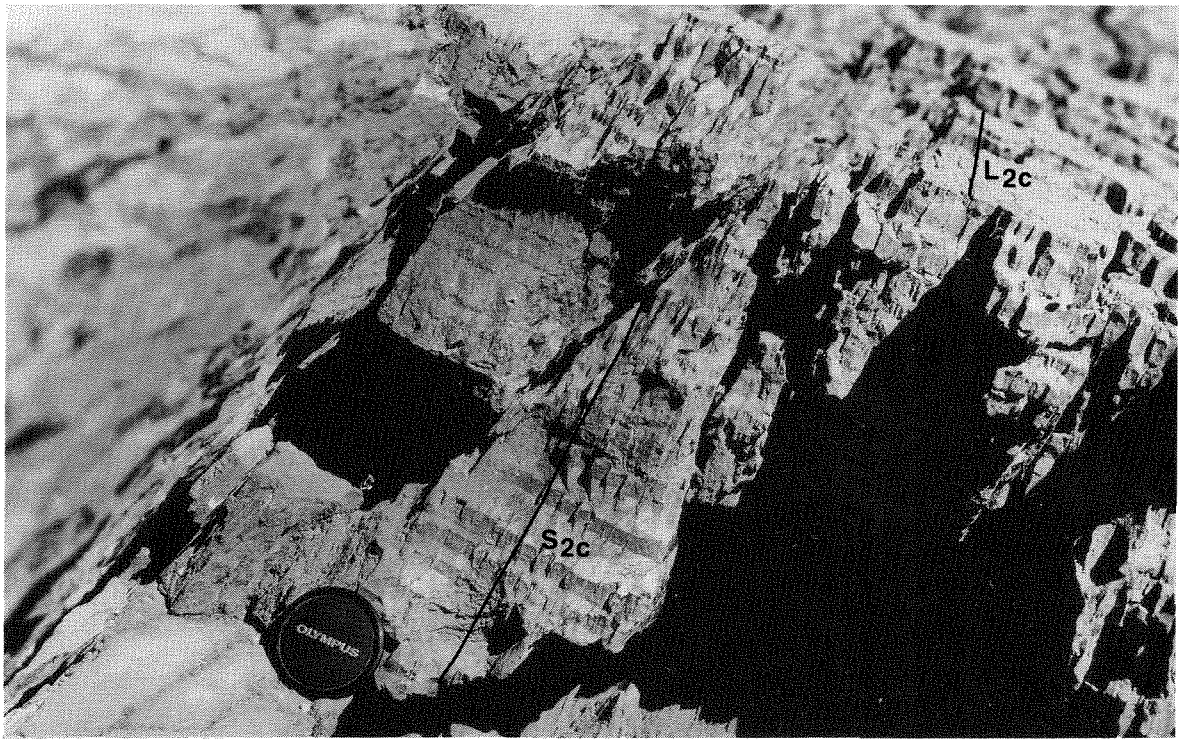

GSWA 25510

Figure 70. S_{2c} cleavage in Jeerinah Formation. A bedding-cleavage intersection lineation (L_{2c}) can be seen on the top bedding surface.

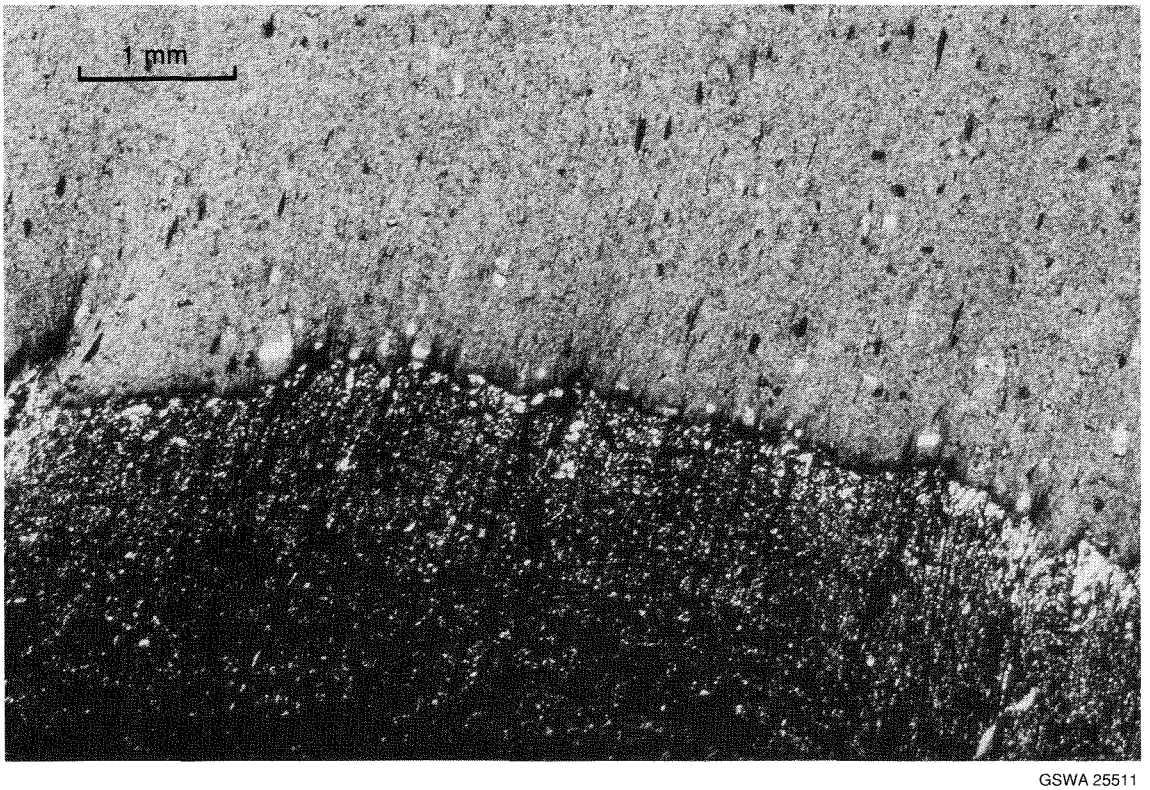

GSWA 25511

Figure 71. Continuous slaty S_{2c} cleavage in shale (upper) passing into a closely spaced disjunctive S_{2c} cleavage in siltstone (lower), Mount McRae Shale, Mount Whaleback (x35). GSWA sample 42222.

During the present study, samples were collected from mafic rocks in the Fortescue Group and from dolerite sills in the Weeli Wolli Formation. The mineral assemblages are consistent with metamorphism to pumpellyite–actinolite facies and to greenschist facies as described by Smith et al. (1982). The isograd pattern is similar to that shown in Figure 35, which is after Smith et al. (1982). Rocks adjacent to the Sylvania Inlier are consistently in the greenschist facies.

The eastern part of the Sylvania Inlier underwent extensive reworking during the Capricorn Orogeny. Suite 1 mafic dykes were deformed and foliated during the M_c event. Towards the northern contact of the inlier, blue-green edenitic amphibole, together with plagioclase, epidote, and quartz, is present. Chlorite may also be present. The plagioclase may be either albite or oligoclase–andesine. The assemblage indicates albite–epidote–amphibolite facies conditions (cf. Miyashiro, 1973; Holland and Richardson, 1979; Laird, 1980). Greenstone-belt rocks adjacent to the Mindoona Bore Thrust have also recrystallized under albite–epidote–amphibolite facies conditions. Mafic rocks south of Sylvania Homestead are higher grade; they have the assemblage hornblende–epidote–oligoclase-andesine–quartz, which is consistent with the upper part of the albite–epidote–amphibolite facies (cf. Apted and Liou, 1983). In some samples collected near Woggaginna Hill, epidote is absent and the assemblage, hornblende–oligoclase-andesine–quartz, indicates amphibolite facies (cf. Miyashiro, 1973). Amphibolite facies assemblages also occur in the Suite 1 mafic dykes sampled between Emerald Bore and Sylvania Homestead.

The main granitoid and the hornblende-bearing granitoid in the eastern part of the inlier were also deformed and foliated during the Capricorn Orogeny. Mineral assemblages are consistent with an overall increase in grade from

GSWA 25512

Figure 72. Cleavage refraction between shale and siltstone units, Jeerinah Formation.

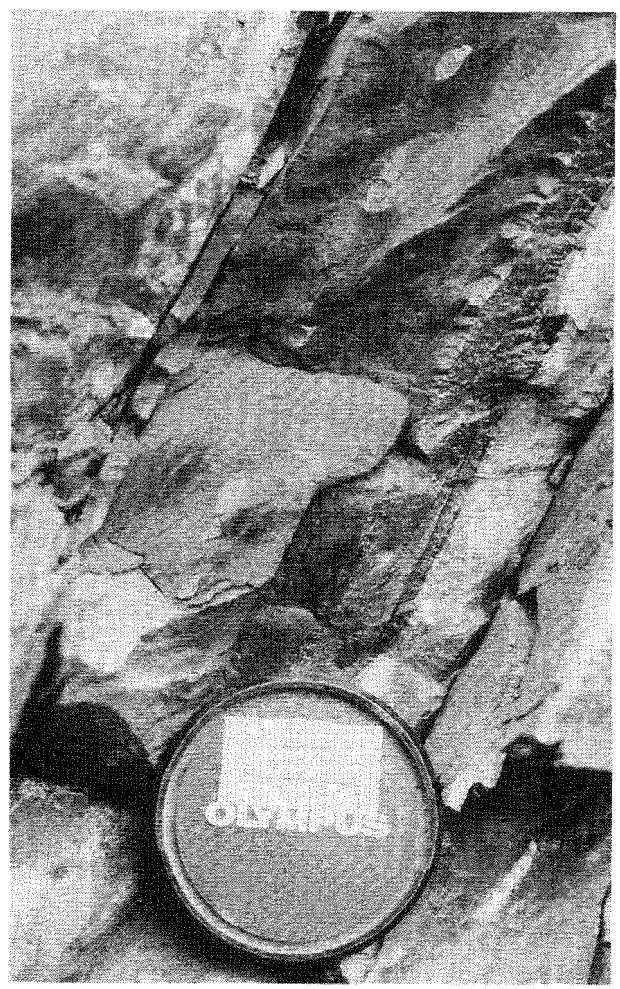

GSWA 25513

Figure 73. Pyrite nodules displaying pressure shadows in plane of S_{2c} cleavage. Mount McRae Shale, Mount Whaleback Mine.

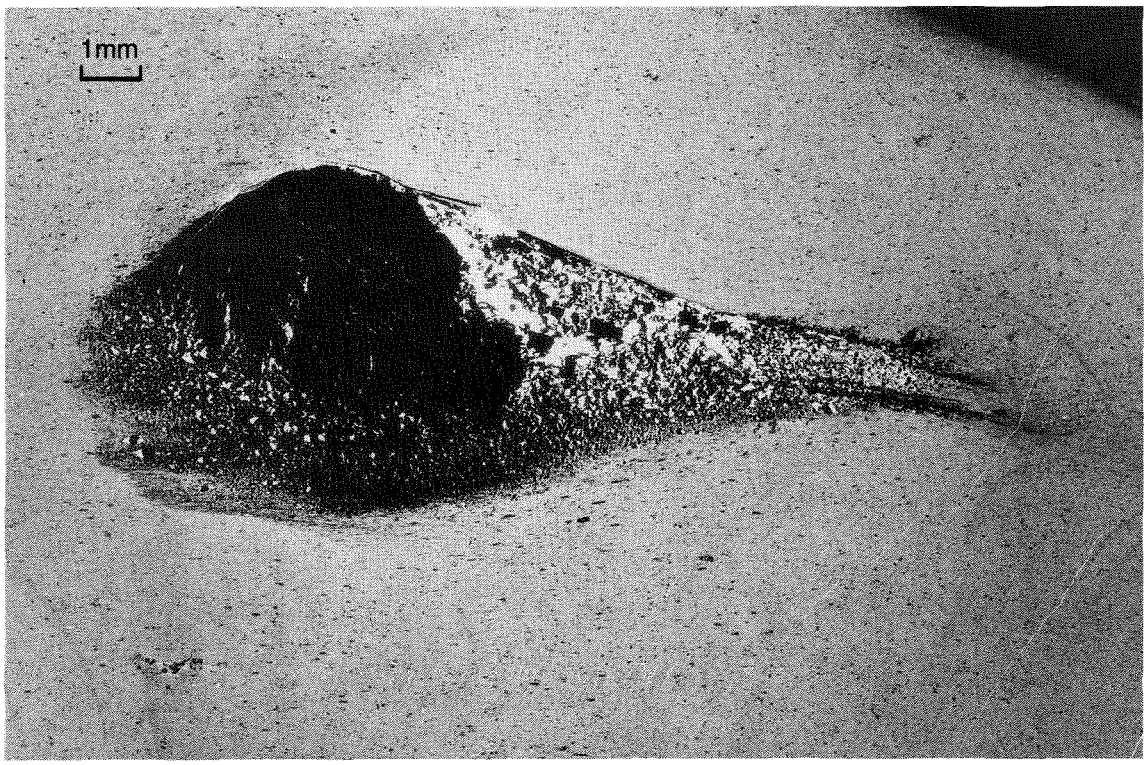

GSWA 25514

Figure 74. Pressure shadows on a pyrite nodule, Mount McRae Shale, Mount Whaleback Mine. The nodule is wrapped by S_{2c} cleavage (x11). GSWA sample 42222.

GSWA 25515

north to south during the M_c event. Towards the northern contact, the mineral assemblage in the main granitoid is quartz–K-feldspar–albite or oligoclase-andesine–epidote–biotite (–muscovite–chlorite). Towards the south, plagioclase is always oligoclase-andesine.

Rocks in shear zones between Sylvania and Woggaginna Hill show a high degree of recrystallization. A schistose rock exposed 6 km south-southeast of Sylvania, which in the field can be traced into a deformed granitoid, has the assemblage kyanite–chlorite–biotite–muscovite–quartz (Fig. 45). Chlorite is well crystallized and is intergrown with muscovite and biotite. From Figure 82 it can be seen that chlorite–kyanite stability may be achieved by an isothermal increase in pressure from the peak burial metamorphism (M_h) conditions. At 550°C, pressure must have been in excess of 500 MPa, equivalent to 18 km of overburden.

Capricorn age metamorphism has also affected Wyloo Group rocks in the Ashburton Basin (Thorne and Seymour, 1991). Grade ranges from pumpellyite–actinolite facies adjacent to the Hamersley Basin to upper greenschist facies adjacent to the Bangemall Basin.

Figure 75. Planar S_{2c} spaced cleavage in Joffre Member BIF, Brockman Iron Formation, Mount Whaleback Mine (x17). GSWA sample 42223.

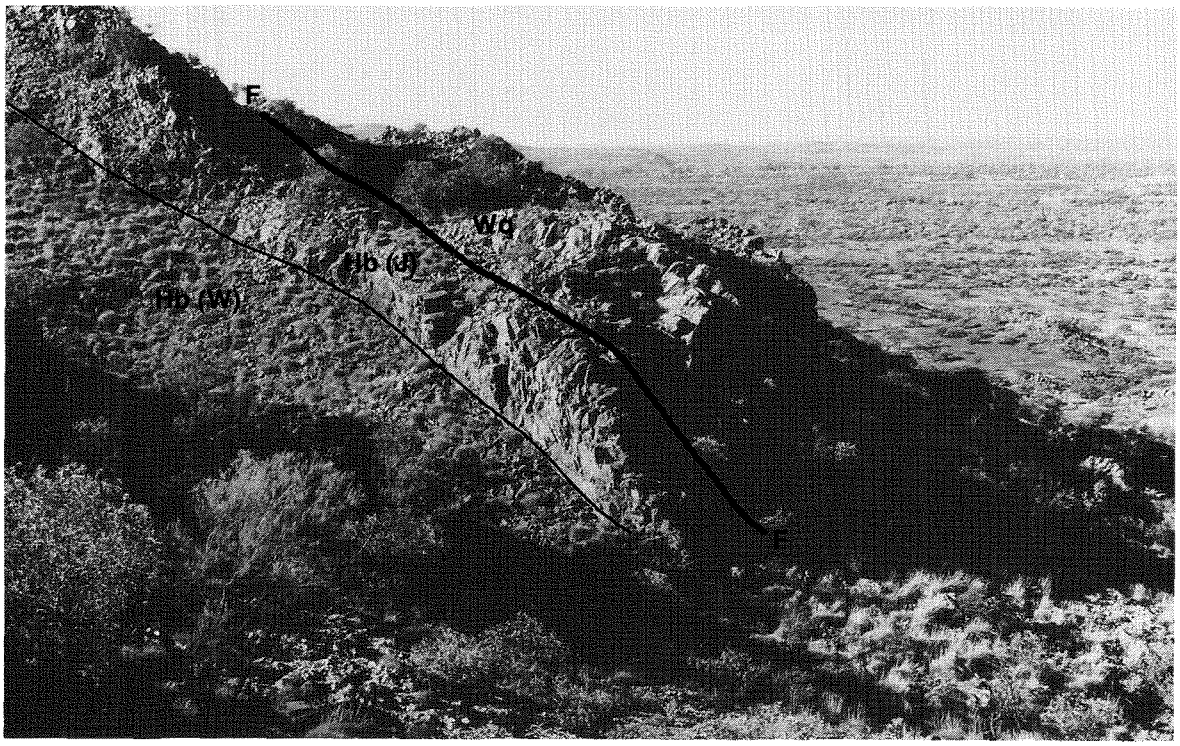

GSWA 25516

Figure 76. Faulted contact between the Joffre Member of the Brockman Iron Formation (Hb(J)) and lowermost Wyloo Group (Beasley River Quartzite - Wq), near Paraburdoo. Whaleback Shale (Hb(W)) underlies the Joffre Member.

Very low-grade assemblages in Hamersley Basin rocks in the Paraburdoo and Hardey Syncline areas were identified by Smith et al. (1982). These assemblages were interpreted to be the result of Hamersley Basin burial metamorphism. The reappearance of zone III assemblages at the southern margin of the basin was attributed to an increase in the thickness of the Fortescue Group combined with thinning of the Hamersley Group. In the present study, pumpellyite has been identified in Cheela Springs Basalt from the core of the Turee Creek Syncline. An alternative explanation for these assemblages is that they are the effect of later burial metamorphism beneath the Ashburton Basin.

Mafic Dykes

Suites 3 and 4

Mafic dykes were intruded during the development of the Capricorn Orogen. Two suites can be identified. The oldest (Suite 3) trends west-southwest and is restricted to a few examples at the southern margin of the Sylvania Inlier in the vicinity of Deadman Flat. This suite is consistently cut by a suite of west-northwest-trending dykes (Suite 4), which occur in the southwest part of the inlier (Fig. 25).

GSWA 25517

Figure 77. Resilicified fault breccia in Beasley River Quartzite, adjacent to the fault seen in Figure 76.

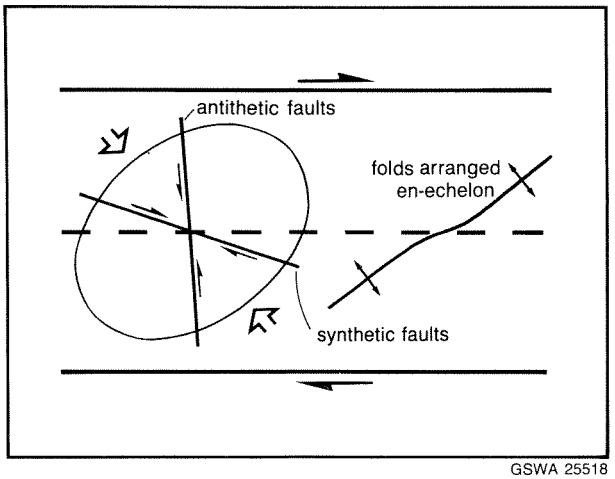

GSWA 25518

Figure 78. Orientation of the strain ellipse and relationship of subsidiary faults and *en-echelon* folds within a dextral wrench fault system. Based on Figure 6 of Wilcox et al. (1973, p.82).

The dykes can also be seen to have intruded Hamersley Basin rocks and Beasley River Quartzite further northwest along the southern Pilbara margin (Plate 2).

The dykes, typically no more than 2–3 m wide, are fine- to medium-grained dolerite with subophitic texture. Primary igneous minerals are usually preserved, although varying degrees of alteration may have taken place. The typical assemblage is pyroxene (partly or wholly replaced by intergrowths of actinolite and chlorite)–plagioclase (labradorite to bytownite, may show alteration to more sodic compositions as well as saussuritization and sericitization)–quartz (primary)–iron oxides (magnetite and ilmenite, replaced by leucoxene). The varying degree of alteration may reflect very low- to low-grade metamorphism controlled by the restricted availability of fluid.

The west-northwest trending Suite 4 dykes cut across folds in the southeast Hamersley Basin. At Paraburdoo they pre-date ore formation, and this restricts them to pre-Mount McGrath Formation in age (Morris, 1980).

Structural Evolution

Previous models

Systematic mapping of the Hamersley Basin and adjacent areas was carried out in the early 1960s, coincident with the discovery and evaluation of important iron-ore deposits (Trendall, 1975b). The results of the first-edition mapping were summarized in publications by MacLeod et al. (1963), Halligan and Daniels (1964), and MacLeod (1966). In general, an increasing intensity of deformation was recognized from the Fortescue valley southwards. The occurrence of two fold periods was inferred from the presence of large-scale dome-and-basin structures, interpreted as fold-interference patterns. Halligan and Daniels (1964) named these the Ophthalmian (northwest and west trends) and the Rocklean (north-northeast trend) fold periods. Folding in the Wyloo Group rocks was regarded as Ophthalmian.

MacLeod (1966) suggested that the dome-and-basin pattern of folds in the Fortescue and Hamersley Groups was due to large differential movements in the underlying basement. Structures such as the Rocklea, Milli Milli, and Sylvania "Domes", were the foci of positive upward movement of basement blocks.

Gee (1979) suggested that the Sylvania Inlier was a rhomb-shaped basement horst, and identified a second rhomb-shaped structural high near the centre of the Ophthalmia Fold Belt. This second high contains two windows

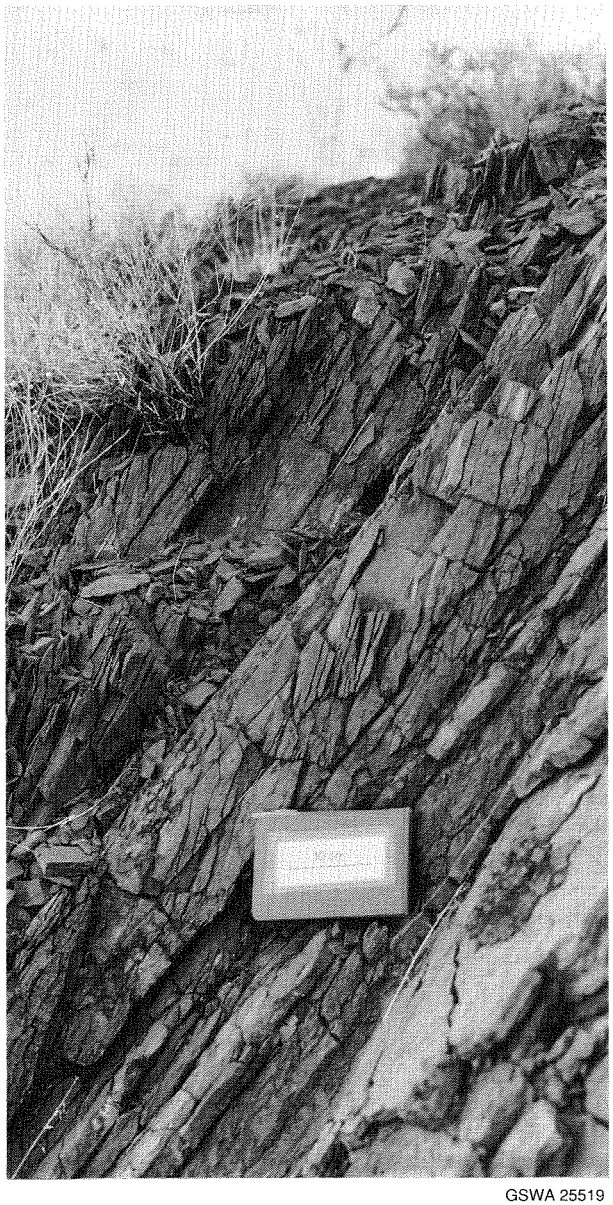

GSWA 25519

Figure 79. Ashburton Fold Belt S_{2a} cleavage in lowermost Turee Creek Group shales south of Nanjilgardy Pool.

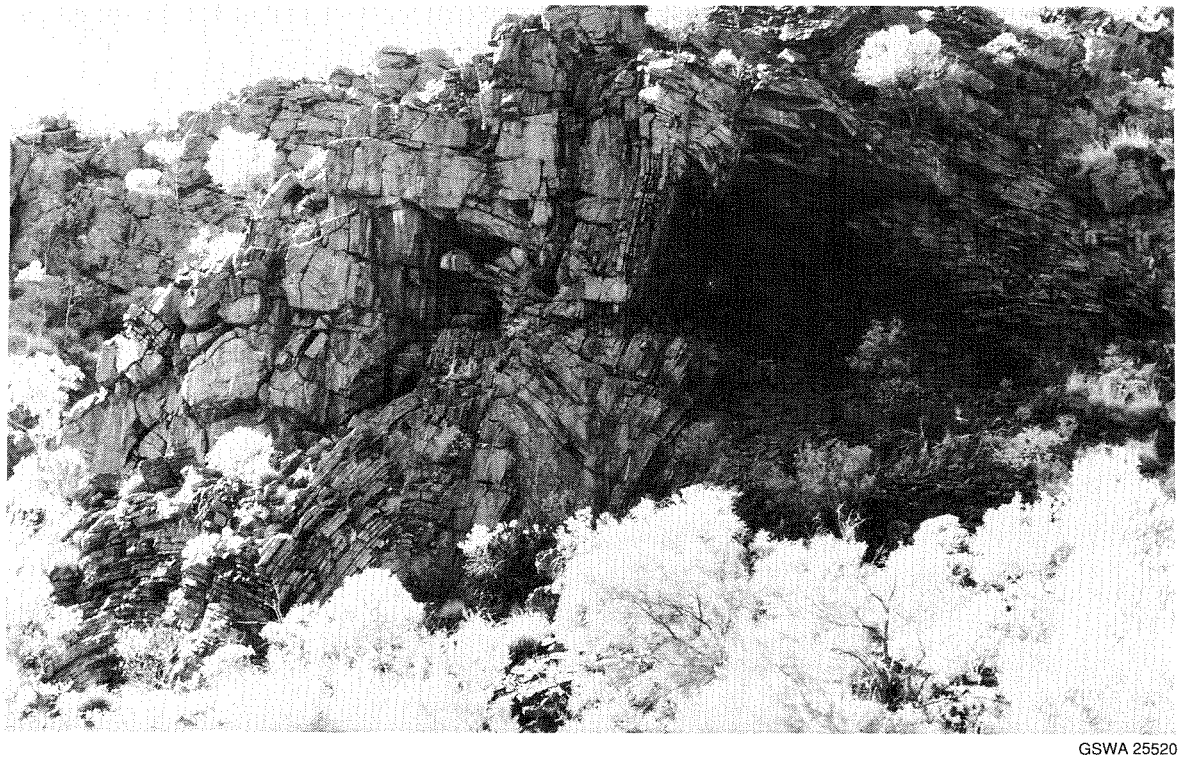

GSWA 25520

Figure 80. Chevron-style D_{2a} folds in Brockman Iron Formation adjacent to faulting associated with the Howies Hole Fault, Doggers Gorge, near Paraburdoo.

GSWA 25521

Figure 81. Upright conjugate D_{2a} fold in Brockman Iron Formation associated with wrench faulting, Howies Hole, near Paraburdoo.

of basement (Rocklea and Milli Milli Domes) and was interpreted as a basement horst still largely cloaked by its cover. Only one curvilinear fold set was recognized, and variations in axial trends were attributed to deflections around basement domes. Tight folding along the northern tangent of the Sylvania "Dome", and virgation of axes away from that point were regarded as evidence for gravity gliding of Hamersley Basin rocks off a rising basement block. Kneeshaw (1975) also suggested that folding at Mount Whaleback was the result of large-scale slumping of units off a rising Sylvania "Dome".

Both MacLeod (1966) and Gee (1979) regarded the folding in the Hamersley Basin as a response to block movements in an almost cratonized basement. Trendall (1983) summed up this model by describing the Mount Bruce Supergroup as behaving as "an overlying and plastically responsive sheet".

Deformation in the Sylvania Inlier

From the structural description presented it should be obvious that the Sylvania Inlier is not a simple domical structure analogous to other basement outcrops, such as the Rocklea and Milli Milli Domes in the southwestern Hamersley Basin. It is a composite structure, the less deformed western third of which outcrops as the cores of two regional anticlines, while the eastern two-thirds is dominated by shear zones. There is also a contrast in metamorphic grade: upper greenschist to amphibolite facies was reached in the inlier, but only pumpellyite–actinolite facies to middle greenschist facies in the overlying Hamersley Basin succession.

The occurrence of extensive shear zones in the eastern part of the inlier is indicative of large inhomogeneities of strain during deformation (Ramsay and Graham, 1970). Shear zones may be produced by simple shear, by an inhomogeneous volume change, or by a combination of the two (Ramsay, 1980, fig. 3). Further complications may arise if the rock has previously been deformed.

Volume change usually involves the removal of relatively soluble material, typically quartz and carbonate minerals. In the shear zones under discussion this was not the case, because there has been no apparent decrease in the leucocratic component compared to undeformed granitoid.

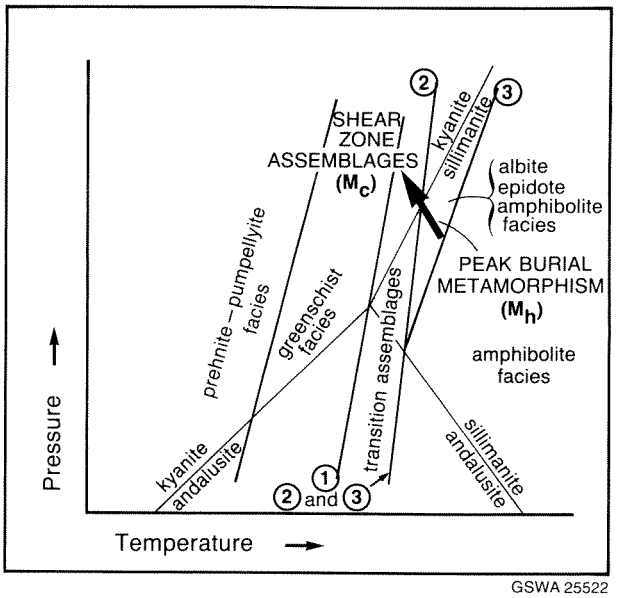

Figure 82. Pressure–temperature diagram showing possible relationship between peak burial metamorphism and metamorphic conditions indicated by mineral assemblages in shear zones. Reactions as for Figure 36.

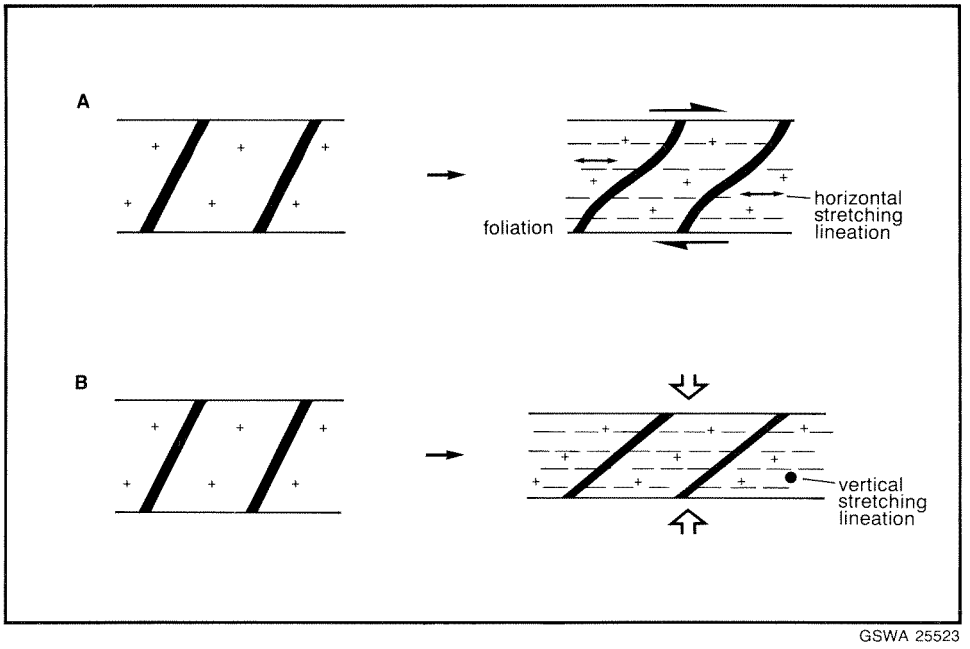

Figure 83. Mechanisms for re-orientating Suite 1 mafic dykes; A — By dextral wrenching; B — By flattening.

In general, shearing was ductile (cf. Ramsay, 1980), and it is possible to continuously trace variations in strain from little-deformed into highly deformed rocks and back out again. Simple shear is, therefore, regarded as the principal deformation mechanism which produced the shear zones themselves (cf. Rathbone et al., 1983). Strain variations are not consistent with inhomogeneous pure shear (e.g. Coward, 1984, Fig. 10).

The observed reorientation of Suite 1 mafic dykes could be interpreted in terms of a regional dextral shear (Fig. 83A). This, however, would not be consistent with stretching lineations within the shear zones, which have been observed to trend north-northeast. The change in the orientation of the dykes, initially at an angle to the main compression, may have been achieved by flattening (Fig. 83B). Some dykes are folded, and the axial surfaces of these folds are parallel to the shear zones. It would appear, therefore, that simple shear has been superimposed onto an initial flattening, and that between the shear zones, granitoid typically acquired a penetrative foliation (S_c) parallel to the shear zones.

The flattening that reorientated the Suite 1 mafic dykes is consistent with a north–south compression. The shear zones developed as part of this regional compression. On their own, the L_c stretching lineations observed in the shear zones are bipolar and do not provide evidence of the sense of shear (Coward, 1984). However, the Mindoona Bore Thrust and the Painkiller Bore Fault both dip to the south and have been interpreted as having a reversed sense of movement (south side up). The observed structures are, therefore, consistent with large-scale northerly directed thrusting.

Deformation in the Ophthalmia Fold Belt related to that in Sylvania Inlier

At the western end of the Sylvania Inlier, the granite - greenstone has been shown to outcrop within anticlinal fold cores (see Plate 3). This relationship effectively rules out a model for deformation involving the gravity gliding of cover rocks off a rising domical structure as envisioned by Gee (1979). Such gliding would require decollement (Fig. 84). Gravity gliding also requires a zone of extension—the "tectonic gap" of Price (1971)—which should balance shortening at the front of a gravity-driven system. North-facing structures in the Hamersley Group rocks south of the inlier are further evidence against gravity gliding, as they indicate the wrong sense of movement (Fig. 84).

In the southeastern part of the Ophthalmia Fold Belt, high-angle reverse faults and upright D_{2c} folds pass to the south into progressively more overturned, tighter, north-facing D_{2c} folds. As the Sylvania Inlier is approached, the deformation becomes more intense. The interpretation of structures in the Sylvania Inlier in terms of a northerly directed thrust system is consistent with the D_{1c} and D_{2c} folding and faulting described, and it would appear that deformation in the two units is linked.

Models of the geometry of fold and thrust belts with their staircase trajectory of "flats" and "ramps" recognize the possible involvement of basement slices (e.g. Elliott and Johnson, 1980; Hatcher, 1981; Boyer and Elliott, 1982). The occurrence of low-angle detachments within crystalline basement and their continuation into the lower crust and beyond, has been confirmed by deep seismic reflection profiles (e.g. Brewer et al., 1981; Brewer and Smythe, 1984). A feature of these is that the "staircase trajectory", thought to be controlled by bedding, is maintained in apparently isotropic crystalline basement rocks (Butler, 1985).

A feature of low-angle thrust systems is that they usually propagate towards their foreland so that the youngest detachment is the lowest (Boyer and Elliott, 1982). This last detachment, usually referred to as the sole thrust, carries all the earlier thrust slices with it "piggy back" fashion. Where the sole thrust passes over a ramp in its footwall, large-scale folding must take place in the hanging wall, deforming the earlier nappes and thrusts. This type of deformation can produce folding of the opposite vergence to the primary transport direction, particularly in early thrusts now high in the sequence (e.g. Price, 1981; Boyer and Elliott, 1982).

The Sylvania Inlier is a complex feature. The western third comprises little-reworked, essentially autochthonous to parautochthonous granite–greenstone within anticlinal fold cores. The eastern two-thirds of the inlier is characterized by ductile thrusting and is interpreted as a stack of parautochthonous to allochthonous thrust sheets. North-dipping shear zones near Woggaginna Hill are interpreted as the result of the passage of the thrust stack over a ramp in the footwall (Fig. 85). Ramping may be caused by irregularities in the basement–cover contact (Wiltschko and Eastman, 1983) and such a feature is provided by the topographic high identified as being present in this area during Fortescue Group times (Horwitz and Smith, 1978; Blake, 1984; this study, Fig. 33).

This interpretation is consistent with the contrast in metamorphic grade between the inlier and the overlying Hamersley Basin succession, and with the observed in-

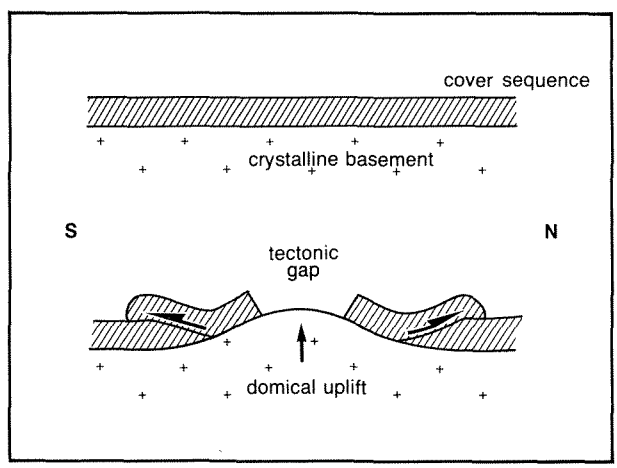

Figure 84. A simple gravity-driven fold and thrust system developed in response to a domical basement uplift.

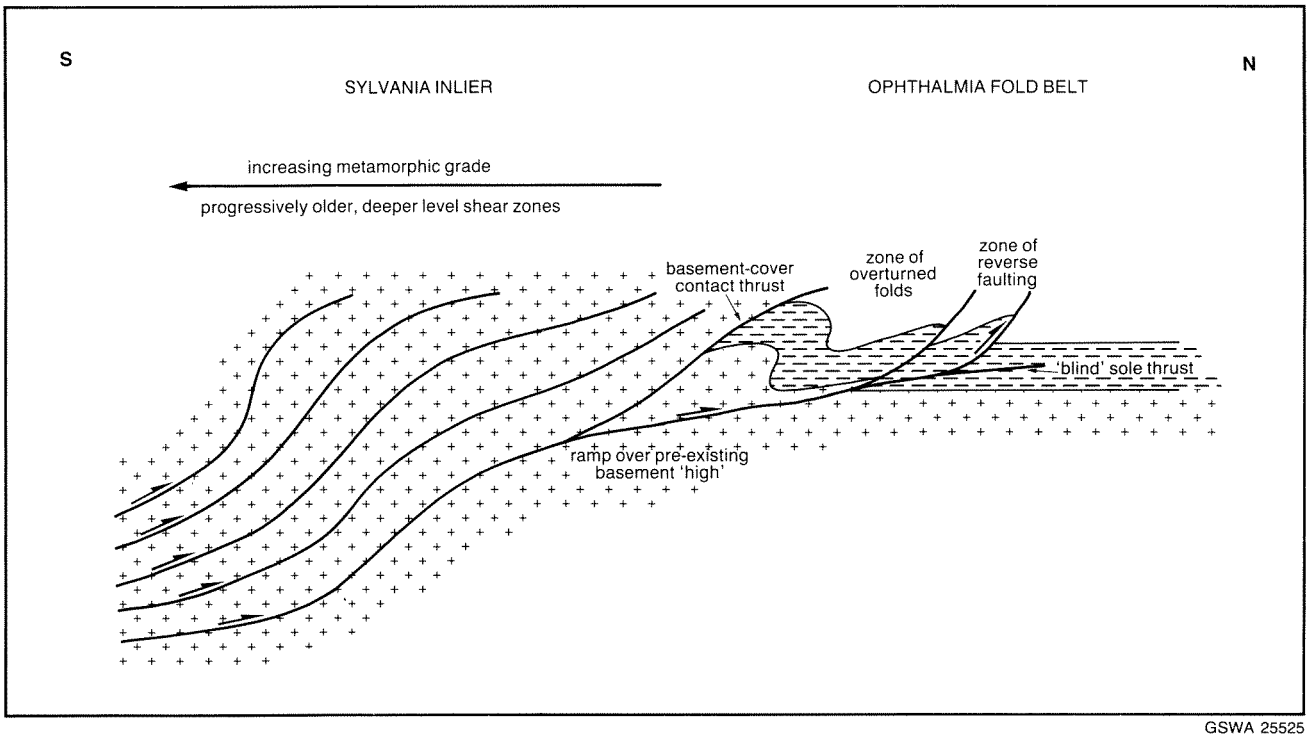

GSWA 25525

Figure 85. Diagrammatic cross-section through the eastern part of the Sylvania Inlier and the southeast part of the Ophthalmia Fold Belt.

crease in metamorphic grade from north to south across the eastern part of the inlier. Such a pattern, together with the ductile nature of the shearing, is also consistent with the exposure of progressively deeper crustal levels (e.g. Rathbone et al., 1983).

Most of the exposed fault structures in the Ophthalmia Fold Belt to the north of the inlier dip steeply south at about 60°. In order to balance folding (Dahlstrom, 1969), a flat lying sole thrust is interpreted beneath the fold belt (Plate 2; see also Elliott and Johnson, 1980; Price, 1981; Hatcher, 1981; Boyer and Elliott, 1982). The steep faults form part of an imbricate fan (Boyer and Elliott, 1982). The conjugate nature of folding north of the fan is consistent with a blind extension to the sole thrust similar to that described by Thompson (1981). The sole thrust is considered to be controlled by the relatively incompetent Fortescue Group.

Direction of thrust transport

From the disposition of faults, shears and stretching lineations in the Sylvania Inlier, and from the pattern of folding in the southeast part of the Ophthalmia Fold Belt (Fig. 40; Plate 3) it is possible to reach some conclusions concerning the principal direction of thrust transport, and the area in which it was concentrated. The most intense deformation in the Sylvania Inlier occurs between Woggaginna Hill and Sylvania. To the east, shear zones and the S_c foliation swing to the southeast. To the west, the trend is southwest. Throughout, the north-northeast trend of L_c stretching lineations is maintained. In the western part of the inlier, the Western Creek Fault, as well as being a thrust, has a sinistral offset.

The most intense deformation in the southeast part of the Ophthalmia Fold Belt occurs between Mount Newman and Shovelanna Hill. Folds to the west of Mount Newman face north—but are not overturned—and swing from a west-northwest to an east–west orientation. East of Shovelanna Hill, folding becomes less intense. This pattern is consistent with the main thrust movement being to the north-northeast and concentrated in the central part of the inlier coincident with the greatest uplift (i.e. deepest exposure levels). To the east and west, the frontal thrusts pass into oblique ramps (Hossack, 1983) which may have relative dextral (eastern ramp) or sinistral (western ramp) offsets.

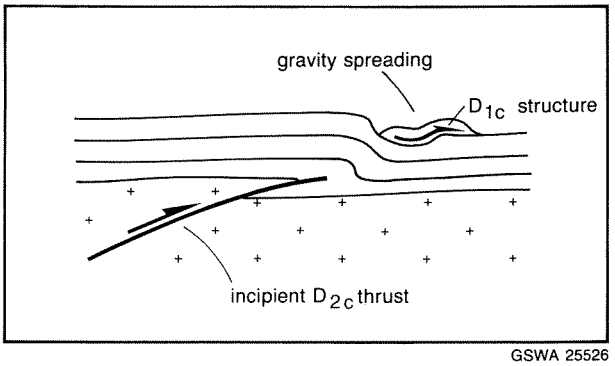

GSWA 25526

Figure 86. Formation of D_{1c} structures during uplift associated with D_{2c} deformation.

Origin of D_{1c} structures

The origin of D_{1c} structures is problematical. Although geographically widespread, any one occurrence appears to be limited in its extent. Deformation is restricted to bedding planes; and ramping—with deformation cutting up or down the stratigraphy—is not seen. No information as to direction of movement is available, and these structures could represent an extensional feature (e.g. Gaudemer and Tapponnier, 1987). Their formation as part of an early extensional fault system (cf. Gibbs, 1984) associated with the formation of the Ashburton Basin is unlikely however, as a direct link with faults on the basin margin has not been seen.

Near the radio transmitter 32 km north-northeast of Newman, the D_{1c} structures are north of the frontal imbricate fan of the D_{2c} thrust system. Deformation does not, then, appear to be directly linked with the thrusting that has produced the D_{2c} structures. An alternative is that it is the result of gravity spreading (cf. Ramberg, 1981) during the early stages of uplift associated with the D_{2c} thrusting (Fig. 86). A similar style of early, restricted, bedding-plane-controlled deformation has been described by Knipe and Needham (1986) from the Southern Uplands of Scotland.

Influence of pre-existing basement structures

Prior to folding in the southeast Hamersley Basin, extensive uplift, up to 9 km according to Smith et al. (1982), took place along the southern margin of the Pilbara Craton. Normal faulting is seen in the vicinity of the Wyloo Dome and may be responsible for localized fan-delta-style deposition of the Beasley River Quartzite in that area (Thorne and Seymour, 1986). Faulting has a general west-northwest to northwest trend, and is parallel to the southern rift which developed during deposition of the Fortescue Group (Blight, 1985; Blake and Groves, 1987).

Folding in the southwestern part of the Hamersley Basin is related to uplift at the end of Turee Creek Group time, and the rhombohedral shape of many of the structures reflects control by a basement segmented along west-northwest and north-northeast shears and faults. This control is the origin of the supposed "Rocklean" cross-fold direction (Halligan and Daniels, 1964) which was attributed by Tyler and Thorne (1990) to plunge culminations and depressions occurring in a single set of west-northwest-trending folds. To some extent the basement blocks can be identified in the seismic refraction data of Drummond et al. (1981, section FDB).

Within the southeastern part of the Ophthalmia Fold Belt, regional plunge culminations can be seen south of the Ophthalmia Range and in the Wonmunna area; there is also a major plunge depression in the Turee Creek syncline area. This reflects the influence of basement-block movements that took place prior to thrusting. Any associated fold would have been very broad, and was tightened up, rather than refolded, by the later thrust event.

Origin of D_{1a} structures in the Ashburton Fold Belt

The origin of D_{1a} structures in the Ashburton Fold Belt is uncertain. The change in facing directions across Zone C may be interpreted in terms of a northeasterly directed thrust system which ramped on the margin of the Pilbara Craton. This could produce back-thrusting and southwest-facing folds at the southern margin of the fold belt. The increase in metamorphic grade from north to south is consistent with crustal thickening caused by thrusting and recumbent folding.

Dextral wrench faulting on the Hamersley Basin–Ashburton Basin margin

The D_{2a} deformation in the Ashburton Fold Belt can be interpreted as the result of major, regional, dextral wrench faulting parallel to the southern margin of the Pilbara Craton (Thorne and Seymour, 1991; Tyler and Thorne, 1990). Harris (1987) suggested that thrusting in the southeast part of the Ophthalmia Fold Belt developed as a part of this wrenching event. Sedimentation patterns within the Ashburton Basin are inconsistent with the view that it represents a strike-slip basin (Thorne and Seymour, 1991). All direct evidence suggests that the D_{2a} event was either synchronous with, or post-dated deposition of the Capricorn Formation. There is a clear separation, therefore, between thrusting in the southeast part of the Ophthalmia Fold Belt, which occurred after the deposition of the Cheela Springs Basalt, and dextral wrenching (Table 7).

Apart from the time separation between the two events, the D_{2c} thrusting in the southeast Ophthalmia Fold Belt is directed north-northeast, normal to the strike-slip direction, and towards the craton margin—a relationship typical of a front-on collision or convergence.

Dextral wrench faulting was controlled by basement structures, and the highest strains developed in the central part of the Ashburton Fold Belt (Zone B)—immediately south of the craton margin as identified by Drummond (1981). In the Paraburdoo area, it is probable that strike-slip movement took place on pre-existing normal faults that were active during deposition of both the Beasley River Quartzite and the Mount McGrath Formation.

The re-orientation of the D_{2c} folds (Ophthalmia Fold Belt) across the Turee Creek Syncline, together with the widespread occurrence of dextral wrench faulting and local northwest-directed thrusting, is consistent with the Turee Creek Syncline having been subjected to a clockwise (i.e. dextral) rotation during the D_{2a} event in the Ashburton Fold Belt (Fig. 40; Plate 3).

A Tectonic model for the northern margin of the Capricorn Orogen

Previous models

Previous models for the Capricorn Orogen have envisioned the development and tectonic evolution of a geosyncline within an intracratonic environment (MacLeod, 1966; Daniels, 1975; Horwitz and Smith, 1978; Gee, 1979; Williams, 1986). In each of the models it has been assumed that the Pilbara and Yilgarn Cratons initially formed part of a single, continuous craton.

Sedimentation in the Capricorn Orogen began with a rifting event, attributed by Williams (1986) to crustal arching as a response to upwelling of hot currents from the mantle. Basement was Archaean gneiss of the Pilbara and Yilgarn cratons (Gee, 1979; Williams, 1986). Separation between the two cratons was indicated by the development of tholeiitic basalts with mid-ocean ridge (MORB) affinities (Hynes and Gee, 1986). Trough sedimentation developed in the rapidly subsiding rift zone with a symmetrical distribution of shelf sedimentation (Gee, 1979) along the flanks of the stable cratons to the north and south. Gee (1979) cited gross lithological similarities, a similar chronological position relative to the major orogenic processes, and the almost complete physical continuity between them, as evidence for correlation of the thick "greywacke-type" sediments of the Glengarry and Wyloo Groups. Deposition of the shelf and trough sediments was accompanied, and followed, by an episode of regional metamorphism; and the Glengarry and Wyloo Groups merged, through steep metamorphic gradients, into the Morrissey Metamorphic Suite (medium- to high-grade metasedimentary rocks) of the Gascoyne Complex (Williams, 1986).

Deformation in the Gascoyne Complex was attributed by Williams (1986) to gravity-induced gliding and plastic flow of metasediments off rising granitoid domes. During peak metamorphism, mantled gneiss domes and diapirs of migmatite and anatectic granitoid were emplaced. Later deformation accompanied the diapiric emplacement of large, late-stage granitoid batholiths derived from large-scale anatexis in the lower part of the sialic crust.

Deformation along the orogenic margins was a consequence of the development and evolution of the geosyncline (MacLeod, 1966). According to Gee (1979) there is marked asymmetry in the tectonic processes operating. The northern margin is characterized by folding that is parallel to the geosyncline, and which has resulted from northward movement against a stable foreland (Pilbara Craton). The southern margin of the Capricorn Orogen is characterized by fault tectonics oblique to the geosyncline. Gee (1990) has attributed these oblique structures to the fact that the initial rifting phase had a sinistral component of movement and that the subsequent convergence had a substantial dextral transcurrent movement.

Both Gee (1979, 1990) and Williams (1986) have commented on the apparent lack of any evidence for subduction or for plate-tectonic processes in general. Central to the intracratonic model outlined above is the question of the original continuity of the Pilbara and Yilgarn Cratons.

Comparison of the Pilbara and Yilgarn Cratons

Gee (1975, 1979) has pointed out apparent differences between the Pilbara and Yilgarn cratons:

(a) The Yilgarn contains a belt of high-grade gneiss, the Narryer Gneiss Complex, which ranges in age from 3700 to 3200 Ma (de Laeter, et al., 1986), and which is older than the Yilgarn granite–greenstone. Such gneiss has not developed in the Pilbara.

(b) The Pilbara granite–greenstone ranges from about 3500 to about 2800 Ma (Trendall, 1983; Blake and McNaughton, 1984) whereas that in the Yilgarn ranges from about 3000 to about 2650 Ma (Fletcher et al., 1984; McNaughton and Dahl, 1987).

(c) Mature sediments occur at stratigraphically higher levels in the Pilbara greenstones than they do in the Yilgarn.

(d) There are differences in tectonic style: the Pilbara batholiths are roughly equant in plan whereas those in the Yilgarn are linear—cf. Gee et al. (1981) and Hickman (1983).

Gee (1979) suggested that the Pilbara and Yilgarn Cratons evolved by similar processes that operated at different times and in different places. Both cratons were regarded as equant volcanic basins developed at different times on older, continuous sialic crust.

Horwitz and Smith (1978) cited the occurrence of east–west and north–south dyke swarms in both cratons as evidence for a common stress system prior to initiation of the Hamersley Basin. Tyler (1990) has pointed out that considerable age differences exist between the various swarms. Those in the Pilbara either pre-date, or developed synchronously with, the Fortescue Group (about 2750 Ma), whereas a dyke of the Widgiemooltha dyke swarm in the Yilgarn, which is the principal east-west suite, has been dated at about 2400 Ma (Fletcher et al., 1987). Also, Horwitz and Smith (1978) suggested that the ultramafic intrusion at Coobina shows both trends. In this study, it has been shown that the intrusion, which was deformed with the Jimblebar greenstone belt, does not form part of either the north–south or east–west swarms.

Data from seismic refraction profiles across the Pilbara Craton and the Capricorn Orogen showed differences between the Pilbara Craton and the northern part of the Yilgarn Craton (Drummond, 1981; Drummond et al., 1981). The crust of the Pilbara Craton is 28 to 33 km thick, but that of the northern Yilgarn Craton is more than 50 km thick. The Pilbara crust has two layers, but three layers are present in the Yilgarn. The first interpreted appearance of the lowest (third) layer marks the southern margin of the Pilbara Craton and is coincident with the middle part of the Ashburton Basin. The third layer is relatively thin beneath the Capricorn Orogen, but thickens rapidly beneath the Yilgarn Craton.

Geochronological data from the Capricorn Orogen have been summarized by Libby et al. (1986). Sm–Nd and Sr–evolution dating indicates that most of the rocks involved in the orogeny were derived directly or indirectly from mantle-like resevoirs between 2400 Ma and 1600 Ma. In the southern part of the orogen, older (>3000 Ma) dates suggest that the Gascoyne Complex developed on Yilgarn basement. To the northwest, a decrease in Sm–Nd dates indicates either gradual migration of crustal formation or progressive northward loss of contaminating Archaean crustal material. This would suggest that there need not have been continuous Archaean basement throughout the orogenic belt.

Blake and Groves (1987) noted that the Norseman–Wiluna belt of the Yilgarn Craton, and the Fortescue Group, which represents the initiation of the Hamersley Basin on the Pilbara Craton, are broadly coeval. The Norseman–Wiluna belt is interpreted by Blake and Groves (1987) as representing a failed rift on stretched, relatively hot crust which has been reworked and then cratonized. The Fortescue Group is a sequence of continental basalts that were extruded on to thick, relatively cold crust after cratonization of the Pilbara. Extensive granitoid emplacement was taking place in the Murchison Province of the Yilgarn Craton during this period (Watkins and Hickman, 1990). Cratonization of the Pilbara was complete some 200 Ma before that of the Yilgarn.

Comparison of the lower Proterozoic sedimentary sequences (Glengarry and Wyloo Groups)

The sequence of depositional environments in the Wyloo Group described earlier in this chapter may be compared with those interpreted for the Glengarry Group rocks by Gee (1987, 1990). Although there are broad similarities, as suggested by Gee (1979), they are such as can be attributed to any sequence deposited during a transition from shelf to deep-water sedimentation. Major internal differences do exist (Table 8).

The lowest units in the Glengarry Group are the Juderina Formation and the Johnson Cairn Shale, which were deposited on a smooth unconformity surface in a shallow epeiric sea. The Beasley River Quartzite at the base of Wyloo Group is associated with active uplift along the Pilbara Craton margin (Thorne and Seymour, 1986). A major carbonate unit, comparable with the Duck Creek Dolomite, has not been found in the Glengarry Group. Gee (1979) has referred to a thick greywacke and volcanic fill; in the Glengarry Group, this is seen as the Doolgunna Formation, comprising granite-derived turbidites, the Thadunna Greywacke, comprising mafic-derived turbidites, and the Narracoota Volcanics, a sequence of basalts chemically similar to tholeiites from mid-ocean ridges

TABLE 8. COMPARISON OF ASHBURTON BASIN AND GLENGARRY SUB-BASIN STRATIGRAPHIES

Ashburton Basin		*Glengarry Sub-Basin*	
Unit	*Lithology*	*Unit*	*Lithology*
Ashburton Formation	sandstone, shale	Labouchere Formation	sandstone
Duck Creek Dolomite	carbonate	Horseshoe Formation	greywacke, shale, BIF
Mount McGrath Formation	conglomerate, sandstone	Thadunna Greywacke	greywacke
—unconformity/disconformity—		Narracoota Volcanics	tholeiitic basalt
Cheela Springs Basalt	basalt	Karalundi Formation	clastic carbonate, chert, tuff
Beasley River Quartzite	conglomerate, sandstone	Doolgunna Formation	sandstone, arkose
		Johnson Cairn Shale	shale
		Juderina Formation	quartzite, siltstone, chert breccia

(Hynes and Gee, 1986). The supposed equivalent in the Wyloo Group is the Ashburton Formation which comprises granite-derived turbidites deposited as part of a submarine fan orientated parallel to the Pilbara Craton margin (Thorne and Seymour, 1991). Rocks equivalent to the Narracoota Volcanics and the Thaduna Greywacke have not been seen. The uppermost part of the Glengarry Group comprises the iron-formation, sandstone, and shale of the Horseshoe and Labouchere Formations. These were basin-fill deposits, and an equivalent is not seen at the top of the Wyloo Group. The Capricorn Formation is a sequence of braided-fluvial, alluvial-fan, and shallow-marine or lacustrine deposits that unconformably overlies the Wyloo Group. It post-dates the initial phase of closure of the Ashburton Basin.

Palaeomagnetic evidence

Construction of a Precambrian apparent-polar-wander-path for Australia (McWilliams, 1981; Idnurm and Giddings, 1988) favours a "single continent" model in which the assemblage of cratons has retained its current or similar spatial relationships since 1600 Ma. The study by Idnurm and Giddings (1988) revealed that the quality of the majority of available pole results is low: only four out of 61 are regarded as "key poles" (well defined in position and age). Certain segments of the path, including the track between 2300 and 1900 Ma remain uncertain because of lack of data. The periods of apparent polar stillstand between 2700 and 2500 Ma and 1900 and 1700 Ma could conceal more complex path behaviour.

The data for the late Archaean to early Proterozoic are equivocal and do not preclude separate histories for the Pilbara and Yilgarn Cratons prior to the Capricorn Orogeny. Even if the data are taken as indicating a "single craton" model, undetected displacement between the Pilbara and Yilgarn cratons could be of the order of 1000 to 2000 km (McWilliams, 1981).

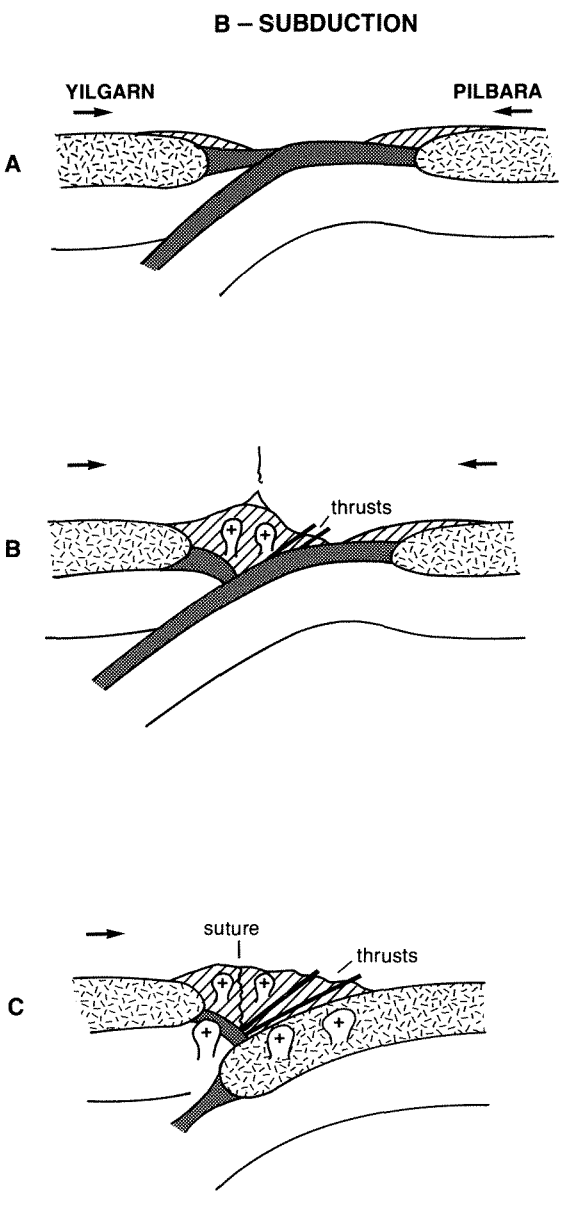

Figure 87. B-subduction model.

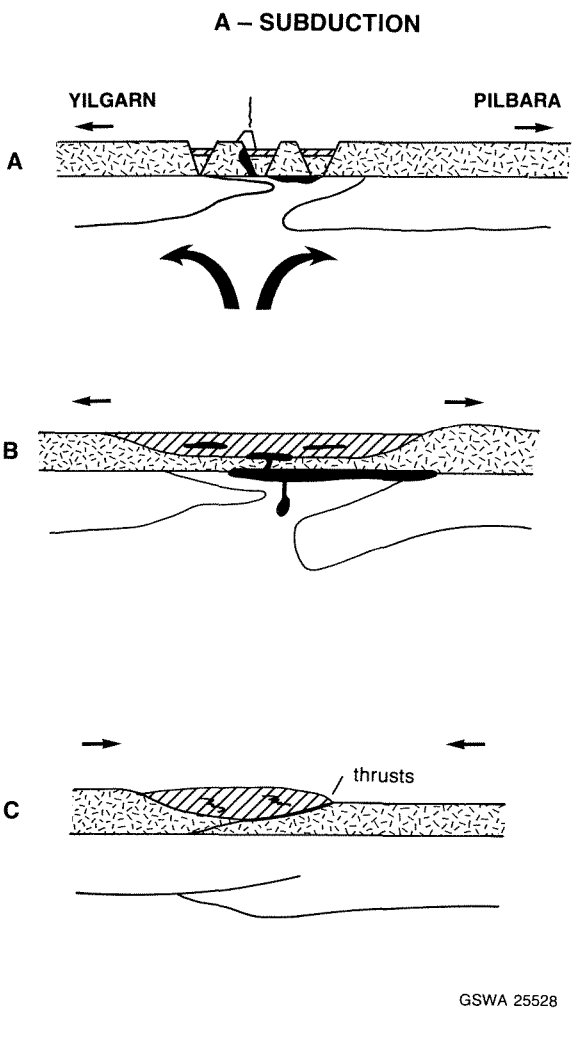

Figure 88. A-subduction model.

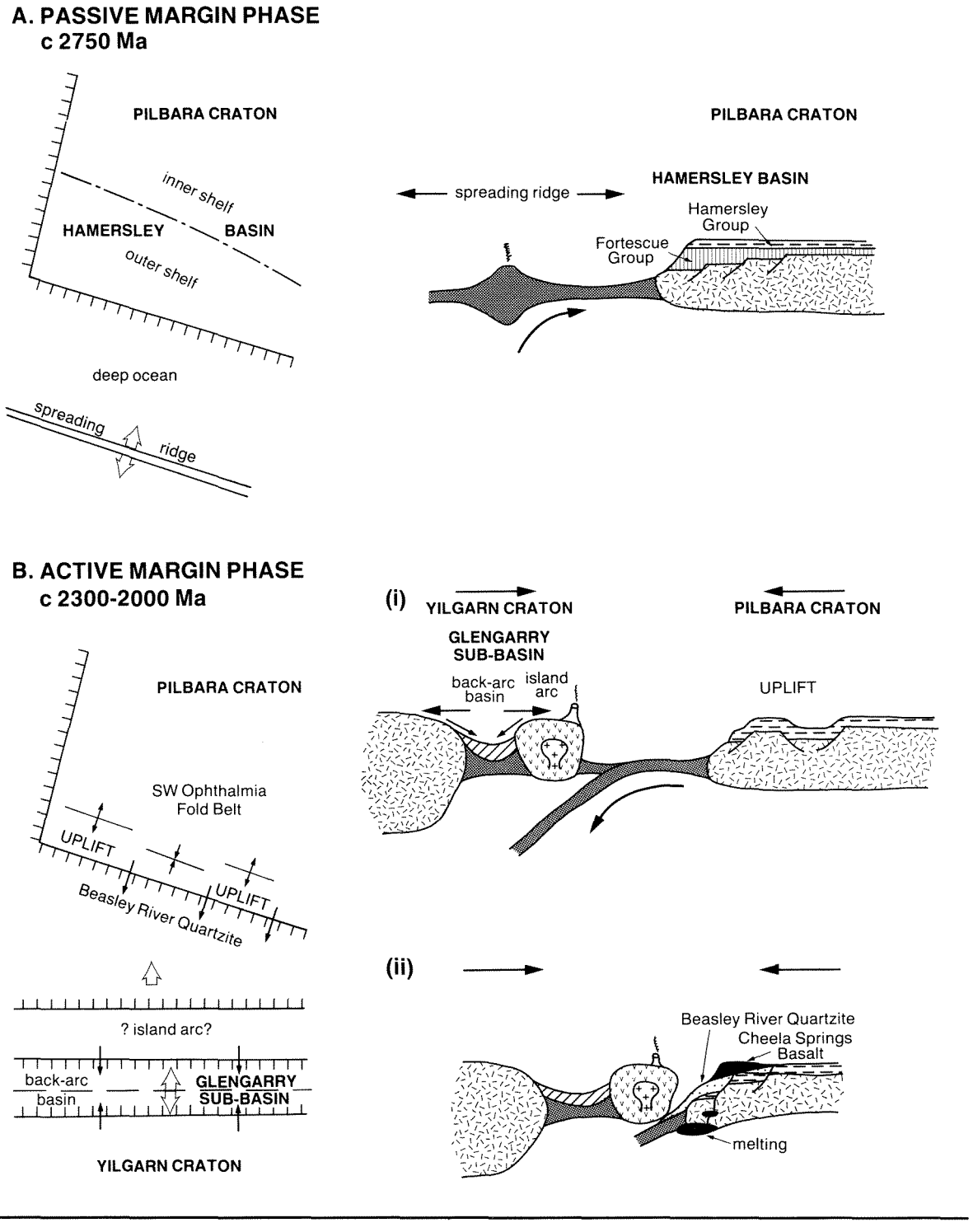

Figure 89. Cartoons illustrating the development of the Capricorn Orogen as part of a B-subduction-style collision; A — Passive margin phase; B — Active margin phase; (i) Post-Turee Creek Group; (ii) Beasley River Quartzite and Cheela Springs Basalt; C — Collision phase; (i) Development of southeast part of the Ophthalmia Fold Belt; (ii) Duck Creek Dolomite - Ashburton Formation; (iii) Suturing - Ashburton Fold Belt D_{1a} and granitoid intrusion.

C. COLLISION PHASE
c 2000-1600 Ma

(i)

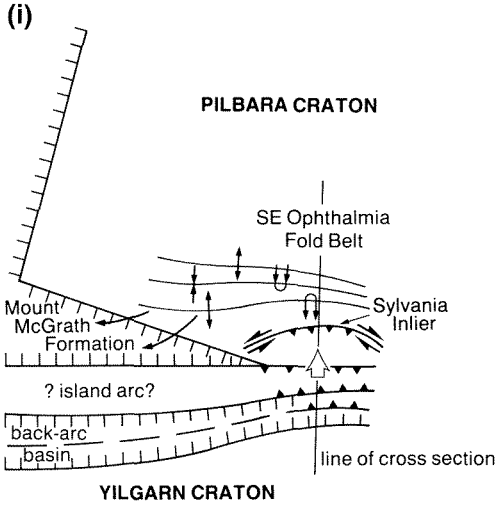

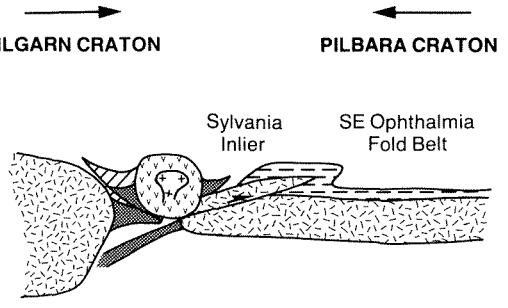

(ii)

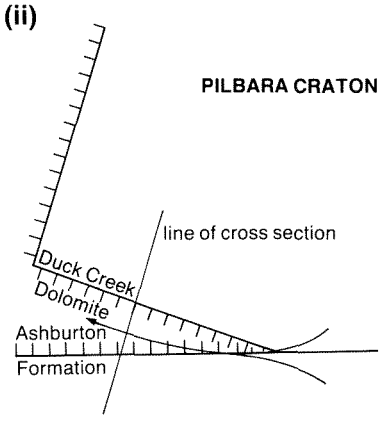

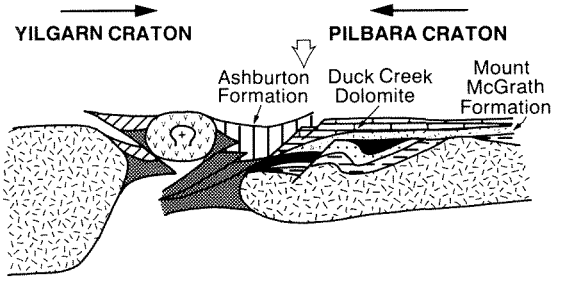

(iii)

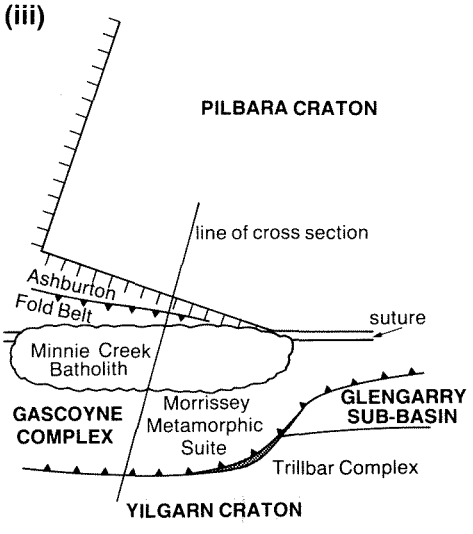

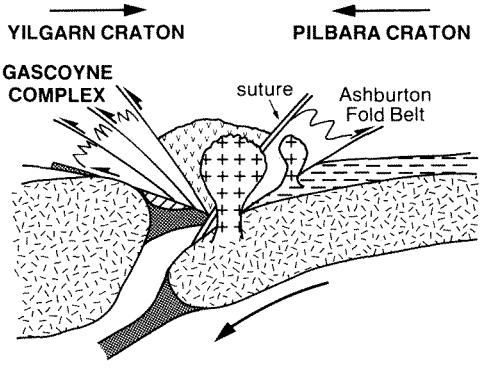

GSWA 25529

Models of Proterozoic orogeny

There has been much debate about the mechanisms of Proterozoic orogeny. With the recognition of the importance of thrust tectonics and other horizontal movement in the Proterozoic crust (e.g. Coward, 1984), attention has focused on the applicability of Phanerozoic-style plate tectonics. This topic was reviewed by Shackleton (1986). Some authors have applied the classical plate tectonic model (Fig. 87, B-subduction) in its entirety (e.g. Burke et al., 1976; Hoffman, 1980; Windley, 1981, 1983). Others, noting the apparent absence of criteria, such as ophiolites, paired metamorphic belts, and island arcs, which would imply B-subduction, have proposed a plate-tectonic model of intracratonic orogeny (Fig. 88, A-subduction) driven by crust–mantle delamination (Kroner, 1981, 1983; Etheridge et al., 1987). Within this debate, models for the Capricorn Orogen, which has developed between two well-exposed and clearly defined Archaean cratons, are significant.

B-subduction model for the Capricorn Orogeny

From the above discussion it is clear that there is no unequivocal evidence that the Pilbara and Yilgarn cratons formed part of a single, continuous craton prior to the development of the Capricorn Orogen. There is, therefore, no *requirement* for intracratonic—i.e. A-subduction-style—orogeny. Any model for the tectonic evolution of the orogen *must* account for the differences that have been recognized between the Pilbara and Yilgarn cratons. In an attempt to overcome this difficulty in an intracratonic model, Harris (1987) has suggested that suturing between the cratons occurred prior to initiation of the rifting phase and that evidence for this suture is masked by the later development of the orogen. The two cratons would have been juxtaposed by transcurrent movements along the line of the suture. At present there is no evidence to support such a model.

It is the opinion of Shackleton (1986) that most of the evidence for A-subduction models is negative. It is possible that the apparently missing criteria, which would imply B-subduction, are present but have not been recognized. This may well be the case for the Capricorn Orogen.

Myers (1990), in a reassessment of the Gascoyne Complex, has attributed extensive shear zones and mylonite formation at its southern margin to the development of a foreland thrust belt. This has formed mainly in rocks of the Narryer Gneiss Complex. They have been overridden by a southward-transported thrust sheet of deformed and metamorphosed gabbro and ultramafic rocks forming the Trillbar Complex. This may represent the lower part of an ophiolite sequence or crustal underplate obducted onto the foreland (Myers, 1989).

A feature of Proterozoic orogenic belts is the occurrence of metamorphic assemblages consistent with high temperature and low to medium pressure. Pressure–temperature–time paths have been interpreted in terms of slow isobaric cooling at depth (e.g. Phillips and Wall, 1981; Hobbs et al., 1984), in contrast with the rapid, isothermal uplifts associated with B-subduction (England and Thompson, 1984). Muhling (1988) and Baker et al. (1987), working on rocks from the southern foreland of the Capricorn Orogen, have identified corona reaction textures between kyanite, garnet, and gedrite, that are consistent with substantial uplift (10 km or more) accompanied by relatively little cooling. Uplift was synchronous with extensive granitoid intrusion. This was taken by Muhling (1988) as evidence consistent with the development of the Capricorn Orogen in a B-subduction-style collision zone.

Within the Narracoota Volcanics, which consist mainly of tholeiitic basalts with MORB affinities, mafic volcanic rocks, whose chemistry resembles some boninites found associated with modern island arcs of the western Pacific are present (Hynes and Gee, 1986).

It appears then, that there is evidence for the operation of B-subduction in the Capricorn Orogen. The tectonic evolution of the Sylvania Inlier and the southeast Hamersley Basin during the Capricorn Orogeny will be discussed in terms of a B-subduction model.

The preferred B-subduction model starts at about 2750 Ma with the development of the Hamersley Basin on the Pilbara Craton as an intracratonic rift (Fig. 89A). The rift evolved into a passive continental margin as crustal separation took place. The southern margin of the rift has not been identified. There is certainly no sequence of rocks preserved on the northern margin of the Yilgarn Craton, or in the Gascoyne Complex comparable, either in age or stratigraphic sequence, with those deposited in the Hamersley Basin. At this stage, the Pilbara Craton would have been remote from the Yilgarn Craton. Iron-formation developed in the quiet waters of an outer shelf adjacent to a deep ocean basin.

The early stages of the closure of the ocean basin were marked by an active continental margin phase and, in Turee Creek Group times (about 2300 Ma), the re-establishment of the supply of terrigenous sediment to the Hamersley Basin. Considerable uplift occurred along the craton margin coincident with large-scale folding in the southwest Hamersley Basin (the western part of the Ophthalmia Fold Belt) controlled by the movement of basement blocks (Fig. 89B(i)). The instability was triggered by a change in plate motion that accompanied the initiation of subduction along the northern margin of the Yilgarn as it began to drift towards the Pilbara.

On the northern margin of the Yilgarn Craton, the lowest part of the Glengarry Group and the equivalent Morrissey Metamorphic Suite were deposited in a shallow sea. As subduction progressed, an island arc with a marginal or back-arc basin separating it from Archaean crust developed. The Narracoota Volcanics and the associated Thadunna Greywacke were deposited in this basin. The Doolgunna Arkose was deposited marginally to the foreland.

The sedimentology of the Ashburton Basin has been interpreted by Thorne and Seymour (1991) in terms of active-margin to foreland-basin evolution. The lower Wyloo Group was deposited during the final stages of ocean-basin closure, and extension along the southwestern part of the margin was the result of arching of the crust (a flexural

bulge) as the adjacent ocean floor was loaded by the approaching continent (e.g. Stockmal et al., 1986). The generation of mafic magma, which erupted as the Cheela Springs Basalt, relates to this flexuring (Fig. 89B(ii)).

The two cratons collided after the eruption of the Cheela Springs Basalt. The collision was oblique, occurring first in the southeast, where a foreland fold-and-thrust belt (the southeast part of the Ophthalmia Fold Belt), was established (Fig. 89C(i)). As a part of this belt, the Sylvania Inlier represents Pilbara Archaean basement, part of which is interpreted as having been thrust back into the Hamersley Basin succession. Some authors have suggested that thrust transport directions can be related directly to plate motions (e.g. Shackleton and Ries, 1984). In the case of the northern Capricorn Orogen, thrust transport was normal to the Pilbara Craton margin and suggests that movement of the Yilgarn Craton relative to the Pilbara was to the north-northeast.

Collision migrated northwest, and migration of the associated flexural bulge produced further, post-folding, uplift and extension (Thorne and Seymour, 1991). A suite of west-northwest-trending mafic dykes was intruded at this time; this was followed by subaerial exposure and formation of iron ore at Paraburdoo. Uplift supplied sediment to the Mount McGrath Formation.

The end of deposition of Mount McGrath Formation deposition was marked by deepening water conditions. Continued loading produced downwarping and drowning of the craton margin, cutting off the supply of terrigenous sediment. The Duck Creek Dolomite was subsequently established in fairly deep water which shallowed as the unit built up to establish a shelf. The end of Duck Creek Dolomite deposition was marked by oversteepening and/or normal faulting of the shelf slope and collapse of the carbonate shelf (Thorne and Seymour, 1991).

With collapse of the carbonate shelf, a deep basin was established parallel to the craton margin (Fig. 89C(ii)). Material eroded from the uplifted granite–greenstone of the Sylvania Inlier was shed into eastern end of the basin and transported westwards by means of an elongate submarine fan, which extended as far as the Wyloo Dome (Thorne and Seymour, 1991). This submarine fan system is now preserved as the Ashburton Formation.

Continent to continent collision now took place along the southern margin of the Ashburton Basin, and granitic detritus from the northern Yilgarn was incorporated into a second submarine fan system which prograded north-northeastwards into the basin, over the easterly derived fan (Thorne and Seymour, 1991). A third fan complex was also recognized in the northwest Ashburton Basin, where sediment was derived from local uplift in the western Hamersley Basin.

Further cratonic convergence produced recumbent folding in the southern Ashburton Basin (Fig. 89C(iii), Ashburton Fold Belt D_{1a}). Tectonic thickening of the sequence by folding and thrusting is indicated by increasing metamorphic grade from north to south across the basin.

Collision also produced extensive deformation and crustal thickening in the northern Yilgarn. This resulted in high-grade metamorphism in the Gascoyne Complex and was accompanied by the generation (1800–1600 Ma) of large volumes of granitic magma (Williams. 1986; Muhling, 1988), the most important example of which is the Minnie Creek Batholith.

Suturing was coincident with the decollement and steep metamorphic gradient that marks the boundary between the Wyloo Group and the Morrissey Metamorphic Suite (Williams, 1986). The Trillbar Complex may represent a slice of ocean floor derived from closure of the back-arc basin.

The last stage of collision involved large-scale dextral wrenching parallel to the margin of the Pilbara craton. This is responsible for the D_{2a} deformation in the Ashburton Fold Belt and for the clockwise rotation of the Turee Creek syncline. The dominance of wrench faulting, together with normal faulting at the southwest corner of the Pilbara Craton, can be explained in terms of the progressive development of an oblique collision (Fig. 90).

The initial collision in the southeast Pilbara was directed north-northeast, normal to the craton margin. The northern margin of the Yilgarn was orientated more east-west (Fig. 2; see also Drummond, 1981). Progressive closure of the oblique margins produced a relative dextral movement on the Pilbara margin. Corresponding sinistral movements on faults and shear zones in the northern Yilgarn have been reported by Williams (1986). A model for this style of lateral extrusion of material caught between two opposing plates is provided by the collision between India and Asia (Tapponnier et al., 1986).

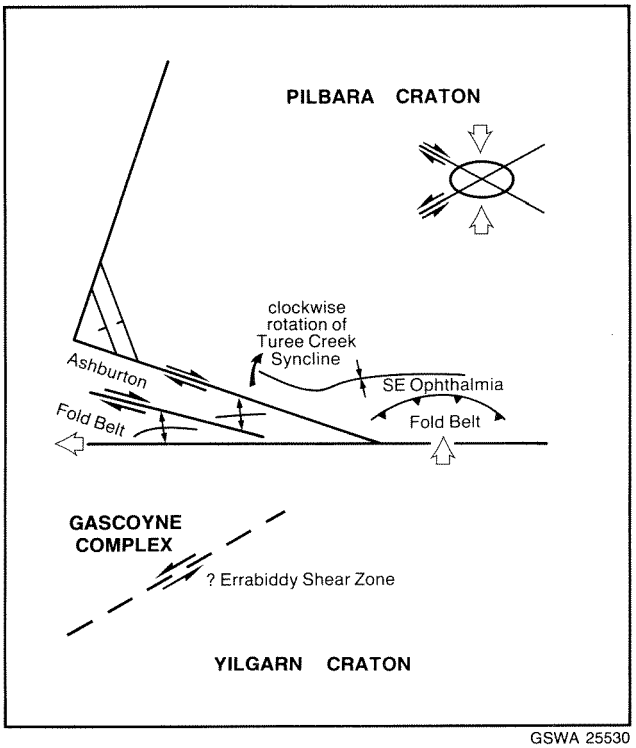

GSWA 25530

Figure 90. Relationship of Ashburton Fold Belt D_{2a} wrench faulting to the overall structure of the Capricorn Orogen developed as part of an oblique collision.

Chapter Five

Post-Capricorn Orogeny Evolution

Deformation

Introduction

Deformation that post-dated the Capricorn Orogeny in the Sylvania Inlier and the southeast Hamersley Basin took the form of faulting and associated folding. Several ages of faulting have been recognized.

The Mount Whaleback Fault System

The earliest set of post-Capricorn Orogeny faults is a series of northeasterly to east-northeasterly orientated normal faults; the most prominent is the Mount Whaleback Fault, which can be traced for 45 km (Plate 3). These normal faults are offset by related west-northwesterly orientated sinistral transfer faults. The two fault directions are consistent with a southeast-directed extension (cf. Gibbs, 1984).

Between Prairie Downs and Horrigans Pool, faults belonging to this system form the boundary between the Hamersley and Bresnahan Basins (Plates 2 and 3). Faulting was active during deposition of the Bresnahan Group, which is a series of at least two, and possibly three, alluvial fans stacked one on top of the other (Hunter, 1990; Tyler et al., in press). The deposition of the fans was probably triggered by faulting; the youngest fan is in the west, centred on Mount Bresnahan. Palaeocurrents were directed to the southeast (Hunter, 1990). This indicates that the fault system was propagating northwestward (Fig. 91). Steep fault structures at the surface are presumed to root into flat-lying detachment faults at depth (cf. Wernicke, 1981; Gibbs, 1984; Lister et al., 1986).

The Mount Whaleback Fault is complex: the single fault present at Western Ridge splits into two at Mount Whaleback itself (Plate 2). The main throw has been transferred by a series of splay and subsidiary faults to a parallel fault 1 km to the south. Kneeshaw (1975) records dip values of 65–75° on this fault (Fig. 92). In its hanging wall, two flat-lying normal faults are present (Fig. 93).

The East Pit Footwall Fault (Swindells et al., in prep.) forms the floor of the orebody under the East Pit and truncates the east syncline. It has an overall west-southwest dip that is shallower than the plunge of the fold. Where it is exposed, the fault juxtaposes the mineralized Dales Gorge Member and the lower part of the Mount McRae Shale.

The Central Fault (Swindells et al., in prep.) originates within the central anticline and truncates the south syncline. It forms the floor to the orebody beneath the West Pit. The mineralized Dales Gorge Member may lie directly on Wittenoom Dolomite. Both the East Pit Footwall Fault and the Central Fault steepen to the north-northwest as they approach the main fault and are presumed to root into it. To the south-southeast they cut into the Wittenoom Dolomite, but are not seen to cut down into the Marra Mamba Iron Formation. Numerous smaller normal faults occur throughout the mine area. At the east end of the East Pit, movement has occurred that offsets the Whaleback Shale–Joffre Member boundary (Fig. 94). Localized high strain is marked by the re-orientation of pre-existing small-scale folds (Fig. 95).

The Homestead Fault parallels the Mount Whaleback Fault, before curving to root into it north of Eastern Ridge (Plates 2 and 3). The throw on the fault appears to increase to the southwest. A southwest continuation of the Homestead Fault controls the Tunnel Creek drainage. The Wheelara Fault also formed as part of this system. It is a complex of east-northeasterly trending normal, reverse, and wrench faults. There is a horizontal offset of 11 km and "drag" associated with dextral movement has affected both the Painkiller Bore Fault and the axes of adjacent D_{2c} folds. Ward et al. (1975) reported dips of 30° to the east on a subsidiary fault.

Other faults that formed as part of this system include the Jillary Well Fault and associated northeast-trending structures at the southwest margin of the Sylvania Inlier. These may also have a dextral strike-slip component, and may degenerate into conjugate folds. Normal faulting occurs to the south and west of Giles Point. Faults affecting lower Fortescue Group south of the Capricorn Roadhouse, and those offsetting the stratigraphy of the Jimblebar greenstone belt are also thought to be of this age.

Northeast-trending normal faults occur along the line of Turee Creek east of Mount Channar, and also separate Wyloo Group from Bresnahan Group at Horrigan Pool. These may reflect re-activation of fault trends established during the Ashburton Fold Belt D_{2a} wrenching event.

Prairie Downs and Poonda Faults

The Prairie Downs Fault (Plates 2 and 3) is a major reverse fault that dips north-northeast, and is marked by massive quartz veining (Blockley, 1971). It cuts the Bangemall Group and was active during its deposition

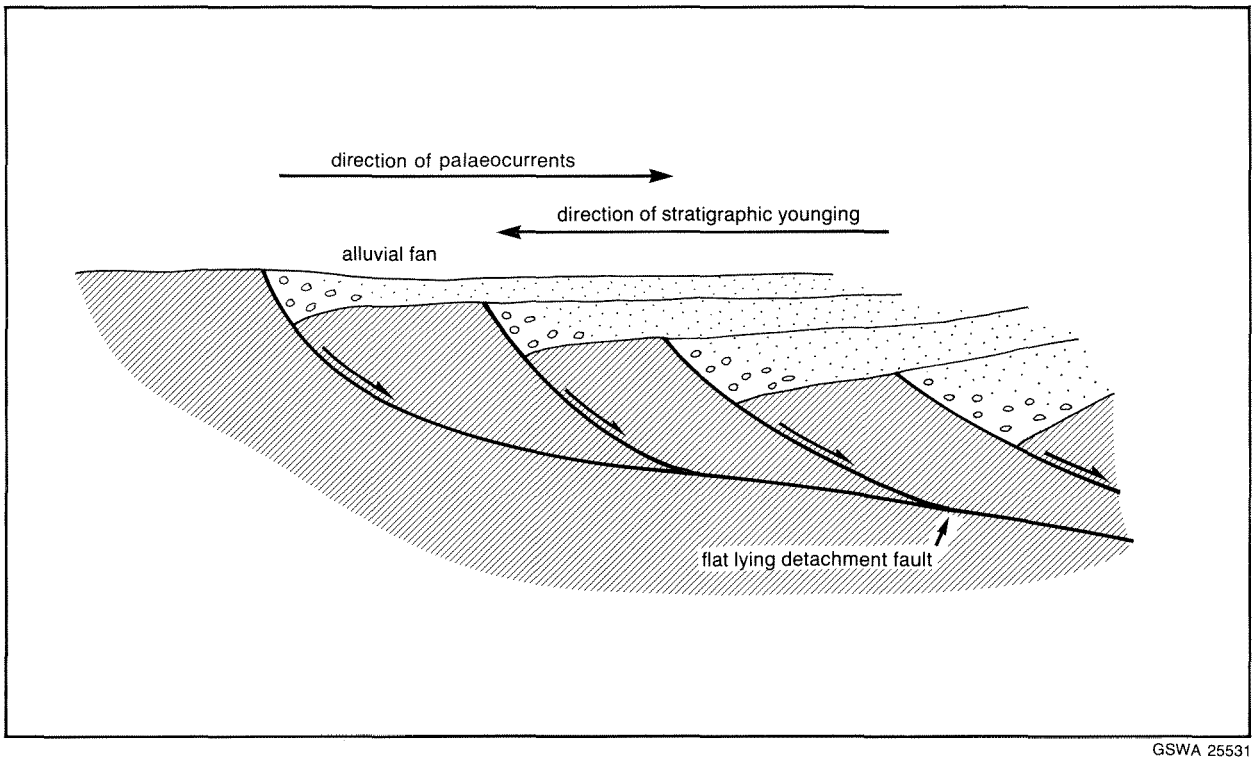

GSWA 25531

Figure 91. Relationship between normal, extensional faulting and deposition of alluvial fans.

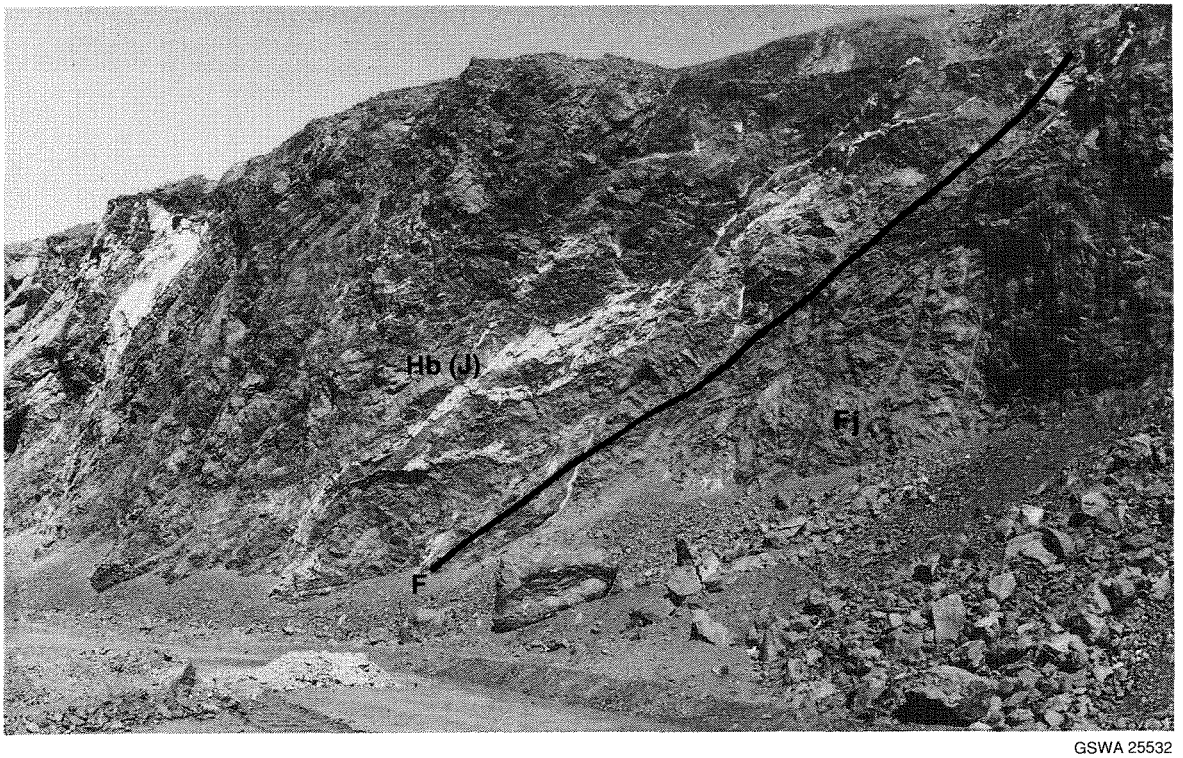

GSWA 25532

Figure 92. The Mount Whaleback Fault, exposed in the Mount Whaleback Mine, juxtaposing the Joffre Member of the Brockman Iron Formation (Hb(J)) and Jeerinah Formation (Fj).

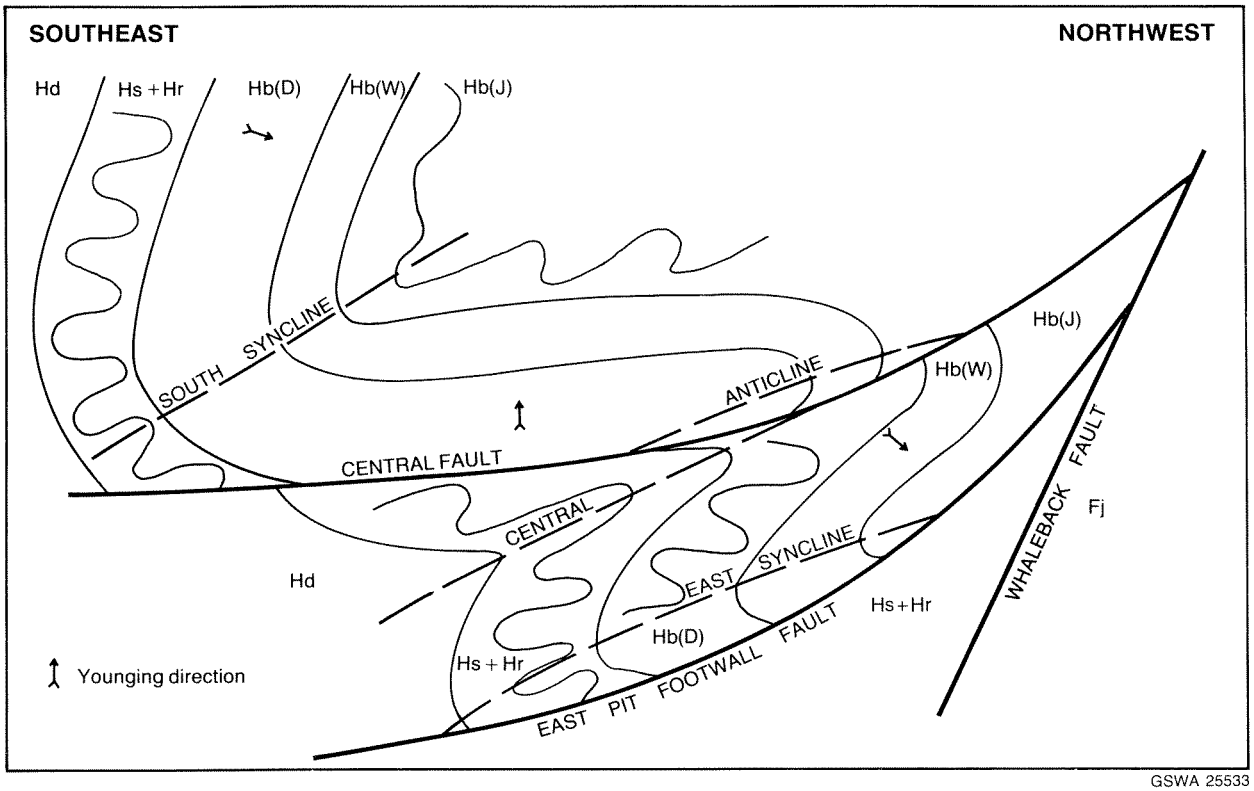

GSWA 25533

Figure 93. Diagrammatic cross-section of the Mount Whaleback Mine. Not to scale.

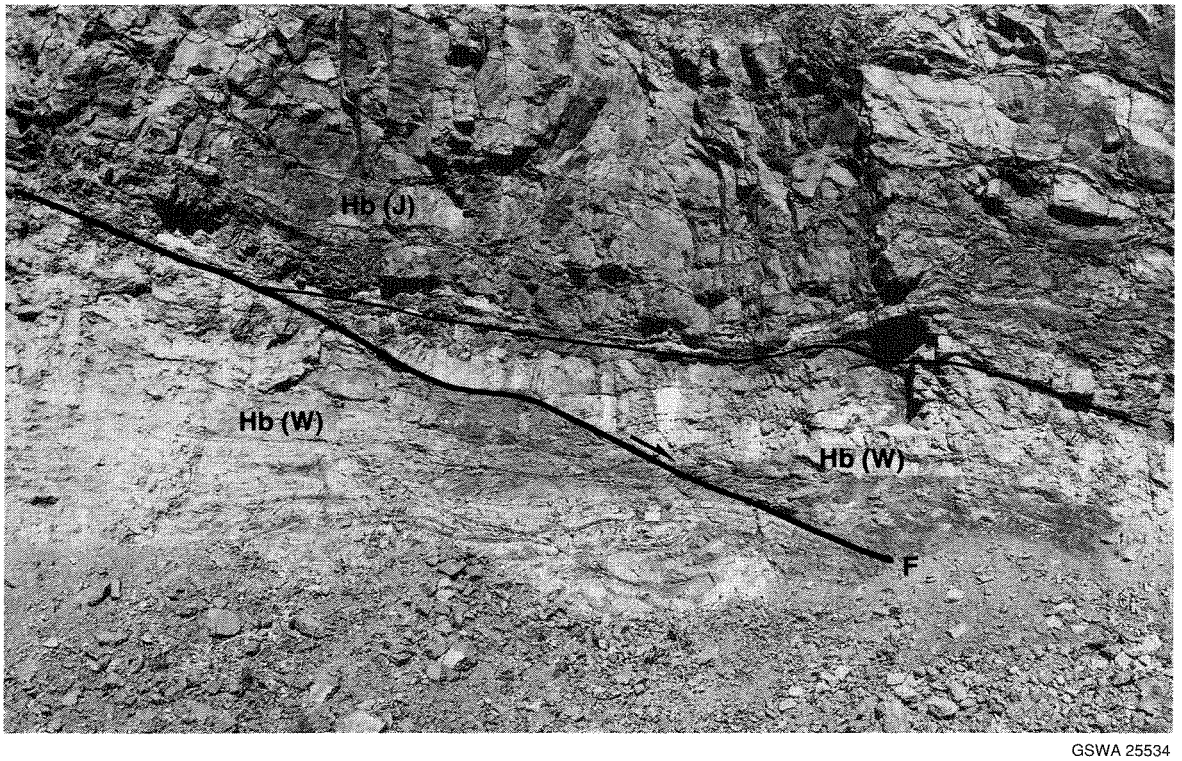

GSWA 25534

Figure 94. Low-angle normal fault offsetting the boundary between the Whaleback Shale (Hb(W)) and the Joffre Member (Hb(J)) of the Brockman Iron Formation, Mount Whaleback Mine.

GSWA 25535

Figure 95. Re-orientated D_{2c} folds adjacent to the normal fault shown in Figure 94.

GSWA 25536

Figure 96. Conjugate fold in Brockman Iron Formation east of Wheelara Hill.

GSWA 25537

Figure 97. Zone of chevron folds in the Joffre Member of the Brockman Iron Formation, Mount Whaleback Mine.

(Tyler et al., 1990). Daniels and MacLeod (1965) estimated vertical displacement in excess of 9 km on this fault. The identification of rocks in the Deadman Hill–Prairie Downs area as being Fortescue Group and Hamersley Group (Horwitz and Smith, 1978; Tyler, 1986; Tyler et al., 1990) means that the throw is of the order of hundreds, rather than thousands, of metres.

The Poonda Fault (Tyler et al., 1990) has the same orientation as the Prairie Downs Fault, but its direction of dip is not known. Its history is complex, requiring initial north-block-up movement to juxtapose Wittenoom Dolomite, which underlies much of the Fortescue Valley, and upper Hamersley Group. Later movement, probably contemporaneous with deposition of the Manganese Subgroup of the Bangemall Group was "north-block-down" (Williams and Tyler, 1989; Tyler et al., 1990). The fault degenerates into a series of splays and subsidiary faults at its termination near Limestone Well.

A fault northwest of Turee Creek shows evidence of both north-block-down and sinistral movement and represents reactivation of an earlier transfer fault.

Shovelanna Bore and Murramunda Faults and related structures

In the eastern part of the Sylvania Inlier, there are two major northwest-trending sinistral strike-slip faults (Plates 2 and 3). These are the Shovelanna Bore Fault and the Murramunda Fault, which between them form the western and eastern limits of the Jimblebar greenstone belt. To the southeast they are seen to affect rocks of the Savory Group (Williams and Tyler, 1989).

Capricorn Orogen age shears and foliations in granitoid to the northwest of Emerald Well have been kinked by movement on the Shovelanna Bore Fault. A cleavage has developed locally in the vicinity of the fault zone and indicates a moderate southwest dip to the fault. An associated down-dip extension lineation suggests a significant vertical component of movement. The fault terminates near the Ophthalmia Dam, where it produces open refolding of D_{2c} folds (S. Slepecki, pers. comm., 1986).

The Murramunda Fault is associated with a system of more west-northwestly orientated faults that cut and displace the eastern part of the Jimblebar greenstone belt and the ultramafic intrusion at Coobina. Displacements are consistently sinistral, and the fault system cuts into the Fortescue Group. Further northwest, the fault degenerates into conjugate folding in Hamersley Group rocks, where small structures are well developed (Fig. 96).

Minor folding and faulting of this age is seen at Mount Whaleback. Structures, although widespread, are not pervasive and generally take the form of kink bands, chevron folds, faults, and minor shears. They can be seen to cut across the main folds, and to fold the associated cleavage. The East Pit Footwall Fault was also folded by this event at both the large and the small scales.

A 20 m wide zone of chevron folds was observed in Joffre Member (Fig. 97). The axial surfaces of the best developed folds dip steeply to the southwest; however, more open folds with northeast-dipping axial surfaces are

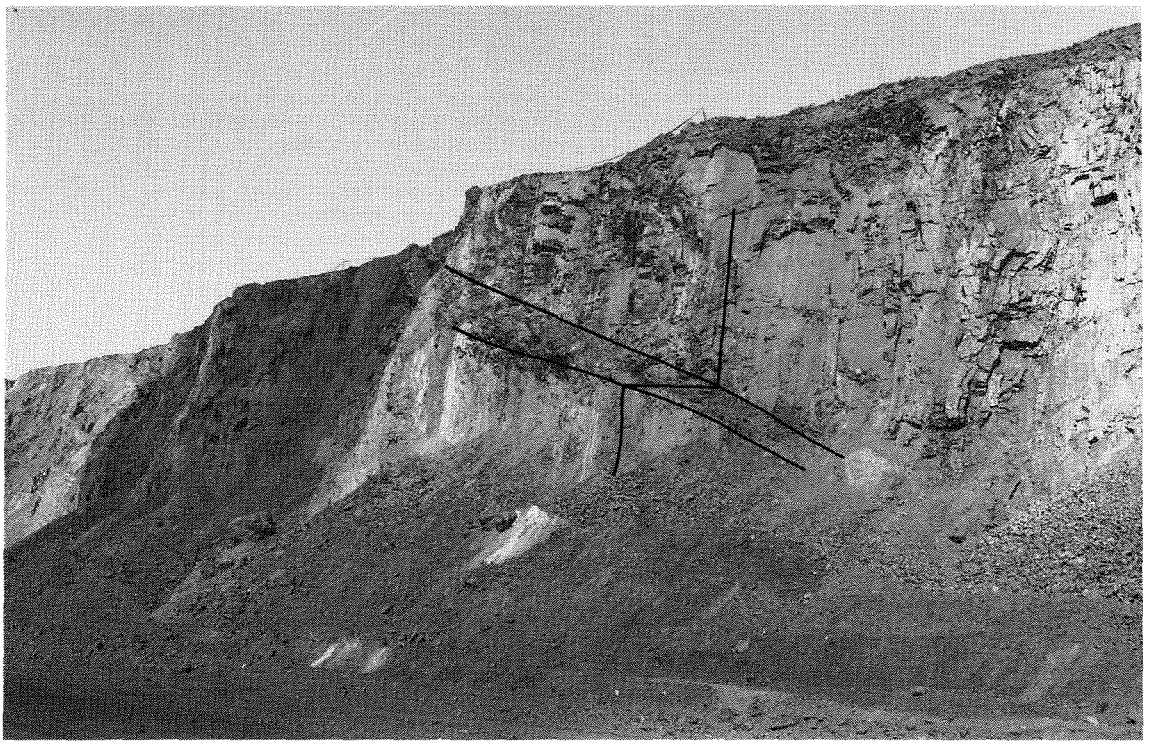

GSWA 25538

Figure 98. Kink band in Brockman Iron Formation, Mount Whaleback Mine.

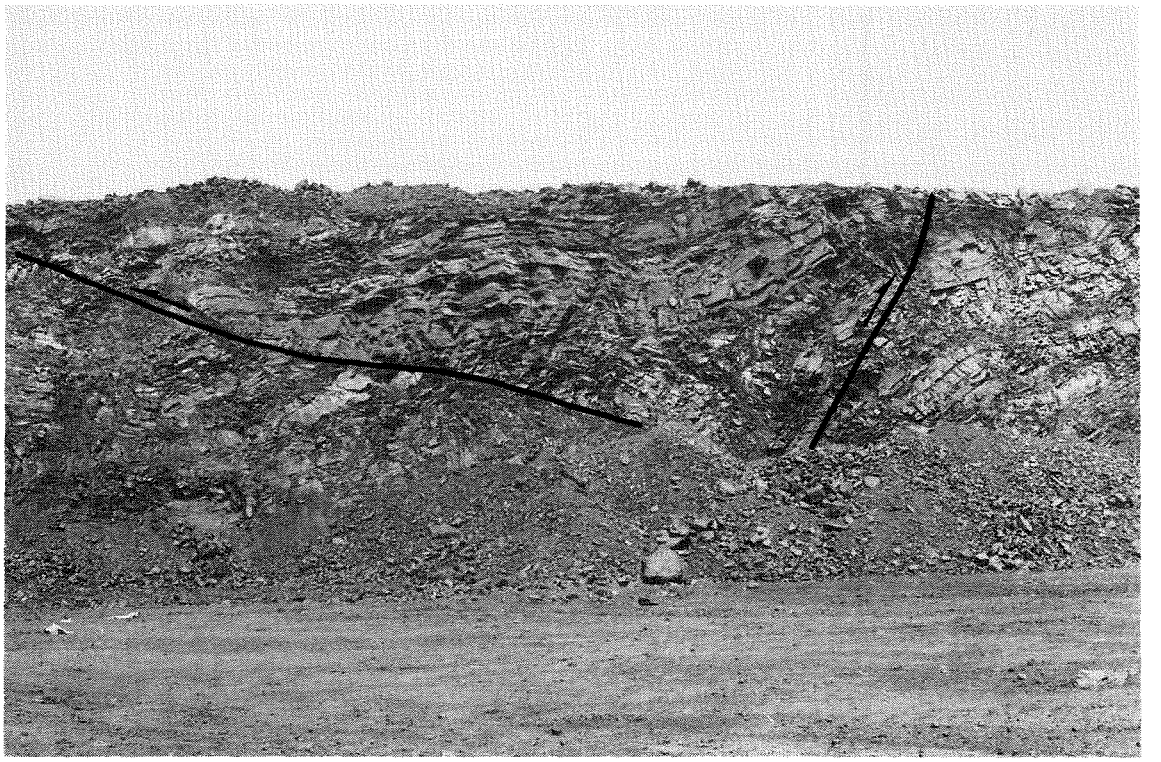

GSWA 25539

Figure 99. "Pop-up" structure in Mount McRae Shale, Mount Whaleback Mine. This structure is developed on the inverted lower limb of the central anticline, stratigraphic way-up is to the right-hand side (north) of the photograph.

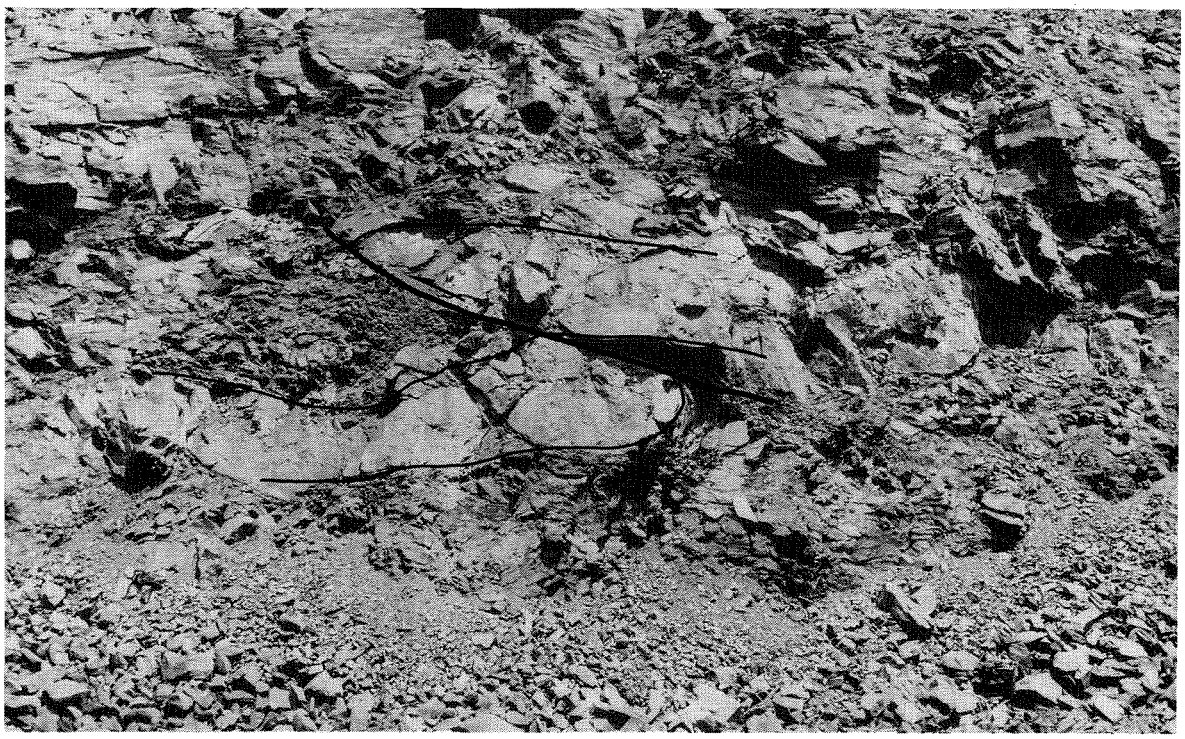

GSWA 25540

Figure 100. Minor reverse fault within D_{2c} fold closure.

also present. The northeast-dipping structures develop into well-defined kink bands (Fig. 98).

In Mount McRae Shale, a medium-scale "pop-up" structure that is bounded by steep southwest, and moderate to gentle northeast-dipping reverse faults was observed (Fig. 99). Associated with this structure are minor reversed faults in downward-facing D_{2c} fold hinges (Fig. 100). Deformation occurs on all scales, and kinking of the main cleavage is common (Fig. 101), particularly at the east end of the East Pit. Here, folds of the bedding can be seen with moderate north-east-dipping axial surfaces.

Fortescue River Fault and related structures

The fault set on which the most recent movement has taken place is a set of north-northeast-trending structures (Plates 2 and 3). The best developed is the Fortescue River Fault, which divides the Sylvania Inlier. The principal displacement is a sinistral strike-slip movement that offsets both the Prairie Downs Fault, and fold and fault structures in Ethel Gorge. The fault can be traced into a lineament recognized in Cainozoic deposits in the Fortescue valley to the north (Williams, 1989). A system of faults extends from Western Creek to the radio transmitter 32 km north of Newman where large-scale refolding of D_{2c} folds can be recognized. A fault of this age, which is downthrown on its eastern side, controls the line of Coondiner Gorge.

The eastern end of the Sylvania Inlier is truncated by faults of similar orientation that are along the line of the Tangadee Lineament. This structure was active during the development of the Bangemall Basin (Muhling and Brakel, 1985), and initial faulting may pre-date the Shovelanna Bore and Murramunda Faults.

Mafic Dykes

Introduction

Four suites of mafic dykes which post-date the Capricorn Orogeny, (Tyler, 1990b) can be recognized (Plate 2),. The earliest of these (Suite 5) is a northwesterly trending suite, which is cut by an east–west orientated suite (Suite 6). Northeast- to north-northeast-trending dykes form Suite 7. The youngest suite (Suite 8) trends west-northwest.

Suite 5

Suite 5 dykes occur frequently in the southwest part of the Sylvania Inlier (Fig. 25) and extend northwest, cutting across fold structures throughout the southwest Hamersley Basin (Fig. 102). Dykes that cut iron-ore deposits in the Brockman Syncline have produced massive recrystallization of adjacent hematite (Evans and Clint, 1975). Tyler (1990b) suggested that they are equivalent to the Round Hummock Suite of Hickman and Lipple (1978).

The dykes are 1–3 m wide (Fig. 103) and may be up to 10 km long. The mineralogy is similar to that of Suite 3 dykes except that orthopyroxene and olivine are both present. Dolerite has a fine- to medium-grained subophitic texture. Plagioclase and/or pyroxene phenocrysts occur in some dykes. Alteration is widespread, and pumpellyite is present.

GSWA 25541

Figure 101. Kinking of the S_{2c} cleavage in Mount McRae Shale, Mount Whaleback Mine (x30). GSWA sample 42228.

Suite 6

Suite 6 dykes are scarce. The best developed example, which occurs near Curleys Bore (Fig. 25) in the western part of the Sylvania Inlier, can be traced for 17 km; individual segments are continuous for between 1 and 7 km and are arranged *en echelon*.

The dykes are doleritic, very fine to medium grained, and show intergranular to subophitic texture. The very fine-grained examples contain infrequent microphenocrysts of plagioclase, olivine, and pyroxene. Plagioclase laths may show a moderate degree of alignment resulting in a subtrachyitic texture. The rock has a distinctive dusting of fine magnetite. The mineralogy is otherwise similar to Suite 3. Alteration is variable and pumpellyite may be present.

Murramunda Dolerite

The Murramunda Dolerite is a large, over 15 km long, north-trending intrusion near the eastern end of the Sylvania Inlier (Plate 2). It intrudes granitoid, which is contact metamorphosed, and cuts across the ultramafic intrusion at Coobina. The dyke is itself cut by a Suite 7 dyke. Its width ranges from five hundred metres to a few metres at its southern end. Although contacts, where observed, appear vertical the intrusion has developed an appreciable scarp along its western edge, possibly corresponding to local moderate to steep easterly dips.

Mineralogy is similar to that seen in Suite 6 dykes, but fine magnetite occurs extensively. A similar mineralogy is also seen in sills and associated dykes of the Davis Dolerite, which are intruded into the Manganese Subgroup of the Bangemall Group (Williams, 1989; Williams and Tyler, 1991).

Suite 7

Dykes belonging to Suite 7 occur throughout the Sylvania Inlier and are also seen in Hamersley Basin, Ashburton Basin and Bangemall Basin rocks. A dyke belonging to this suite cuts the Channar iron-ore deposit near Paraburdoo and has significantly recrystallized adjacent hematite (Bourn and Jackson, 1979). The suite corresponds to the Mundine Well Suite of Hickman and Lipple (1978) (Tyler, 1990b).

Although dykes generally trend north-northeast, some conjugate northwest-trending examples do occur. Dykes may intrude into fault zones at Wheelara Hill (Ward et al., 1975). They are usually 1–2 m thick. An intrusion of two parallel dykes can be seen west of Curleys Bore in the Sylvania Inlier (Fig. 25).

The dykes are doleritic and vary from fine to coarse grained. Textures range from subophitic to weakly porphyritic. Orthopyroxene as well as clinopyroxene is present in some examples; and olivine, pseudomorphed by a clay-like mineral, also occurs.

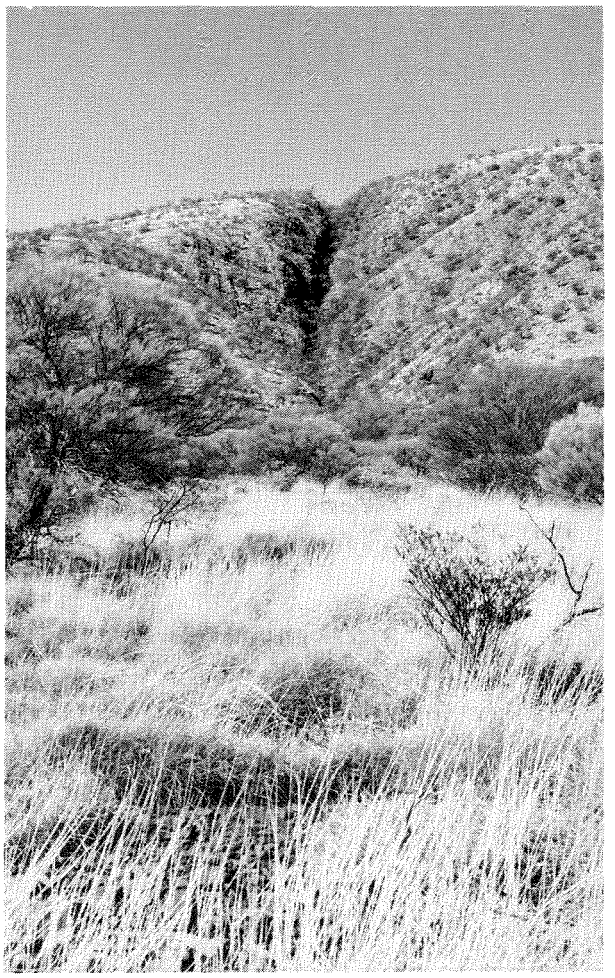

GSWA 25542

Suite 8

Dykes of Suite 8 are restricted to the southern part of the Sylvania Inlier, where they occur south of the Southern ultramafic intrusion. They trend west-northwest and clearly cut Suite 7 dykes. Dykes with a west-northwest to west-southwest orientation cut the Bangemall Group (Tyler, 1990b).

Dolerite is fine- to medium-grained with subophitic textures. Mineralogy is as for Suite 3 dykes.

Figure 102. Gully in Brockman Iron Formation ridge produced by erosion of a Suite 5 dolerite dyke.

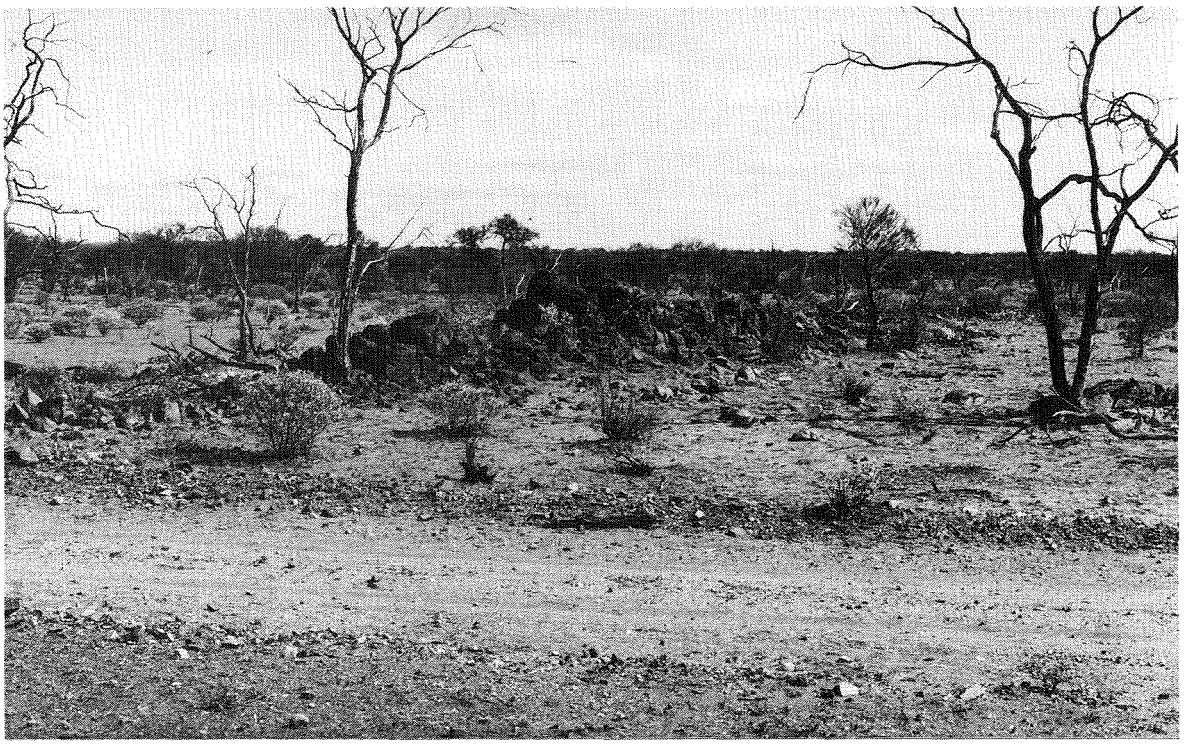

GSWA 25543

Figure 103. Suite 5 dolerite dyke exposed in the Sylvania Inlier near Curleys Bore.

Chapter Six

Economic Geology

Introduction

The iron-ore mines at Mount Whaleback and Paraburdoo are located within the area described and naturally dominate the economic geology. However, interest is not confined solely to iron ore. Within the Sylvania Inlier, gold has been mined from banded iron-formation at Jimblebar; and Australia's largest known deposit of chromite occurs at Coobina. Exploration for copper has taken place in the Jimblebar greenstone belt and within the Fortescue Group. Minor occurrences of galena, cerusite, barite, uranium, ochre, crocidolite, and chrysoprase, have also been reported in the area.

Gold

Sylvania Inlier

Gold has been mined at Jimblebar, and a government battery was established during the 1930s to treat the ore (Wilson, 1930). Most production was from two leases, Shearers, and Sunny South (Plate 2). Production figures are given in Table 9.

The deposits are BIF-hosted, and gold is associated with sulphide minerals. At Shearers, the main lode is parallel to layering within leached and altered banded iron-formation. At Sunny South, mineralization is again parallel to layering, but here it occurs at the margin of the BIF. Sulphide minerals—dominantly pyrite, but including small amounts of pyrrhotite and chalcopyrite—are present in a host rock that comprises quartz, feldspar, blue-green amphibole, biotite, carbonate, and small amounts of epidote and apatite (Fig. 104). This assemblage is probably the result of metasomatic alteration of mafic rocks adjacent to the BIF.

TABLE 9. GOLD PRODUCTION AT JIMBLEBAR, PEAK HILL MINERAL FIELD, 1930–1987

	Alluvial (kg)	*Dollied* (kg)	*Ore treated* (t)	*Gold therefrom* (kg)	*Total gold* (kg)
Jimblebar Mining Centre	1.74	7.424	8712	97.544	106.708

Both deposits, together with a small show 3.5 km to the north, are closely associated with the Battery Fault, which most probably provided a pathway for mineralizing fluids (cf. Groves et al., 1985). Mineralization and D_{2g} deformation occurred synchronously. The reported occurrence of gold in quartz veins in granitoid 3 km southwest of Jimblebar (de la Hunty, 1969) suggests that there may have been later remobilization associated with systems of fluid circulation established during intrusion of the main granitoid.

Alluvial gold has been found associated with the greenstone belt at Deadman Flat, but there has been no recorded production.

Fortescue Group

Potential for placer gold mineralization exists within the basal metasedimentary unit of the Fortescue Group. This is based on the perceived similarities between the Hamersley Basin and the Witwatersrand Basin in South Africa (Hickman and Harrison, 1986), which is the world's largest producer of gold.

Gold has been produced from conglomerates at the base of the Fortescue Group near Nullagine, and from the "Just-in-Time" mine west of Marble Bar (Hickman, 1983). However, large-scale mineralization is not known; and both Blake (1984) and Blight (1985) suggested that this may reflect the lack of extensive gold mineralization within the underlying granite–greenstone (Groves et al., 1984), which was the source of the sediments. Hickman and Harrison (1986) argue that the potential for high-grade placer deposits remains, particularly where sedimentary basins have developed in close proximity to high-grade epigenetic deposits. If this is the case, then around the Sylvania Inlier detrital gold from the Jimblebar deposit could have been incorporated in the basal rocks of the Fortescue Group.

Iron

Introduction

Hamersley Group rocks lie within the Hamersley Iron Province (Fig. 105) of MacLeod et al. (1963). Extensive exploration for iron ore took place throughout the 1960s and 1970s (Blockley et al., 1990). Identified economic resources of iron ore in Australia, of which the Hamersley

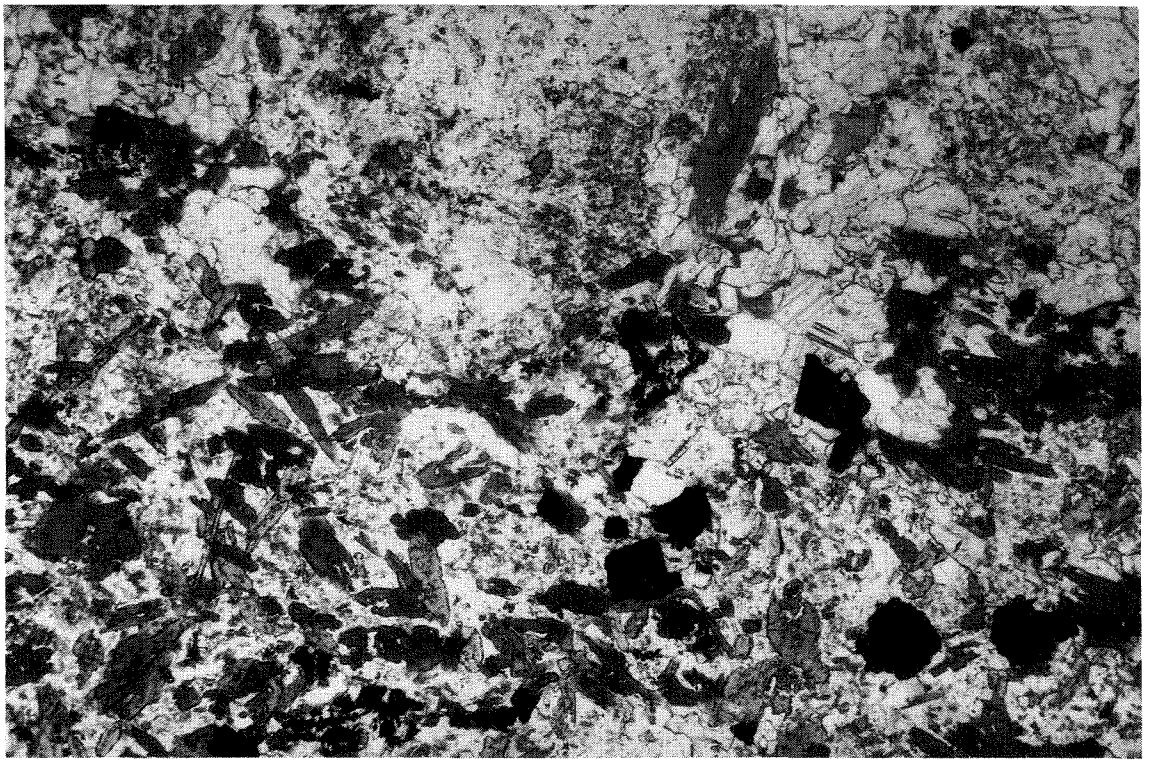

GSWA 25544

Figure 104. Metasomatized and recrystallized sulphide-bearing quartz–feldspar–blue-green amphibole–biotite–calcite rock from the Sunny South Mine, Jimblebar (x25). GSWA sample 81882.

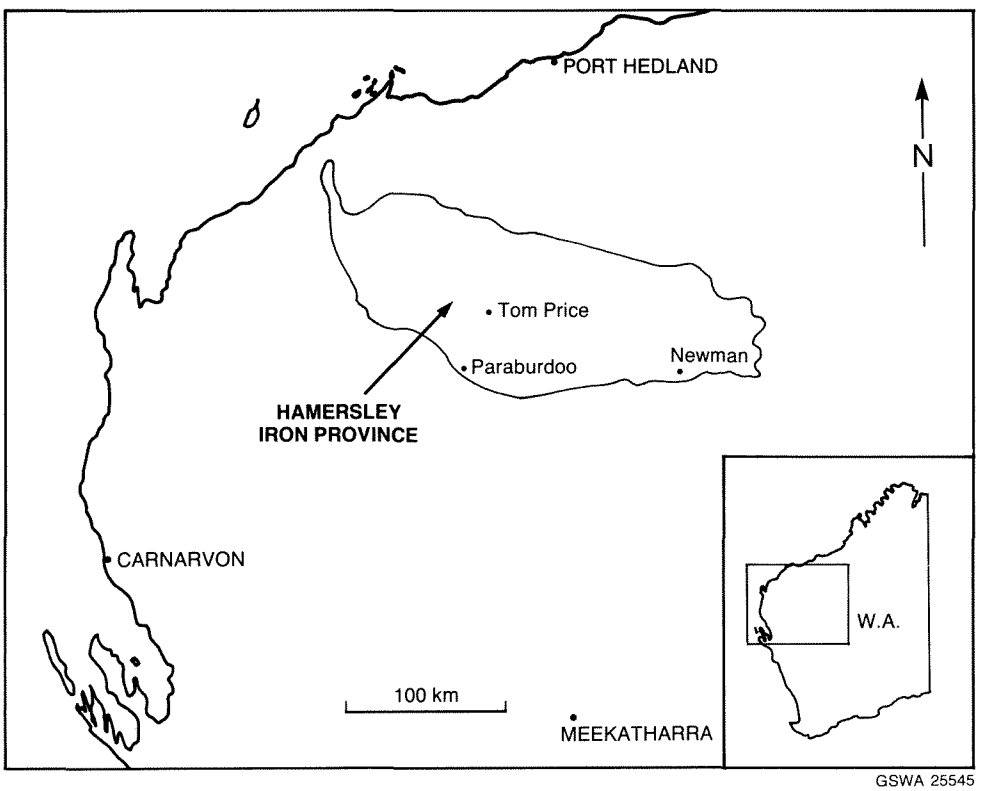

GSWA 25545

Figure 105. Location map of the Hamersley Iron Province.

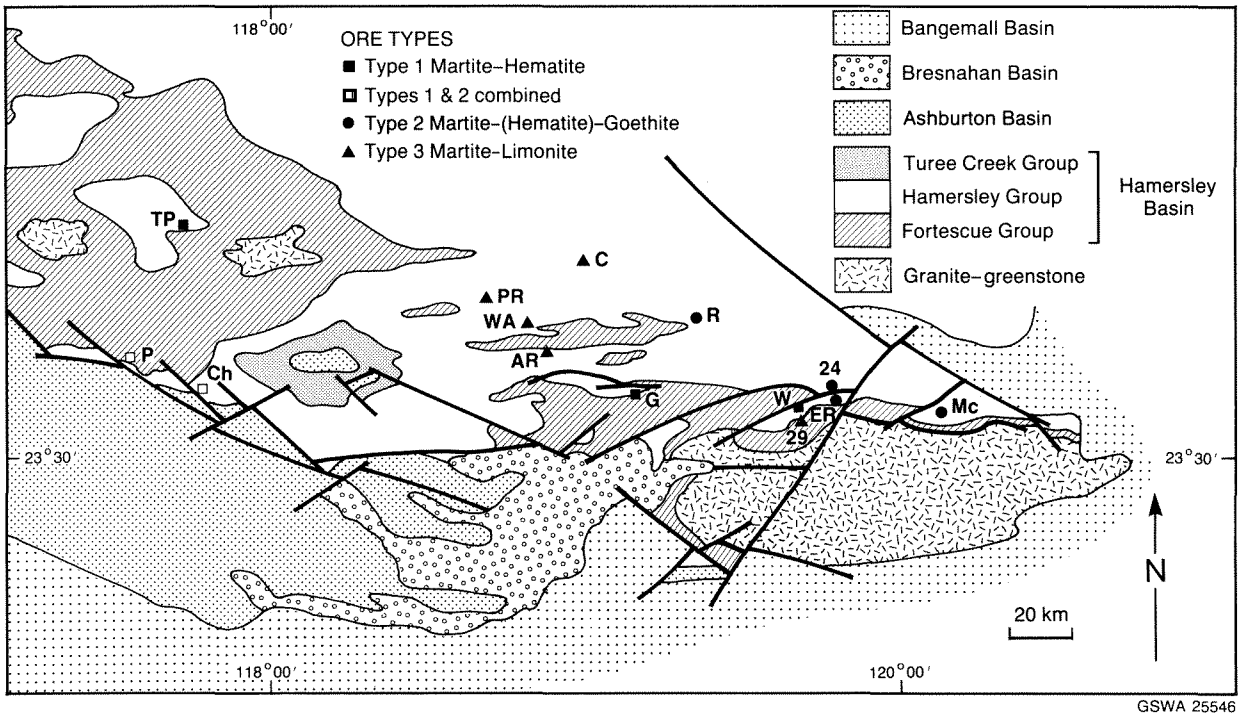

Figure 106. Simplified geology map of the southeastern Pilbara showing the location and ore type of major hematite orebodies. AR—Angelo River; C—Area C; Ch—Channar; ER—Eastern Ridge; G—Giles; Mc—McCamey's Monster; P—Paraburdoo; PR—Parallel Ridge; R—Rhodes Ridge; TP—Tom Price; W—Mount Whaleback; WA—West Angelas; 24—Orebody 24; 29—Orebody 29.

Basin contains some 95%, were quoted at 20 610 Mt in 1986 (BMR, 1987). In the area covered by this report (Fig. 106), Mount Newman Mining Pty. Ltd. is producing ore from its Mount Whaleback and Marra Mamba Mines (Kneeshaw, 1975; Slepecki, 1981), and Hamersley Iron Pty. Ltd. is producing ore from the 4E and 4W deposits at Paraburdoo (Baldwin, 1975; Bourn and Jackson, 1979). Further large deposits are present in the southeast Hamersley Basin at McCamey's Monster (Ward et al., 1975), Eastern Ridge, Rhodes Ridge, Giles, West Angelas, Angelo River, Parallel Ridge Area C (Neale, 1975), and Channar (Bourn and Jackson, 1979). At least two (McCamey's Monster and Channar), are currently at the development stage.

Ore Types

Three types of ore are present (Kneeshaw, 1984). The first (Type 1) is martite–hematite ore: martite has replaced primary magnetite in the parent BIF; secondary microplaty hematite has formed by metamorphism of earlier goethite; and unconverted goethite has subsequently been leached out.

The second type (Type 2) is martite (–hematite)–goethite. This is the typical, high-phosphorous ore that forms most of the reserves. It comprises martite, primary hematite, and goethite. Secondary hematite, which is not always present, results from the dehydration of goethite, and is fine-grained rather than microplaty.

The third type (Type 3) is martite–limonite. This is typical of ores in the Marra Mamba Iron Formation. The term limonite is used to designate yellow, ochreous goethite.

Model of supergene enrichment

A model (Fig. 107) for the formation of the various ore bodies by supergene enrichment of banded iron-formation has been presented by Morris (1980; 1985) and Morris et al. (1980). Hydraulic systems resembling small artesian basins were established, and the ore formed initially at depth under the influence of large electrochemical cells. Ore formed preferentially against faults or minor intrusions that controlled the fluid flow. Ore zones extended up dip. Iron was added to the ore body from BIF eroded at the surface. The ore formation process is slow, and large ore bodies formed over millions, to hundreds of millions, of years.

Continuing erosion removed many of the early-formed deposits; these are unmetamorphosed and characterized by abundant hydrous iron oxides (Type 2 ore). Some of those that survived were buried by later sedimentary basins and were metamorphosed. Increased temperatures formed secondary, characteristically microplaty, hematite from the goethite (Type 1 ore). Erosion has exposed many of these metamorphosed ores to renewed supergene processes and their textures have been further modified by oxidation, leaching, and precipitation. Preferential leaching of residual goethite results in significant upgrading to nearly pure hematite.

Ore bodies that have been subjected to weathering for extended periods are capped by a goethite-rich ferricrete, formed by repeated solution and deposition in the vadose zone. This process destroys original BIF textures which are preserved in the metasomatic ores.

Structural controls on mineralization

The supergene-enrichment model for ore formation detailed above has two requirements for the production of deep ore: that the BIF outcrops at the surface and acts as an aquifer; and that there is a suitable pathway for fluid to reach the BIF at depth. Suitable conditions are found in faulted synclines and perhaps the best example of this is the Mount Whaleback deposit.

However, it seems that the simple requirement of a faulted syncline is not enough to produce the vast tonnages of ore which are present at Mount Whaleback. Five kilometres to the west-southwest, a superficially similar structural environment occurs at Western Ridge, but there has been limited formation of ore (Ward et al., 1975).

It is noticable that the largest deposits are formed in areas where faulting is complex. At Mount Whaleback, the Mount Whaleback Fault splits into two, and the main throw is transferred to a fault offset 1 km to the south-southeast (Plate 2). Between the two faults is a zone of complex faulting that constitutes the footwall of the ore body. Extensive faulting also occurred in the hanging wall. At Western Ridge only a single fault plane is present.

At Paraburdoo, extensive dextral strike-slip faulting is present. This is regarded as having taken place on pre-existing normal faults that developed marginal to the Ashburton Basin. Examples of normal faulting are preserved within the orebody where Morris (1985) regards them as a major control on mineralization. The complexity of faulting at Paraburdoo reflects its position at the termination of the Nanjilgardy Fault (Plate 3), which locally forms the boundary between the Hamersley Basin and the Ashburton Basin.

Sibson (1987) has suggested a model of mineralization in fault zones where fluid flow is concentrated in what are known as fault "jogs" (Fig. 108). These are localized zones of extension caused by fault curvature or segmentation arranged *en echelon*, and are best developed in normal and strike-slip fault systems. The intervening, driving faults are usually barren. Similar dilational structures can occur at fault terminations. Mineralization occurred during active faulting, when, as the result of earthquake rupturing, fluid was pumped into dilational structures.

Such a model is applicable to the formation of deep ore bodies (Fig. 109). Ore formation would be initiated at jogs and fault terminations during active fault growth along the margin of a sedimentary basin. The resultant fault scarps would be zones of active erosion that provided additional iron to the ore body. As the margins of the basin migrated, active faulting would cease, allowing the scarps and, therefore, the juvenile ore bodies to be buried by on-lapping sediments. Sufficient depth of burial would produce metamorphic martite - hematite ore.

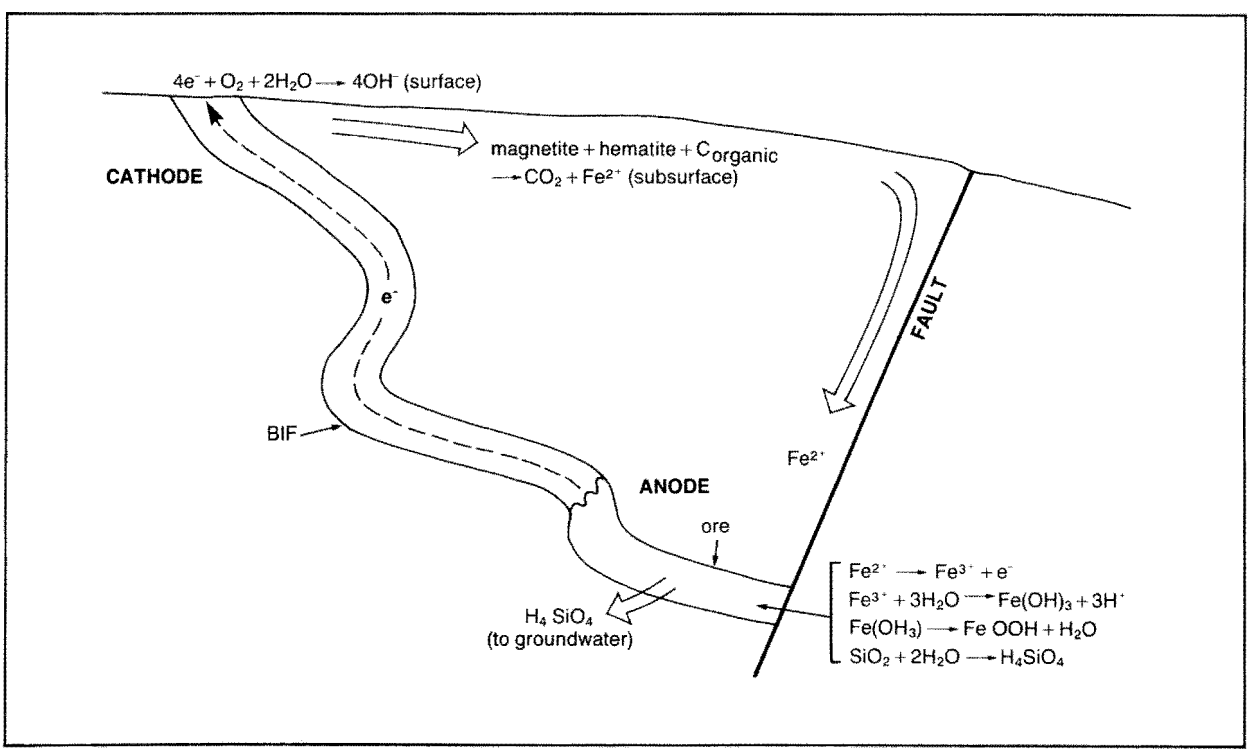

GSWA 25547

Figure 107. The "Morris" model for supergene enrichment of banded iron-formation to form deep hematite orebodies. Taken from Morris (1985) and Morris et al. (1980).

Age of ore formation

The hematite ore bodies that formed within the Brockman Iron Formation were initially presumed to be Tertiary (MacLeod et al., 1963). It was soon realized, however, that the Tertiary surface, to which their formation had been related, had actually eroded down into and modified the ore bodies (MacLeod, 1966).

Morris (1985) concluded that, throughout the world, the first significant BIF-hosted enrichment ores formed around 2.0±0.2 Ga. This was related to a change from a generally "anoxic" atmosphere to one in which very low concentrations of oxygen were present. In the Hamersley Basin, the oldest ore bodies were formed during the early stages of the development of the 1.84 Ga Ashburton Basin. Ore pebbles containing microplaty hematite occur in conglomerates from the Mount McGrath Formation near Paraburdoo (Morris, 1980). Conglomerates lower in the sequence contain only unenriched BIF. The time of ore formation is further constrained by the presence of post-folding, but pre-ore, mafic dykes. Morris (1985) favoured a post-Beasley River Quartzite, pre-Cheela Springs Basalt age for ore formation at Paraburdoo and surmised that the volcanics contributed to the heat required to metamorphose the ore. However, Cheela Springs Basalt crops out in the core of the Turee Creek Syncline. This implies that folding in this area and, therefore, dyke intrusion and ore formation, took place after eruption of the Cheela Springs Basalt. Ore formation would then be related to the period of uplift and subaerial exposure which followed deformation. The burial model requires the deposition of sediments that were then stripped before deposition of the currently exposed Mount McGrath Formation (Morris, 1985).

Horwitz (1982) and Morris (1985) related ore bodies in the southeastern part of the Hamersley Basin (Western Ridge, Mount Whaleback, Giles, McCamey's Monster) to the supposed margins of the "McGrath Trough", which was thought to have developed during Turee Creek Group and early Wyloo Group times. From evidence presented in this study, and from work carried out on the depositional history of the Wyloo Group by Thorne and Seymour (1991), major uplift took place in the southeastern Hamersley Basin following continental collision. As indicated above, deformation occurred after Cheela Springs Basalt time; and uplift provided sediment first to the Mount McGrath Formation and later to the Ashburton Formation. It is difficult to reconcile this with a syn-Wyloo Group age for ore formation in the southeastern Hamersley Basin. The difficulties are compounded by the close association of ore bodies in this area to faults belonging to the Mount Whaleback Fault system. The faults are regarded as an integral part of the ore-forming process (Morris et al., 1980; Morris, 1985). As discussed in Chapter 5, the faults are related to the formation of the Bresnahan Basin. Suitable hydrological conditions for ore formation are indicated by the occurrence of lacustrine deposits within the Bresnahan Group sequence (Hunter, 1990).

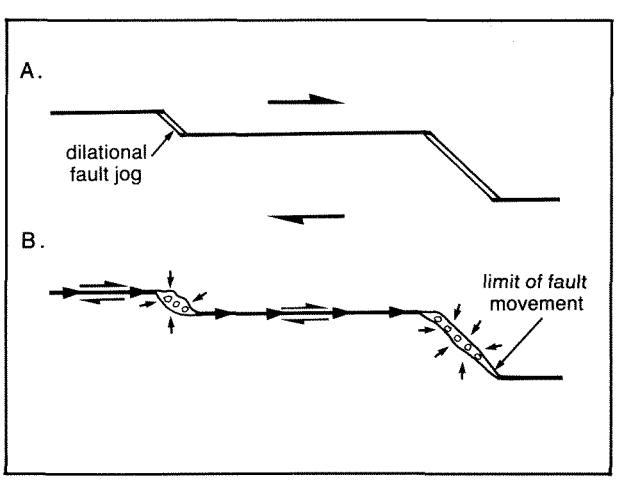

GSWA 25548

Figure 108. Development of dilational fault jogs within a dextral wrench fault system. Taken from Sibson (1987). A—Pre-rupture–uniform fluid pressures. B—Post-rupture–fluid influx into jogs, arrows indicate flow directions.

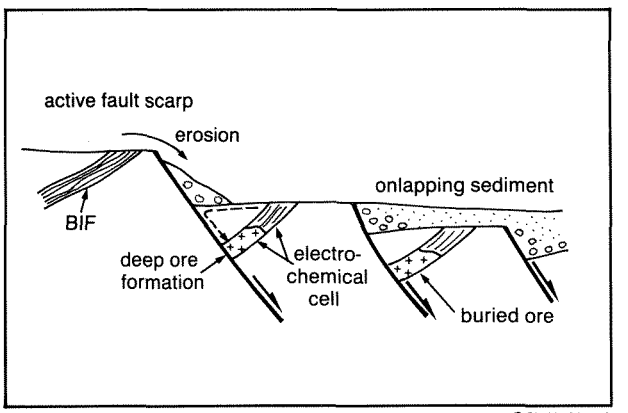

GSWA 25549

Figure 109. Formation of deep orebodies associated with active faulting at a basin margin.

It is suggested, therefore, that ore bodies of two ages have formed within Brockman Iron Formation. The earliest are those in the southwest Hamersley Basin (e.g. Paraburdoo, Tom Price), which formed during development of the Ashburton Basin. Then followed the formation of ore bodies in the southeastern part of the basin, which were initiated during development of the Bresnahan Basin. This occurred sometime between 1.6 Ga (the age of completion of the Capricorn Orogeny; Libby et al., 1986) and 1.5 Ga (the age of the overlying Bangemall Group; Williams, 1990).

Ore bodies of Type 3 ore developed in the Marra Mamba Iron Formation. The initial burst of exploration activity concentrated on the Brockman Iron Formation. Later it was realized that significant mineralization could occur in the upper BIF unit of the Marra Mamba Iron Formation (Neale, 1975). Ore formation was concentrated in synclinal structures, and the ore bodies are often buried beneath Tertiary and Quaternary alluvial and colluvial deposits adjacent to outcrops of the lower BIF unit. At Marandoo, relationships between ore and Tertiary alluvium indicate a Mesozoic to early Tertiary age for this ore type (Morris, 1985). This is consistent with the ore's immature nature compared with Types 1 and 2 (Morris, 1985).

Exploration for high-grade ores

As has been pointed out by Morris (1985), the obvious targets for the further discovery of low-phosphorous martite–hematite ore bodies are unconformity-related deposits. Morris (1985) suggested that the recognition of features equivalent to the "McGrath Trough" and their relationship to post-2.0 Ga metamorphism, will help to delimit search areas.

The Bresnahan Basin offers a possible exploration target. The occurrence of Brockman Iron Formation at Deadman Hill suggests that Hamersley Group rocks provide basement to at least part of the basin. Areas of complex faulting which form part of the Mount Whaleback Fault System offer the best sites for potential deep mineralization.

Chrome

Chromite occurs in the ultramafic intrusion at Coobina within the Sylvania Inlier. The main deposit is at Coobina itself (Plates 1 and 2). Chromitite pods and lenses also occur 3.5 km east of Garden Well in a serpentinite sill that is regarded as part of the main intrusion. The intrusion has been described in detail in Chapter 2.

The main deposit at Coobina represents the largest known deposit of chromite in Australia. It has been described by several authors. The most recent descriptions are those of Bye (1975) and Baxter (1978); see de la Hunty (1969) for references to early investigations. The deposit has been the subject of extensive exploration by BHP Pty. Ltd.

Chromitite occurs in some 200 pods and lenses that are concentrated at the western end of the Coobina intrusion; some reach a length of 250 m and a width of 6 m. They are regarded as preserving primary magmatic layering, which was disrupted during later deformation. Baxter (1978) reported the lenses as having sharp southern, and diffuse northern contacts. The lenses are discontinuous, and their continuation at depth is uncertain (Bye, 1975). This makes calculation of ore reserves difficult.

The chromite ore consists of aggregates of euhedral to subhedral chromite (up to 2 mm across) and intergranular chlorite and serpentine. Grades are low: grades in individual lenses range from 46.4% to 50.8% Cr_2O_3, and the ratio, Cr_2O_3:FeO, ranges from 1.35:1 to 2.3:1 (Baxter, 1978).

Copper

Sylvania Inlier

Copper in the Jimblebar greenstone belt is associated with the felsic volcanic unit (Plate 1). Several copper shows, principally malachite veinlets and disseminations in anastomosing networks of limonitic veins (Marston, 1979), extend along the length of the unit from the main occurrence at Copper Knob. Production of ore took place between 1959 and 1962 totalling 84.09 t averaging 8.37% Cu (Marston, 1979). Low nickel:cobalt ratios of iron-sulphides (<0.5:1) indicate a magmatic–hydrothermal origin for mineralization (Barley, 1974).

Exploration by Vam Ltd and Endeavour Resources identified one million tonnes of very low-grade disseminated mineralization (0.77% Cu); but, in the absence of higher grade concentrations, the prospect appears to have no economic potential (Marston, 1979).

Fortescue Group

Copper occurs in uppermost Jeerinah Formation shales in the Wonmunna area. The geology of the prospects was summarized by Marston (1979).

Typically, mineralization takes the form of veinlets and stainings of cuprite, malachite, and chrysocolla, which are associated with limonite. The mineralized zones may extend for more than 25 m across strike. However, there is little continuity of mineralization along strike. The observed surface mineralization is derived from the oxidation of sulphide minerals. Pyrite and subordinate pyrrhotite, and small amounts of chalcopyrite and sphalerite, occur as thin laminae, lenses, and small nodules within the shales. Values up to 3.43% Cu have been recorded but are exceptional and mineralization is generally very low grade and of little economic interest.

Production of 13.53 t of copper ore (25.6% Cu) and 5.96 t of cupreous ore (23.75% Cu) from the Wonmunna prospect took place in 1953 (Low, 1963).

Prairie Downs Fault

Minor copper mineralization (assaying up to 2.69% Cu) associated with lead occurs along the Prairie Downs Fault (Blockley, 1971).

Lead, barium, and zinc

Sylvania Inlier

Galena and associated barite occur in veins within a fault zone forming the northern margin of the Coobina ultramafic intrusion near Murramunda.

Prairie Downs Fault

Galena and cerusite, together with copper minerals, occur in a gangue of barite and ferruginous quartz that outcrops discontinuously along a 2.4 km length of the Prairie Downs Fault. The prospect was described by Blockley (1971).

Mineralization occurs in veins, ranging up to 2 m wide, which are arranged *en echelon* in zones up to 61 m long. Assays range from 0.43% to 32.4% Pb and 0.05% to 11.3% Zn.

Uranium

Exploration for uranium in the southeastern Pilbara has been concentrated on the basal unconformity of the Bresnahan Group. Anomalies are associated with the basal sedimentary unit of the Fortescue Group near Jillary Well.

Ochre

Between 1938 and 1941, 1651 t of red ochre was mined from Boolgeeda Iron Formation 29 km north-northeast of Mount Newman (Matheson, 1945). A further 8 t was produced from Weeli Wolli Formation 7 km north of Mount Newman Homestead.

Crocidolite

The northern part of the southeastern Hamersley Basin lies within the Wittenoom sub-province of the Hamersley Crocidolite Province. The deposits have been described in detail by Trendall and Blockley (1970). East of Yampire Gorge, crocidolite is restricted mainly to the upper part of the Dales Gorge Member of the Brockman Iron Formation.

The main occurrence in the area of interest is at Lamb Creek, where fibres approach ore grade. Other occurrences are at Coondiner Creek, Weeli Wolli Spring, and Fish Pool. None of these deposits has any current economic potential.

Chrysoprase

Chrysoprase has been mined from the massive silica capping that has developed on the southern ultramafic intrusion in the Sylvania Inlier.

Appendix

Localities mentioned in text

	Latitude (S)	Longitude (E)
Benchmark 627	23° 42'	120° 09'
Bubbacurry Well	23° 32'	119° 56'
Cairn Hill Well	23° 09'	117° 19'
Capricorn Roadhouse	23° 27'	120° 48'
Channar iron ore deposit	23° 18'	117° 48'
Coobina	23° 30'	120° 16'
Coondiner Creek	23° 01'	119° 36'
Copper Knob	23° 27'	120° 09'
Curleys Bore	23° 42'	119° 26'
Deadman Flat	23° 46'	119° 28'
Deadman Hill	23° 48'	119° 25'
Divide Well	23° 28'	118° 22'
Doggers Gorge	23° 16'	117° 44'
Eagle Pool	23° 06'	119° 35'
Eastern Ridge	23° 20'	119° 47'
Emerald Bore	23° 30'	120° 05'
Ethel Gorge	23° 17'	119° 52'
Fish Pool	23° 07'	118° 05'
Garden Well	23° 30'	120° 10'
Giles Mini camp	23° 17'	119° 10'
Giles Point	23° 15'	119° 10'
Horrigans Pool	23° 33'	118° 15'
Howies Hole	23° 17	117° 45'
Jillary Well	23° 44'	119° 24'
Jimblebar	23° 28'	120° 11'
Juna Downs	22° 53'	118° 29'
Junction Pool	23° 29'	120° 29'
Kalgan	23° 11'	119° 54'
Lamb Creek	22° 50'	118° 56'
Limestone Well	23° 22'	120° 27'
McCamey's Iron camp	23° 24'	120° 09'
Mindoona Bore	23° 26'	120° 04'
Mount Channar	23° 20'	118° 00'
Mount Maguire	23° 20'	117° 45'
Mount Meharry	22° 59'	118° 35'
Mount Newman	23° 16'	119° 34'
Mount Robinson	23° 02'	118° 53'
Mount Whaleback	23° 22'	119° 40'
Murramunda	23° 30'	120° 22'
Nanjilgardy Pool	23° 22'	117° 50'
Newman	23° 21'	119° 44'
Nirran Nirrie Bore	23° 41'	119° 17'
Noddy Bore	23° 22'	119° 59'
Ophthalmia Dam	23° 21'	119° 52'
Outcamp Well	23° 28'	119° 52'
Packsaddle camp	22° 54'	118° 37'
Painkiller Bore	23° 24'	120° 02'
Pamelia Hill	23° 10'	119° 25'
Paraburdoo	23° 12'	117° 40'
Prairie Downs	23° 33'	119° 09'
Radio Hill (Newman)	23° 06'	119° 50'
Radio Hill (Paraburdoo)	23° 14'	117° 40'
Ratty Spring	23° 13'	117° 32'
Red Hill	23° 36'	120° 19'
Rhodes Ridge camp	23° 06'	119° 22'
Round Hill Bore	23° 38'	119° 28'
Sandy Creek Bore	23° 43'	119° 20'
Shearers	23° 28'	120° 11'
Shovelanna Bore	23° 26'	120° 01'
Shovelanna Hill	23° 20'	120° 01'
Snowy Mountain	23° 24'	118° 04'
Spearhole Yard	23° 31'	119° 21'
Sunny South	23° 29'	120° 11'
Weeli Wolli Spring	22° 55'	119° 13'
West Angelas camp	23° 07'	118° 42'
Western Ridge	23° 24'	119° 37'
Wheelarra Hill	23° 23'	120° 07'
Woggaginna Hill	23° 41'	120° 01'
Wonmunna	23° 07'	119° 08'

References

APTED, M. J. and LIOU, J. G., 1983, Phase relations among greenschist, epidote amphibolite and amphibolite in a basaltic system: American Journal of Science, v. 283-A, p. 328–354.

ARNDT, N. T., NELSON, D. R., COMPSTON, W., TRENDALL, A. F., and THORNE, A. H., 1991, The age of the Fortescue Group, Hamersley Basin, Western Australia, from iron microprobe zircon U–Pb results: Australian Journal of Earth Sciences, v. 38, p. 261–281.

AYERS, D. E., 1972, Genesis of iron-bearing minerals in banded iron formation mesobands in the Dales Gorge Member, Hamersley Group, Western Australia: Economic Geology, v. 67, p. 1214 - 1233.

AYERS, L. D. and THURSTON, P. C., 1985, Archaean supracrustal sequences in the Canadian Shield—An overview, *in* Evolution of Archaean supracrustal sequences *edited by* L. D. Ayers, P. C. Thurston, K. D. Card, and W. Weber: Geological Association of Canada, Special Paper 28, p. 343–380.

BAKER, J., POWELL, R., SANDIFORD, M., and MUHLING, J., 1987, Corona textures between kyanite, garnet and gedrite in gneisses from Errabiddy, Western Australia: Journal of Metamorphic Geology, v. 5, p. 357–370.

BALDWIN, J. T., 1975, Paraburdoo and Koodaideri iron ore deposits, and comparison with Tom Price ore deposits, Hamersley Iron Province, *in* Economic geology of Australia and Papua New-Guinea 1. Metals, *edited by* C. L. Knight: Australasian Institute of Mining and Metallurgy, Monograph 5, p. 906–910.

BARLEY, M. E., 1974, Geology of the Copper Range, Jimblebar, Western Australia: University of Western Australia, B.Sc. Honours thesis (unpublished).

BAXTER, J. L., 1978, Molybdenum, tungsten, vanadium and chromium in Western Australia: Western Australia, Geological Survey, Mineral Resources Bulletin 11.

BEARD, J. S., 1975, The vegetation of the Pilbara area—Vegetation survey of Western Australia, Explanatory notes to sheet 5, Pilbara: Nedlands, University of Western Australia Press.

BECKER, R. H. and CLAYTON, R. N., 1976, Oxygen isotope study of a Precambrian banded iron-formation, Hamersley Range, Western Australia: Geochimica et Cosmochimica Acta, v. 40, p. 1153–1165.

BICKLE, M. J., BETTANAY, L. F., BOULTER, C. A., GROVES, D. I., and MORANT, P., 1980, Horizontal tectonic interactions of an Archaean gneiss belt and greenstones, Pilbara Block, Western Australia: Geology, v. 8, p. 525–529.

BICKLE, M J., MORANT, P., BETTENAY, L. F., BOULTER, C. A., BLAKE, T. S., and GROVES, D. I., 1985, Archaean tectonics of the Shaw Batholith, Pilbara Block, Western Australia—Structural and metamorphic tests of the batholith concept, *in* Evolution of Archaean supracrustal sequences, *edited by* L. D. Ayers, P. C. Thurston, K. D. Card, and W. Weber: Geological Association of Canada, Special Paper 28, p. 325 - 341.

BICKLE, M. J., BETTENAY, L. F., CHAPMAN, H. J., GROVES, D. I., McNAUGHTON, N. J., CAMPBELL, I. H., and de LAETER, J. R., 1989, The age and origin of younger granitic plutons of the Shaw Batholith in the Archaean Pilbara Block: Contributions to Mineralogy and Petrology, v. 101, p. 361–376.

BLAKE, T. S., 1984, The lower Fortescue Group of the northern Pilbara Craton—Stratigraphy and palaeogeography, *in* Archaean and Proterozoic basins of the Pilbara, Western Australia, *edited by* J. R. Muhling, D. I. Groves, and T. S. Blake: University of Western Australia, Geology Department and University Extension, Publication 9, p. 123–143.

BLAKE, T. S. and GROVES, D. I., 1987, Continental rifting and the Archaean–Proterozoic Transition: Geology, v. 15, p. 229–232.

BLAKE, T. S. and McNAUGHTON, N. J., 1984, A geochronological framework for the Pilbara region, *in* Archaean and Proterozoic basins of the Pilbara, Western Australia, *edited by* J. R. Muhling, D. I. Groves, and T. S. Blake: University of Western Australia, Geology Department and University Extension, Publication 9, p. 1–22.

BLIGHT, D. F., 1985, Economic potential of the lower Fortescue Group and adjacent units in the southern Hamersley Basin: Western Australia, Geological Survey, Report 13.

BLOCKLEY, J. G., 1971, The lead, zinc and silver deposits of Western Australia: Western Australia, Geological Survey, Mineral Resources Bulletin 9.

BLOCKLEY, J. G., 1980, The tin deposits of Western Australia with special reference to the associated granites: Western Australia, Geological Survey, Mineral Resources Bulletin 12.

BLOCKLEY, J. G., REID, I. R., and TRENDALL, A. F., 1990, Geological aspects of Australian iron ore discovery and development, *in* Geological aspects of the discovery of some important mineral deposits in Australia, *edited by* K. R. Glasson and J. H. Rattigan: Australasian Institute of Mining and Metallurgy, Monograph 17, p. 263–285.

BLOCKLEY, J. G., TEHANAS, I., MANDYCZEWSKY, A., and MORRIS R. C., in press, Proposed stratigraphic subdivision of the Marra Mamba Iron Formation and the lower Wittenoom Dolomite: Western Australia, Geological Survey, Professional Papers.

BLOCKLEY, J. G., TRENDALL, A. F., de LAETER, J. R., and LIBBY, W. G., 1980, Two anomalous isochrons from the vicinity of Newman: Western Australia, Geological Survey, Annual Report for 1979, p. 93–96.

BOURN, R. and JACKSON, D. G., 1979, A generalised account of the Paraburdoo iron orebodies: Australasian Institute of Mining and Metallurgy, Annual Conference, Perth, p. 187–201.

BOYER, S. E. and ELLIOTT, D., 1982, Thrust systems: American Association of Petroleum Geologists, Bulletin, v. 66, p. 1196–1230.

BREWER, J. A. and SMYTHE, D. K., 1984, MOIST and the continuity of crustal reflector geometry along the Caledonian–Appalachian Orogen: Geological Society of London, Journal v. 141, p. 105 - 120.

BREWER, J. A., COOK, F. A., BROWN, L. D., OLIVER, J. E., KAUFMAN, S., and ALBAUGH, D. S., 1981, COCORP seismic reflection profiling across thrust faults, *in* Thrust and nappe tectonics, *edited by* K. R. McClay and N. J. Price: Geological Society of London, Special Publication 9, p. 501–512.

BUREAU OF MINERAL RESOURCES, 1987, Australian Mineral Industry Quarterly: Australia, BMR, v. 39, p. 138.

BURKE, K., DEWEY, J. F., and KIDD, W. S. F., 1976, Precambrian palaeomagnetic results compatible with contemporary operation of the Wilson Cycle: Tectonophysics, v. 33, p. 287–299.

BUTLER, R. W. H., 1985, Thrust tectonics—A personal view: Geological Magazine, v. 122, p. 223–232.

BYE, S. M., 1975, Chromite mineralisation within the Coobina ultramafic, *in* Economic geology of Australia and Papua-New Guinea, 1. Metals, *edited by* C. L. Knight, Australasian Institute of Mining and Metallurgy, Monograph 5, p. 205–206.

CAMPANA, B., HUGHES, F. E., BURNS, W. G., WHITCHER, I. G., and MUCENIEKAS, E., 1964, Discovery of the Hamersley iron deposits: Australasian Institute of Mining and Metallurgy, Proceedings, v. 210, p. 1–30.

COMPSTON, W., WILLIAMS, I. S., McCULLOCH, M. T., FOSTER, J. J., ARIENS, P. A., and TRENDALL, A. F., 1981, A revised age for the Hamersley Group: Geological Society of Australia, 5th Annual Convention, Perth, Abstracts 3, p. 40.

COWARD, M. P., 1984, Major shear zones in the Precambrian crust—Examples from NW Scotland and southern Africa and their significance, *in* Precambrian tectonics illustrated, *edited by* A. Kroner, and R. Greiling: E. Schweizerbart'sche Verlagsbuchhandlung, Stuttgart, p. 207–235.

COWLEY, W. M., 1979, Petrochemistry of the Mount Jope Volcanics and a mafic–ultramafic sill in the Fortescue Group near Mount Turner, Hamersley Ranges, W A: University of Adelaide, B Sc Honours thesis, (Unpublished).

DAHLSTROM, C. D. A., 1969, Balanced cross sections: Canadian Journal of Earth Sciences, v. 6, p. 743–757.

DANIELS, J. L., 1968, Turee Creek, W A: Western Australia, Geological Survey, 1:250 000 Geological Series—Explanatory Notes.

DANIELS, J. L., 1970, Wyloo, W A: Western Australia, Geological Survey, 1:250 000 Geological Series—Explanatory Notes.

DANIELS, J. L., 1975, Palaeogeographic development of Western Australia — Precambrian, in Geology of Western Australia: Western Australia, Geological Survey, Memoir 2, p. 437–450.

DANIELS, J. L. and MacLEOD, W. N., 1965, Newman, W A: Western Australia, Geological Survey, 1:250 000 Geological Series—Explanatory Notes.

de la HUNTY, L. E., 1965, Mount Bruce, W A: Western Australia, Geological Survey, 1:250 000 Geological Series—Explanatory Notes.

de la HUNTY, L. E., 1969, Robertson, W. A.: Western Australia, Geological Survey, 1:250 000 Geological Series—Explanatory Notes.

de LAETER, J. R., FLETCHER, I. R., BICKLE, M. J., MYERS, J. S., LIBBY, W. G., and WILLIAMS, I. R., 1985, Rb–Sr, Sm–Nd and Pb–Pb geochronology of ancient gneisses from Mount Narryer, Western Australia: Australian Journal of Earth Sciences, v. 32, p. 349– 358.

DIMROTH, E., IMREH, L., GOULET, N., and ROCHELEAU, M., 1983, Evolution of the south-central segment of the Archaean Abitibi Belt, Quebec. Part II—Tectonic evolution and geomechanical model: Canadian Journal of Earth Sciences, v. 20, p. 1355–1373.

DROOP, G. T. R., 1982, A clinopyroxene paragenesis of albite–epidote–amphibolite facies in metasyenites from the southeast Tauern Window, Austria: Journal of Petrology, v. 23, p. 163–185.

DRUMMOND, B. J., 1981, Crustal structure of the Precambrian terrains of northwest Australia from seismic refraction data: BMR Journal of Australian Geology and Geophysics, v. 6, p. 123–135.

DRUMMOND, B. J., SMITH, R. E., and HORWITZ, R. C., 1981, Crustal structure in the Pilbara and northern Yilgarn Blocks from deep seismic sounding, *in* Archaean Geology, *edited by* J. E. Glover and D. I. Groves: Geological Society of Australia, Special Publication 7, p. 33–42.

ELLIOTT, D. and JOHNSON, M. R. W., 1980, Structural evolution in the northern part of the Moine thrust belt, NW Scotland: Royal Society of Edinburgh, Transactions, Earth Sciences, v. 71, p. 69–96.

ENGELDER, T. and MARSHAK, S., 1985, Development of cleavage formed at shallow depths in sedimentary rocks: Journal of Structural Geology, v. 7, p. 327–343.

ENGLAND, P. C. and THOMPSON, A. B., 1984, Pressure–temperature–time paths of regional metamorphism. I—Heat transfer during the evolution of regions of thickened continental crust: Journal of Petrology, v. 25, p. 894–928.

ETHERIDGE, M. A., RUTLAND, R. W. R., and WYBORN, L. A. I., 1987, Orogenesis and tectonic process in the early to middle Proterozoic of northern Australia, *in* Proterozoic lithospheric evolution, *edited by* A. Kroner: American Geophysical Union, Geodynamic Series, v. 17, p. 131–147.

EVANS, W. J. and CLINT, P., 1975, Iron deposits of the Brockman Syncline, Hamersley Iron Province, *in* Economic geology of Australia and Papua New Guinea 1. Metals, *edited by* C. L. Knight: Australasian Institute of Mining and Metallurgy, Monograph 5, p. 906–910.

EWERS, W. E. and MORRIS, R. C., 1981, Studies on the Dales Gorge Member of the Brockman Iron Formation: Economic Geology, v. 76, p. 1929–1953.

FLETCHER, I. R., ROSMAN, K. J. R, WILLIAMS, I. R., HICKMAN, A. H., and BAXTER, J. L., 1984, Sm–Nd geochronology of greenstone belts in the Yilgarn Block, Western Australia: Precambrian Research, v. 26, p. 333–361.

FLETCHER, I. R., LIBBY, W. G., and ROSMAN, K. J. R., 1987, Sm–Nd dating of the 2411 Ma Jimberlana dyke, Yilgarn Block, Western Australia: Australian Journal of Earth Sciences, v. 34 p. 523–526.

FRASER, A. R., 1976, Gravity provinces and their nomenclature: BMR Journal of Australian Geology and Geophysics, v. 1, p. 350–352.

GAUDEMER, Y. and TAPPONIER, P., 1987, Ductile and brittle deformations in the northern Snake Range, Nevada: Journal of Structural Geology, v. 9, p. 159–180.

GEE, R. D., 1975, Regional geology of the Archaean nucleii of the Western Australian Shield, *in* Economic geology of Australia and Papua New Guinea 1. Metals, *edited by* C. L. Knight: Australasian Institute of Mining and Metallurgy, Monograph 5, p. 43–55.

GEE, R. D., 1979, Structure and tectonic style of the Western Australian Shield: Tectonophysics, v. 58, p. 327–369.

GEE, R. D., 1987, Peak Hill, W. A. (2nd edn): Western Australia, Geological Survey, 1:250 000 Geological Series —Explanatory Notes.

GEE, R. D., 1990, Nabberu Basin, in Geology and mineral resources of Western Australia: Western Australia, Geological Survey, Memoir 3, p. 202–210.

GEE, R. D., BAXTER, J. L., WILDE, S. A., and WILLIAMS, I. R., 1981, Crustal development in the Archaean Yilgarn Block, Western Australia, *in* Archaean Geology, *edited by* J. E. Glover and D. I. Groves: Geological Society of Australia, Special Publication 7, p. 43–56.

GEOLOGICAL SURVEY OF WESTERN AUSTRALIA, 1990, Geology and mineral resources of Western Australia: Western Australia, Geological Survey, Memoir 3.

GIBBS, A. D., 1984, Structural evolution of extensional basin margins: Geological Society of London, Journal, v. 141, p. 711–732.

GRIFFIN, T. J., 1990a, Southern Cross Province, *in* Geology and mineral resources of Western Australia: Western Australia, Geological Survey, Memoir 3, p. 60–77.

GRIFFIN, T. J., 1990b, Eastern Goldfields Province, *in* Geology and mineral resources of Western Australia: Western Australia, Geological Survey, Memoir 3, p. 77–119.

GROVES, D. I., PHILLIPS, G. N., HO, S. E., HENDERSON, C. A., CLARK, M. E., and WOAD, G. M., 1984, Controls on distribution of Archaean hydrothermal gold deposits in Western Australia, in Gold 82, *edited by* R. P. Foster: A. A. Balkema, Rotterdam.

GROVES, D. I., PHILLIPS, G. N., HO, S. E., and HOUSTOUN, S. M., 1985, The nature, genesis and regional controls of gold mineralisation in Archaean greenstone belts of the Western Australian Shield—A brief review: Geological Society of South Africa, Transactions, v. 88, p. 135–148.

HALLIGAN, R. and DANIELS, J. L., 1964, The Precambrian geology of the Ashburton valley region: Western Australia, Geological Survey, Annual Report for 1963, p. 38–46.

HARKER, A., 1904, The Tertiary igneous rocks of Skye: United Kingdom, Geological Survey,, Memoir, (HMSO, Edinburgh).

HARRIS, L. B., 1987, A tectonic framework for the Western Australian Shield and its significance to gold mineralisation—A personal view, *in* Recent advances in understanding Precambrian Gold Deposits, *edited by* S. E. Ho and D. I. Groves: University of Western Australia, Geology Department and University Extension, Publication 11, p. 1–27.

HASSLER, S. W., 1990, The main tuff interval of the Wittenoom Dolomite—Evidence for the palaeogeography and tectonic setting of the Hamersley Basin, Western Australia, *in* Extended abstracts volume—Third international Archaean symposium, *compiled by* J. E. Glover and S. E. Ho: Perth, Geoconferences Inc, p 331–333.

HATCHER Jr., R. D., 1981, Thrusts and nappes in the North American Appalachian Orogen, *in* Thrust and nappe tectonics, *edited by* K. R. McClay, and N. J. Price: Geological Society of London, Special Publication 9, p. 491–500.

HICKMAN, A. H., 1975, Precambrian structural geology of part of the Pilbara region: Western Australia, Geological Survey, Annual Report for 1974, p. 68–73.

HICKMAN, A. H., 1983, Geology of the Pilbara Block and its environs: Western Australia, Geological Survey, Bulletin 127.

HICKMAN, A. H., 1984, Archaean diapirism in the Pilbara Craton, Western Australia, in Precambrian tectonics illustrated, *edited by* A. Kroner and R. Greiling: E. Schweizerbart'sche Verlagsbuchhandlung, Stuttgart, p. 113—127.

HICKMAN, A. H. and HARRISON, P. H., 1986, A review of the occurrence of, and potential for, Precambrian conglomerate-hosted gold mineralisation within Western Australia, *in* Geocongress '86, Extended Abstracts: Geological Society of South Africa, p. 301–306.

HICKMAN, A. H. and LIPPLE, S. L., 1975, Explanatory notes on the Marble Bar 1:250 000 geological sheet, W A: Western Australia, Geological Survey, Record 1974/20.

HICKMAN, A. H. and LIPPLE, S. L., 1978, Marble Bar, W A: Western Australia, Geological Survey, 1:250 000 Geological Series—Explanatory Notes.

HOBBS, B. E., ARCHIBALD, N. J., ETHERIDGE, M. A., and WALL, V. J, 1984, Tectonic history of the Broken Hill Block, Australia, *in* Precambrian tectonics illustrated, *edited by* A. Kroner and R. Greiling: E. Schweizerbart'sche Verlagsbuchhandlung, Stuttgart, p. 353–368.

HOFFMAN, P. F., 1980, Wopmay Orogen—A Wilson cycle of early Proterozoic age in the northwest of the Canadian Shield, *in* The continental crust and its mineral deposits, *edited by* D. W. Strangway: Geological Association of Canada, Special Paper 20, p. 523–549.

HOLLAND, T. J. B. and RICHARDSON, S. W., 1979, Amphibole zonation in metabasites as a guide to the evolution of metamorphic conditions: Contributions to Mineralogy and Petrology, v. 70, p. 143–148.

HORWITZ, R. C., 1976, Two unrecorded basal sections in older Proterozoic rocks of Western Australia: Australia, CSIRO, Mineral Research Laboratories, Division of Mineralogy, Report FP 17.

HORWITZ, R. C., 1980, Discussion on—A progress review of the Hamersley Basin of Western Australia *by* A. F. Trendall: Finland, Geological Survey, Bulletin, v. 53, p. 63–66.

HORWITZ, R. C., 1982, Geological History of the early Proterozoic Paraburdoo hinge zone, Western Australia: Precambrian Research, v. 19, p. 191–200.

HORWITZ, R. C, 1987, Structural trends of the Archaean to lower Proterozoic Hamersley Province, Western Australian Shield: Australia, CSIRO, Division of Minerals and Geochemistry, Report MG 31.

HORWITZ, R. C. and SMITH, R. E., 1978, Bridging the Pilbara and Yilgarn Blocks, Western Australia: Precambrian Research, v. 6, p. 293–322.

HOSSACK, J. R., 1983, A cross-section through the Scandanavian Caledonides constructed with the aid of branch-line maps: Journal of Structural Geology, v. 5, p. 103–111.

HUNTER, W. M., 1990, Bresnahan Basin, *in* Geology and mineral resources of Western Australia: Western Australia, Geological Survey, Memoir 3, p. 304–308.

HYNES, A and GEE, R. D., 1986, Geological setting and petrochemistry of the Narracoota Volcanics, Capricorn Orogen, Western Australia: Precambrian Research, v. 31, p. 107–132.

IDNURM, M. and GIDDINGS, J. W., 1988, Precambrian polar wander—A review: Precambrian Research, v. 40 - 41, p. 61–88.

KNEESHAW, M., 1975, Mt. Whaleback iron orebody, Hamersley Iron Province, *in* Economic geology of Australia and Papua New Guinea 1. Metals, *edited by* C. L. Knight: Australasian Institute of Mining and Metallurgy, Monograph 5, p. 910–916.

KNEESHAW, M., 1984, Pilbara iron ore classification—A proposal for a common classification for BIF-derived supergene iron ore: Australasian Institute of Mining and Metallurgy, Proceedings, v. 289, p. 157–162.

KNIPE, R. J. and NEEDHAM, D. T., 1986, Deformation processes in accretionary wedges—Examples from the SW margin of the Southern Uplands, Scotland, *in* Collision tectonics, *edited by* M. P. Coward and A. C. Ries: Geological Society of London, Special Publication 19, p. 51–66.

KOKELAAR, B. P., 1982, Fluidization of wet sediments during the emplacement and cooling of various igneous bodies: Geological Society of London, Journal, v. 139, p. 21–34.

KRONER, A., 1981, Precambrian plate tectonics, *in* Precambrian plate tectonics, *edited by* A. Kroner: Elsevier, Amsterdam, p. 57–90.

KRONER, A., 1983, Proterozoic mobile belts compatible with the plate tectonic concept: Geological Society of America, Memoir 161, p. 59–74.

LAIRD, J., 1980, Phase equilibria in mafic schist from Vermont: Journal of Petrology, v. 21, p. 1–37.

LAIRD, J. and ALBEE, A. L., 1981, Pressure, temperature and time indicators in mafic schist—Their application to reconstructing the polymetamorphic history of Vermont: American Journal of Science, v. 281, p. 127–175.

LIBBY, W. G., de LAETER, J. R., and MYERS, J. S., 1986, Geochronology of the Gascoyne Province: Western Australia, Geological Survey, Report 20.

LIOU, J. G., KUNIYOSHI, S., and ITO, K., 1974, Experimental studies of the phase relations between greenschist and amphibolite in a basaltic system: American Journal of Science, v. 274, p. 613–632.

LISTER, G. S., ETHERIDGE, M. A., and SYMONDS, P. A., 1986, Detachment faulting and the evolution of passive continental margins: Geology, v. 14, p. 246–250.

LOW, G. H., 1963, Copper deposits of Western Australia: Western Australia, Geological Survey, Mineral Resources Bulletin 8.

McCALL, G. J. H., 1971, Some ultrabasic and basic igneous rock occurrences in the Archaean of Western Australia: Geological Society of Australia, Special Publication 3, p. 429–442.

McCONCHIE, D., 1984, A depositional environment for the Hamersley Group—Palaeogeography and geochemistry, *in* Archaean and Proterozoic basins of the Pilbara, Western Australia—Evolution and mineralisation potential, *edited by* J. R. Muhling, D. I. Groves, and T. S. Blake: University of Western Australia, Geology Department and University Extension, Publication 9, p. 144–190.

McCULLOCH, M. T., 1987, Sm–Nd isotopic constraints on the evolution of Precambrian crust in the Australian continent: American Geophysical Union, Geodynamics Series, v. 17, p. 115–130.

McNAUGHTON, N. J. and DAHL, N., 1987, A geochronological framework for gold mineralisation in the Yilgarn Block, Western Australia, *in* Recent advances in understanding Precambrian gold deposits, *edited by* S. E. Ho and D. I. Groves: University of Western Australia, Geology Department and University Extension, Publication 11, p. 29–49.

McWILLIAMS, M. O., 1981, Palaeomagnetism and Precambrian tectonic evolution of Gondwana, *in* Precambrian plate tectonics, *edited by* A. Kroner: Elsevier, Amsterdam, p. 649–687.

MacLEOD, W. N., 1966, The geology and iron deposits of the Hamersley Range area: Western Australia, Geological Survey, Bulletin 117.

MacLEOD, W. N. and de la HUNTY, L. E., 1966, Roy Hill, W A: Western Australia, Geological Survey, 1:250 000 Geological Series—Explanatory Notes.

MacLEOD, W. N., de la HUNTY, L. E., JONES, W. R., and HALLIGAN, R., 1963, Preliminary report on the Hamersley Iron Province, North West Division: Western Australia, Geological Survey, Annual Report for 1962, p. 44–54.

MARSTON, R. J., 1979, Copper mineralization in Western Australia: Western Australia, Geological Survey, Mineral Resources Bulletin 13.

MARUYAMA, S., SUZUKI, K., and LIOU, J. G., 1983, Greenschist–amphibolite transition equilibria at low pressures: Journal of Petrology, v. 24,p. 583–604.

MATHESON, R. S., 1945, Report on red ochre deposits, ML370H, Ophthalmia Range: Western Australia Geological Survey, Annual Report for 1944, p. 92–95.

MIYASHIRO, A., 1973, Metamorphism and Metamorphic Belts: George Allen and Unwin, London.

MOODY, J. B., MEYER, D., and JENKINS, J. E., 1983, Experimental characterisation of the greenschist/amphibolite boundary in mafic systems: American Journal of Science, v. 283, p. 48–92.

MORRIS, R. C., 1980, A textural and mineralogical study of the relationships of iron ore to banded iron-formation in the Hamersley Iron Province of Western Australia: Economic Geology, v. 75, p. 184–209.

MORRIS, R. C., 1985, Genesis of iron ore in banded iron-formation by supergene and supergene–metamorphic processes—A conceptual model, *in* Handbook of strata-bound and stratiform ore deposits, *edited by* K. Wolf: Elsevier, Amsterdam, v. 13, p. 73–235.

MORRIS, R. C. and HORWITZ, R. C., 1983, The origin of the iron-formation-rich Hamersley Group of Western Australia—Deposition on a platform: Precambrian Research, v. 21, p. 273–297.

MORRIS, R. C., THORNBER, M. R., and EWERS, W. E., 1980, Deep-seated iron ores from banded iron-formation: Nature, v. 288, p. 250–252.

MUHLING, J. R., 1986, Tectonothermal history of the Mukalo Creek area, southern Gascoyne Province, Western Australia—Crustal evolution of Archaean gneisses reworked during Proterozoic orogenesis: University of Western Australia, Ph. D. Thesis, (unpublished).

MUHLING, J. R., 1988, The nature of Proterozoic reworking of early Archaean gneisses, Mukalo area, Southern Gascoyne Province, Western Australia: Precambrian Research, v. 40/41, p. 341–362.

MUHLING, P. C. and BRAKEL, A. T., 1985, The geology of the Bangemall Group—The evolution of an intracratonic Proterozoic Basin: Western Australia, Geological Survey, Bulletin 128.

MYERS, J. S., 1989, Thrust sheets on the southern foreland of the Capricorn Orogen, Robertson Range, Western Australia: Western Australia, Geological Survey, Professional Papers.

MYERS, J. S., 1990, Gascoyne Complex, *in* Geology and mineral resources of Western Australia: Western Australia, Geological Survey, Memoir 3.

MYERS, J. S. and WATKINS, K. P., 1986, Origin of granite–greenstone patterns, Yilgarn Block, Western Australia: Geology, v. 13, p. 778–780.

NEALE, J., 1975, Iron ore deposits in the Marra Mamba Formation at Mining area "C", Hamersley Iron Province, *in* Economic Geology of Australia and Papua New Guinea 1. Metals, *edited by* C. L. Knight: Australasian Institute of Mining and Metallurgy, Monograph 5, p. 924–932.

NISBET, E. G., 1984, The continental and oceanic crust and lithosphere in the Archaean—Isostatic, thermal, and tectonic models: Canadian Journal of Earth Sciences, v. 21, p. 1426–1441.

PHILLIPS, G. N. and WALL, V. J., 1981, Evaluation of prograde regional metamorphic conditions—Their implications for the heat source and water activity during metamorphism in the Willyama Complex, Broken Hill, Australia: Bullétin de la Société Français de Minéralogie et de Cristallographie, v. 104, p. 801–810.

PIDGEON, R. T., 1984, Geochronological constraints on early volcanic evolution of the Pilbara Block, Western Australia: Australian Journal of Earth Sciences, v. 31, p. 237–242.

PIDGEON, R. T. and HORWITZ, R. C., 1991, The origin of olistoliths in Proterozoic rocks of the Ashburton Trough, Western Australia, using zircon U–Pb isotopic characteristics: Australian Journal of Earth Sciences, v. 38, p. 55–63.

POWELL, C . McA., 1979, A morphological classification of rock cleavage: Tectonophysics, v. 58, p. 21–34.

PRICE, R. A., 1971, Gravitational sliding and the foreland–thrust belt of the North American Cordillera: Geological Society of America, Bulletin, v. 82, p. 1133–1138.

PRICE, R. A., 1981, The Cordilleran foreland thrust and fold belt in the southern Canadian Rocky Mountains, *in* Thrust and nappe tectonics, *edited by* K. R. McClay and N. J. Price: Geological Society of London, Special Publication 9, p. 427–448.

RAMBERG, H., 1981, The role of gravity in orogenic belts, *in* Thrust and nappe tectonics, *edited by* K. R. McClay and N. J. Price: Geological Society of London, Special Publication 9, p. 125–140.

RAMSAY, J. G., 1967, Folding and fracturing of rocks: New York, McGraw Hill.

RAMSAY, J. G., 1980, Shear zone geometry—A review: Journal of Structural Geology, v. 2, p. 83–89.

RAMSAY, J. G. and GRAHAM, R. H., 1970, Strain variation in shear belts: Canadian Journal of Earth Sciences, v. 7, p. 786–813.

RAMSAY, J. G., and HUBER, M. I., 1983, The techniques of modern structural geology Volume 1—Strain analysis: London, Academic Press.

RAMSAY, J. G. and HUBER, M. I., 1987, The techniques of modern structural geology Volume 2—Folds and fractures: London, Academic Press.

RATHBONE, P. A., COWARD, M. P., and HARRIS, A. L., 1983, Cover and basement—A contrast in structural style and fabrics: Geological Society of America, Memoir 158, p. 213–223.

RICHARDS, J. R. and BLOCKLEY, J. G., 1984, The base of the Fortescue Group, Western Australia—Further galena lead isotope evidence on its age: Australian Journal of Earth Sciences, v. 31, p. 257–268.

RUST, B. R. and KOSTER, E. H., 1984, Coarse alluvial deposits, *in* Facies models, *edited by* R. G. Walker (2nd edn): Geoscience Canada, Reprint Series 1, p. 53–69.

RUTLAND, R. W. R., 1981, Structural framework of the Australian Precambrian, *in* The Precambrian of the southern hemisphere, *edited by* D. R. Hunter: Amsterdam, Elsevier, p. 3–32.

RUTTER, E. H., 1983, Pressure solution in nature, theory and experiment: Geological Society of London, Journal, v. 140, p. 725–740.

SEYMOUR, D. B., THORNE, A. M., and BLIGHT, D. F., 1988, Wyloo, W. A. (2nd edn): Western Australia Geological Survey, 1:250 000 Geological Series—Explanatory Notes.

SHACKLETON, R. M., 1986, Precambrian collision tectonics in Africa, *in* Collision tectonics, *edited by* M. P. Coward and A. C. Ries: Geological Society of London, Special Publication 19, p. 329–349.

SHACKLETON, R. M. and RIES, A. C., 1984, Relation between stretching lineations and plate motions: Journal of Structural Geology, v. 6, p. 111–117.

SIBSON, R. H., 1987, Earthquake rupturing as a mineralizing agent in hydrothermal systems: Geology, v. 15, p. 701–704.

SLEPECKI, S., 1981, Marra Mamba iron ore—A case history in exploration and development of a new ore type: Australasian Institute of Mining and Metallurgy, Annual Conference, Sydney, p. 195–207.

SMITH, R. E., PERDRIX, J. L., and PARKS, T. C., 1982, Burial metamorphism in the Hamersley Basin, Western Australia: Journal of Petrology, v. 23, p. 75–102.

SNOWDEN, P. A., 1984, Non-diapiric batholiths in the north of the Zimbabwe Shield, *in* Precambrian tectonics illustrated, *edited by* A. Kroner and R. Greiling: E. Schweizerbart'sche Verlagsbuchhandlung, Stuttgart, p. 135–145.

STOCKMAL, G. S., BEAUMONT, C., and BOUTILIER, R., 1986, Geodynamic models of convergent margin tectonics—Transition from rifted margin to overthrust belt and consequences for foreland - basin development: American Association of Petroleum Geologists, Bulletin, v. 70, p. 181–190.

SWINDELLS, C. E., TYLER, I. M., RANSOM, D. B., and JAMES, T., in prep., Low angle normal faulting at Mount Whaleback, Western Australia.

TAPPONNIER, P., PELTZER, G., and ARMIJO, R., 1986, On the mechanics of the collision between India and Asia, *in* Collision tectonics, *edited by* M. P. Coward, and A. C. Ries: Geological Society of London, Special Publication 19, p. 115–157.

THOMPSON, A. B. and ENGLAND, P. C., 1984, Pressure–temperature –time paths of regional metamorphism II. Their inference and interpretation using mineral assemblages in metamorphic rocks: Journal of Petrology, v. 25 ,p. 929–955.

THOMPSON, R. I., 1981, The nature and significance of large "blind" thrusts within the northern Rocky Mountains of Canada, *in* Thrust and nappe tectonics, *edited by* K. R. McClay and N. J. Price: Geological Society of London, Special Publication 9, p. 449–473.

THORNE, A. M., 1985, Upward-shallowing sequences in the Precambrian Duck Creek Dolomite, Western Australia: Western Australia, Geological Survey, Professional Papers for 1983, Report 14, p. 81–93.

THORNE, A. M., 1990, Fortescue Group volcanism and sedimentation in the southern Hamersley Basin, Pilbara Craton, Western Australia, *in* Recent advances in understanding the Archaean and Early Proterozoic geology of the Pilbara Block—Program and abstracts: University of Western Australia, Department of Geology and University Extension, p. 25–29.

THORNE, A. M. and SEYMOUR, D. B., 1986, The sedimentology of a tide influenced fan-delta system in the early Proterozoic Wyloo Group on the southern margin of the Pilbara Craton, Western Australia: Western Australia, Geological Survey, Professional Papers for 1984, Report 19, p. 70–82.

THORNE, A. M. and SEYMOUR, D. B., 1991, Geology of the Ashburton Basin: Western Australia, Geological Survey, Bulletin 139.

THORNE, A. M. and TYLER, I. M., in press, Turee Creek, W. A. (2nd edn): Western Australia, Geological Survey, 1:250 000, Geological Series—Explanatory Notes.

TRENDALL, A. F., 1975a, Hamersley Basin, in Geology of Western Australia: Western Australia, Geological Survey, Memoir 2, p. 118–141.

TRENDALL, A. F., 1975b, Geology of Western Australian iron ore, *in* Economic geology of Australia and Papua-New Guinea 1. Metals, *edited by* C. L. Knight: Australasian Institute of Mining and Metallurgy, Monograph 5, p. 883–892.

TRENDALL, A. F., 1979, A revision of the Mount Bruce Supergroup: Western Australia, Geological Survey, Annual Report for 1978, p. 63–71.

TRENDALL, A. F., 1983, The Hamersley Basin, *in* Iron formations—Facts and problems, *edited by* A. F. Trendall and R. C. Morris: Amsterdam, Elsevier, p. 69–129.

TRENDALL, A. F. and BLOCKLEY, J. G., 1970, The iron formations of the Precambrian Hamersley Group, Western Australia: Western Australia Geological Survey Bulletin 119.

TWIDALE, C. R., HORWITZ, R. C., and CAMPBELL, E. M., 1985, Hamersley landscapes of the northwest of Western Australia: Revue de Géologie Dynamique et de Géographie Physique, v. 26, p. 173–186.

TYLER, I. M., 1986, Age and stratigraphy of a sequence of metavolcanic and metasedimentary rocks in the Prairie Downs–Deadman Hill area, southwestern margin of the Sylvania Dome: Western Australia, Geological Survey, Professional Papers for 1984, Report 19, p. 83–87.

TYLER, I. M., 1990a, Explanatory Notes on the Newman 1:100 000 sheet (2851): Western Australia, Geological Survey.

TYLER, I. M., 1990b, Mafic dyke swarms, in Geology and mineral resources of Western Australia: Western Australia, Geological Survey, Memoir 3, p. 191–194.

TYLER, I. M., FLETCHER, I. R., de LAETER, J. R., WILLIAMS, I. R. and LIBBY, W. G., in press, Isotope and rare earth element evidence for a late Archaean terrane boundary in the southeastern Pilbara Craton, Western Australia: Precambrian Research.

TYLER, I. M., HUNTER, W. M. and WILLIAMS, I. R., 1990, Newman, W. A. (2nd edn): Western Australia Geological Survey, 1:250 000 Geological Series—Explanatory Notes.

TYLER, I. M. and THORNE, A. M., 1990, Capricorn Orogen—Structural evolution of the northern margin, in Geology and mineral resources of Western Australia: Western Australia, Geological Survey, Memoir 3, p 223–232.

WALKER, R. G., 1984, Turbidites and associated coarse clastic deposits, *in* Facies models, *edited by* R. G. WALKER (2nd edn): Geoscience Canada, Reprint Series 1, p. 171–188.

WARD, D. F., COLES, I. G., and CARR, W. M. B., 1975, Jimblebar and Western Ridge iron ore deposits, Hamersley Iron Province, *in* Economic geology of Australia and Papua-New Guinea 1. Metals, *edited by* C. L. Knight: Australasian Institute of Mining and Metallurgy, Monograph 5, p. 916–924.

WATKINS, K. P. and HICKMAN, A. H., 1990, Geological evolution and mineralization of the Murchison Province, Western Australia: Western Australia, Geological Survey, Bulletin 137.

WATTERSON, J., 1968, Plutonic development of the Ilordleq area, South Greenland, Part II—Late kinematic basic dykes: Gronlands Geologiske Undersogelse, Bulletin 70.

WERNICKE, B., 1981, Low-angle normal faults in the Basin and Range Province—Nappe tectonics in an extending orogen: Nature, v. 291, p. 645–648.

WHITE, S., 1979, Grain and sub-grain size variations across a mylonite zone: Contributions to Mineralogy and Petrology, v. 70, p. 193–202.

WIEDENBECK, M. and WATKINS, K. P., in prep., U–Pb zircon ages from granitoids of the Murchison Province, Western Australia.

WILCOX, R. E., HARDING, T. P., and SEELY, D. R., 1973, Basic wrench tectonics: American Association of Petroleum Geologists, Bulletin, v. 57, p. 74–96.

WILLIAMS, I. R., 1989, Balfour Downs, W A (2nd edn): Western Australia, Geological Survey, 1:250 000 Geological Series—Explanatory Notes.

WILLIAMS, I. R., 1990, Bangemall Basin, in Geology and mineral resources of Western Australia: Western Australia, Geological Survey, Memoir 3, p. 308–329.

WILLIAMS, I. R. and TYLER, I. M., 1991, Robertson, W A (2nd edn): Western Australia, Geological Survey, 1:250 000 Geological Series—Explanatory Notes.

WILLIAMS, S. J., 1986, Geology of the Gascoyne Province, Western Australia: Western Australia, Geological Survey, Report 15.

WILSON, R. C., 1930, Jimble Bar: Western Australia, Department of Mines, Annual Report for 1929, p. 49–52.

WILTSCHKO, D. and EASTMAN, D., 1983, Role of basement warps and faults in localizing thrust fault ramps: Geological Society of America, Memoir 158, p. 177–190.

WINDLEY, B. F., 1981, Precambrian rocks in the light of the plate-tectonic concept, *in* Precambrian plate tectonics, *edited by* A. Kroner: Elsevier, Amsterdam, p. 1–20.

WINDLEY, B. F., 1983, A tectonic review of the Proterozoic: Geological Society of America, Memoir 161, p. 1–9.

WINKLER, H. G. F., 1979, Petrogenesis of metamorphic rocks: New York, Springer Verlag.

02208/5/91-500-L/5415 GARRY L. DUFFIELD, Government Printer, Western Australia

REFERENCE

PHANEROZOIC — CAINOZOIC — QUATERNARY

- Q — Alluvium, colluvium and eolian sand
- Czc, Czl, Czk
  - Czc Colluvium — partly consolidated valley-fill deposits
  - Czl Laterite — massive and pisolitic ferruginous duricrust
  - Czk Calcrete — sheet carbonate, usually formed in major drainage channels
- q — Quartz veins, various ages
- d_r — Dolerite dyke
- d_4 — MURRAMUNDA DOLERITE: fine-grained to weakly porphyritic dolerite

HAMERSLEY BASIN — c. 2750 Ma

- Hamersley Group
  - Hm — MARRA MAMBA IRON FORMATION: chert, ferruginous chert, minor shale
  - Fj — JEERINAH FORMATION: interbedded shale, chert, minor felsic tuff
- Fortescue Group
  - Fpu — Upper mafic volcanic unit: andesitic and basaltic lavas, minor thin tuff units
  - Fs — Basal metasedimentary unit: coarse conglomeratic sandstone, shale

ARCHAEAN — > 2750 Ma

SYLVANIA INLIER

- d_1 — Amphibolite dyke, foliated and lineated
- d_3 — Schistose amphibolite dyke; intruded into and deformed with the greenstone belt
- g, gr, gv, gc
  - g Granitoid rocks, undifferentiated, deeply weathered
  - gr Metagranite to metagranodiorite, medium-, even-grained
  - gv Metagranite to metagranodiorite, medium-grained, sparse feldspar phenocrysts
  - gc Metagranite, coarse-grained; feldspar and quartz megacrysts
- m — Greenstone belt extensively veined by granitoid rocks
- sq — Interbedded chert, fuchsitic quartzite, quartzofeldspathic schist, calc-silicate schist, minor pelitic and semi-pelitic schist
- i, ih, ia
  - i Banded iron-formation, undifferentiated
  - ih Hematite-magnetite-quartz banded iron-formation
  - ia Amphibole (grunerite and hornblende) - magnetite-quartz banded iron-formation
- zc, zh
  - zc Quartz-chlorite-amphibole-feldspar (-garnet) schist; relict textures indicate tuff
  - zh "Hybrid" intermediate rock; grades into recrystallized garnet-bearing granitoid rock
- bb, bg, bo, bu, ba
  - bb Metabasalt; tholeiitic, locally amygdaloidal
  - bg Metagabbro; medium- and coarse-grained; includes some serpentinite, metaperidotite and metapyroxenite layers
  - bo Metaleucogabbro; <30% mafic minerals, minor quartz
  - bu Komatiitic metabasalt
  - ba Amphibolite, fine- and medium-grained; lineated and foliated
- ua, us, ux, uz
  - ua Tremolite-chlorite-talc schist; minor talc-chlorite(-serpentine) schist
  - us Serpentinite; cumulate textures may be preserved
  - ux Metapyroxenite; amphibole-chlorite rock
  - uz Silicified cap rock developed on ultramafic rocks

SYMBOLS

- Geological boundary
- Fault
  - exposed
  - concealed
- Small- scale fold showing orientation of axial surface, direction of plunge and nature of vergence (Z, S or M)
- Bedding
  - inclined
  - vertical
  - overturned
- Way-up indicator
  - differentiation in mafic sills
- Cleavage, slaty or spaced
- Pre-Capricorn Orogeny
  - inclined
  - vertical
- Capricorn Orogeny
  - inclined
  - vertical
- Late, post-orogenic, inclined
- Foliation
- Pre-Capricorn Orogeny
  - inclined
  - vertical
- Capricorn Orogeny
  - inclined
- Lineation
  - plunge of stretching lineation
  - axis of crenulation hinges
- Formed road
- Track
- Mining camp
- Building
- Yard
- Landing ground
- Watercourse intermittent
- Pool
- Well
- Bore
- Windpump
- Pump engine
- Mine with recorded production (gold unless otherwise stated)
- Open-cut or pit
- Mineral prospect
- Mineral occurrence
  - Barite
  - Chromite
  - Copper
  - Lead

STRUCTURAL INTERPRETATION MAP

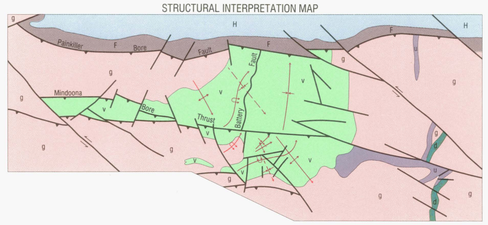

- g — Murramunda Dolerite
- H — Hamersley Group
- F — Fortescue Group
- Hamersley Basin
- g — Granitoid rocks
- u — Coobina ultramafic intrusion
- v — Jimblebar greenstone belt
- Sylvania Inlier

- Fault
- Thrust
- Sinistral wrench fault
- D_3g, overturned anticline
- D_3g, syncline
- D_3g, overturned syncline
- D_3g, anticline
- D_3g, syncline

INDEX TO 1:250 000 SHEETS

ROY HILL SF 50-12	BALFOUR DOWNS SF 51-9	RUDALL SF 51-10
NEWMAN SF 50-16	ROBERTSON SF 51-13	GUNANYA SF 51-14
OLLER SG 50-4	BULLEN SG 51-1	TRAINOR SG 51-2

LOCALITY DIAGRAM

HON. JEFF CARR, M.L.A.
MINISTER FOR MINES
D.R. KELLY, DIRECTOR GENERAL OF MINES

P.E. PLAYFORD
DIRECTOR, GEOLOGICAL SURVEY
OF WESTERN AUSTRALIA

BULLETIN 138 PLATE 1

GEOLOGICAL MAP OF THE JIMBLEBAR GREENSTONE BELT

SCALE 1:50 000

1 0 1 2 3 4 5

KILOMETRES

TRANSVERSE MERCATOR PROJECTION

Grid lines indicate 10 000 metre interval of the Australian Map Grid Zone 51

Geology by I.M. Tyler 1983

Cartography by the Surveys and Mapping Division, Department of Mines, Western Australia.
Topographic and Cadastral bases from compilations by the Department of Land Administration.
Published by and available from the Geological Survey of Western Australia, Department of Mines, 100 Plain Street, East Perth, W. A. 6004.
Printed by the State Printing Division, Department of Services, Western Australia, 1991.

HON. JEFF CARR, M.L.A.
MINISTER FOR MINES
D.R. KELLY, DIRECTOR GENERAL OF MINES

P.E. PLAYFORD
DIRECTOR, GEOLOGICAL SURVEY
OF WESTERN AUSTRALIA

BULLETIN 138 PLATE 2E

GEOLOGICAL MAP OF THE SYLVANIA INLIER AND SOUTHEAST HAMERSLEY BASIN

SCALE 1: 250 000

5000 0 5 10 15 20 25
Metres Kilometres

TRANSVERSE MERCATOR PROJECTION

Grid lines indicate 20 000 metre interval of the Australian Map Grid Zone 50

Geology by I.M. Tyler 1983–1986, with additional mapping by D.F. Blight 1981, A.M. Thorne 1983–1984, D.B. Seymour 1983, W.M. Hunter 1986, I.R. Williams 1985–1986.
Cartography by the Surveys and Mapping Division, Department of Mines, Western Australia.
Topographic and cadastral bases from compilations by the Department of Land Administration.
Published by and available from the Geological Survey of Western Australia, Department of Mines, 100 Plain Street, East Perth, 6004.
Printed by the State Printing Division, Department of Services, Western Australia, 1991.

INDEX TO 1:250 000 SHEETS

MT BRUCE SF 50–11	ROY HILL SF 50–12	BALFOUR DOWNS SF 51–9
THREE CREEK 2W SG 50–15	NEWMAN 2E SG 50–16	ROBERTSON SF 51–13
MT EGERTON SG 50–3	COLLIER SG 50–4	BULLEN SG 51–1

LOCALITY DIAGRAM

REPRESENTATIVE DIAGRAMMATIC CROSS-SECTIONS

NATURAL SCALE

SECTION E – F

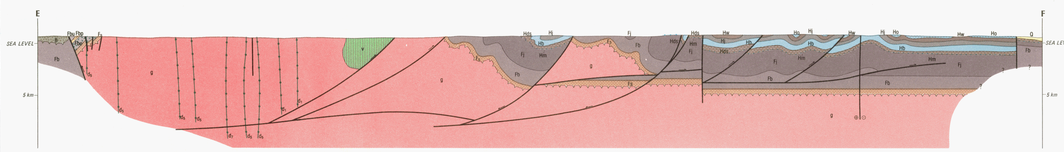

SECTION G – H

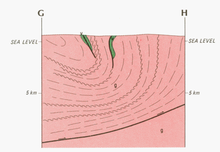

SECTION I – J – K

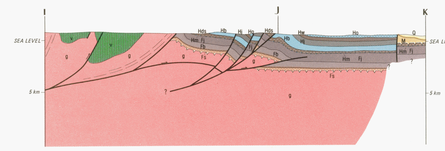

REFERENCE

PHANEROZOIC — CAINOZOIC — QUATERNARY

Q — Colluvium, alluvium and eolian sand

Czc Czr Czk Czp

Czc Colluvium — partly consolidated valley-fill deposits
Czr Laterite and siliceous duricrust; includes surficial hematite-goethite deposits over banded iron-formation; forms the Hamersley Surface
Czk Calcrete; includes massive opaline silica
Czp **ROBE PISOLITE:** pisolitic limonite

q Quartz veins
d_{3-4} Dolerite and metadolerite dykes. Numbers identify different suites, lowest number earliest

PROTEROZOIC — c. 750 Ma — Savory Group — BASIN

S — Shale, siltstone, sandstone

c. 1500—1050 Ma — Bangemall Group — BASIN

M — Sandstone, siltstone, shale, conglomerate, dolomite, chert. Intruded by dolerite sills

c. 1600 Ma — Bryah Basin Group — BLACK BRIDGE BASIN — EARAHEDY BASIN

B — Conglomerate, conglomeratic sandstone, sandstone, mudstone. Intruded by dolerite sills

R — **CAPRICORN FORMATION:** sandstone, siltstone, mudstone

c. 2000 Ma — Wyloo Group — ASHBURTON BASIN

W — Undifferentiated
Wa — **ASHBURTON FORMATION:** sandstone, mudstone, dolomite. Intruded by dolerite sills
Wd — **DUCK CREEK DOLOMITE:** dolomite, locally stromatolitic; chert, mudstone
Wm — **MOUNT McGRATH FORMATION:** mudstone, sandstone, conglomerate, dolomite
Wv — **CHEELA SPRINGS BASALT:** vesicular and amygdaloidal basalt
Ww — **BEASLEY RIVER QUARTZITE:** fine to coarse sandstone, may be silicified. Intruded by dolerite sills

2500 Ma — Hamersley Group — HAMERSLEY BASIN

Ok — **PINJIAN CHERT BRECCIA:** chert breccia, poorly banded chert

Tyee Creek Group

TU — Mudstone, sandstone, carbonate. Intruded by metadolerite sills

H — Undifferentiated
Ho — **BOOLGEEDA IRON FORMATION:** fine-grained, flaggy iron-formation, chert, jaspilite and shale
Hw — **WOONGARRA VOLCANICS:** quartz- or feldspar-phyric rhyolite and rhyodacite as sills or flows, jaspilitic banded iron- formation
Hi — **WEELI WOLLI FORMATION:** interlayered banded iron-formation, often jaspilitic, and metadolerite sills
Hb — **BROCKMAN IRON FORMATION:** banded iron-formation, chert, shale
Hdu — **MOUNT McRAE SHALE – MOUNT SYLVIA FORMATION – WITTENOOM DOLOMITE:** dolomite, chert; banded iron-formation, shale
Hm — **MARRA MAMBA IRON FORMATION:** chert, ferruginous chert, banded iron–formation, shale
Shown as a line on cross–sections

Fortescue Group

Fj — **JEERINAH FORMATION:** mudstone, siltstone, chert, sandstone, dolomite, felsic tuff, pillowed metabasalt. Intruded by metadolerite sills
Fb — Mafic and felsic volcanic rocks — undifferentiated. Intruded by metadolerite sills
Fbu — Upper mafic volcanic unit: metabasalt, pyroxene spinifex–textured basalt, serpentinite. Intruded by metadolerite sills
Fp — Felsic pyroclastic unit: felsic metatuff, chert
Fbl — Lower mafic volcanic unit: interbedded metabasalt and mafic metatuff

c. 2750 Ma

Fh Fs

Fh **HARDEY SANDSTONE:** sandstone, siltstone, mudstone, chert; tuff, basalt. Intruded by metadolerite sills
Fs Basal metasedimentary unit: phyllite, quartz–muscovite schist, metasandstone, metaconglomerate, carbonate rock

Fr — **MOUNT ROE BASALT – BELLARY FORMATION:** vesicular basalt and basaltic agglomerate, pelite, feldspathic sandstone and conglomerate, pillowed metabasalt, metatuff

ARCHAEAN

Mfu — Serpentinite

d_{1-2} — Metadolerite and amphibolite dykes

g gr ge gy gm gh

g Granitoid rocks — undifferentiated
ge Medium-, even-grained metagranite to metagranodiorite
gy Medium–grained metagranite to metagranodiorite, sparse feldspar phenocrysts
gh Medium–grained metagranite to metagranodiorite, with hornblende and relict clinopyroxene
gm Mixed granitoid unit: extensive veins and patches of ge and gy into foliated and/or banded metagranite to metagranodiorite
gr Mesocratic to melanocratic metamonzogranite to meta–quartz– diorite

Mfu — Greenstone belt rocks, mafic intrusive rocks — undifferentiated
Shown only on cross–sections

Mg — Interbedded chert, fuchsitic quartzite, quartzofeldspathic schist, calc–silicate schist, minor pelitic and semi–pelitic schist

> 2750 Ma — Banded iron–formation, chert

zc zh

zc Quartz–chlorite–amphibole–feldspar (–garnet) schist after tuff
zh "Hybrid" intermediate rock

ba bg

ba Amphibolitic schist
bg **Metagabbro;** includes serpentinite, metaperidotite, metapyroxenite, metaleucogabbro and anorthosite

ua uc

ua Ultramafic rocks; includes tremolite–chlorite– talc schist, serpentinite, metapyroxenite
uc Coobina ultramafic intrusion: serpentine, metapyroxenite, chromite

BASEMENT ROCKS OF THE SYLVANIA INLIER

SYMBOLS

Geological boundary
Unconformity/disconformity on cross–sections
angular unconformity
disconformity
Fault
exposed
concealed
on cross–sections, showing sense of movement, thrust or normal fault
vertical wrench fault, movement towards viewer
away from viewer
shear zone
Small–scale folds showing orientation of axial surface, direction of plunge and nature of vergence (Z, S or M)
Capricorn Orogeny $D1_C$
Capricorn Orogeny $D2_C$ inclined, vertical
Late, post–orogenic fold inclined, vertical
Bedding
inclined
vertical
overturned
horizontal
dip estimated from aerial photography
horizontal
0 – 15°
15 – 45°
45 – 90°

Highway
Formed road
Track
Railway
Homestead or building
Yard
Airfield
Major watercourse, intermittent
Bore or well, with windpump
Mine with recorded production
Open–cut or pit
Major
Minor

Cleavage, slaty or spaced
Pre–Capricorn Orogeny
inclined
vertical
Capricorn Orogeny
Ophthalmia Fold Belt
inclined
vertical
Ashburton Fold Belt
inclined
vertical
Cleavage, parallel to bedding
Ashburton Fold Belt
inclined
vertical
Foliation
Gneissic banding
inclined
Pre–Capricorn Orogeny
inclined
Capricorn Orogeny
inclined
vertical
trend of foliation
Lineation
plunge of stretching lineation
fold hinge orientation
axis of crenulation hinge
Ashburton Fold Belt
fold hinge orientation showing vergence
Isotopic age determination site

Mineral prospect
Mineral occurrence
Barite Ba
Chromite Cr
Chrysoprase Ce
Copper Cu
Crocidolite Ad
Gold Au
Iron Fe
Lead Pb
Ochre Oc
Road metal Rm
Uranium U
Zinc Zn

HON. JEFF CARR, M.L.A.
MINISTER FOR MINES
D.R. KELLY, DIRECTOR GENERAL OF MINES

P.E. PLAYFORD
DIRECTOR, GEOLOGICAL SURVEY
OF WESTERN AUSTRALIA

BULLETIN 138 PLATE 2W

GEOLOGICAL MAP OF THE SYLVANIA INLIER AND SOUTHEAST HAMERSLEY BASIN

SCALE 1:250 000

5000 0 5 10 15 20 25
Metres Kilometres

TRANSVERSE MERCATOR PROJECTION

Grid lines indicate 20 000 metre interval of the Australian Map Grid Zone 50

Geology by I.M. Tyler 1983–1986, with additional mapping by D.F. Blight 1981, A.M. Thorne 1983–1984, D.B. Seymour 1983, W.M. Hunter 1986, I.R. Williams 1985–1986.
Cartography by the Surveys and Mapping Division, Department of Mines, Western Australia.
Topographic and cadastral bases from compilations by the Department of Land Administration.
Published by and available from the Geological Survey of Western Australia, Department of Mines, 100 Plain Street, East Perth, 6004.
Printed by the State Printing Division, Department of Services, Western Australia, 1991.

SEE PLATE 2 E FOR REFERENCE

INDEX TO 1:250 000 SHEETS

MT BRUCE SF 50–11	ROY HILL SF 50–12	BALFOUR DOWNS SF 51–9
TUREE CREEK SG 50–15	NEWMAN 2E SG 50–16	ROBERTSON SF 51–13
MT EGERTON SG 50–3	COLLIER SG 50–4	BULLEN SG 51–1

2W

LOCALITY DIAGRAM

REPRESENTATIVE DIAGRAMMATIC CROSS-SECTIONS

NATURAL SCALE

SECTION A – B

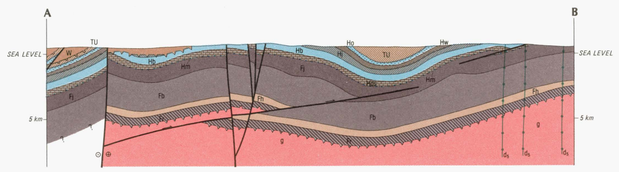

SECTION C – D

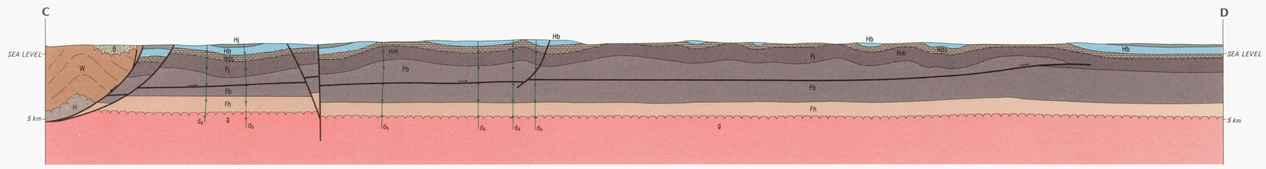

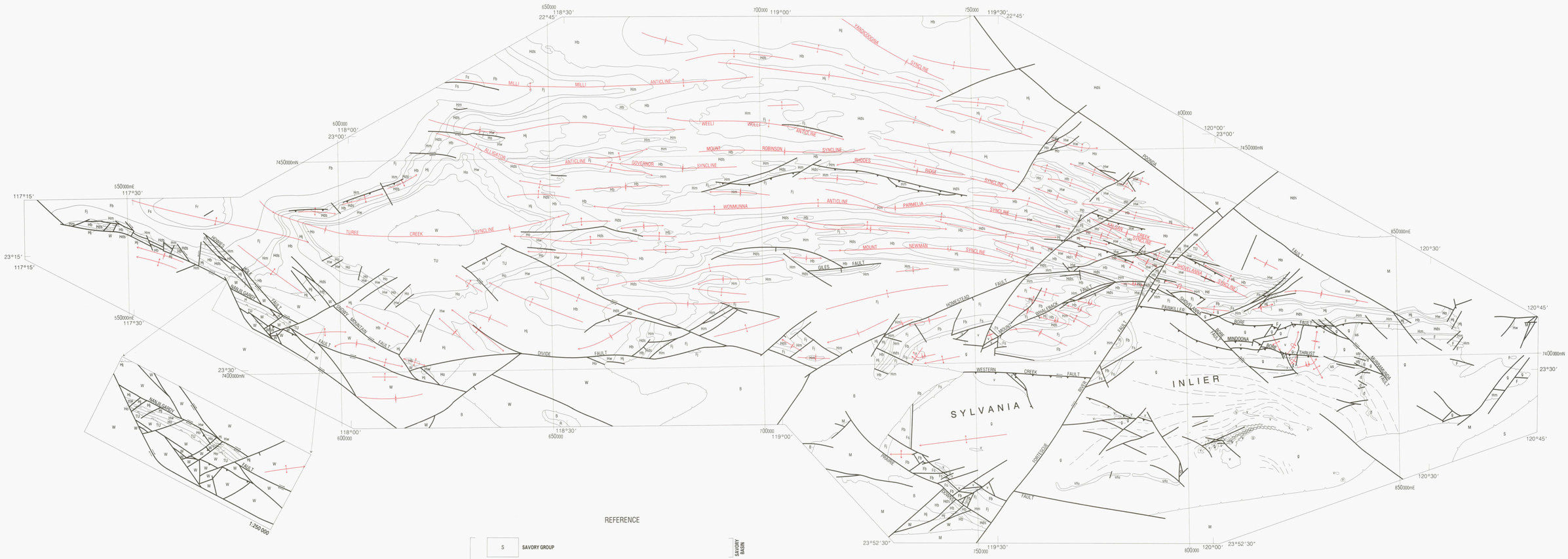

REFERENCE

		S	SAVORY GROUP	SAVORY BASIN
		d	MURRAMUNDA DOLERITE	
		M	BANGEMALL GROUP	BANGEMALL BASIN
		B	BRESNAHAN GROUP	BRESNAHAN BASIN
PROTEROZOIC		R	CAPRICORN FORMATION	BLAIR BASIN
		W	WYLOO GROUP	ASHBURTON BASIN
		TU	TUREE CREEK GROUP	
		H	HAMERSLEY GROUP :undifferentiated	HAMERSLEY BASIN
		Ho	BOOLGEEDA IRON FORMATION	
		Hw	WOONGARRA VOLCANICS	
		Hj	WEELI WOLLI FORMATION	
		Hb	BROCKMAN IRON FORMATION	
		Hds	MOUNT McRAE SHALE-MOUNT SYLVIA FORMATION-WITTENOOM DOLOMITE	
		Hm	MARRA MAMBA IRON FORMATION	
		F	FORTESCUE GROUP :undifferentiated	
		Fj	JEERINAH FORMATION	
		Fb	Mafic and felsic volcanic rocks – undifferentiated	
		Fs	Metasedimentary unit	
ARCHAEAN		Fr	MOUNT ROE BASALT-BELLARY FORMATION	
		us_2	Serpentinite	
		g	Granitoid rocks – undifferentiated	PILBARA CRATON Basement rocks
		us	Coobina Ultramafic Intrusion	
		v	Greenstone belt rocks – undifferentiated	

SYMBOLS

- Geological boundary
- Unconformity/disconformity
  - angular unconformity
  - disconformity
- Fault
  - normal
  - thrust
  - wrench, showing sense of movement
  - shear zone
- Fold (axial trace and plunge)
  - anticline
  - syncline
  - overturned anticline
  - overturned syncline
- Trend of foliation

LOCALITY DIAGRAM

INDEX TO 1:250 000 SHEETS

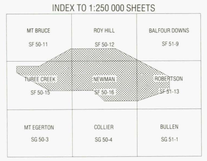

HON. JEFF CARR, M.L.A.
MINISTER FOR MINES
D.R. KELLY, DIRECTOR GENERAL OF MINES

P.E. PLAYFORD
DIRECTOR, GEOLOGICAL SURVEY
OF WESTERN AUSTRALIA

GEOLOGICAL SURVEY OF WESTERN AUSTRALIA

BULLETIN 138 PLATE 3

STRUCTURAL INTERPRETATION OF THE SYLVANIA INLIER AND SOUTHEAST HAMERSLEY BASIN

SCALE 1:500 000

5000 0 10 20 30 40 50
Metres Kilometres

TRANSVERSE MERCATOR PROJECTION
Grid lines indicate 50 000 metre interval of the Australian Map Grid Zone 50

Interpretation by I.M. Tyler 1988
Cartography by the Surveys and Mapping Division, Department of Mines, Western Australia.
Published by and available from the Geological Survey of Western Australia, Department of Mines, 100 Plain Street, East Perth, W.A. 6004.
Printed by the State Printing Division, Department of Services, Western Australia 1991.